THE GENETIC BASIS OF PUSTULAR PSORIASIS AND ITS OVERLAP WITH PSORIASIS VULGARIS

Berki, Dorottya Maria

Awarding institution:
King's College London

THE GENETIC BASIS OF PUSTULAR PSORIASIS AND ITS OVERLAP WITH PSORIASIS VULGARIS

By

Dorottya M Berki

A thesis submitted in fulfilment of the requirements for the degree of Doctor of Philosophy at King's College London

Department of Medical and Molecular Genetics
King's College London
9th floor, Tower Wing Guy's Hospital
Great Maze Pond London SE1 9RT

March 2016

CONTRIBUTION

I hereby declare the work presented in this thesis was performed exclusively by me, with the following exceptions. The whole-exome sequencing experiment was undertaken by technical staff from the Genomics Core facility of Guy's and St Thomas' Hospital Biomedical Research Centre (BRC). The raw sequence data was processed by the BRC Bioinformatics Core. The imputation using SNPTEST and the re-analysis of *IL36RN* genotypes generated in a previous genome-wide association scan was implemented by Jo Knight. Satveer Mahil and Safia Hussain contributed to the screening of the plaque and pustular psoriasis cohorts for *IL36RN* mutations, respectively. Finally, Francesca Capon performed the meta-analysis of the p.Asp176His variant in the *CARD14* study. I would like to acknowledge the contribution of everyone mentioned to the completion of my project.

Dorottya M Berki

ACKNOWLEDGEMENTS

My laptop was the foremost appendage of mine lately and has been through quite rhapsodic times. It visited numerous quiet libraries and lively cafeterias around Europe and the US, and writing this thesis on it transformed many things around (and within) myself. Public transportation was revealed to be as much of a thesis-writing arena as my current lab after hours.

Most importantly; however, this thesis could have not been completed without the help of numerous people to whom I owe sincere gratitude for supporting me in the past four years.

First of all, I am beyond words thankful for my supervisor, Dr. Francesca Capon, whose approach shaped my personality and research in many ways. Her consistent help, scientific and otherwise, was crucial in guiding me through my years at King's College London and completing this thesis. I cannot overstate my appreciation for all her support.

I am grateful to Professors Richard Trembath and Jonathan Barker for providing me with the opportunity to carry out work in their research group, and allowing me to be a part of a professional, collaborative environment. Furthermore, I gratefully acknowledge the funding received towards my PhD from the Psoriasis Association.

I am also indebted to many friends of mine. Foremost, Agnes Czako and Zita Galantai, "Nagy köszönet" for the memorable, fun, occasionally artistic, and always emotionally supportive time we spent together in London. Thanks are due to Dr. Andrea Schnúr, Dr. Lajos Maurovich-Horvát, and Dr. Zsombor Kovács for our inspiring discussions, Skype conversations, and e-mails, beyond and above molecular biology, chemistry, and the lovely statistics.

My deep appreciation also goes out to those I had the opportunity to work with in Boston prior to the start of my PhD. Very special thanks to Professor Jane Lopilato, Simmons College, whose kindness, unswerving helpfulness, and great enthusiasm toward science driven my

interest in genetics. I am also immensely grateful to Professor Raju Kucherlapati, Harvard University, for allowing me to complete an internship at his lab and awakening my interest in the application of genetics in medicine. Working with him offered me numerous opportunities, and I greatly appreciate his support and scientific advice. I also owe sincere thanks to Dr. Ildiko Hajdu from Harvard University for being an excellent supervisor and a friend.

Lastly, and most importantly, I would like to say thank to my family. My gratitude to them is impossible to express, even remotely. Hence I would like to finish this part with a Hungarian quotation, given that my fundamental source of life energy originates from that part of the world.

“Mert nem mindenkivel esik meg, hogy egy felhő színe, egy szél melege, egy gondolat izgalma érvén őt, meglepetve néz körül és azt mondja: "élek. - Milyen csodálatos!" - és pillanatnyi jelenségekben megérinti a létezés életöntudata.”

Balazs Bela

ABSTRACT

Pustular Psoriasis (PP) is a rare and disabling inflammatory skin disorder that is associated with an increased risk of plaque psoriasis (also known as psoriasis vulgaris or PV). While two PP genes (*IL36RN* and *AP1S3)* have been discovered, less than 30% of the patients harbour mutations at these loci. Moreover, the main genetic determinant for PV susceptibility (HLA-Cw6) is not associated with pustular psoriasis. Therefore, the molecular pathogenesis of PP and its clinical association with psoriasis vulgaris remain poorly understood. The aim of the current study was to investigate these issues through the genetic analysis of extended patient resources.

In the first part of the project, the possibility that the *IL36RN* gene may contribute to PV susceptibility was investigated by sequencing the gene in 363 unrelated individuals and re-analysing genome-wide association data. No enrichment of *IL36RN* mutations was detected in cases compared to controls, indicating that this important genetic determinant of pustular psoriasis does not confer PV susceptibility.

Next, the *CARD14* locus, which had been previously associated with familial PV, was screened in an extended pustular psoriasis cohort (n=205). This revealed a low-frequency p.Asp176His allele that caused constitutive CARD14 activation in functional assays and was significantly enriched in Asian cases compared to controls (P=8.4x10^{-5}; OR=6.4).

In the final part of the project, 17 patients affected by pustular psoriasis were exome-sequenced to identify genes that may be involved in the pathogenesis of the disease and contribute to the increased PV risk. Stepwise filtering of variant profiles uncovered a number of candidate genes that were followed-up in European (n=92) and

Asian validation cohorts (n=94). Although extensive genetic heterogeneity was observed, a number of loci deserving further investigation were defined, paving the way for the identification of novel genetic determinants of skin inflammation.

TABLE OF CONTENT

LIST OF TABLES

1 INTRODUCTION

2 MATERIALS AND METHODS

3 GENETIC ANALYSIS OF *IL36RN* ALLELS IN PSORIASIS VULGARIS

LIST OF FIGURES

1 INTRODUCTION

2 MATERIALS AND METHODS

3 GENETIC ANALYSIS OF *IL36RN* ALLELS IN PSORIASIS VULGARIS

4 GENETIC ANALYSIS OF *CARD14* ALLELES IN DIFFERENT SUBTYPES OF PSORIASIS

5 IDENTIFICATION OF NOVEL CANDIDATE GENES BY WHOLE-EXOME SEQUENCING

ABBREVATIONS

AA	amino acid
ACH	acrodermatitis continua of Hallopeau
AD	autosomal dominant
all	total allele count
alt	alternative allele count
AP	adaptor protein
AP-1	adaptor protein complex 1
AP1S3	adaptor-related protein complex 1, sigma subunit 3 gene
APP	Acral pustular psoriasis
APS	ammonium persulphate
AR	autosomal recessive
ARFGAP2	ADP-Ribosylation Factor GTPase Activating Protein 2 gene
ARHGAP11A	Rho GTPase Activating Protein 11A gene
ARHGEF16	Rho Guanine Nucleotide Exchange Factor (GEF) 16 gene
ATP	adenosine triphosphate
BCR	B-cell receptor
bp	base pair
BSA	bovine serum albumin
CADD	combined annotation dependent depletion
CARD9	caspase recruitment domain family,

	member 9 gene
CARD11	caspase recruitment domain family, member 11 gene
CARD14	caspase recruitment domain family, member 14 gene
CARMA1	Caspase recruitment domain (CARD)-containing protein 1
CARMA2	Caspase recruitment domain (CARD)-containing protein 2
CARMA3	Caspase recruitment domain (CARD)-containing protein 3
CC	coiled-coil domain
CCDS	consensus coding sequence
CCL20	Chemokine (C-C Motif) Ligand 20 gene
cDNA	complementary DNA
CEPH	Centre d'Etude du Polymorphisme Humain
CEU	Utah residents with ancestry from northern and western Europe
CHB	Han Chinese in Beijing
Chip-seq	chromatin immunoprecipitation sequencing
CI	confidence interval
CIP	calf intestinal alkaline phosphatase
COPI	coat protein I
CRP	C-reactive protein
CRF	Case Report Form
CSF	colony-stimulating factor

ctr	control
CYP1A1	Cytochrome P450, Family 1, Subfamily A, Polypeptide 1 gene
DAMP	damage-associated molecular pattern
DC	dendritic cell
DIRA	deficiency of IL-1 receptor agonist
DITRA	deficiency of the IL-36 receptor antagonist
DMEM	Dulbecco's modified Eagle's medium
DMSO	dimethyl sulphoxide
DNA	deoxyribonucleic acid
DNAH12	Dynein, Axonemal, Heavy Chain 12 gene
dNTP	deoxynucleotide triphosphate
DOCK8	Dedicator Of Cytokinesis 8 gene
dsDNA	double-stranded DNA
dsRNA	double-stranded RNA
DTT	Dithiothreitol
EDTA	ethylenediamine tetraacetic acid
EP	erythrodermic psoriasis
EPHA8	EPH Receptor A8 gene
ER	endoplasmic reticulum
ERASPEN	European rare and severe psoriasis expert network
ESP	exome sequencing project
ESR	erythrocyte sedimentation rate
EVI5	Ecotropic Viral Integration Site 5 gene
ExAC	Exome Aggregation Consortium

F	Female
FBN3	Fibrillin 3 gene
FCS	foetal calf serum
FL	full length
FMN1	Formin 1 gene
FRAS1	Fraser Extracellular Matrix Complex Subunit 1 gene
F8	Coagulation Factor VIII, Procoagulant Component gene
Gb	giga base
GIH	Gujarati Indian from Houston Texas
GO	grand opportunity
GLI2	GLI Family zinc finger 2 gene
GPP	generalised pustular psoriasis
GRR	Genotype Relative Risk
HEK293T	human embryonic kidney 293T cell line
HLA-C	Human Leukocyte Antigen C
HET	heterozygous
HKR1	GLI-Kruppel Zinc Finger Family Member gene
HOM	homozygous
IBD	inflammatory bowel disease
IFN-α	interferon-α
IFN-β	interferon-β
IFN-γ	interferon-γ
IGSF10	Immunoglobulin Superfamily, Member 10 gene
IGV	Integrative genomics viewer

IκB	Inhibitor of NF-κB
IKK	IκB kinase
ILC	innate lymphoid cells
IL-1	interleukin-1
IL-6	interleukin-6
IL-10	interleukin-10
IL-17	interleukin-17
IL-18	interleukin-18
IL-18R1	interleukin 18 receptor 1
IL-18RAP	interleukin-18 receptor accessory protein
IL-1R	interleukin-1 receptor
IL1Ra	interleukin 1 receptor antagonist
IL1RN	interleukin 1 receptor antagonist gene
IL-1RAcP	interleukin-1 receptor accessory protein
IL-1RL2	interleukin-1 receptor-like 2
IL-21	interleukin-21
IL-22	interleukin-22
IL-23	interleukin-23
IL-36	interleukin-36
IL-36Ra	IL-36 receptor antagonist
IL36RN	IL-36 receptor antagonist gene
IL-6	interleukin-6
IL-8	interleukin-8
IL-36	interleukin-36
ILC	innate lymphoid cells
in/del	insertion/deletion
IPEX	immune dysfunction, polyendocrinopathy enteropathy, X-

	linked
IRAK	IL-1 receptor associated kinase
ITU	Indian Telegu from the UK
IκB	inhibitor of NF-κB
IKK	inhibitor of NF-κB
JAK	Janus kinase
JNK	c-Jun N-terminal protein kinases
JPT	Japanese in Tokyo Japan
KC	Keratinocytes
KCl	potassium chloride
LB	Luria broth
LD	linkage disequilibrium
LL-37	Antimicrobial peptide *LL-37*
LPS	lipopolysaccharide
LRO	lysosome-related organelle
LRR	leucine-rich region
LUBAC	linear-ubiquitin-chain-assembly complex
M	Male
MAPKBP1	Mitogen-Activated Protein Kinase Binding Protein 1 gene
MAF	minor allele frequency
MAL	MyD88-adapter-like
MAPK	mitogen-activated protein kinase
MEGF11	Multiple EGF-Like-Domains 11 gene
MDA-5	Melanoma Differentiation-Associated protein 5
MgCl2	magnesium chloride

MgSO4	magnesium sulfate
MHC	major histocompatibility complex
ml	Millilitre
µl	Microlitre
µM	Micromolar
LGP2	Laboratory of genetics and physiology 2
MAVS	mitochondrial antiviral signaling protein
MPEG1	Macrophage Expressed 1 gene
mRNA	messenger RNA
MYOM2	Myomesin 2 gene
N	no
n/a	not available
n/s	not significant
NaCl	sodium chloride
NaOAc	sodium acetate
NF-κB	nuclear factor κB
ng	nanogram
NGS	next-generation sequencing
NK	natural killer
NLR	nod-like receptor
NLRP3	NLR family, pyrin domain containing 3
nM	nanomolar
NR3C2	Nuclear Receptor Subfamily 3, Group C, Member 3 gene

NS	not synonymous
nt	nucleotide
N-ter	N-terminal
OMIM	online mendelian inheritance in man
OR	odds ratio
OR51G1	Olfactory Receptor, Family 51, Subfamily G, Member 1 gene
P/S	Penicillin-Streptomycin
PACT	PKR activator
PAMP	pathogen-associated molecular patterns
PBS	phospate buffer saline
pCMV	human cytomegalovirus early promoter
PCR	polymerase chain reaction
PJL	Punjabi from Lahore Pakistan
PLCH1	Phospholipase C, Eta 1 gene
PNK	polynucleotide kinase
PPIA	cyclophilin A
PPP	palmar-plantar pustulosis
PRP	pityriasis rubra pilaris
PRR	pattern recognition receptor
PsA	psoriatic arthritis
PSORS1	psoriasis susceptibility locus 1
PSORS2	psoriasis susceptibility locus 2
PSORS4	psoriasis susceptibility locus 4
PV	psoriasis vulgaris
QC	quality control

RA	rheumatoid arthritis
RBMXL1	RNA Binding Motif Protein, X-Linked-Like 1 gene
RD	repressor domain
RIG-I	retinoic acid-inducible gene 1
RISC	RNA-induced silencing complex
RLR	RIG-I-like receptors
RNA	ribonucleic acid
rpm	revolutions per minute
SD	standard deviation
SDS	sodium dodecyl sulphate
SE	standard error
SH2	Src homology 2
SLC45A4	Solute Carrier Family 45, Member 4 gene
SNP	single nucleotide polymor phism
SSIP	Singapore Sequencing Indian Project
SSMP	Singapore Sequencing Malay Project
ssRNA	single-stranded RNA
ST2	interleukin 1 receptor-related protein
STAT	signal transducer and activator of transcription
STING	stimulator of interferon genes
STOX1	Storkhead Box 1 gene
STU	Sri Lankan Tamil from the UK
T1D	type 1 diabetes
TAK	TGF β-activated kinase
TAS2R3	Taste Receptor 2, type 3 gene
TBE	Tris-borate-EDTA
TBS	Tris-buffered saline

Tc	T cytotoxic
TCR	T-cell Receptor
TEMED	Tetramethylethylenediamine
TGN	trans-Golgi network
Th	T helper cell
Th1	T helper 1 cell
Th17	T helper 17 cell
Th2	T helper 2 cell
Th22	T helper 22 cell
TIR	Toll/IL-1R
TLR	Toll-like receptor
Tm	annealing temperature
TNF	tumour-necrosis factor
TNF- α	tumour-necrosis factor alpha
TRAF	TNF receptor associated factor
TRIF	TIR-domain-containing adapter-inducing interferon-β
TREG	Regulatory T-cells
U	Unit
UCSC	university of California Santa Cruz
VCF	variant call format
WES	whole-exome sequencing
WGS	whole-genome sequencing
WT	wild-type

1 INTRODUCTION

1.1 The skin immune system

The skin is the largest organ in humans. As the outermost layer of the body, it confers protection against environmental insults such as temperature changes, solar radiation and most importantly, infections. Therefore, the skin has a very important immune function (Burns and Breathnach, 2010).

1.1.1 The structure of skin

The skin consists of two layers, the epidermis and the dermis. Each is further divided into sub-layers and contains distinct cell types that are essential to its function.

1.1.1.1 The epidermis

The epidermis is a rapidly self-renewing tissue that forms the outermost portion of the skin. While keratinocytes are its major constituent, immune (e.g. Langerhans cells and CD8+ T lymphocytes), sensory (e.g. Merkel cells), and melanin producing cells (melanocytes) are also present (Burns and Breathnach, 2010).

The epidermis encompasses a number of cell layers. The *stratum corneum* is the outermost part of the tissue and is composed of corneocytes (anucleated, nonviable keratinocytes) surrounded by a lipid-rich intercellular matrix. This layer represents a physical barrier, which protects against water loss, and most importantly, against invading microorganisms (Burns and Breathnach, 2010).

The *stratum basale* is a single layer of continuously proliferating stem cells from

where keratinocytes migrate to the *stratum corneum*. To further support the structure of the epidermis, these basal keratinocytes adhere to each other via their desmosomes and to the basement membrane via hemi-desmosomes (Burns and Breathnach, 2010).

The *stratum spinosum* and *stratum granulosum* are both composed of multiple cell layers. While the keratinocytes of the *stratum spinosum* contain thick bundles of intermediate filaments in their cytoplasm, the cells of the *stratum granulosum* are characterized by the presence of keratohyalin granules that contain profillaggrin and promote the cross-linking of keratin fibres (Burns and Breathnach, 2010).

Of note, the skin of the palms and soles includes an additional layer (*stratum lucidum*) between the *stratum granulosum* and *stratum corneum* (Burns and Breathnach, 2010).

1.1.1.2 The dermis

The dermis lies beneath the epidermis and can be divided into papillary dermis, which is the uppermost layer, and reticular dermis, which lies between the papillary dermis and the subcutaneous fat, and hosts blood vessels, hair follicles, and sweat glands (Burns and Breathnach, 2010). The dermis mostly consists of fibroblasts and matrix components such as collagen and elastin, which provide mechanical support (Nestle et al., 2009; Szun et al., 2014). However, capillary and lymphatic vessels are also present and allow the infiltration of immune cells such as dendritic cells, CD4+ T lymphocytes, macrophages and mast cells (Nestle et al., 2009; Szun et al., 2014).

1.1.2 Innate immunity

The protective role of the immune system is mediated by two interconnected arms known as innate and adaptive immunity. While the former promotes a rapid first reaction to pathogens, the latter ensures that the response is antigen-specific (Table 1.1.2; Figure 1.1.2).

The skin, as an anatomical barrier is the first line of protection against invading organisms. If a pathogen penetrates through this layer, it will be recognized by germline encoded innate receptors, which are expressed by a variety of skin resident cells.

Table 1.1.2. Comparison between the innate and adaptive immune system

	Innate immunity	**Adaptive immunity**
Response time	Immediate	Immediate or delayed response (3-5 days)
Memory	Absent	Present
Receptors	Pattern recognition receptors (PRRs) are encoded in the germline	B-cell and T-cell receptors are generated by somatic recombination
Pathogen recognition	Receptors recognize pathogen-associated molecular patterns (PAMPs)	Receptors bind antigen-specific sequences (epitopes)

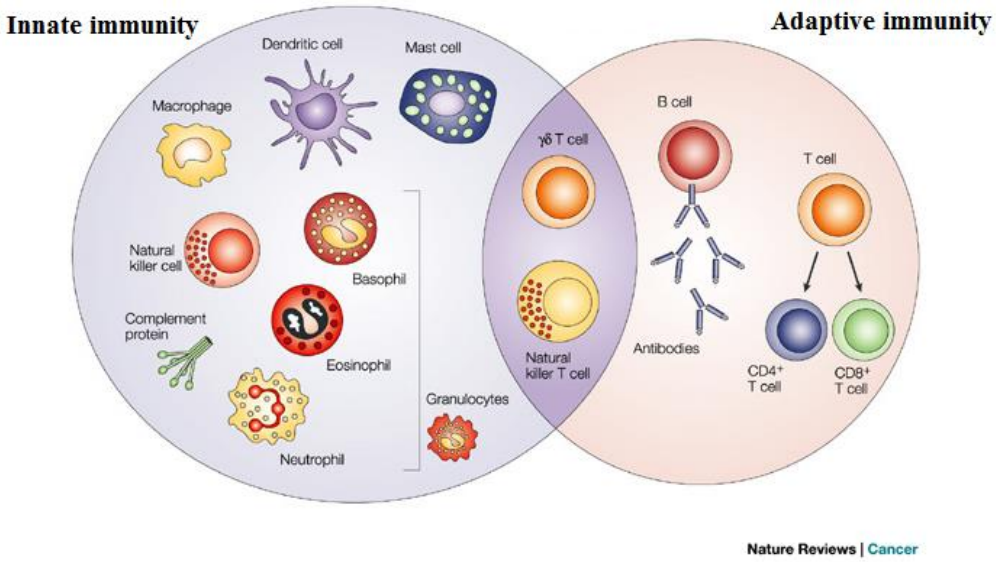

Figure 1.1.2. Comparison between innate and adaptive immune cells

Innate immunity is mediated by diverse cell populations including dendritic cells, macrophages, mast cells, natural killer cells, granulocytes (basophils, eosinophils and neutrophils), as well as soluble factors (complement proteins). The adaptive immune response consists of B and T ($CD4^+$ and $CD8^+$) lymphocytes, as well as antibodies. There is also an overlap between the two systems, since natural killer T cells and γ δ T cells can function at the interface between innate and adaptive immunity.

Figure originally published by Dranoff, 2004.

1.1.2.1 Innate immune receptors

The innate immune system senses pathogens by recognizing evolutionally conserved structures called pathogen-associated molecular patterns (PAMPs). These are detected by three families of pattern recognition receptors (PRRs): Toll-like receptors, RIG-I-like receptors, and NOD-like receptors. The latter can also recognize endogenous molecules called damage associated molecular patterns (DAMPs), which are released following cell death or tissue injury (Takeuchi and Akira, 2010).

Toll-like receptors (TLRs) are a family of evolutionary conserved, membrane-bound proteins located on the cell surface (TLR- 1, 2, 4, 5, 6, 10), or within the endosomal membrane (TLR- 3, 7, 8, 9) (Takeuchi and Akira, 2010). TLRs recognize features present on the cell walls (e.g. lipoproteins and peptidoglycan recognized by TLR-2) or outer membrane (e.g. lipopolysaccharide recognised by TLR-4) of pathogens, as well as viral nucleic acids (recognized by TLR-3, -7, -8) (Takeuchi and Akira, 2010). Once bound to a ligand, TLRs activate two different pathways known as the MyD88-dependent and the TRIF-dependent cascade, leading to the production of inflammatory cytokines and type I interferons (IFNs), respectively (Takeuchi and Akira, 2010).

RIG-I-like receptors (RLRs) are localized in the cytoplasm and their main role is the sensing of viral nucleic acids. RLRs include RIG-I (retinoic acid inducible gene-I), MDA-5 (Melanoma Differentiation-Associated protein 5), and LGP2 (laboratory of genetics and physiology 2). In the N terminal end of RIG-I and MDA5, there are two caspase activation and recruitment domains (CARDs) that mediate signaling toward downstream proteins (Wu and Chen, 2014). While RIG-I detects small (<1kB)

molecules, MDA5 recognizes longer (>2kB) RNA fragments (Wu and Chen, 2014). Upon nucleic acid binding, both receptors signal through the mitochondrial antiviral signaling protein (MAVS), leading to IRF3, IRF7, and NF-κB activation, plus the production of type I IFNs and pro-inflammatory cytokines (Takeuchi and Akira, 2010; Wu and Chen, 2014). As to LGP2, it is involved in MDA5 signaling, and acts as a positive regulator (Wu and Chen, 2014).

Nucleotide oligomerisation domain (NOD)-like receptors (NLRs) are soluble cytoplasmic proteins that detect cytoplasmic pathogens and danger-associated molecules released during cell damage or stress (Fukata et al., 2009). NLRs can be classified in two main families: NOD (nucleotide-binding oligomerization domain) and NALP (NACHT, LRR and PYD containing) proteins (Mathews et al., 2008). Although they share two common domains (the ligand-sensing LRRs and the NACTH 2 oligomerization motif), NOD and NALP proteins differ in their effector regions. Upon ligand recognition, NOD receptors activate NF-κB and mitogen-activated protein kinase (MAPK) signaling, while NALPs cause the cleavage of the pro-inflammatory precursors pro-IL-1β and pro-IL-18 into their mature forms, through activation of caspase 1 and 5 (Mathews et al., 2008; Fukata et al., 2009).

1.1.2.2 Innate immune cells in the skin

Keratinocytes are the most abundant cell type in the epidermis, and besides their aforementioned role in providing structural support to the skin; they have key functions in pathogen detection and host defense. Due to the diverse receptors they express, they are able to sense bacterial components trough their TLRs, as well as viral and fungal molecules through NLRs (Nestle et al., 2009). As a result, keratinocytes can release a

wide-range of cytokines (e.g. IL-1, IL-6, IL-10, IL-18, IL-22 and IL-36), antimicrobial peptides (e.g. LL-37 and β-defensin), and chemokines (e.g. IL-8), and attract further immune cells to the site of infection (Nestle et al., 2009).

Macrophages are professional antigen presenting cells, which express major histocompatibility complex (MHC) molecules as well as co-stimulatory ligands such as CD80 and CD86 (Bendke and Stenzl, 2010). Macrophages also express many PRRs that allow them to sense both pathogen- and damage-associated signals (Szun et al., 2013). Once activated, macrophages produce pro-inflammatory cytokines (e.g IL-1) and chemokines (e.g Chemikine C-C ligand motif 3, CCL3) (Foss et al., 1999). At the same time, macrophages can terminate inflammation by engulfing apoptotic cells (Szun et al., 2013).

Under normal conditions, macrophages are the most abundant hematopoietic cell type in the skin (Szun et al., 2013). They can be either tissue-resident or bone marrow-derived monocytes/macrophages, but the functional difference between these two populations remains to be understood (Szun et al., 2013; Nestle et al., 2009). What is known is that skin-resident macrophages originate from the yolk sac and are able to self-renew during inflammation, while bone marrow-derived monocytes circulate through the skin and transport antigens to the lymph nodes (Pasparakis et al., 2014).

Dendritic cells (DC) are antigen-presenting cells that can migrate to skin draining lymph nodes upon pathogen recognition (Szuen et al., 2013). They are a diverse population and are able to sense numerous microbial components through their pattern recognition receptors (Heath and Carbone, 2013).

Under homeostatic conditions, Langerhans cells are the only DCs that reside within the basal and suprabasal layers of the epidermis, where they can induce Th17 cell

responses (Heath and Carbone, 2013), but also activate regulatory T cells. The dermal DC population is more heterogeneous and can be subdivided into different subsets, based on the expression of surface markers such as Langerin, CD103 and CD11b. These DCs are involved in capturing dead cells, presenting antigens to CD4+ and CD8+ T-cells and inducing Th17 cell response (Heath and Carbone, 2013).

Mast cells are located in the dermis, close to the blood vessels and are involved in wound healing, as well as Th2 activation (Szun et al., 2013).

Innate lymphoid cells (ILC) are a recently characterized group of effector cells, which originate from the lymphoid lineage but do not express antigen-specific surface receptors. They are typically found within barrier surfaces (gut, lung and skin) and can be classified into different subtypes (ILC1, ILC2 and ILC3) according to the cytokine they produce and the immune cells they activate (Pasparakis et al., 2014). Under homeostatic conditions, all three subsets are found in skin, where they contribute to the fight against intracellular pathogens (ILC1), helminths (ILC2), and extracellular bacteria (ILC3) (Pasparakis et al., 2014).

Neutrophils are also important mediators of early immune responses, but they are not found in the dermis or the epidermis, under homeostatic conditions (Nestle et al., 2009).

1.1.3 Adaptive immunity

The adaptive immune system is composed of specialized lymphocytes, which can mount a humoral or T-cell mediated response. This reaction is antigen-specific and is typically stronger after an initial encounter with a pathogen (immunological memory)

(Luckheeram et al., 2012).

T lymphocytes are activated following the presentation of antigens to their T-cell receptor (TCR) and the engagement of co-stimulatory surface molecules such as CD28. Depending on the cytokine milieu, activated CD4+ T cells differentiate into Th subsets (e.g. Th1, Th2 and Th17 lymphocytes) or regulatory T-cells (T-regs) (Figure 1.1.3) (Luckheeram et al., 2012). While the former can activate additional immune cells (e.g. Th1 lymphocytes act on macrophages and NK-cells; Th2 cells act on B-cells), T-regs modulate the function of the aforementioned T-cell populations through the production of IL-10 (Luckheeram et al., 2012).

CD8+ T cells are also known as cytotoxic-lymphocytes, as they kill infected and malignant cells, upon recognising intra-cellular peptides presented by MHC molecules (Luckheeram et al., 2012).

B-lymphocytes express the B cell receptor on their surface and mediate the humoral adaptive response. They can become activated through T-cell dependent or T-cell independent mechanisms, leading to the secretion of antibodies into the bloodstream (Egbuniwe et al., 2015). B-lymphocytes can also act as antigen presenting cells and produce cytokines (Egbuniwe et al., 2015).

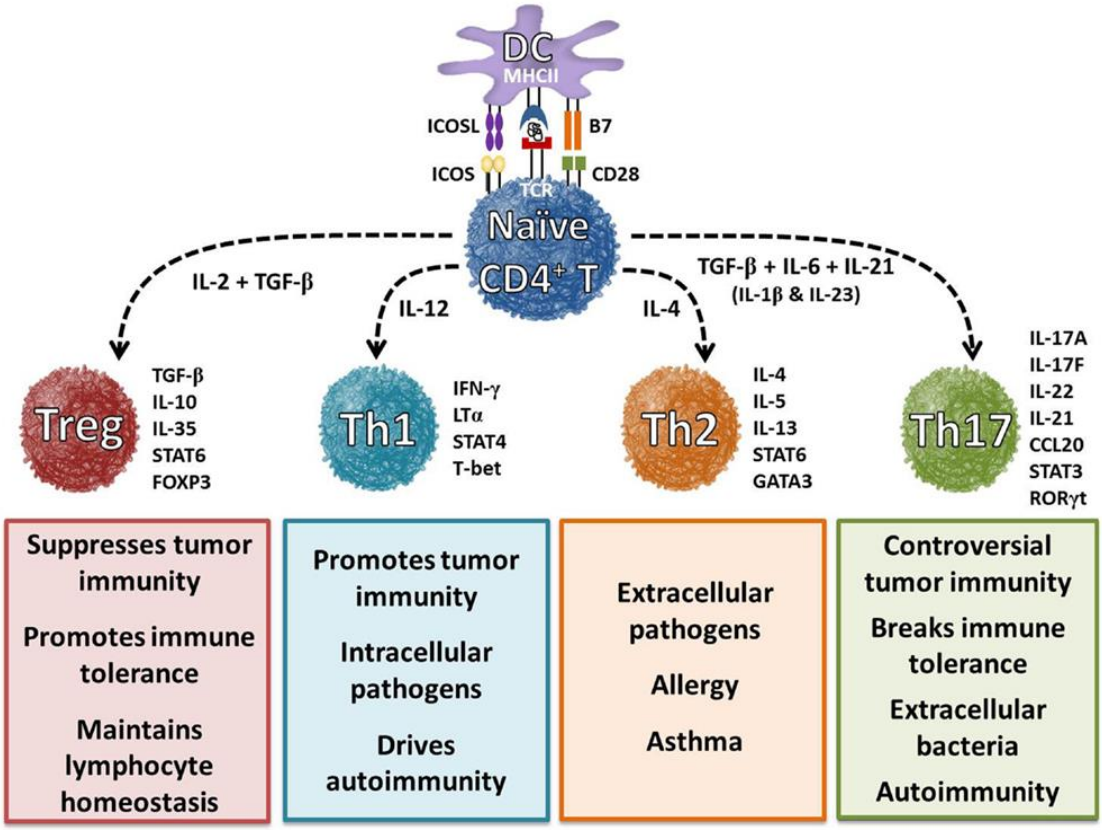

Figure 1.1.3. The differentiation of helper T cells is driven by cytokines

The presence of Interleukin 2 (IL-2) and transforming growth factor-beta (TGF-β), and the transcription factor FOXP3 drives the differentiation of the naïve $CD4^+$ T cells into Treg cells, while the cytokines IL-4 and TGF-β, and transcription factors T-bet and GATA3 induce Th1 and Th2 cell development, respectively. These three T-cell subsets regulate the immune response to self, foreign, as well as tumor antigens. IL-6, IL-21, TGF-β, and the transcription factor RORγt were implicated in the development of Th17 cells. Figure retrieved from Bailey et al., 2014.

1.1.3.1 Skin-resident adaptive immune cells

The skin contains twice as many T-cells as peripheral blood (Nestle et al., 2009). In the basal- and suprabasal-layer of the epidermis, the majority of these are CD8+ α β T lymphocytes (Nestle et al., 2009). In contrast, the dermal population is a mixture of CD8+ and CD4+ T cells, which are found in proximity of the dermal-epidermal junction (Nestle et al., 2009). The migration of these cells into the skin is mediated by the cutaneous lymphocyte antigen (CLA) (Egbuniwe et al., 2015).

There are also "innate-like" populations present in the skin, including γ δ T cells and NKT cells found within the dermis. While the exact role of the γ δ T cells remains poorly defined, they were shown to produce several growth factors (e.g. fibroblast growth factor 9 and keratinocyte growth factor) implicated in wound healing. They can also release antimicrobial molecules such as cathelicidins (Nestle et al., 2009).

NKT cells share features with natural killer cells and T-lymphocytes. Upon activation, they can produce both Th1 (IFN γ) and Th2 (IL-4) cytokines (Nestle et al., 2009).

B-cells are rarely seen in the skin under physiological conditions, and it is still unknown whether they form a tissue-resident population (Egbuniwe et al., 2015).

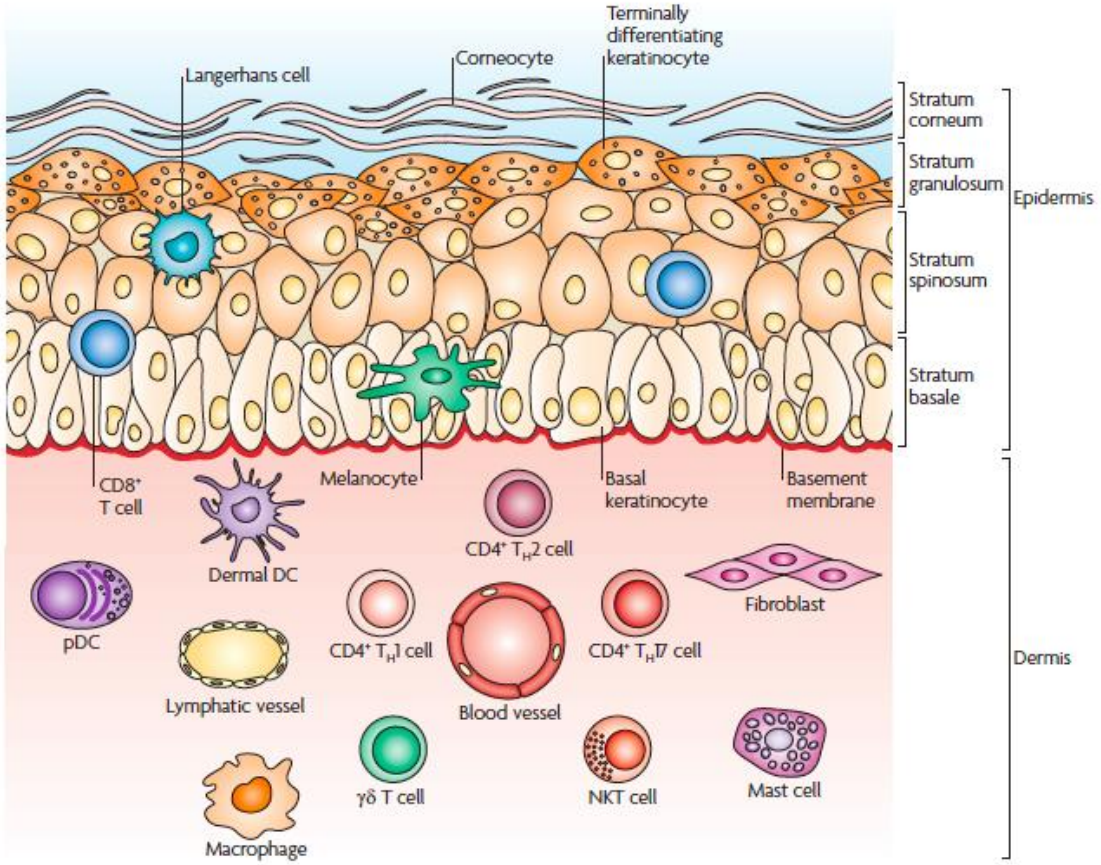

Figure 1.1.3.1. Skin-resident immune cells

The human skin hosts both innate and adaptive immune cells. Those found in the epidermis are keratinocytes, Langerhans cells and $CD8^+$ cytotoxic T cells. The dermis contains a more complex immune population, including dendritic cells (dermal DCs and, under inflammatory conditions, plasmacytoid DCs), several T cell subsets (memory T lymphocytes γδ T cells, NKT cells and under inflammatory conditions activated CD4+ T lymphocytes), macrophages and mast cells. Figure retrieved from Nestle et al., 2009.

1.2 Psoriasis and related phenotypes

Psoriasis is a non-contagious, chronic inflammatory skin disorder that has a profound impact on the well-being of patients. It is estimated to affect up to 2% of the population worldwide, but is more prevalent in ethnic groups of European descent (Crow, 2012; Nestle et al., 2009). Disease onset shows two peaks, which occur at 15-30 (early onset disease) and 50-60 years of age (late onset disease) (Mahil et al., 2015). In either case, males and females are affected with equal frequency.

Triggering factors include trauma (e.g, piercings, tattoos), sunburn, chemical irritants, as well as systemic drugs (e.g. β blockers) and non-steroidal anti-inflammatory agents (Boehncke and Schön, 2015).

Several clinical variants of psoriasis have been described. These can co-exist or more often appear in succession**.** The subtypes that are relevant to this study are described below.

1.2.1 Psoriasis vulgaris and non-pustular disease variants

1.2.1.1 Clinical features

The most common type of psoriasis is psoriasis vulgaris (PV, also known as chronic plaque psoriasis), which accounts for 90% of disease cases (Boehncke and Schön, 2015). PV is characterized by the appearance of red, scaly plaques, which mostly affect symmetric sites on the elbows, knees, scalp, and intergluteal cleft (Figure 1.2.1.1.1). Around 50% of patients also have nail involvement and experience pitting and nail-plate thickening (Boehncke and Schön, 2015).

At the histological level, psoriatic lesions show epidermal hyperplasia and increased vascularity of the dermis (Griffiths and Barker, 2007). An inflammatory

infiltrate is also present. It includes abundant numbers of CD4+ and CD8+ T cells, which underscores the importance of adaptive immunity in disease pathogenesis (Griffiths and Barker, 2007).

The impact of psoriasis can be compounded by several important co-morbidities. Approximately 25% of PV patients suffer from a sero-negative form of joint inflammation, known as psoriatic arthritis (Naldi and Gambini, 2007). This causes pain and swelling in/around the joints, which can lead to occupational or functional disability (Naldi and Gambini, 2007; Boehncke and Schön, 2015).

Epidemiological studies have also demonstrated an increased prevalence of cardiovascular disease among psoriatic patients, which is especially noticeable among individuals suffering from severe PV (Ryan and Kirby, 2015). Furthermore, PV is associated with hypertension and type II diabetes (Ryan and Kirby, 2015). Whether or not the association of PV with cardiovascular comorbidities is caused by concurrent systemic inflammation remains to be understood (Ryan and Kirby, 2015).

Less frequent and site-specific subtypes of the disease include flexural (inverse) psoriasis, which presents with shiny, red, scale-free lesions in intertriginous sites (Griffiths and Barker, 2007; Crow, 2012) (Figure 1.2.1.1.2). Acute forms also exist, such as guttate psoriasis, which is characterised by papule eruptions that mostly affect the trunk (Griffiths and Barker, 2007; Crow, 2012).

Finally, the most severe non-pustular variant of the disease is erythrodermic psoriasis. This is a rare condition (it accounts for less than 3% of psoriasis cases) that can be triggered by severe sunburn, use of systemic steroids or excessive alcohol intake (Thomas et al., 2014). It presents with widespread exfoliation, severe itching, pain, and fiery redness of the skin (Thomas et al., 2014; Griffiths and Barker, 2007). These

symptoms are associated with systemic involvement and increased heart rate. Erythrodermic psoriasis is therefore a potentially life-threatening condition, so that disease flares require urgent hospitalisation (Griffiths and Barker, 2007; Crow, 2012) (Figure 1.2.1.1.2).

Figure 1.2.1.1.1. Clinical presentation of PV

The incidence (80-90% of psoriasis cases) and typical presentation of PV are shown in the lower panels. The anatomical regions that are most often affected are represented as red spots in the upper panel diagram. Figure originally published in Crow, 2012; and Griffiths and Barker, 2007.

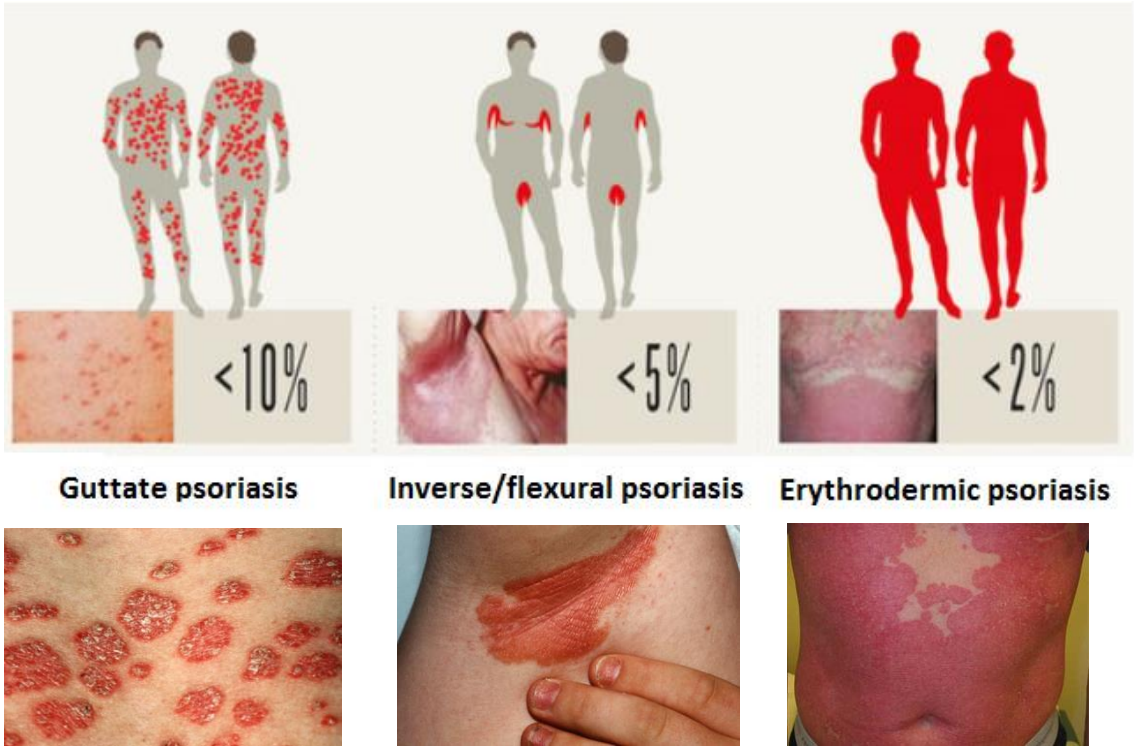

Figure 1.2.1.1.2. Clinical presentation of further non-pustular variants of psoriasis

The incidence (% of psoriasis cases) and typical presentation of gutatte psoriasis, inverse psoriasis, and Erytrodermic psoriasis are shown in the lower panel, while the most often affected anatomical regions are represented as red areas in the upper panel diagram. Figures retrieved from Crow, 2012; http://psoriasismedication.org; and http://www.skindiseasehospital.org.

1.2.1.2 Immune pathogenesis

The effort to elucidate the immune pathogenesis of psoriasis has mostly been focused on PV, so that very little is known about the aetiology of other non-pustular disease variants.

PV was first considered to be a Th1-mediated disease, as cytokines like IL-2, IL-12 and IFN-γ, were found to be highly expressed in psoriatic plaques compared to normal skin (Griffiths and Barker, 2007; Di Cesare et al., 2009). However, more recent studies have convincingly implicated the IL-23/Th17 axis in disease pathogenesis (Di Cesare et al., 2009; Boehncke and Schön, 2015). Over-activation of the latter immune pathway is thought to drive the progression of psoriasis vulgaris and account for most of the phenotypic features of psoriatic plaques (Figure 1.2.1.2).

The cross-talk between innate and the adaptive immunity, which is mediated by cytokines such as TNF-α and interleukin 1, is also important in disease pathogenesis (Boehncke and Schön, 2015).

Following injury, keratinocytes produce antimicrobial peptides (e.g. β-defensins and cathelicidin) that contribute to host defense by killing pathogens (e.g. Escherichia coli) and activating further immune cells (Morizane et al., 2012). One such molecule, the cathelicidin LL37, plays a key role in the establishment of psoriatic lesions. In fact, the most likely initial step in disease pathogenesis is the binding of host nucleic acid (originating from stressed or dying cells) by LL37. The resulting DNA/LL37 complexes aberrantly stimulate plasmacytoid dendritic cells (pDCs), a population of DC expressing TLR-7 and TLR-9, which infiltrates the dermis under inflammatory conditions (Morizane et al., 2012; Ganguly et al., 2009; Lande et al., 2007). The subsequent release of interferon α by pDCs activates myeloid DCs, which in turn promote the differentiation of CD4+ T-cells into Th1 and Th17 subsets (Figure 1.2.1.2) (Nestle et

al., 2009; Morizane et al., 2012; Lande et al., 2007). These lymphocytes migrate to the epidermis, where they release a number of pro-inflammatory cytokines, including TNF-α, IFNγ (Th1 cells), IL-17 and IL-22 (Th17 cells). The resulting pro-inflammatory milieu activates keratinocytes to produce chemokines (e.g. IL-8 and CCL20), which attract further Th1 and Th17 cells and propagate an abnormal immune response.

Of note, recent studies demonstrated the presence of LL37 dependent T-cell populations in psoriatic skin, indicating that cathelicidin LL37 also acts as an autoantigen in psoriasis (Lande et al., 2014).

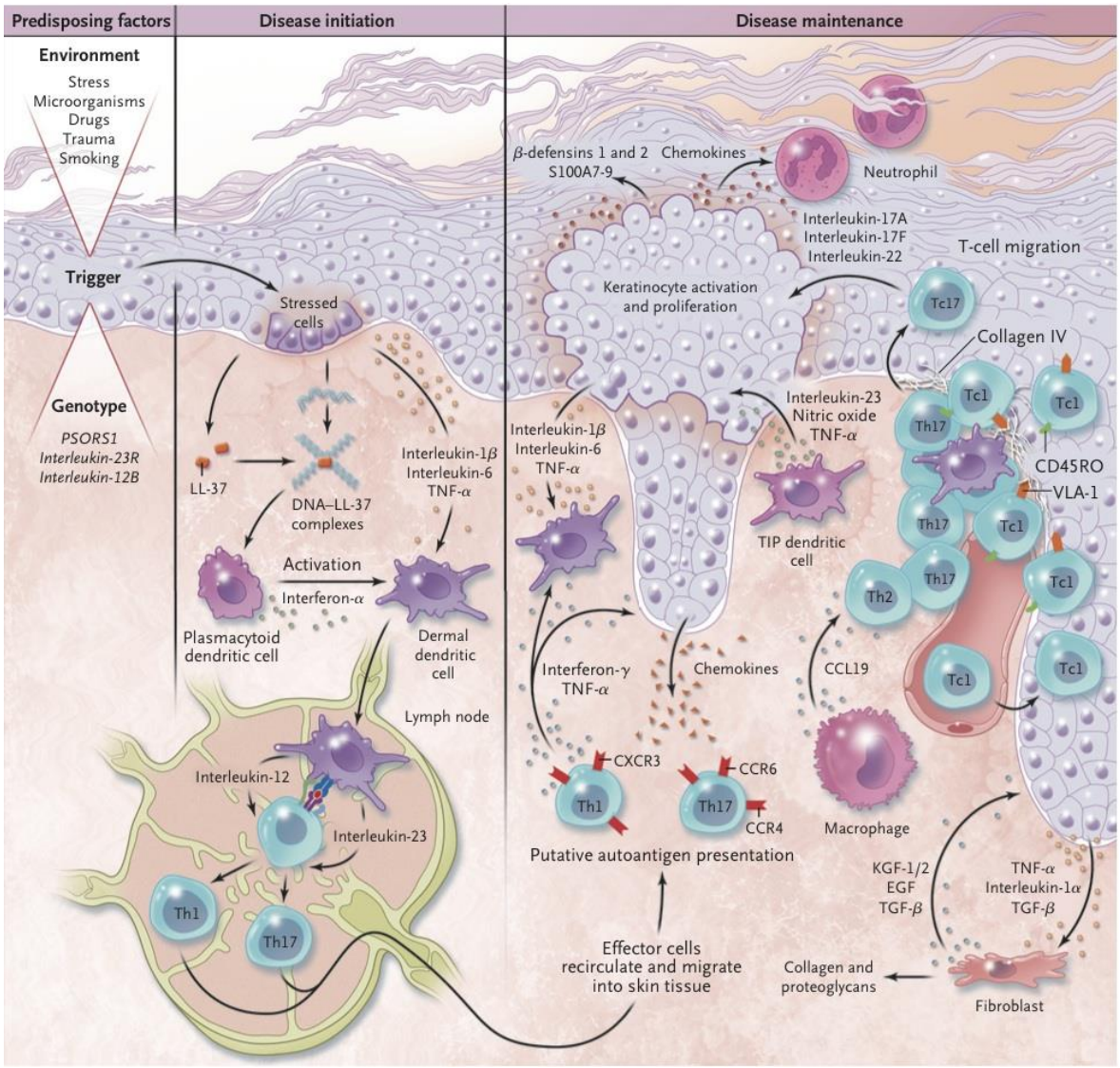

Figure 1.2.1.2. Immune pathogenesis of PV

Self nucleic acids released following cell-damage are recognised by LL-37. The resulting complexes cause pDCs to release IFNα, which activates myeloid dermal dendritic cells. Myeloid DC-induced IL-12 and IL-23 promotes the differentiation of Th1 and Th17 cells, respectively. T lymphocytes migrate into the skin and secrete pro-inflammatory cytokines, leading to keratinocyte activation. This effect is reinforced by the release of keratinocyte growth factor from fibroblasts. Activated keratinocytes propagate the inflammatory response by producing chemokines, which attract neutrophils, macrophages and further T cells. Figure retrieved from Nestle et al., 2009.

1.2.1.3 Genetics

A genetic component of PV has long been apparent, due to the higher incidence of the disease among individuals with affected family members. This is particularly noticeable in early onset cases, with almost 70% of patients with childhood psoriasis reporting a family history of the condition (Capon et al., 2012; Mahil et al., 2015). Several studies have also documented increased disease concordance in monozygotic (35-73%) compared to dizygotic twins (12-20%) (Capon et al., 2012; Nestle et al., 2009; Mahil et al., 2015). Indeed, psoriasis has one of the highest genetic components among complex diseases, with heritability estimates ranging between 60% and 90% (Mahil et al., 2015).

In the 1990s, linkage studies identified 9 genomic regions (*PSORS1-9*) that co-segregated with the disease in multiplex pedigrees (Capon et al., 2012; Mahil et al., 2015). Of these, *PSORS1*, a 220 kB interval of the Major Histocompatibility Complex (MHC) class I region, was found to confer the highest risk for the disease (Capon et al., 2012).

While the *PSORS1* (chromosome 6p21), *PSORS2* (chromosome 17q25) and *PSORS4* (chromosome 1q21) loci were replicated in multiple follow-up studies, the remaining genomic regions were not (Mahil et al., 2015), highlighting the lack of reproducibility of linkage studies in complex traits.

In recent years, genome-wide association scans (GWAS) and targeted studies of immune loci have led to the identification of over 40 disease susceptibility regions (Capon et al., 2012; Tsoi et al., 2012; Mahil et al., 2015). Based on the results of these studies, *HLA-C* (located in *PSORS1*) is widely regarded as the major genetic determinant for the disease, as it account for ~50% of its familial aggregation (Capon et

al., 2012).

The *HLA-C* gene encodes a class I major histocompatibility molecule that mediates antigen presentation to CD8+ T-cells (Mahil et al., 2015). Although the causal susceptibility variant at the *HLA-C* locus has yet to be identified, the *HLA-Cw*062* allele is a prime candidate, as it is strongly associated with psoriasis in several ethnic groups and consistently generates the highest odds ratios in GWAS (Capon et al., 2012). Of note, fine mapping studies have demonstrated the existence of multiple secondary signals within the MHC, implicating other HLA (e.g. HLA-B) and non-HLA molecules (e.g. MICA) in disease pathogenesis (Knight et al., 2012; Okada et al., 2014).

Although the susceptibility loci identified outside of the MHC typically contain several genes, it is noteworthy that the strongest biological candidates cluster to a limited number of immune pathways, most notably the IL-23/Th17 and NF-κB signalling cascades (Capon et al., 2012).

The IL-23/Th17 pathway has been implicated by the identification of psoriasis-associated variants in genes such as *IL12B, IL23A,* and *IL23R* (Mahil et al., 2015). *IL23A* and *IL12B* code for the two subunits of IL-23, which signals through the IL-23 receptor complex (encoded by *IL12RB1* and *IL23R*) and activates Th17 cells (Mahil et al., 2015).

NF-κB is a transcription factor for genes involved in apoptosis and innate-immune responses (Scudiero et al., 2011; Scudiero et al., 2014). It is activated by TLR ligands as well as cytokines such as TNF, IL-17 and IL-1 (Scudiero et al., 2011; Mahil et al., 2015). Several genes regulating NF-κB activation have been implicated in psoriasis pathogenesis. Examples include *TRAF3IP2,* which encodes an adaptor for IL-17 mediated NF-κB signalling, and *NFKBIA,* which encodes a molecule inhibiting the

formation of NF-κB /REL complexes (Hayashi et al., 2012; Harden et al., 2015).

Another important PV locus involved in the activation of NF-κB is *CARD14*. Its gene product (CARD14/CARMA2) belongs to the CARMA family of scaffold proteins, which also includes CARD11/CARMA1 and CARD10/CARMA3 (Scudiero et al., 2014). All three proteins encompass the same conserved functional motifs: a caspase activation and recruitment domain (CARD) located at the amino-terminus, a coiled coil (CC), a SRC homology 3 (SH3) motif and a guanylate kinase-like domain (MAGUK) at the carboxy-terminus of the protein (Scudiero et al., 2014). Although they show different expression patterns across human tissues, all three CARMAs are able to activate the NF-κB transcription factor through an interaction with the BCL10 adaptor protein (Scudiero et al., 2014). CARD14 is predominantly expressed in the skin, and it is the only CARMA protein that has several, alternately spliced isoforms (Jordan et al., 2012; Fuchs-Telem et al., 2012; Scudiero et al., 2011).

Common *CARD14* variants were convincingly associated with PV in GWAS (Tsoi et al., 2012). Moreover, the c.349G>A (p.Gly117Ser) and c.349+5G>A mutations were shown to underlie rare, monogenic forms of PV linked to the *PSORS2* locus (Jordan et al., 2014). Functional genomics demonstrated that the above disease alleles are gain-of-function mutations, which cause abnormal NF-κB activation (Jordan et al., 2014).

Very little is known about the genetic determinants underlying other non-pustular forms of psoriasis. Guttate psoriasis shows a very strong association with the *HLA-Cw*0602* allele, but no other susceptibility loci have been identified (Asumalhti et al., 2003). Likewise, no disease alleles have been associated with erythrodermic psoriasis, as the rarity of the condition has prevented the ascertainment of adequately

powered patient resources.

1.2.1.4 Treatment

An important criterion in determining the most appropriate treatment for a patient is disease severity. This can be measured using the Psoriasis Area and Severity Index (PASI), which ranges from 0 (not affected) to 72 (severely affected) and is calculated based on the severity of psoriatic lesions and the percentage area of affected skin (Boehncke and Schon, 2015).

For mild disease (PASI <7), topical therapies (e.g. gluco-corticosteroids) and/or vitamin D derivatives are usually prescribed, while moderate (PASI: 7-12) and severe (PASI >12) disease can often be managed with systemic treatment, either alone or in combination with photo-therapy (Boehncke and Schon, 2015).

In recent years, disease treatment has been improved by the availability of biologics that directly target disease associated pathways (Boehncke and Schon, 2015) (Figure 1.2.1.4). These drugs can be used when patients do not show a durable response to topical treatment or conventional therapies. Such therapeutics include TNF-α inhibitors (e.g. infliximab, which is a monoclonal anti-TNF-α antibody), IL-12 and IL-23 blocking agents (e.g. ustekinumab, which blocks the p40 subunit shared by IL-12 and IL-23) and IL-17 inhibitors (e.g. secukinumab, which targets IL-17A) (Mease, 2015). Although their long-term usage does not cause organ toxicity - an advantage of these agents compared to other systemic drugs such as cyclosporin and acitretin-, biologics can have many side effects, most notably a decreased ability to fight serious infections (http://www.bad.org.uk). Hence, patients are required to have regular blood tests and clinical assessments.

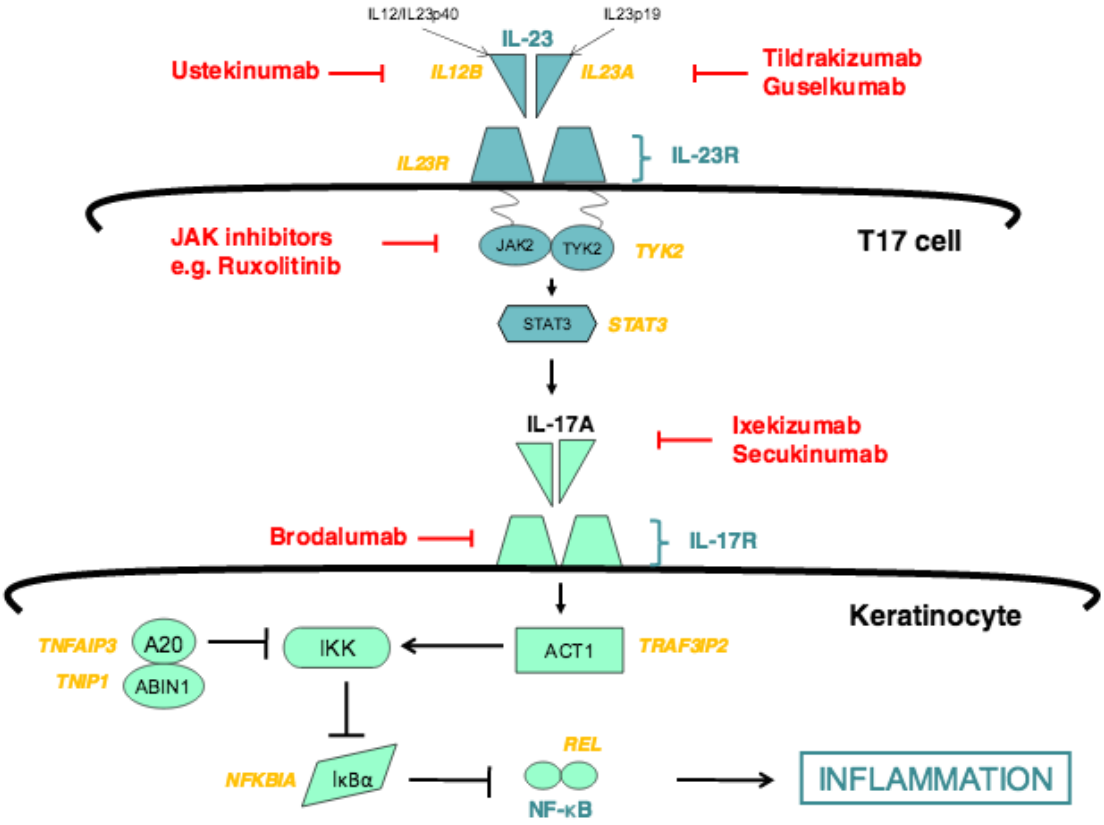

Figure 1.2.1.4. The IL-23/Th17 pathway as a therapeutic target in psoriasis

GWAS have greatly helped the understanding of psoriasis pathogenesis and have identified key inflammatory cytokines, which have been successfully targeted for disease treatment. The diagram shows a schematic representation of the IL-23/Th17 axis, with the names of selected disease associated genes in yellow. The names of biologics that target this pathway are highlighted in red. Figure retrieved from Mahil et al., 2016.

1.2.2 Pustular Psoriasis

1.2.2.1 Clinical features

The term pustular psoriasis refers to a group of inflammatory skin diseases which present with sterile pustules on erythematous background and are associated with an increased risk of psoriasis vulgaris (Burns et al., 2010).

At the histological level, pustular psoriasis presents with marked infiltration of neutrophils in the epidermis, which gives rise to characteristic Kogoj's spongiform pustules (Augey et al., 2006). Other histological findings are similar to those observed in PV and include parakeratosis, elongation of the rete ridges, as well as thinning of the supra-papillary epidermis (Augey et al., 2006).

At the clinical level, the disease can manifest as generalised or localised pustular psoriasis.

Generalised Pustular psoriasis (GPP) is the most rare and severe form of the disease. It affects 1-2 individuals per million, with a sex bias towards females (the estimated male female ratio is 0.7) (Augey et al., 2006).

GPP is a potentially lethal condition, characterized by episodes of systemic inflammation and skin pustulation (Figure 1.2.2.1) (Augey et al., 2006). During disease flares the skin becomes red and numerous small pustules appear all over the body (Naldi and Gambini, 2007). The pustules might coalesce to form lakes of pus, but eventually dry out ad peel off (Naldi and Gambini, 2007). During these attacks, the patients often show signs of systemic upset, such as fever, malaise, neutrophilia and increased levels of acute phase reactants. GPP flares are therefore considered a dermatological emergency, requiring the immediate hospitalisation of the patient.

The impact of GPP can also be complicated by co-morbidities as a significant

proportion of cases suffer from concurrent PV and/or psoriatic arthritis (Naldi and Gambini, 2007).

GPP triggers include recurrent infections, hypocalcaemia, pregnancy (*impetigo herpetiformis* is a form of GPP triggered by pregnancy), high stress, and ultrapotent tropical therapies (Griffiths and Barker, 2007; Augey et al., 2006). However, many patients are not exposed to any of these agents, which underscores the need for further studies of disease pathogenesis (Griffiths and Barker, 2007; Augey et al., 2006).

There are two main subtypes of localised pustular psoriasis: acrodermatitis continua of Hallopeau and palmoplantar pustulosis.

Acrodermatitis continua of Hallopeau (ACH) is a rare, chronic condition characterised by pustular eruptions on the tips of fingers and toes (Naldi and Gambini, 2007). These lesions may also spread to the dorsal surface of the hands and forearms (Naldi and Gambini, 2007) (Figure 1.2.2.1). Importantly, the pustulation of patients' nail-bed is often associated with onychodystophy (the malformation of the nail), osteolysis (dissolution of the bone), and arthritis (Naldi and Gambini, 2007).

Patients with palmoplantar pustulosis (PPP) experience hyperkeratosis and sterile pustulation on the palms and the soles (Naldi and Gambini, 2007). The pustules appear in crops on red skin, which is prone to develop painful cracks (fissures). The lesions later turn brown and then scaly (Naldi and Gambini, 2007) (Figure 1.2.2.1).

PPP accounts for approximately 1% of psoriasis cases and shows a very robust sex-bias, with a female to male ratio of 9:1. Of note, the vast majority of patients (~90%) are smokers (95%) (Griffits and Barker, 2007). Both PPP and ACH manifest with a chronic disease course. While this is not life threatening, both conditions have a profound effect on quality of life and often cause occupational or functional disability.

Figure 1.2.2.1. Clinical presentation of Generalised Pustular Psoriasis (GPP; left); Acrodermatitis continus of Hallopeau (ACH; middle) and palmaplantar pustulosis (PPP; right)

The photos illustrate the presence of widespread pustulation in GPP patients and localized lesions in individuals affected by ACH and PPP.

Figures retrieved from Naldi and Gambini, 2007.

1.2.2.2 Genetics and immune pathogenesis

Although the rarity of pustular psoriasis has hindered the implementation of case-control studies, it has long been apparent that the disease is not associated with *HLA-Cw*0602*, the major genetic determinant of PV (Asumalahti et al., 2003)

In more recent years, the advent of next-generation sequencing has greatly helped the study of GPP, enabling the discovery of two disease genes.

The first genetic determinant to be robustly associated with the disease was the *IL36RN* locus. Bialleleic *IL36RN* mutations were first uncovered in Tunisian consanguineous pedigrees and in unrelated British patients with GPP (Marrakchi et al., 2011, Onoufriadis et al., 2011). Further disease alleles have been subsequently identified in German, Japanese and Malaysian cases, with a total of 17 deleterious variants identified so far (Sugiura et al., 2013; Farooq et al., 2012; Setta-Kaffetzi et al., 2013; Kanazawa et al., 2013).

The most prevalent mutations in the Asian population are the c.115+6T>C and p.Arg10X variants, which are null alleles causing early protein truncation. In Europe and North-Africa, the most frequent disease alleles are the p.Ser113Leu and p.Pro27Leu amino acid changes; respectively, and both affect highly conserved amino acid residues (Marrakchi et al., 2011; Setta-Kaffetzi et al., 2013).

Of note, a small but significant number of individuals carrying a single p.Ser113Leu allele has been reported, indicating that the mutation may under certain circumstances, be pathogenic in the heterozygous state (Setta-Kaffetzi et al., *2013).*

IL36RN is mostly expressed in skin and it codes for an anti-inflammatory protein (IL-36 receptor antagonist or IL-36Ra) that antagonizes the effects of IL-36α, -β, and –γ (Gabay and Towne, 2015). While the binding of the latter cytokines to the IL-

36 receptor drives NF-κB and MAPK signalling, IL-36Ra blocks the recruitment of the IL-1Rrp2 accessory protein and therefore hinders the activation of downstream pathways (Marrakchi et al., 2011; Onoufriadis et al., 2011).

In individuals carrying *IL36RN* mutations, the IL-36Ra protein no longer functions as an antagonist, resulting in increased production of NF-κB induced pro-inflammatory cytokines (Figure 1.2.2.2) (Marrakchi et al., 2011; Onoufriadis et al., 2011). In these subjects, activated keratinocytes secrete IL-36 cytokines that can activate dermal DCs, and in the absence of a functional antagonist, induce the increased production of TNF-α and IL-17α (Gabay and Towne, 2015), leading to the recruitment of T cells, neutrophils, and DCs (Gabay and Towne, 2015). An association was also observed between the expression of IL-36 cytokines in psoriatic skin and that of IL-17, IL-23, and TNF, further supporting the notion that IL-36 cytokines govern the pathogenesis of psoriasis in patients with *IL36RN* mutations (Gabay and Towne, 2015).

The second locus to be associated with pustular psoriasis is *AP1S3*. This gene encodes a small subunit of the AP-1 adaptor complex, a cytosolic tetramer that regulates vesicular trafficking between the *trans*-Golgi network and the endosomes (Setta-Kafettzi et al., 2014). Two founder *AP1S3* mutations (p.Phe4Cys and p.Arg33Trp) were found in the heterozygous state in all subtypes of pustular psoriasis, but only in patients of European origin (Setta-Kafettzi et al., 2014). The mechanisms whereby *AP1S3* alleles cause skin inflammation are still under investigation.

Finally, a p.Asp176His *CARD14* substitution has been tentatively associated with GPP in a small Japanese study (Sugiura et al., 2014) but the pathogenic potential of this change remains to be understood.

Importantly *IL36RN* and *AP1S3* mutations have been observed in patients affected by all forms of pustular psoriasis, demonstrating a common genetic basis for common localized and acute generalized variants of the disease (Setta-Kaffetzi et al., 2013; Setta-Kaffetzi et al., 2014)

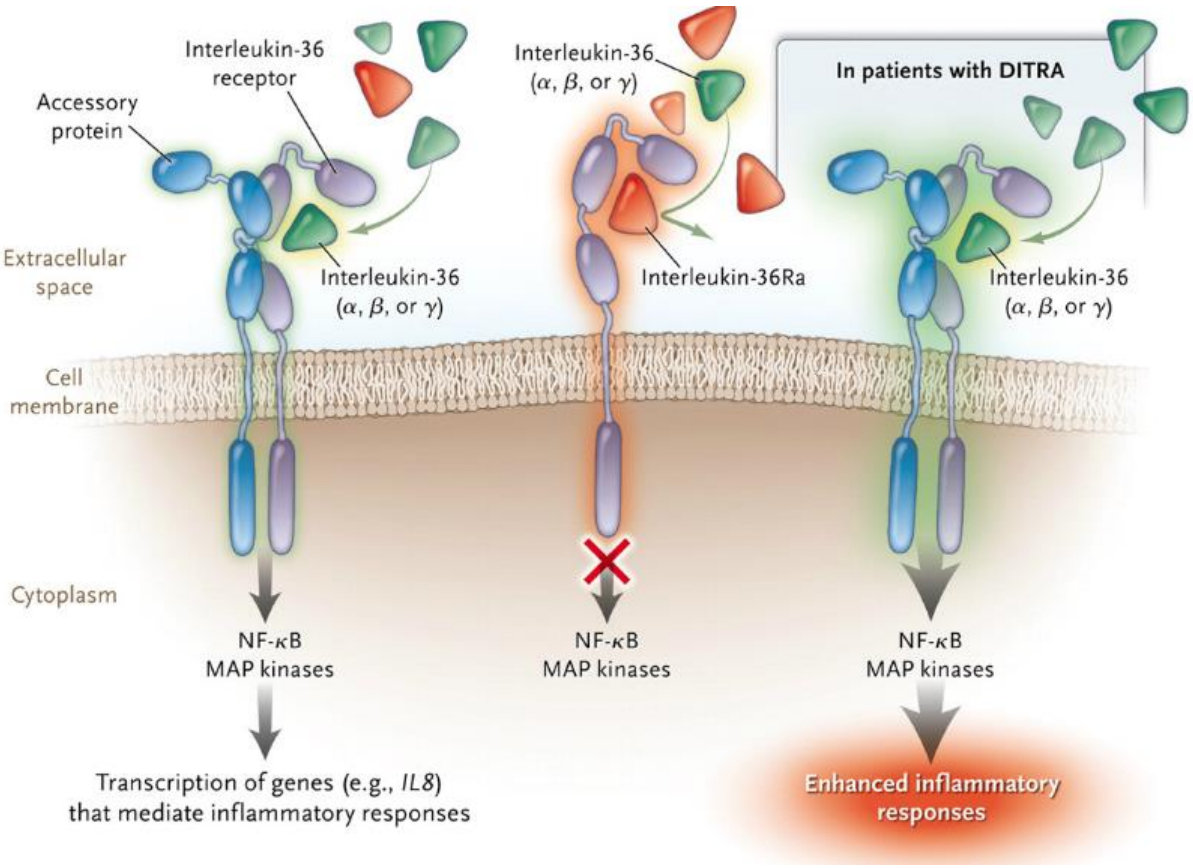

Figure 1.2.2.2. Mutations in *IL36RN* lead to increased NF-κB and MAPK signalling

As a result of *IL36RN* mutations, the IL-36Ra protein is not able to function as an antagonist and prevent the binding of IL-36α, -β, and –γ, to the IL-36 receptor. This leads to increased activation of the NF-κB and MAPK signalling and abnormal production of pro-inflammatory cytokines. DITRA: Deficiency of Interleukin Thirty-six Receptor Antagonist. Figure retrieved from Marrakchi et al., 2011.

1.2.2.3 Treatment

The biologics that have transformed the treatment of plaque psoriasis show limited efficiency in the pustular forms of the disease, indicating that the latter are likely to have a distinct aetiology. In fact, the results of genetic studies suggest that blocking IL-1 signalling downstream of the IL-36 receptor might be a more efficient therapeutic approach than targeting the IL-23/Th17 axis. Of note, pilot studies of Anakinra (a recombinant form of the IL-1 receptor antagonist) have given promising results in GPP (Rossi-Semeraro et al., 2015; Huffmeier et al., 2014). However, larger trials or case series will be required to rigorously assess the efficacy of IL-1 blockade.

In the context of a limited efficiency of biologics, the use of retinoids, either alone or in combination with PUVA appears to be more effective compared to other systemic therapies (Augey et al., 2006; Marsland et al., 2006). However, therapeutic options are extremely limited overall, highlighting the need for an improved understanding of disease pathways.

1.2.3 Pityriasis Rubra pilaris

1.2.3.1 Clinical features

Pityriasis Rubra pilaris (PRP) is a chronic inflammatory skin disorder of unknown etiology which affects 1:5,000 patients with dermatological conditions (Griffiths, 1980). The disease is characterized by keratotic follicular papules, reddish, scaly plaques, and palmoplantar keratoderma, that may progress to erytroderma with distinct islands of uninvolved skin (Griffiths, 1980) (Figure 1.2.3.1). Compared to PV, the major differences are the prominent involvement of the face and the absence of psoriasis-like nail changes (Fuchs-Telem et al., 2012).

At the histological level PRP lesions also have a distinctive appearance characterised by parakeratosiss, orthokeratosis, hypergranulosis, and follicular hyperkeratosis (Fuchs-Telem et al., 2012).

At the clinical level, PRP can be classified into five subtypes based on age of onset, clinical presentation, and prognosis: classic adult type (type I, accounting for 50% of cases); atypical adult type (type II, 5% of cases); classic juvenile (type III, 10% of cases); circumscribed juvenile (type IV, 25% of cases), and atypical juvenile (type V, 10% of cases) (Griffiths, 1980). Familial PRP is part of the type V group and accounts for a minority of all PRP cases (Fuchs-Telem et al., 2012).

Figure 1.2.3.1. Clinical presentation of Pityriasis Rubra Pilaris

The picture illustrates the presence of widespread, erythematous plaques surrounded by uninvolved skin-areas. Figure retrieved from Fuchs-Telem et al., 2012.

1.2.3.2 Genetics and immune pathogenesis

The only known genetic determinant of the disease is *CARD14*, with a small number of heterozygous gain-of function mutations detected in familial forms of PRP (Fuchs-Telem et al., 2012). Interestingly, these variants do not overlap with those identified in familial PV, suggesting that mutations are disease-specific.

Immunostaining of patient skin showed an abnormal accumulation of the p65 NF-κB subunit compared to healthy controls. Furthermore, the expression of NF-κB target genes (*CCL20*, *IL1B*, and *NOS2*) was increased in lesional skin, supporting the notion that the *CARD14* mutations associated with PRP lead to increased NF-κB signaling (Fuchs-Telem et al., 2012).

1.2.3.3 Treatment

There are no efficient treatments against the disease, with modest improvements reported for the use of retinoids, cyclosporine, and TNF-α blockers (Fuchs-Telem et al., 2012).

1.3 Gene identification by next-generation sequencing

1.3.1 Traditional approaches to gene discovery

Understanding the genetic background of a disease has great translational impact, as it enables early diagnosis, prenatal testing and appropriate counselling for high-risk individuals. The identification of disease genes can also provide mechanistic insights into the aetiology of the condition, which has the potential to inform the development of targeted therapies.

Historically, gene discovery was pursued by positional cloning or mutational analysis of candidate loci. The former approach was based on the linkage analysis of extended pedigrees and the subsequent sequencing of genes located within the critical disease interval. This hypothesis-free approach allowed the identification of genes underlying important Mendelian disorders (e.g. spinal muscular atrophy and cystic fibrosis) and monogenic forms of cancer (e.g. early onset breast cancer).

The analysis of candidate genes, on the other hand, relied on previous knowledge of disease processes or assumptions on likely pathogenic mechanisms.

The cornerstone of both approaches was Sanger sequencing, a method that defines the order of nucleotides in a DNA sequence through the incorporation of labelled, chain-terminating di-deoxynucleotides. The reaction is carried out *in-vitro* by DNA-polymerase and the sequence is determined upon electrophoretic size-separation of the DNA fragments (Venter et al., 2001) (Figure 1.3.1).

Sanger sequencing – also termed capillary sequencing- has been a commonly used technology since its discovery. Importantly, it underpinned the completion of the Human Genome Project in 2001, which derived the entire sequence of the first reference human genome (Venter et al., 2001).

Although the method has been automated, it was still too time-consuming and expensive for the systematic analysis of extended genomic regions. This hindered gene identification efforts for conditions where linkage studies had defined large linkage intervals and/or the knowledge of the underlying pathway was insufficient to priorities candidate genes for analysis.

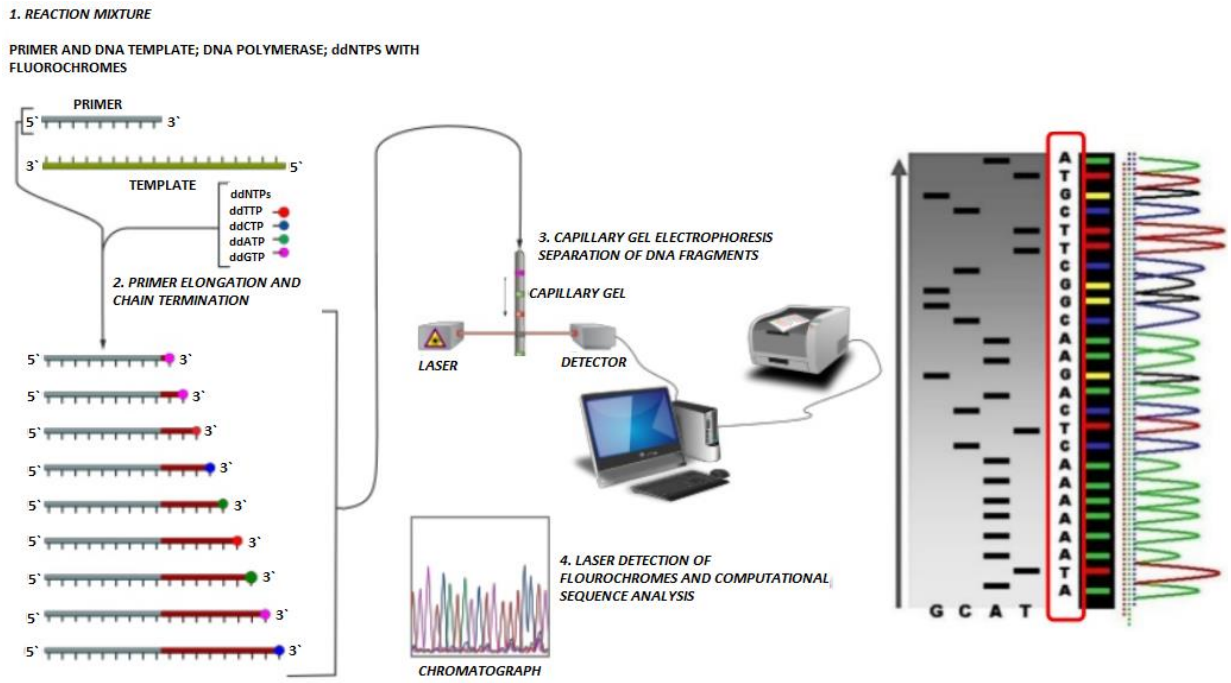

Figure 1.3.1. Sanger sequencing workflow

In a sequencing reaction, a primer is first annealed to a single-stranded DNA template, upon which the DNA polymerase incorporates both deoxy-nucleotide triphosphates (dNTPs) and labelled di-deoxynucleotides (ddNTPs). Given that ddNTPs lack a hydroxyl group, their random insertion terminates the DNA synthesis at various stages of elongation, generating a mixture of labelled DNA fragments of differing lengths. These products are then separated by capillary gel electrophoresis. Finally the fluorescent signals are captured by a detector, and an imaging system shows the identity of each base along the DNA template. Figure retrieved from http://www.slideshare.net/suryasaha/sequencing-the-next-generation.

1.3.2 Next-generation sequencing

In the last few years, the field of gene discovery has been revolutionised by the advent of next-generation sequencing methods, which allow the rapid and cost effective analysis of entire genomes. The use of these technologies has transformed Mendelian genetics, with hundreds of disease causing genes identified since the first proof of principle study was published in 2010 (Ng et al., 2010) (Figure 1.3.2).

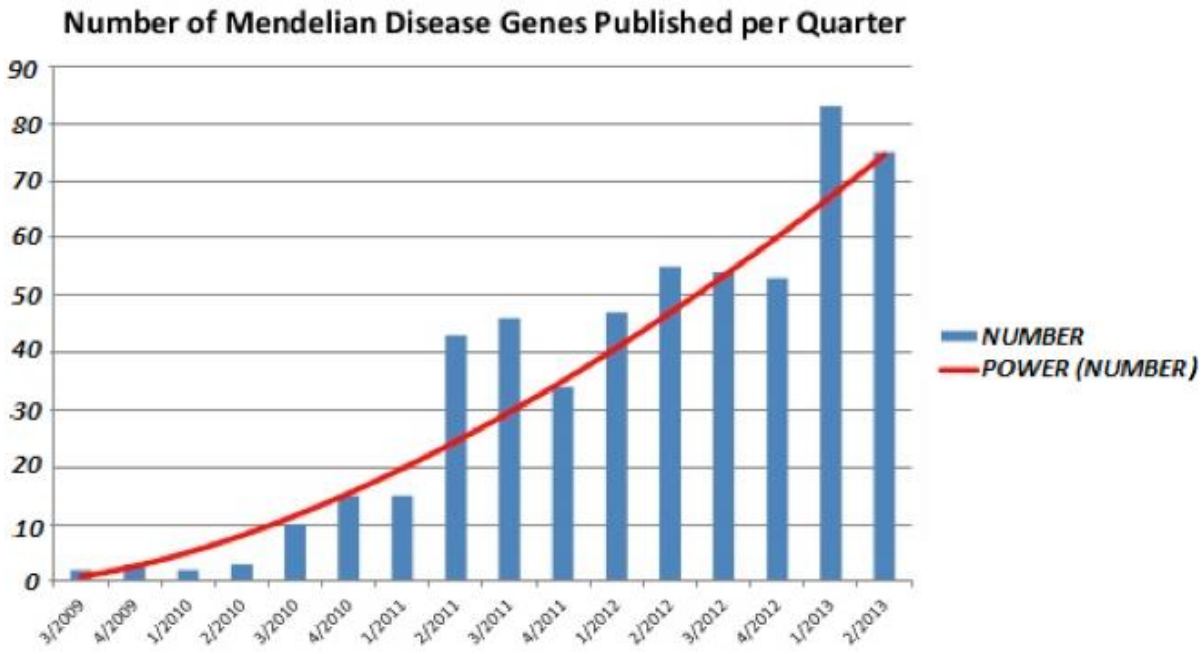

Figure 1.3.2. The use of whole-exome sequencing accelerated our understanding of Mendelian disease

Figure retrieved from http://www.slideshare.net/informaoz/michael-buckley-seals (Appendix III).

1.3.2.1 Sequencing platforms

` Next-generation sequencing is currently implemented in one of three major platforms: Roche 454 (which, however, is going to be discontinued in mid-2016), ABI Solid, and the Illumina HiSeq System (Liu et al., 2012).

The key steps in the underlying protocols are fundamentally similar. These include the preparation of libraries by DNA shearing and adaptor ligation, the massively parallel sequencing of short DNA fragments, the alignment of reads to a reference genome, and the variant calling (Liu et al., 2012).

The Roche 454 platform employs the pyrosequencing technology where a pyrophosphate is released during nucleotide incorporation and the number of incorporated nucleotides is derived from the signal intensity (Liu et al., 2012). The main advantages of this system are the long read length (700 bp) and the high sequencing speed (a run can be completed in less than a day) (Table 1.3.2.1) (Liu et al., 2012). However, the cost-per base is high compared to other technologies and the error rate at homo-polymer detection is high (Liu et al., 2012).

The ABI SOLiD System determines the DNA sequences by ligating fluorescently labeled probes (two bases long) to the template. What makes this platform to stand out from the rest is its accuracy. However, sequence runs are more time-consuming compared to the other platforms (they can take up to 14 days) and the reads that are generated are shorter (85bp), which complicates the alignment process (Liu et al., 2012).

Illumina introduced the cheapest technology (Table 1.3.2.1). This technique applies a sequencing-by-synthesis approach and reads one incorporated nucleotide per sequencing cycle (Liu et al., 2012). The read length is relatively short, but is increasing

with the latest models, supporting the generation of 300 bp reads in a paired-end arrangement. The error rate remains significant, though (2%).

A number of "third-generation sequencing" approaches have also been emerging in recent years. An example is the Single Molecule sequencing in Real Time (SMRT) system devised by Pacific Biosciences, which can generate very long reads (10-15kb) and has allowed scientists to sequence the E. Coli genome with 99.9999% accuracy (Chin et al., 2013). Another example is the Nanopore sequencing method that is being developed by Oxford Nanopore Technologies (Schmidt, 2016). This is based on single-use DNA sequencing devices that can generate 5-10kb long reads. Although this technology shows great promise, its accuracy is currently low (Schmidt, 2016).

(a) Advantage and mechanism of sequencers. (b) Components and cost of sequencers. (c) Application of sequencers.

(a)

Sequencer	454 GS FLX	HiSeq 2000	SOLiDv4	Sanger 3730xl
Sequencing mechanism	Pyrosequencing	Sequencing by synthesis	Ligation and two-base coding	Dideoxy chain termination
Read length	700 bp	50SE, 50PE, 101PE	50 + 35 bp or 50 + 50 bp	400 ~ 900 bp
Accuracy	99.9%*	98%, (100PE)	99.94% *raw data	99.999%
Reads	1 M	3 G	1200~1400 M	—
Output data/run	0.7 Gb	600 Gb	120 Gb	1.9~84 Kb
Time/run	24 Hours	3~10 Days	7 Days for SE 14 Days for PE	20 Mins~3 Hours
Advantage	Read length, fast	High throughput	Accuracy	High quality, long read length
Disadvantage	Error rate with polybase more than 6, high cost, low throughput	Short read assembly	Short read assembly	High cost low throughput

(b)

Sequencers	454 GS FLX	HiSeq 2000	SOLiDv4	3730xl
Instrument price	Instrument $500,000, $7000 per run	Instrument $690,000, $6000/(30x) human genome	Instrument $495,000, $15,000/100 Gb	Instrument $95,000, about $4 per 800 bp reaction
CPU	2* Intel Xeon X5675	2* Intel Xeon X5560	8* processor 2.0 GHz	Pentium IV 3.0 GHz
Memory	48 GB	48 GB	16 GB	1 GB
Hard disk	1.1 TB	3 TB	10 TB	280 GB
Automation in library preparation	Yes	Yes	Yes	No
Other required device	REM e system	cBot system	EZ beads system	No
Cost/million bases	$10	$0.07	$0.13	$2400

(c)

Sequencers	454 GS FLX	HiSeq 2000	SOLiDv4	3730xl
Resequencing		Yes	Yes	
De novo	Yes	Yes		Yes
Cancer	Yes	Yes	Yes	
Array	Yes	Yes	Yes	Yes
High GC sample	Yes	Yes	Yes	
Bacterial	Yes	Yes	Yes	
Large genome	Yes	Yes		
Mutation detection	Yes	Yes	Yes	Yes

Table 1.3.2.1. Comparing traditional and next-generation sequencing platforms that differ in read length, accuracy, times needed to complete a sequence run, and required informatics for data analysis. Figure retrieved from Liu et al., 2012.

1.3.2.2 Next-generation sequencing applications

The use of NGS technologies in gene discovery includes different applications.

Targeted sequencing is performed when the analysis can be focused on a discrete genomic region or a relatively small number of candidate genes (Rehm, 2013). This is the case when linkage data are available or previous knowledge of disease mechanisms can be leveraged to define a panel of candidate genes. In either case, probes that hybridise the target genomic regions are designed, so that the relevant genomic segments can be captured and then sequenced (Rehm, 2013).

Whole-exome sequencing (WES) is currently the most popular NGS application in gene discovery. It allows researchers to focus on the coding portion of the genome (i.e. the exome), based on the assumption that it is more likely to harbour disease-causing mutations. As coding regions only represents 1% of the human genome, whole-exome sequencing can be more cost- and time-effective than whole-genome sequencing (WGS) (Singleton, 2011).

The underlying protocol of WES is similar to those described in the earlier section. The difference is that upon library preparation, the coding regions are captured by hybridization with complementary probes (Figure 1.3.2.2.1) (Singleton, 2011). The latter are commercially available as reagents are provided by Agilent (SureSelect Human All Exon kits), Roche/Nimblegen (SeqCap EZ Exome Library), and Illumina (TruSeq Exome Enrichment system).

The above products differ in various aspects of probe design. While Nimblegen relies on overlapping baits and provides the highest coverage among the three suppliers, Agilent uses longer oligonucleotides that are adjacent to each other. Finally, Illumina

sequencers generate paired-reads that are extended from the baits (Figure 1.3.2.2.2) (Singleton, 2011).

Another dissimilarity between these platforms are their target regions, given that the capture probes are designed on the basis of information provided in different repositories, such as RefSeq, Ensembl, and UCSC Knonw Genes. Thus, Illumina probes cover the most untranslated regions, Nimblegen provides better coverage of micro-RNAs and Agilent was the most specific platform for the analysis of Ensembl genes (Figure 1.3.2.2.2) (Singleton, 2011).

The platforms also differ in their target specificity, with Nimblegen probes performing best on this parameter (98.6% of target bases covered at least once; 96.8% covered at >10X) (Clark et al., 2011).

Despite their success, it is important to bear in mind that WES studies suffer from some significant limitations. The most important is uneven coverage of target regions. In a typical experiment, 5-10% of exonic sequences are not captured or sequenced at a sufficient depth (Rehm, 2013). This is due to numerous factors, most importantly, probes that fail to tile their targets either due to repetitive sequences, GC-richness, or low mapping quality (Rehm, 2013).

Whole-genome sequencing does not suffer from the above limitations but is more expensive. As the protocol generates a very substantial volume of data, the costs associated with data storage and data analysis are also much higher.

.

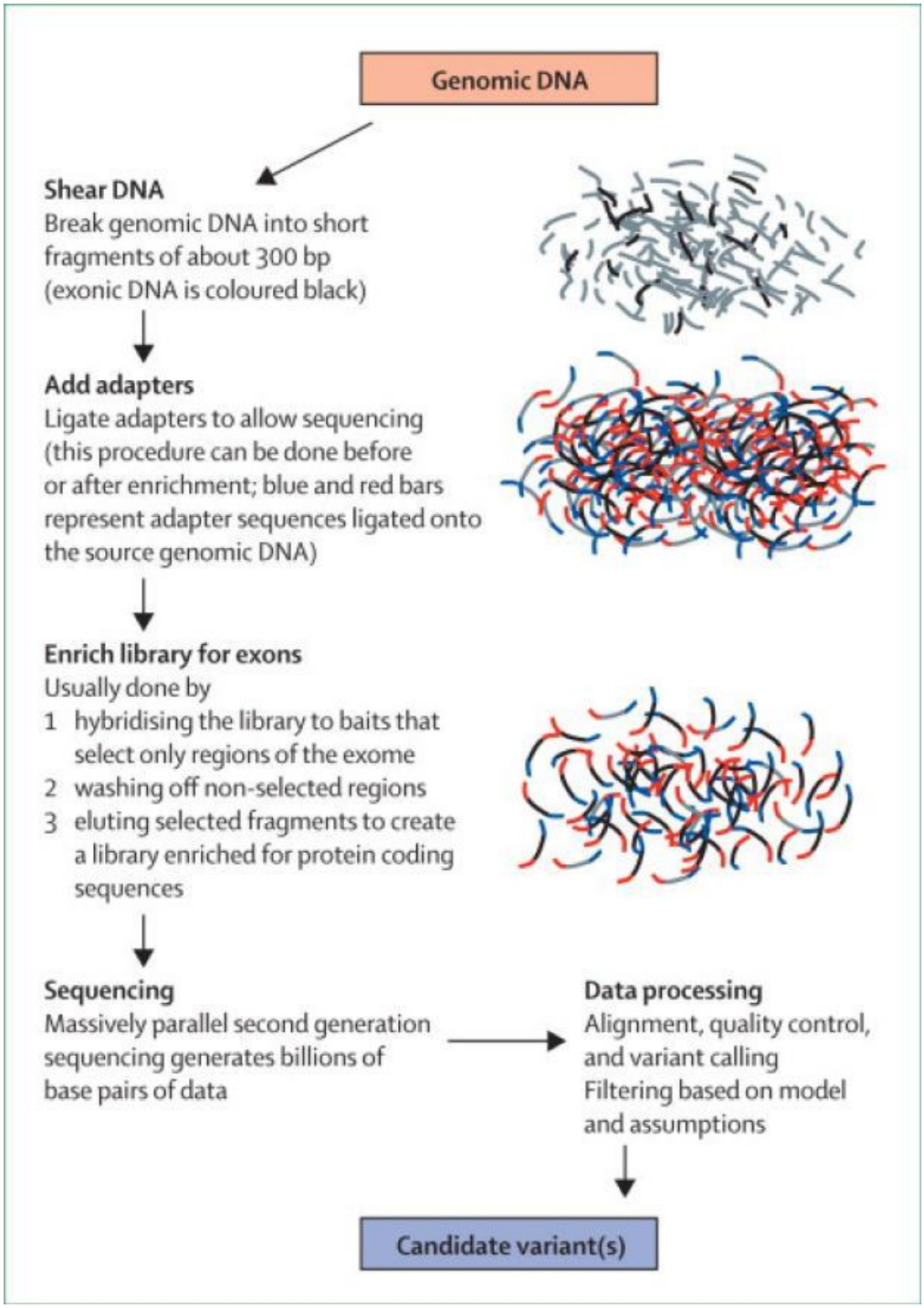

Figure 1.3.2.2.1. Overview of the experimental procedure for whole-exome sequencing

Figure retrieved from Singleton et al., 2011.

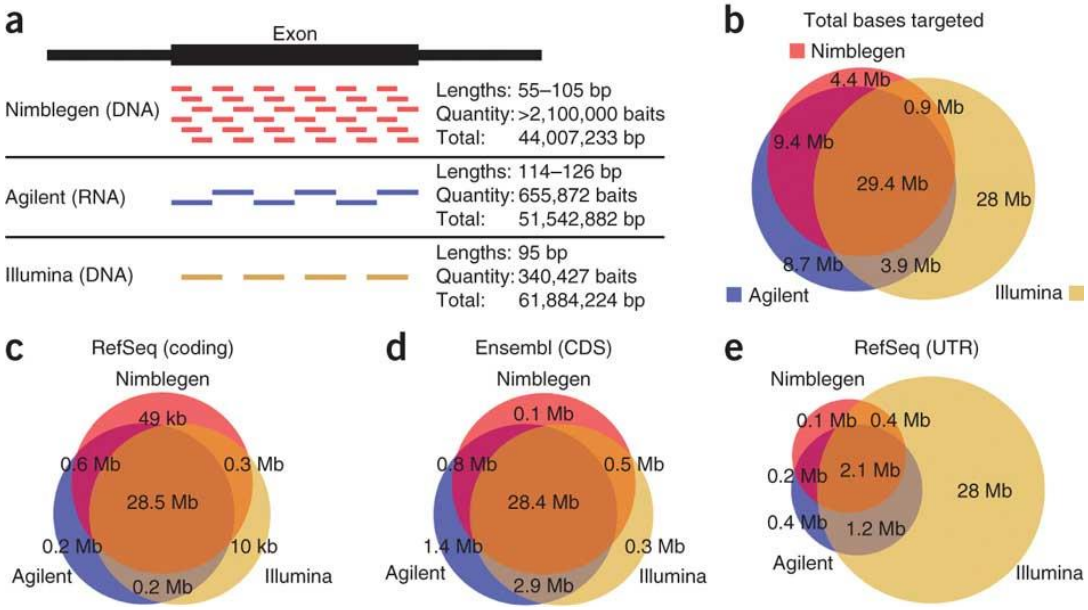

Figure 1.3.2.2.2 Performance comparison of exome sequencing technologies

Commercially available platforms for exome enrichment differ in the length and density of oligonucleotide baits (a) and composition of their target regions (b). While the coverage of coding exons represented in RefSeq (c) and Ensembl (d) is comparable across platforms, Illumina probes performs better in targeting UTR regions (e).

Figure retrieved from Clark et al., 2011.

1.3.2.3 Data analysis

The most challenging part of the whole-genome/whole-exome sequencing workflow is the computational analysis of the data (Figure 1.3.2.3).

Next-generation sequencing instruments generate FASTA/FASTAQ files that include the sequence itself and its quality scores (Pabinger et al., 2013). After the reads have been aligned to a reference genome, this information is converted to a Sequence Alignment Map (SAM) file, in a tab-delimited text format (Olson et al., 2015). There are different programs available for this conversion step; one of them is the Burrows-Wheler Aligner (BWA).

For easier storage, SAM files are converted to a BAM binary format (Olson et al., 2015). Read qualities are recalculated as Phred scores, which provide base-calling error probabilities on a logarithmic scale (Olson et al., 2015). Phred scores typically go from 10 (1:10 probability of incorrect base call, 90% accuracy) to 40 (1 in 10,000 probability of incorrect base call, 99.999% accuracy). In a typical analysis pipeline, a minimum Phred score is specified (e.g. Phred $\geq$ 20) and bases that are below this threshold are excluded from further consideration.

The next step is SNP annotation from BAM files. This can be achieved using software packages such as the Genome Analysis Tool Kit (GATK), which identify sites that show differences compared to the reference genome and generate output files in the variant call format (vcf) (Pabinger et al., 2013; Olson et al., 2015). The latter lists the exact genomic position of the base change, the reference and the alternative base at that position as well as the quality score of the variant.

Further downstream analyses can be completed using this format as input. For instance, the sequence changes can be annotated with the ANNOVAR software, to

determine their frequency in the relevant population. Information on the gene and amino acid affected by the variant can also be retrieved. This data is extremely valuable for the filtering of variant profiles, as explained in the next section.

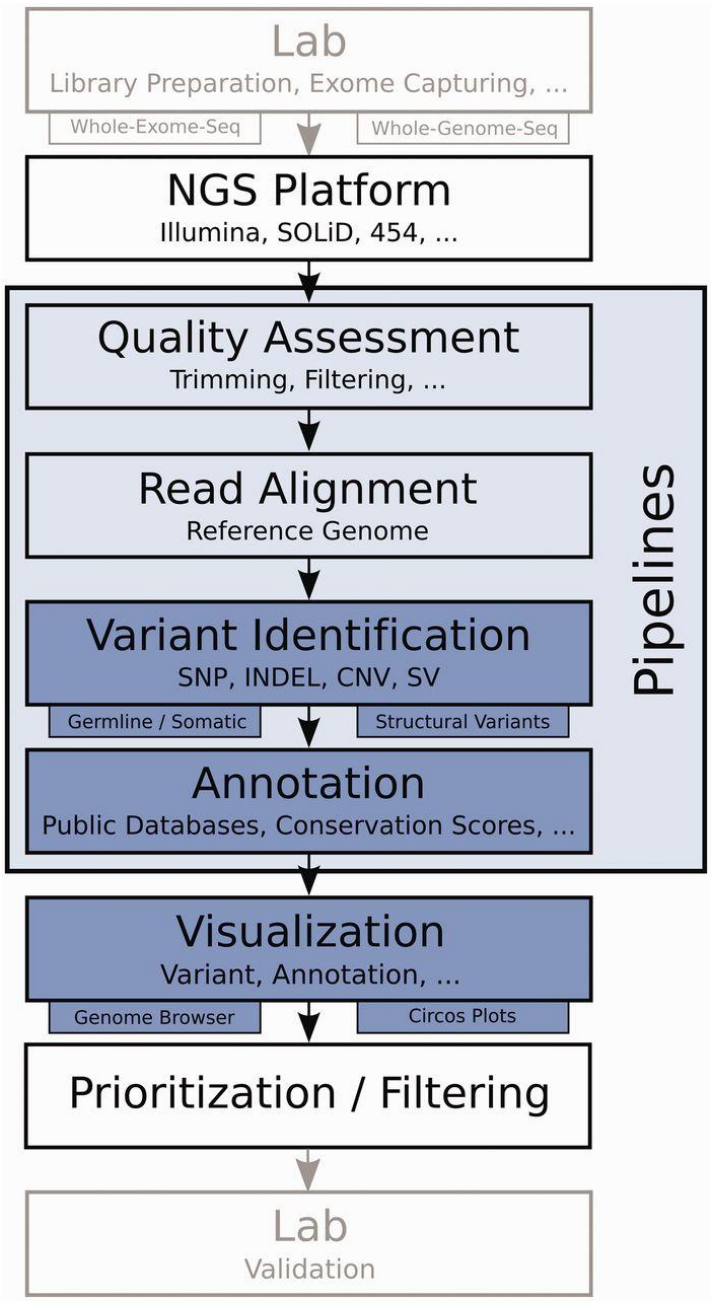

Figure 1.3.2.3. The general workflow for next-generation sequencing

Once the library preparation is completed, the samples are sequenced on the chosen platform. The quality of the reads is assessed, and those passing this QC are aligned against a reference genome. Finally, variants are annotated and filtered to identify the most likely disease-causing changes.

Figure retrieved from Pabinger et al., 2013.

1.3.2.4 Data filtering

The sequence analysis of typical Caucasian exome identifies more than 20,000 nucleotide changes (Ng et al., 2009*).* Thus, variant profiles need to be carefully filtered to find disease causing mutations among the numerous variants that have been detected.

First, all synonymous variants are removed. Next, one needs to define the most likely mode of disease inheritance, in order to establish whether the mutation is likely to occur in the heterozygous or homozygous/compound heterozygous state.

The expected penetrance and prevalence of the disease allele also need to be estimated, so that a Minor Allele Frequency (MAF) threshold can be defined and changes that exceed it can be filtered out, using publicly available datasets (e.g. the 1000 Genome Project, 1000 Genomes Project Consortium, 2012) and in-house reference panels. Given that the frequency of rare alleles can vary widely among populations and that some variants may only be found in certain ethnic groups, it is important that the origin of the patient(s) is taken into consideration and appropriate control sequences are used during the filtering process. Fortunately, exome data is now available for several non-European populations, thanks to the efforts of the 1000 Genomes Consortium and the NHLBI Grand Opportunity (GO) Exome sequencing project, among others (1000 Genomes Project Consortium, 2012; Johnston and Biesecker, 2013).

Further filtering steps can be introduced at this stage, depending on the design of the study. If multiple family members are being examined, the variants that are not shared by all affected individuals are filtered out. Likewise, in the analysis of multiple isolated cases, the genes that are only mutated in a small number of patients can be excluded from further consideration.

Finally, variants can be prioritized for follow-up, based on *in-silico* pathogenicity predictions. These can be implemented by a variety of algorithms that take into account the biochemical properties and evolutionary conservation of the amino acid residues that are affected by sequence variants. Given that none of these methods is completely accurate, it is advisable to use multiple programs and look for consensus predictions rather than rely on the output of a single tool (Miosge et al., 2015).

Of note, the studies that originally identified *IL36RN* and *AP1S3* as GPP genes were executed in our lab, showing that rigorous filtering of exome sequencing data has the power to detect disease-causing alleles for pustular psoriasis (Onoufriadis et al., 2011).

1.4 Aims of the study

While genetic studies have identified more than 40 susceptibility loci associated with plaque psoriasis, our understanding of pustular psoriasis (PP) genetics is still very limited. Of note, the identification of the *IL36RN* and *AP1S3* genes in PP has suggested that the disease is driven by innate rather than adaptive immune mechanisms, indicating a distinct etiology.

Hence the aim of the current study was to further investigate the above issues by comparing and contrasting the genetic basis of plaque and pustular psoriasis. This was achieved by investigating the genetic overlap between PV and GPP, as well as by identifying novel genetic determinants for pustular psoriasis:

The first two parts of the study focused on the candidate genes *IL36RN* and *CARD14* and on their in depth examination:

To address the possibility that *IL36RN* loss-of-function alleles may contribute to PV susceptibility, the locus was systematically screened in 363 unrelated patients with familial forms of the disease and genetic data extracted from large-scale association studies was re-analysed.

To validate the involvement of *CARD14* in monogenic forms of PV and explore the gene contribution to pustular psoriasis, the locus was screened in large datasets of patients with familial psoriasis vulgaris (n=159) and pustular psoriasis (n=205).

The last part of the study sought to further characterise the molecular pathogenesis of pustular psoriasis:

Since the majority (almost 70%) of PP patients do not carry mutations in *IL36RN* or *AP1S3*, whole-exome sequencing was undertaken in twelve carefully selected

individuals with generalised pustular psoriasis and five unrelated cases of Acrodermatitis Continua of Hallopeau.

2 MATERIALS AND METHODS

2.1 Materials

2.1.1 General reagents and buffers

Reagent	Supplier
2-Mercaptoethanol	Sigma-Aldrich
Acetic Acid	BDH
Adenosine triphosphate (ATP)	Fermentas
Amersham ECL Western Blotting Detection Reagent	GE Healthcare
Bovine Serum Albumin (BSA)	Cell Signalling
Bromophenol Blue	Sigma-Aldrich
Complete Protease Inhibitor Cocktail Tablet	Roche
Deoxynucleotide Triphosphates (dNTPs)	Thermo Scientific
Dimethyl Sulphoxide (DMSO)	Sigma-Aldrich
Dried Skimmed Milk	Marvel
Dithiothreitol (DTT)	Invitrogen
Ethanol	BDH
EthylenediamineTetraacetic Acid (EDTA)	BDH
Glycerol	BDH
Glycine	Sigma-Aldrich
Isopropanol	BDH
Magnesium Chloride ($MgCl_2$)	BDH
Methanol	BDH
Nonidet-P40	Sigma-Aldrich
Normal Goat Serum	Cell Signalling

Paraformaldehyde, 4%	Alfa Aesar
Potassium Chloride (KCl)	Sigma-Aldrich
Ponceau S	Sigma-Aldrich
RNaseZap RNase Decontamination Solution	Life Technologies
Sodium Acetate (NaOAc)	Sigma-Aldrich
Sodium Chloride (NaCl)	VWR
Sodium Dodecyl Sulphate (SDS)	Sigma-Aldrich
TAMRA Sizing Standard	Applied Biosystems
Tris-Base	Sigma-Aldrich
Tris-HCl	Sigma-Aldrich
Tween-20	Sigma-Aldrich
Urea	Life Technologies

2.1.2 Enzymes, buffers and supplements

Reagent	**Supplier**
10X PCR Buffer	Thermo Scientific
Agencourt AMPure XP beads	Beckman Coulter
Big Dye 5X Sequencing Buffer	Applied Biosystems
Bovine Serum Albumin (BSA)	New England Biolabs
DreamTaq Polymerase	Thermo Scientific
Magnesium Sulfate ($MgSO_4$)	Novagen
Taq Polymerase	Thermo Scientific
TaqMan Universal Master Mix II	Applied Biosystems

2.1.3 Gel Electrophoresis Reagents

Reagent	Supplier
5X DNA Loading Buffer	Bioline
10X Tris-Borate-EDTA (TBE)	Geneflow
Agarose	VWR
Ammonium Persulphate (APS)	Sigma-Aldrich
Ethidium Bromide	Sigma-Aldrich
GeneScan 500 TAMRA Size Standard	Life Technologies
HiDi Formamide	Applied Biosystems
HyperLadder I Molecular Weight Marker	Bioline
HyperLadder II Molecular Weight Marker	Bioline
Precision Plus Dual Colour Protein Marker	Biorad
Tetramethylethylenediamine (TEMED)	Sigma-Aldrich
Ultra PureProtoGel 30% Acrylamide Mix	National Diagnostics

2.1.4 Bacterial culture reagents

Reagent	Supplier
5-Alpha Competent E.coli	New England Biolabs
Ampicillin	Sigma-Aldrich
Bacto-Agar	BD
Bacto-Tryptone	BD
Bacto-Yeast Extract	BD
SOC Outgrowth Medium	New England Biolabs
XL10-Gold ultracompetent cells	Agilent Technologies

2.1.5 Plasmid

Reagent	Supplier
pcDNA3-CARMA2-sh.1	Prof. Pasquale Vito (Università del Sannio, Italy)

2.1.6 Tissue culture reagents

Reagent	Supplier
Dulbecco's Modified Eagle's Medium (DMEM)	Life Technologies
Foetal Calf Serum (FCS)	LabTech
Lipofectamine2000	Life Technologies
Penicillin-Streptomycin (P/S)	Life Technologies
Phospate Buffer Saline (PBS)	Life Technologies
ProLong Diamond Antifade Reagent	Life Technologies
Tryple	Life Technologies

2.1.7 Antibodies

Reagent	Supplier	Dilution
Alexa Fluor® 488 Goat Anti-Rabbit IgG	Invitrogen	1 : 800
Donkey monoclonal anti-rabbit IgG	GE Healthcare	1 : 10000
DYKDDDDK Tag Antibody	Cell-Signalling	1 : 600
Goat polyclonal anti-mouse IgG	Dako	1 : 10000
Monoclonal ANTI-FLAG M2, Clone M2	Sigma-Aldrich	1 : 3000
Rabbit polyclonal anti-β–actin	Cell-Signalling	1 : 1000

2.1.8 Molecular biology kits

Reagent	Supplier
Agilent Sure SelectXT Kit	Agilent Technologies
Agilent Sure Select Human All Exome Kit v.4	Agilent Technologies
Big Dye Terminator v3.1 Cycle Sequencing Kit	Life Technologies
Herculase II Fusion DNA Polymerase Kit	Agilent Technologies
High-Capacity cDNA Reverse Transcription Kit	Life Technologies
HiSpeed Plasmid Midi	Qiagen
IllustraExoStar 1-Step	GE Healthcare
KAPA SYBR FAST qPCR kit	KAPA Biosystems
MycoSensor PCR Assay Kit	Agilent Technologies
Oragene DNA kit	DNA Genotek
QIAprepMiniprep Kit	Qiagen
QIAshredder Columns	Qiagen

QuikChange Lightning Kit	Agilent Technologies
Rneasy Plus Mini Kit	Qiagen
SureSelect Library Prep Kit	Agilent Technologies

2.1.9 Stock solutions

Solution	**Composition**
Denaturing Cell Lysis / HU Buffer	5%SDS 200Mm Tris-HCL (pH6.8) 1mM EDTA 1.5% β -Mercaptoethanol 8M Urea
Immunofluorescence Antibody Dilution Buffer	1% BSA 0.3% TritinX-100 1X PBS
Immunofluorescence Blocking Buffer	5% Goat Serum 0.3% TritinX-100 1X PBS
Laemmli Buffer (6X)	0.375 M Tris-HCl (pH 6.8) 9% (v/v) SDS 50%(v/v) Glycerol 5% (w/v) β-Mercaptoethanol 0.03% Bromophenol Blue

LB Agar	1% (w/v) NaCl 1% (w/v) Bacto-Tryptone 0.5% (w/v) Bacto-Yeast 1.5% (w/v) Bacto-Agar
Luria Broth (LB)	1% (w/v) NaCl 1% (w/v) Bacto-Tryptone 0.5% (w/v) Bacto-Yeast
Non-denaturing buffer	50mM Tris-HCl (pH 7.4) 50mM NaCl 10% (v/v) Glycerol 5mM EDTA 0.03% Bromophenol Blue 1% (v/v) NP-40
Poly-Acrylamide Gel Electrophoresis Running Buffer (10X)	0.25 M Tris-base 1.92 M Glycine 1% (v/v) SDS
Sanger Sequencing Precipitation Solution	95% (v/v) Ethanol 0.12 M NaOAc (pH 4.6)
Tris-buffered Saline (TBS)(pH 7.6, 10X)	1.5 M NaCl 0.2 M Tris-base
Tris-EDTA (pH.8.0, 1X)	0.1 mM EDTA 10 mMTris-HCl
Western Blot Transfer Buffer (10X)	0.25 M Tris-base 1.92 M Glycine 20% (v/v) Methanol

2.2 Study Resource

This study was performed in accordance with the principles of the Helsinki Declaration. Ethical approval was granted by St Thomas Hospitals' ethics research committee (ref 06/Q0702/7; 11th May 2006) and all patients gave their written informed consent for the use of their DNA.

2.2.1 Patients with familial psoriasis vulgaris and eryhtrodermic psoriasis

Patients were recruited through St John`s Institute of Dermatology (London, UK) and Glasgow Western Infirmary (Glasgow, UK), based on the standard diagnostic criteria reported by Griffiths and Barker (Griffiths and Barker, 2007). Individuals who had at least one first degree relative affected by plaque psoriasis were considered cases of familial PV. The cohort recruited on this basis consisted of 349 unrelated probands (175 females, 174 males) (Table 2.2.1), while the erythrodermic psoriasis dataset included 23 unrelated cases (5 females and 18 males). All subjects were of British (white) European descent.

2.2.2 Pityriasis Rubra Pilaris patients

Twenty-nine unrelated individuals (13 females and 16 males) with sporadic pityriasis rubra pilaris were ascertained by Professor John McGrath from the records of St John's Institute of Dermatology (London, UK) and classified based on the criteria listed by Griffiths (Griffiths, 1975) (Table 2.2.2.).

Table 2.2.1. Disease recurrence in the familial PV resource

Number of affected individuals in the pedigree					
>5	**5**	**4**	**3**	**2**	**Total**
15	11	33	121	169	**349**

Number of affected family members found in the pedigree of each PV proband.

Table 2.2.2. Pityriasis Rubra Pilaris resource

PRP Type	**Ethnicity**
Type 1, classic adult type (n=26)	North-European (n=21) Afro-Caribbean (n=2) Unknown (n=3)
Type 3, classic juvenile type (n=2)	North-European
Type 5, atypical juvenile type (n=1)	North-European

2.2.3 Sporadic pustular psoriasis cases

This cohort consisted of 194 unrelated cases (8 Acrodermatitis continua of Hallopeau, 94 Generalised Pustular Psoriasis, and 92 Palmoplantar pustulosis patients; Table 2.2.3), who did not carry mutations within the *IL36RN* or *AP1S3* genes. Participants were recruited from St. John's Institute of Dermatology (London, UK) by Professor Catherine Smith and Jonathan Barker, Glasgow Western Infirmary (Glasgow, UK) by Professor David Burden, University of Manchester (Manchester, UK) by Professor Chrisopher Griffits, Hospital Sultanah Aminah (Johor Bahru, Malaysia) by Professor SE Choon, Singapore National Skin Center (Singapore) by Professor Siew-Eng Tan, Our Lady's Children's Hospital and St Vincent University Hospital (Dublin, Ireland) by Professor Allan Irvine, Helsinki University Central Hospital (Helsinki, Finland) by Dr Annamari Ranki, Hopital Necker-Enfants Malades (Paris, France) by Professor Asma Smahi, Geneva University Hospital and Zurich University Hospital (Switzerland) by Dr Alexander Navarini, Radboud University Nijmegen Medical Centre (Nijmegen, The Netherlands) by Professor Marieke Seyger. Clinical data were collated in the Case Report Form (CRF) attached in Appendix I and patients were classified according to the standard diagnostic criteria reported by Griffiths and Barker, (Griffiths and Barker, 2010). The screening of *IL36RN* and *AP1S3* genes was undertaken prior to the onset of the study (Onoufriadis et al., 2011; Setta-Kaffetzi et al., 2014).

Table 2.2.3. Sporadic pustular psoriasis cases

Disease	**N. of Cases**	**Gender**	**Concomitant PV**	**Mean Age of onset**	**Ethnicity**
Acrodermatitis Continua of Hallopeau	8	3M, 5F	4/8 (50%)	53+/-19	North-European
Generalised Pustular Psoriasis	94	32M, 62F	65/94 (69.15%)	31+/-16	Chinese (n=21**)** Indian (n=17) Malay (n=48) North-European (n=7) Romani (n=1)
Palmar Plantar Pustulosis	92	31M, 61F	14/92 (15.21%)	49+/-26	North-European

M: male; F: female; PV: psoriasis vulgaris

2.2.4 Familial GPP cases

Six affected relative pairs were recruited from Sultanah Aminah Hospital in Johor Bahru (Malaysia) (Table 2.2.4). All individuals were of Asian origin.

Table 2.2.4. Familial GPP cases

Sample ID	Ethnicity	Gender	Age of Onset	PV	Relatedness
16GPP1/ T014368	Chinese	Female	25	Yes	Aunt and niece
16GPP2 T014369	Chinese	Female	3	No	
38GPP1/ T014395	Malay	Female	25	Yes	Father and daughter
38GPP2/ T014394	Malay	Male	27	Yes	
23GPP1/ T014376	Malay	Female	31	Yes	Great aunt and niece
23GPP2/ T020702	Malay	Female	12	Yes	
8GPP1/ T012409	Chinese	Female	30	Yes	Sisters
8GPP2/ T012410	Chinese	Female	21	No	
41GPP1/ T14398	Malay	Female	25	Yes	Sisters
41GPP2/ T014399	Malay	Female	35	No	

PV: psoriasis vulgaris

2.2.5 Controls

Several control panels of European and Asian descent were analysed at various stages of the study. The following populations were represented: North-American (n=5,548), British (n=4,098), European (n=54,658), Chinese (n=416), Japanese (n=424), Malay (n=96), and Indian (n=340). The individual datasets are described in Table 2.2.5.

2.2.6 DNA extraction and sample storage

DNA was isolated by technical employees at St John's Institute of Dermatology, either from 2 ml saliva or 10 ml blood, using the Oragene DNA kit or the "salting out" method (Miller Dykes et al., 1988), respectively. DNA concentrations were quantified with a NanoDrop ND-1000 Spectrophotometer and samples were stored as duplicate aliquots at -20°C. Working dilutions (25 ng/µl in 1X TE) were aliquoted in skirted 96-well plates and stored at -20°C.

Table 2.2.5. Control datasets

Origin	**Dataset**	**Reference**	**Application**
American (White European)	Controls genotyped by the International Psoriasis Genetics Consortium (n=5,548)		*IL36RN* association analysis
British (White European)	1000 Genomes GBR sample (n=91) Exomes sequenced in-house (n=2,222) Exomes sequenced by collaborator (n=1,785)	Abecasis et al., 2012. Setta-Kaffetzi et al., 2014.	Filtering of variant profiles *ARFGAP2* association analysis
Chinese	1000 Genomes project CHB (n =206) and CHS (n =210) samples	Abecasis et al., 2012.	Filtering of variant profiles *CARD14* association analysis *CYP1A1* association analysis
European	Exome Aggregation Consortium European (Non-Finnish) sample (n=33,000) Controls genotyped by the International Psoriasis Genetics Consortium (n=21,658)		*ARFGAP2* association analysis *IL36RN* association analysis

Japanese	1000 Genomes project JPT sample (n=104) Population controls analysed in the literature (n=100) Population controls genotyped in-house (n=220)[1]	Abecasis et al., 2012. Sugiura et al., 2014.	*CARD14* association analysis
Indian	1000 Genomes project GIH (n=103), ITU (n=102), STU (n=102), and PJL (n=96) samples Singapore sequencing Indian project, SSIP (n=38)	Abecasis et al., 2012. Wong et al., 2014.	Filtering of variant profiles (SSIP only) *CYP1A1* association analysis
Malay	Singapore sequencing Malay project (n=96)	Wong et al., 2013.	Filtering of variant profiles *CYP1A1* association analysis

[1] Recruited at National Cerebral and Cardiovascular Center, Osaka. Abbreviations are as follows: GBR, British in England and Scotland; CHB, Han Chinese in Bejing China; CHS, Southern-Han Chinese, JPT, Japanese in Tokyo Japan; GIH, Gujarati Indian from Houston Texas; ITU, Indian Telegu from the UK; STU, Sri Lankan Tamil from the UK; PJL, Punjabi from Lahore Pakistan.

2.3 Sanger sequencing and genotyping

2.3.1 Polymerase Chain Reaction (PCR)

2.3.1.1 Primer design and storage

PCR primer pairs were designed with Primer3Plus (Untergrasser et al., 2012), in order to amplify the relevant exons and intron/exon junctions. All oligonucleotides were aligned to their target region on the Ensembl genome browser in order to avoid, wherever possible, an overlap with single nucleotide polymorphisms. The primer sequences were also analysed with BLAST (Zhang et al., 2000) to verify their specificity. For highly polymorphic or GC rich regions, oligonucleotides were designed manually, based on the following criteria: GC content: 45-55% Tm: 54-64°C; oligonucleotide length:18-24 bases; product size: 300-700 bp. Oligonucleotides were purchased from Eurofins MWG Operon, diluted in RNAse/DNAse free water to a 100pmol/μl concentration and stored at -20°C. Stock solutions were subsequently diluted to a 10pmol/μl working concentration.

All primer sequences are listed in Appendix II.

2.3.1.2 PCR conditions

After optimising annealing temperatures by gradient PCR, target regions were amplified under the following cycling conditions: 5 min initial denaturation at 95 °C; 30 replication cycles at 95 °C for 30 sec, 52-68°C for 30 sec (Appendix II) , 72 °C for 30 sec, followed by a final extension at 72 °C for 10 min. Each 15 μl reaction contained the components listed in Table 2.3.1.2. For primers encompassing GC-rich regions, PCR reactions were also supplemented with 10%v/v DMSO.

Table 2.3.1.2. PCR reaction components

Component	**Volume [µl]**
10X Polymerase Buffer	1.5
10 µM Forward Primer	0.5
10 µM Reverse Primer	0.5
25 ng/µl DNA Template	2
2 µM dNTPs	1.5
5U/µlTaq Polymerase	0.15
ddH2O	8.85
Total	**15**

2.3.1.3 Agarose gel electrophoresis

The outcome of PCR reactions was determined by agarose gel electrophoresis. PCR products (3.5µl) were diluted in 5X DNA loading buffer (1.5µl), and loaded on a 2% agarose gel supplemented with 0.5 mg/ml ethidium bromide. Hyper ladder II was used as a molecular weight marker. Amplification products were separated at 200 Volts for 15 minutes, and visualized under UV light (UVP, GelDoc-It310 Imaging Syetem).

2.3.2 Sanger sequencing

2.3.2.1 PCR Product purifications

In order to remove unincorporated dNTPs and primers, 2 µl of each PCR product were transferred into a non-skirted 96-well plate, treated with 3 µl of IllustraExoStar 1 solution (0.125µl of Illustra ExoStar1 diluted in 2.875 µl ddH_2O), and incubated at 37°C for 30 min and 80 °C for 15 min.

2.3.2.2 Sequencing reaction

One point twenty five microliter of 5X BigDye Terminator sequencing buffer, 0.25 µl of BigDye Terminator v3.1, and 0.25 µl of 10µM sequencing primer were added to each purified sample. Sanger sequencing reactions were performed under the following cycling conditions: 30 cycles at 96 °C for 30 sec, 50°C for 15 sec, and 60°C for 1 min. For sequencing plasmid DNA, 1µl of 5X BigDye Terminator sequencing buffer, 2 µl of BigDye Terminator v3.1, and 0.32 µl of 10 µM sequencing primer were added to 3 µl of 30 ng/µl plasmid DNA, and diluted

in water to a final volume of 10 µl.

2.3.2.3 Purification of sequencing reaction

Sequencing reaction products were treated with 26 µl of precipitation solution (50ml of 95% ethanol solution mixed with 2ml of 3M NaOAc, pH=4.6), incubated at room temperature for 10 min, and then centrifuged at 3000 rpm for 30 min at room temperature. Supernatants were removed by inverting the plates and centrifuging them for a few seconds at 300 rpm. Pellets were resuspended in 100 µl 70% ethanol solution and centrifuged at 3000 rpm for 15 min at room temperature. Supernatants were removed as described above, and pellets were air dried for at least 15 min at room temperature. Dried pellets were resuspended in 10 µl of HiDi formamide and denatured at 96 °C for 2 min. The samples were run on a 3730xl ABIsequencer (Applied Biosystems).

2.3.3 Microsatellite genotyping

Primer sequences were obtained from the GeneLoc database (Appendix III). After optimising annealing temperatures by gradient PCR, the region spanning the microsatellite was amplified by standard PCR , using a forward primer that was labelled with 5'-FAM. Gel electrophoresis was performed to confirm target amplification. PCR products were diluted 1:20 to 1:80 depending on band intensity. Next, 1 µl of diluted sample was supplemented with 8.75 µl HiDi and 0.25 µl of TAMRA Sizing Standard. Reactions were run on a 3730xl AB Sequencer. Fragments were analysed with Peak Scanner (v1.0).

2.4 Whole-exome sequencing

2.4.1 Sample selection for whole-exome sequencing

The samples were selected to provide a phenotypically homogeneous cohort of patients.

The foremost criterion was the presence of a severe disease, manifesting at an early age (<35 years old), with signs of systemic inflammation. To obtain the relevant clinical information, all available CRFs were systematically interrogated. Once a small number of cases were selected for analysis, the accuracy of the data reported in the CRF was validated by contacting the dermatologist who had recruited the patient. Individuals with a family history of generalised pustular psoriasis were further prioritised,.

2.4.2 Sample preparation for whole-exome sequencing

Genomic DNA samples were diluted in 130 µl TE to a final concentration of 30 ng/µl. Sample concentration was determined by using a Qubit 2.0 Fluorometer.

2.4.3 Whole-exome sequencing

Sequencing libraries were prepared by the personnel of Guy's and St Thomas Hospital Biomedical Research Centre (BRC) core genomics facility. Briefly, 3 µg DNA were diluted in 130 ml 1X TE and sheared into150-200 bp fragments with a Covaris M220 ultrasonicator. Libraries were prepared using the SureSelect Library Prep Kit. DNA fragments were purified with Agencourt AMPure XP beads and repaired to produce blunt-ended 5'-phosphorylated ends. 3'-dA overhangs were added to these repaired fragments, and indexing-specific paired-

end adapters were ligated. Each library was amplified with a Herculase II Fusion DNA Polymerase Kit under the following cycling conditions: 98°C for 2 minutes, (98°C for 30 seconds, 65°C for 30 seconds, 72°C for 60 seconds) x 5, 72°C for 10 minutes. The quality and concentration of amplification products were determined using an Agilent 2100 Bioanalyzer and a Qubit 2.0 Fluorometer, respectively.

The BRC technicians also undertook the exome capture procedure, using the Agilent Sure Select Human All Exome Kit v.4, according to the manufacturer's protocol. Briefly, libraries were hybridised for 24h at 65C, purified on a Dynal magnetic separator, and amplified under the following cycling conditions: 98°C for 2 minutes, (98°C for 30 seconds, 57°C for 30 seconds, 72°C for 60 seconds) x 10, 72°C for 10 minutes. After index tags were added, the quality and concentration of the preparation were assessed with the Agilent 2100 Bioanalyzer High Sensitivity DNA assay. Following that, samples were pooled for multiplex sequencing and prepared for cluster amplification.

2.5 Plasmid DNA manipulation

2.5.1 Plasmid transformation and propagation

Thirty nanograms of wild-type pcDNA3-CARMA2-sh.1 plasmid were added to 50 μl of NEB 5-alpha competent E.coli cells thawed on ice. The cells were incubated on ice for at least 45 minutes, heat shocked at 42°C for 45 seconds, and incubated on ice for another 5 minutes. Five hundred microliters of pre-warmed SOC medium was added to the bacteria and the culture was incubated at 37°C for at least one hour. The cultures were centrifuged for 3 minutes at 6000 rpm and 400 μl of the supernatant was discarded. The bacteria were re-suspended in the remaining 100 μl medium and the cell suspension was spread on LB agar

plates containing 100 μg/ml ampicillin. The plates were incubated at 37°C overnight;, single colonies were picked next day and used for the inoculation of 5 ml LB broth supplemented with 100 μg/ml ampicillin. The small cultures were grown in a Barnstead SHKE6000 shaker incubator, at 37°C and 180 rpm for 8 hours. Plasmid DNA was isolated by using the QIAprep Miniprep Kit, while 500 μl of culture was used to inoculate 50 ml of LB broth supplemented with 100μg/ml ampicillin. Large cultures were incubated overnight as described above and plasmid DNA was isolated using the HiSpeed Midi Kit according to the manufacturer's protocol. The concentration of the plasmid DNAs was assessed with a NanoDrop ND-1000 Spectrophotometer and the sequence of the insert was verified by Sanger sequencing.

Plasmids were stored as glycerol stocks (750ml overnight culture supplemented with 250 ml 80% glycerol) and recovered by streaking 30 μl bacteria on an LB agar plate supplemented with 100 μg/ml ampicillin. Single colonies were picked the next day and processed as described above.

2.5.2 Site-directed mutagenesis

Mutagenic primers were designed with the QuikChange Primer Design tool, according to the manufacturer's instructions (Table 2.5.2, Figure 2.5.2). The mutagenesis reactions were set up in a final volume of 50 μl, using 30 ng plasmid DNA and the reagents provided by the QuikChange Lightning Site-directed Mutagenesis Kit. The protocol provided by the manufacturer was used with minor modifications. In particular, the DpnI digestion time was extended from 5 to 15 min and the reaction products were concentrated by ethanol precipitation. Briefly, 1/10 volume of NaOAc and 3 volumes of 95% ethanol were added to the reaction. After a 15 minute incubation on ice, the reactions were centrifuged for 30

minutes at 13,000 rpm, at 4°C. The supernatants were discarded and the pellets were rinsed with 70% ethanol before a 15 minute centrifugation at 13,000 rpm. After discarding the supernatant, the pellets were air-dried for 5 minutes and re-suspended in 10 µl water. The mutagenised constructs were transformed into E.coli XL-10 Gold ultracomptent cells, according to the manufacturer's guidelines. Cells were propagated as described in 2.5.1 and constructs were validated by direct sequencing of the entire *CARD14* coding sequence, pCMV promoter, Bovine Growth Hormone polyadenylation site (BGH pA) and FLAG-tag sequence.

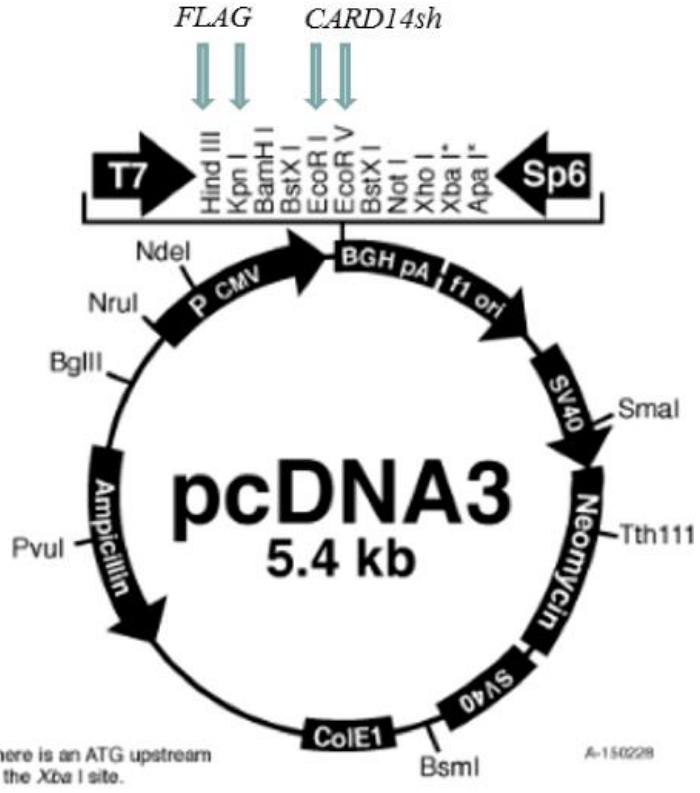

Figure 2.5.2. Plasmid used for site-directed mutagenesis

The position of the FLAG tag and CARD14 cDNA within the multiple cloning site is indicated by arrows.

Table 2.5.2. Primers used for site directed mutagenesis

Target change	**Primer ID**	**Primer sequence (5' to 3')**
p.Gly117Ser	G117S F	GCT TGG ATG TCT CCA TGA GAC TGC TAA AGT TAC TGA AGT C
	G117S R	GAC TTC AGT AAC TTT AGC AGT CTC ATG GAG ACA TCC AAG C
p.Glu138Ala	E138A F	CCT TTT CCT GGT TCA GCG CCT CCT GCA GGC TGC C
	E138A R	GGC AGC CTG CAG GAG GCG CTG AAC CAG GAA AAG G
p.Leu156Pro	L156P F	AGG TGC TCC TGC GGC TGC TGG CAC C
	L156P R	GGT GCC AGC AGC CGC AGG AGC ACC T
p.Asp176His	D176H F	CAT GCG GCT GTG GTG AGC CTC CAG CTG GT
	D176H R	ACC AGC TGG AGG CTC ACC ACA GCC GCA TG

2.6 Cell culture

2.6.1 Cell lines

Human embryonic kidney (HEK293) cell cultures were handled under aseptic conditions, in a laminar flow hood contained in a designated tissue culture room. Cell lines were grown at 37°C, in a NuAir Air-Jacketed Automatic CO_2 Incubator (NU-5500) providing humidified atmosphere with 5% CO_2. Cultures were tested for mycoplasma contamination once every 3 months, using the MycoSensor PCR Assay Kit according to the manufacturer's instructions. Cells were cultured in Dulbecco's Modified Eagle Medium (DMEM) supplemented with 10% Foetal Calf Serum (FCS), 2mM L-Glutamine, 50 U/ml of penicillin and 50 μg/ml of streptomycin (complete medium). Cultures were stored in liquid nitrogen. When thawing aliquots, cryo-vials were hand warmed and sequentially diluted in 1 ml of FCS and 9 ml of pre-warmed complete medium. Next day, at passage no.1, the medium was removed; cells were washed with 3 ml of PBS, and then trypsinised by adding 3 ml of TrypLE. After 5 min incubation at room temperature, detached cells were diluted in pre-warmed complete medium to stop trysinisation, and then centrifuged at 1500 rpm for 5 minutes. Supernatants were discarded, cell pellets re-suspended in 10 ml of complete medium, and plated in a T75 flask. These steps were repeated every time the cells reached ~80-90% confluency, when cultures were passaged by transferring 1 ml of cell suspension to a new T75 flask.

For storage in liquid nitrogen, $2x10^6$ cells were diluted in 1ml of chilled, freshly prepared and filter-sterilised freezing medium consisting of 90% FCS and 10% of DMSO. The cryo-vials were immediately placed in a MrFrosty container at -80°C for ~24hours and then transferred to a liquid nitrogen tank.

2.6.2 Transfection

To investigate the impact of *CARD14* variants on protein expression, $2.5x10^5$ HEK293 cells were seeded in 1 ml of DMEM supplemented with 10% of FCS, in 12-well plates. The following day, 1.6 µg of plasmid DNA was transfected using the Lipofectamine2000 Transfection reagent according to the manufacturer's guidelines. The medium was changed 6 hours after transfection to 1 ml of DMEM supplemented with 10% FCS per well. Cells were harvested for protein extraction 48 hours after transfection.

For immunofluorescence microscopy, HEK293 cells were seeded on poly-D-lysin coated coverslips (Becton Dickinson) in a 24-well plate, at a density of $1.25x10^5$ cells per well, in 500 ml of DMEM supplemented with 10% FCS. The following day, 0.8 µg of plasmid DNA was transfected using the Lipofectamine2000 Transfection reagent according to the manufacturer's guidelines. Media was changed 5 hours after transfection to 500 ml of DMEM supplemented with 10%FCS per well.

2.6.3 Immunofluorescence microscopy

Twenty-four hours after transfection, the medium was aspirated and cells were carefully washed in 500 µl PBS for two times. Coverslips were covered with 350 µl of 4% paraformaldehyde freshly diluted in PBS and cells were fixed for 15 min at room temperature. The formaldehyde solution was aspirated and cells carefully rinsed in 350 µl of PBS for 5 minutes. After the washing step was repeated three times, specimens were incubated in 350 µl Blocking Buffer for 1 hour at room temperature. The blocking solution was aspirated and 0.6 µl DYKDDDDK Tag primary antibody (targeting FLAG) diluted in 350 µl Antibody Dilution Buffer was directly applied to each well. After an overnight incubation at 4°C, the primary

antibody was aspirated and coverslips were rinsed three times in PBS, for 5 min per wash. Specimens were incubated in Alexa Fluor® 488 Goat Anti-Rabbit IgG diluted in 350 µl Antibody Dilution Buffer for 1 hr and 10 min at room temperature, in the dark. Coverslips were carefully rinsed three times in PBS for 5 min and mounted onto slides using ProLong Diamond Antifade reagent containing 4', 6-diamino-2-phenylindole (DAPI). Coverslips were sealed with transparent nail polish to prevent drying out of the samples. Slides were stored in the dark at 4°C and imaged at least 24 hours later, using immunofluorescence microscopy (ZEISS, AxioCAM MRm microscope and ZEISS Axiovision Software Version 4). A minimum of 25 cells per coverslips were examined for the presence of CARD14 oligomers in their cytoplasm.

2.7 Transcript analysis

2.7.1 RNA extraction

The procedure was performed under hood, using filter tips. Prior to RNA extraction, all surfaces and pipettes were treated with RNaseZap Decontamination Solution. Cell pellets were homogenised using the QIAshredder columns and RNA was extracted with the RNeasy Mini Kit according to the manufacture's guidelines. RNA was eluted in 30µl of RNase-free water and quantified with a NanoDrop ND-1000 Spectrophotometer. Samples were stored in RNAase free Eppendorfs at -80°C.

2.7.2 cDNA synthesis

One microgram of total RNA was reverse-transcribed using the High Capacity cDNA Reverse Transcription Kit, according to the manufacturer's protocol. The reactions were incubated at 25°C for 10 minutes, 37°C for 120 minutes, and 85°C for 5 minutes. After the reverse transcription was completed, the cDNAs were diluted by adding 30 µl of nuclease-free water to each reaction. Skin, CD4+T lymphocyte, and RNAs used in the *ARFGPA2* study were generously provided by Prof. Nestle's group at KCL. The remaining samples were generated by other members of the Capon group.

2.7.3 Real-time PCR

PPIA transcript levels were measured using a fluorescent, VIC labelled TaqMan probe purchased from Life Technologies (see Table 2.7.3). Reactions were set up in duplicate, in a final volume of 20µl containing 1 µl probe, 1X TaqMan Universal Master Mix II, and 2µl of diluted cDNA.

ARFGAP2 transcript levels were measured with the KAPA SYBR FAST qPCR kit, using primers designed in house and purchased from Eurofin Genomics. Reactions were set up in duplicate, in a final volume of 20µl containing 1X KAPA SYBR FAST Universal qPCR Master Mix, 45 nM primers (Table 2.7.3, Appendix II), and 2 µl of cDNA. Samples were loaded on a 7900HT Fast Real Time PCR System and run under the following cycling conditions: 95°C for 10 minutes, (95°C for 15 seconds, 60°C for 60 seconds) x 40.

2.7.4 Gene expression analysis

Relative gene expression was quantified with the ΔΔCt method (Livak et al., 2001). *PPIA* was used as endogenous control. The average detection threshold cycle (Ct) of each duplicate sample was calculated and the ΔCt was derived with the following formula:

$\Delta Ct = Ct[sample] - Ct[PP1A]$

ΔCt values were then normalized to those of a calibrator sample:

$$\Delta\Delta Ct = \Delta Ct[sample] - \Delta Ct[calibrator]$$

Finally, relative gene expression levels (RQ) were calculated using the following formula:

$RQ = 2^{-\Delta\Delta Ct}$

Table 2.7.3. Primers and probe used for real-time PCR

Primer ID	**Transcript target**
ARFGAP2 Main	*ARFGAP2* full length transcript (ENST000000524782)
ARFGAP2 2nd Main	*ARFGAP2* isoform lacking exon 5 (ENST000000426335)
4310883E	*PPP1A* (ENST00000312989)

2.8 Protein analysis

2.8.1 Sample preparation

Cells were trypsinized as described in 2.6.1, centrifuged at room temperature for 5 minutes at 5000 rpm, and washed twice with 500 µl PBS. The pellets were stored at -20°C overnight.

For the preparation of whole-cell extracts, pellets were thawed and re-suspended in 70 ml of HU buffer. Suspensions were incubated for 5 min at room temperature, centrifuged for 15min at 65°C, and sonicated for 45 sec with a W-375 ultrasonic sonicator (Heat Systems Ultrasonics) to reduce their viscosity. Following that, samples were ready to load on a gel or store at -20 °C.

For the separation of the soluble and insoluble cell fraction, pellets were thawed on ice and initially re-suspended in 70 µl of ice-cold, non-denaturing cell lysis buffer, freshly supplemented with 10µl 7X protease inhibitors. Cell suspensions were incubated on ice, in a 4°C cold room, for at least 40 minutes, and centrifuged at 13000 rpm at 4°C for 15 minutes. Supernatants were transferred to new, pre-chilled Eppendorf tubes and stored at -80°C or immediately loaded on a gel. Pellets were re-suspended in denaturing buffer, and processed as described above.

2.8.2 Gel preparation

The 8% separating gel contained 2.7 ml Ultra PureProtoGel 30% Acrylamide Mix, 2.5 ml 1.5M Tris pH 8.8, 100 µl 10% SDS, 100 µl 10% Ammonium Persulfate, and 6 µl TEMED, in a final volume of 10 ml. To create a straight, clear cut junction between the stacking and separating gel, 500 ml of isopropanol was applied to the top of the gel. After the separating

gel had polymerized (~5-10 min), the isopropanol was removed, and 2 ml of stacking gel (330 µl acrylamide mix, 250 µl Tris pH 6.8, 20 µl 10% SDS, 20 µl 10% Ammonium Persulfate, 2 µl TEMED) was poured on top. The gel was stored at 4°C overnight, soaked in 1X Running buffer.

2.8.3 Western Blotting

Thirty five microliters of lysate were mixed with 10 ul 6X Laemmli buffer, denatured at 95-98°C for 5 minutes and loaded on the polyacrylamide gel, alongside 7 µl of Precision Plus molecular weight marker. The gel was electrophoresed in 1X running buffer for at least 60 minutes at 150 Volt. Wet transfer to a nitrocellulose membrane (brand) was carried out in a Biorad Mini Trans-Blot Electrophoresis transfer cell apparatus at 200 mA for 1 hour 45 min, at 4°C. To evaluate transfer efficiency, the membrane was stained with Ponceau S red dye. To inhibit unspecific antibody binding, the membrane was incubated in 5% milk-1X TBS-0.1% Tween 20 for at least one hour at room temperature. After blocking, the membrane was incubated overnight at 4°C with the primary antibody (Monoclonal ANTI-FLAG M2, Clone M2, or Rabbit polyclonal anti-β–actin, see 2.1.7 for dilutions). The membrane was then washed 6 times in 1X TBS-0.1% Tween 20 for 5 minutes. For the secondary antibody staining, the membrane was incubated at room temperature with a peroxidase-linked species-specific antibody (Goat polyclonal anti-mouse IgG or Donkey monoclonal anti-rabbit IgG) diluted in 5% skimmed milk/1X TBS-0.1% Tween 20 (see 2.1.7 for dilutions). After 1 hour, the antibody was discarded and the membrane was washed 6 times as described above. For signal detection the membrane was treated with the Amersham ECL Western Blotting System for 1 minute. Fujifilm Super RX autoradiography films were exposed to the ECL-treated

membrane and developed using an automated film developer (KONICA MINOLTA SRX-101A).

2.8.4 Densitometric analysis

Autoradiographs were scanned with a Canon CanoScanLiDE 25 device and densitometric analysis was performed with the ImageJ software, according to the manufacturer's directions. The densities of both the protein of interest and loading control (β -Actin) were determined.

2.9 Bioinformatics

2.9.1 Sanger sequence data analysis

Reference sequences were obtained from the Ensembl genome browser (Flicek et al., 2014, Genome assembly: GRCh38) and chromatograms were analysed with the Sequencher software (v4.9, Genecodes). Variants were detected by visual inspection of contigs.

2.9.2 Pathogenicity predictions

The SIFT/PROVEAN (Ng and Heinkoff, 2003), Align GVD (Tavtigian et al., 2005) and Polymorphism Phenotyping v2 (PolyPhen-2, Adzhubei et al., 2010) online tools were used to analyse the likely impact of single nucleotide changes and small (~up to 6 basepairs) deletions/insertions. The effects of splice site variants were investigated with SROOGLE (Schwartz et al., 2009) and MaxEntScan (Yeo and Burge, 2004), while Mutation Taster (Schwartz et al., 2014) and CADD (Kircher M, 2014) were used for both class of changes. The ClustalW2 program was used to estimate whether a variant affected an evolutionarily

conserved residue (Thompson, 1994). Reference sequences for all tools mentioned above were obtained from the Ensemble Genome browser (Flicek et al., 2014, Genome assembly: GRCh38).

2.9.3 Coiled-coil prediction

The following tools were used to assess what portions of the CARD14 protein were more likely to form coiled-coil domains and to assess the impact of mutations lying in such regions: COILS (Lupas, 1991), MultiCoil (Wolf, 1997), NCOILS (Lupas, 1996) and STRAP project (Gille, 2008). Reference DNA and protein sequences were obtained from Ensembl (Flicek et al., 2014).

2.9.4 Haplotype analysis of the *CARD14* locus

Haploview (v4.2, Barrett et al., 2005) (Appendix III) was used to visualize linkage disequilibrium blocks within the *CARD14* locus and to identify informative SNPs (rs4889991, rs2044103, rs3829612, rs8068433; Sugiura et al., 2014) tagging common *CARD14* haplotypes in the Chinese population. The analysis was carried out on the CHB (Han Chinese from Beijing) genotypes generated by International HapMap Project Consortium (The International HapMap Consortium, 2007). Primers were designed according to Sugiura et al, for genomic regions spanning the above four SNPs. The relevant regions were sequenced in the four patients harbouring the p.Asp176His variant.

2.9.5 Exome sequence data processing

The raw sequence data generated by an Illumina HiSEq1000 sequencer was processed

through a software pipeline, originally established by Prof Michael Simpson and currently managed by Guy's and St Thomas' Hospitals BRC Bioinformatics core. Briefly, 100 bp paired-end reads were aligned to the reference hg19 genome with Novoalign (Novocraft Technologies), duplicates and poor quality reads were removed with MarkDuplicates and SAMtools (Li et al., 2009), while capture efficiency was assessed with BEDtools (Quinlan et al., 2010). Changes that were covered by more than four reads were called with SAMtools, and annotated to known genes with Annovar (Wang et al., 2010).

2.9.6 Exome sequence data filtering

Annovar annotated files were imported and analysed in Microsoft Excel. Variant profiles were initially filtered by removing synonymous substitutions and common alleles occurring with a minor allele frequency (MAF) > 0.015 in 2,222 exomes sequenced in-house or the 1000 Genomes Project CEU dataset. Rare changes were further filtered based on the predicted mode of inheritance of the disease allele:

A) In the analysis of cases born into consanguineous marriages, sequencing profiles were filtered to exclude all heterozygous changes. Homozygosity clusters were determined by the manual analysis of variant profiles around rare variants. Stretches of homozygous markers spanning at least 2 Mb were considered as most likely autozygous, based on the observations of Alsalem et al., and McQuillan et al. Hence variants lying in such regions were prioritised.

B) In the analysis of familial GPP cases, the predicted mode of inheritance was inferred from the pedigree structure and variant profiles were filtered by excluding single heterozygous (for recessive pedigrees) or homozygous changes (for dominant

pedigrees), as appropriate.

C) In the isolated cases, both homozygous and heterozygous changes were studied, as it was not possible to infer the most likely mode of disease inheritance.

Filtered profiles were allocated to different analysis groups according to the predicted mode of inheritance of the disease allele. Genes that were mutated in multiple families were prioritised for analysis and the variants they harboured were assessed for pathogenicity, using the online tools described in 2.9.2. Changes that were predicted to be deleterious by four out of five algorithms were followed-up, the rest were filtered out. In individuals of Asian descent, allele frequencies in relevant control populations were also taken into account, and variants with frequencies of higher than 0.015 were removed from the list of possible candidates (Table 2.2.5). Given the numerous candidates in the dominant group, putative mutations were further prioritised by ranking them on the basis of their CADD scores.

2.9.7 Quality control of exome sequence reads

The accuracy of all variant calls that passed the above filtering steps was verified using the Integrative Genomic Viewer (IGV) tool (Robinson et al., 2011). Changes supported by a small number of reads ($n<6$) and variants surrounded by numerous mismatches were deemed to be artifacts and excluded from further analyses (Figure 2.9.7).

If the sequence change was validated by the IGV analysis, reads spanning the relevant gene were also inspected in samples that did not appear to present any damaging alleles. This was to make sure that the lack of mutation was not the consequence of poor coverage.

a)

b)

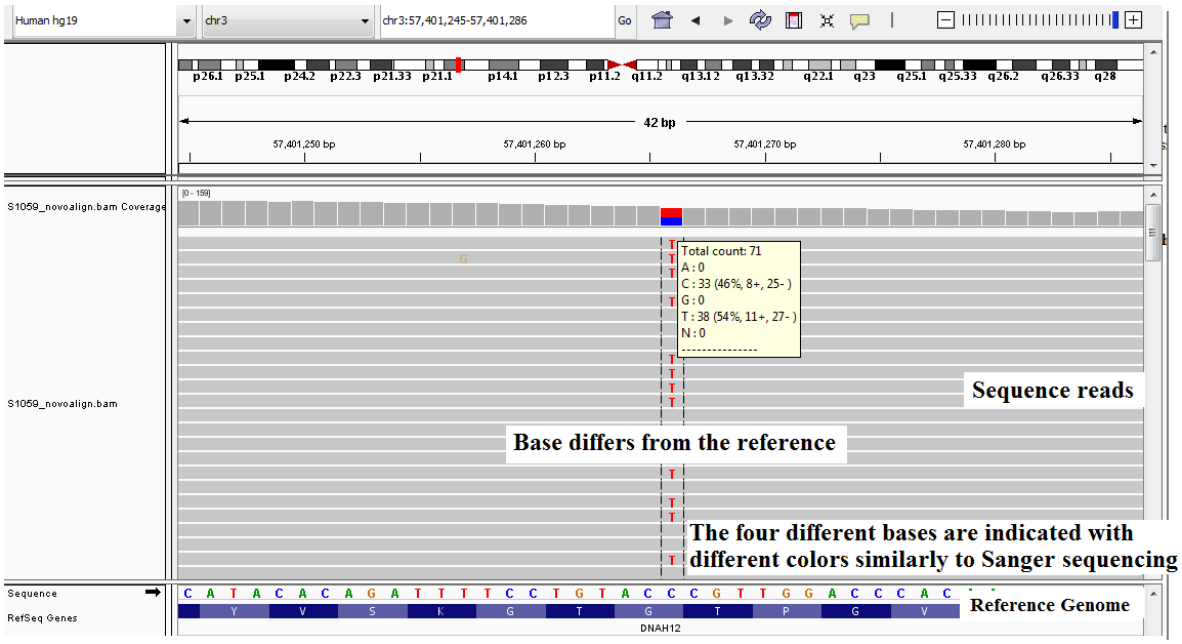

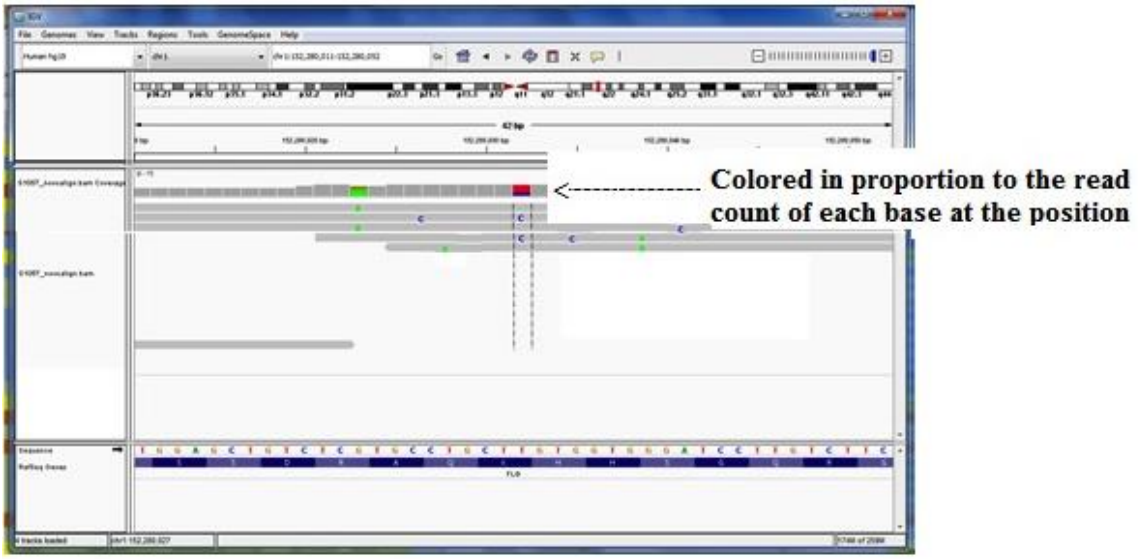

Figure 2.9.7. Examples of high confidence (a) and low confidence (b) variant calls using IGV. The IGV program aligns sequence reads to a reference genome. In case of complete sequence homology only reference bases are shown. Variants covered by many reads are considered high confidence calls (a), whereas the presence of numerous mismatches around the base change indicates that the reads have probably been misaligned. The calls are therefore considered as unreliable (b).

2.9.8 Analysis of Copy Number Variants (CNV)

The occurrence of CNVs was assessed by using the ExomeDepth tool (Plagnol et al., 2012) to analyse read counts. The frequency of CNVs in the general population was determined by querying the Ensembl genome browser (Flicek et al., 2014).

2.10 Statistical analyses

2.10.1 Power calculations

In order to measure the probability of detecting variants with varying MAFs, a power calculation was performed with an online binomial calculator (Appendix III). The Genetic Power Calculator (Purcell et al., 2003) was used to estimate the probability of identifying disease associated SNPs occurring with varying frequencies and effect sizes. Power ≥80% was considered adequate.

2.10.2 Association testing

Because there is a very strong expectation that rare deleterious variants will be enriched and not reduced in frequency among affected patients, all analyses were implemented as one-tailed association tests. Depending on the sample size, Fisher's exact test or Chi-square tests with Yates correction were used to assess the association between individual gene variants and disease phenotypes. In the study of *ARFGAP2*, and *CYP1A1,* burden tests were used to assess the cumulative effects of deleterious changes in the relevant gene region. All tests were performed using Graphpad and cases were always compared to controls of similar ethnicity.

In the investigation of *CARD14* and *CYP1A1*, a meta-analysis of different association studies

was performed by using the RevMan 5.2 software to calculate a weighted pooled odds ratio and Z score (Cochrane Collaboration, 2012).

For the study of common *IL36RN* alleles in PV, genome-wide association data was available for 2,622 patients with psoriasis and 5,667 controls (Strange et al., 2010). Genotype data was extracted for a 26 kb interval (2:113,806,215- 113,832,325 , GRCh37) spanning the *IL36RN* gene and 10 kb of flanking regions. Experimental genotypes were integrated by imputing additional SNPs with IMPUTE v2 (Howie et al., 2009), using the 1000 Genome haplotypes as a reference set. Imputed SNPs showing minor allele frequencies < 0.01, info scores < 0.5, or extreme deviations from Hardy-Weinberg equilibrium ($P < 1x10^{-6}$) were excluded from further analyses. Association tests accounting for the uncertainty in the imputed genotypes were implemented under additive and recessive models using SNPTEST (Marchini et al., 2007).

For the analysis of rare *IL36RN* variants in PV, genotypes were extracted from a large case-control dataset (11,801 cases and 27,233 unrelated controls), which had been typed by the International Psoriasis Consortium, using Illumina's HumanExome Beadchip. Combined allele counts were compared in cases vs. controls, using Fisher's exact test.

2.10.3 Multiple testing and significance thresholds

For candidate gene studies, *P* values smaller than 0.05 were considered to be nominally significant. No correction for multiple testing was required for the *IL36RN* analysis (no *P* values < 0.05 were observed) or the *CARD14* study (only one SNP was examined). For the follow-up of WES, the issue of multiple statistical testing was addressed by adopting an exome-wide significance threshold of $P<1.5 \times 10^{-6}$ (Kiezun et al, 2012).

2.10.4 Densitometry data analysis

The densitometry data were analysed with GraphPad Prism 6.0 (GraphPad Software, La Jolla, CA) using one-way ANOVA, followed by a Dunnett's post-test. *P* values < 0.05 were considered statistically significant. Standard devitaions were calculated with GraphPadPrism.

3 GENETIC ANALYSIS OF *IL36RN* ALLELES IN PSORIASIS VULGARIS

Generalised pustular psoriasis often presents with concomitant psoriasis vulgaris, suggesting the existence of shared genetic determinants between the two conditions (Sugiura et al., 2014). In this context, the possibility that *IL36RN* alleles may confer susceptibility to plaque psoriasis looks particularly plausible given that IL-36 cytokine levels are elevated in the lesional skin of PV patients (Blumberg et al., 2007; Carrier et al., 2011; Johnston et al., 2011), and that *il36rn* knockout exacerbates psoriasis-like skin inflammation in *il36a* transgenic mice (Blumberg et al., 2007; Carrier et al., 2011; Tortola et al., 2012). Therefore, the aim of this project was to investigate in association studies whether *IL36RN* variation contributes to PV susceptibility.

3.1 Common variant analysis

Single nucleotide polymorphisms in *IL36RN* detected in a previous genome-wide association study were re-examined first (Strange et al., 2010).

3.1.1 Power calculations

The study included 2,600 PV patients and 5,700 controls of British origin. Calculations were undertaken by assuming a 2% population prevalence of psoriasis and indicated that the study had 80% power to detect disease associated alleles occurring with a frequency ≥1.5%, provided the Genotype Relative Risk (GRR) exceeded 1.4. Variants with a GRR ≥1.1 could also have been detected (80% power), if their frequency was above 40% (Figure 3.1.1).

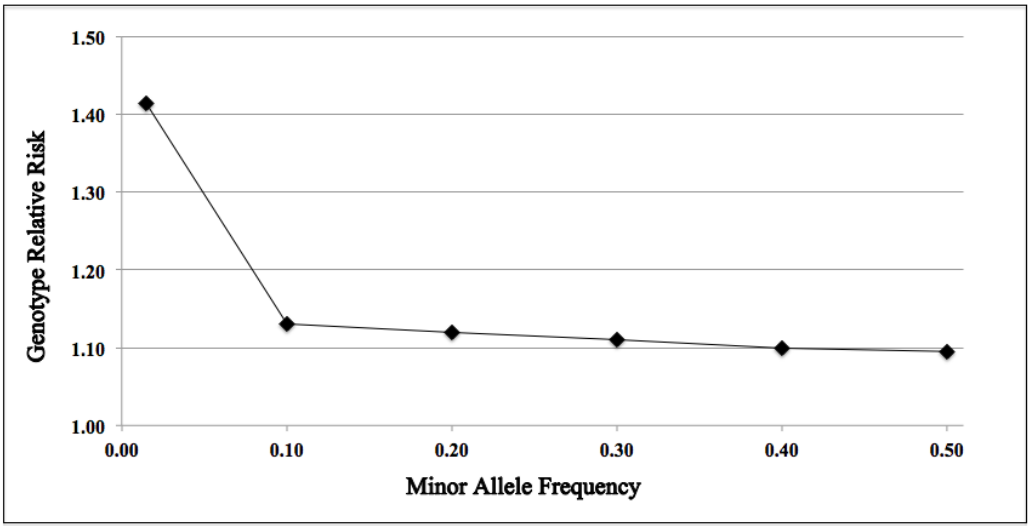

Figure 3.1.1. Required Genotype Relatives Risk and Minor Allele Frequency values to reach 80% power. Calculations were performed by the online Genetic Power Calculator (Purcell et al., 2003).

3.1.2 Analysis of *IL36RN* genotypes from genome-wide association data

The genotypes generated by Strange et al. were supplemented by imputing additional markers with IMPUTE v.2 (Howie et al., 2009), using the 1000 Genomes haplotypes as a reference. The resulting dataset included a total of 130 single-nucleotide polymorphisms spanning the *IL36RN* locus and 10 kb of flanking regions (the latter were included in the analysis so as to cover likely regulatory regions lying in proximity of the gene). The genotypes were examined under a recessive model, using SNPTEST. No markers generated a *P*-value <0.05, indicating that common *IL36RN* variants are unlikely to confer a substantial PV risk.

3.2 Rare variant analysis

3.2.1 Case selection

IL36RN mutations are highly penetrant in GPP (Capon, 2013). Therefore, it was assumed that *IL36RN* alleles associated with psoriasis vulgaris would result in familial recurrence of the disease, or lead to very severe phenotypes. On this basis, 349 probands (175 females, 174 males) with a family history of PV (Table 2.2.1 in methods**)** and 14 individuals (10 females, 4 males) with severe erythrodermic psoriasis were selected for analysis.

3.2.2 Power calculations

Power calculations were undertaken at the outset of the study. The first analysis was performed with an online binomial calculator and demonstrated that Sanger sequencing the patient resource (726 chromosomes) would have 80% power to detect alleles occurring with a frequency of at least 0.25% (Figure 3.2.2/A), while variants with lower frequencies might

have been missed.

A further analysis was carried out with the Genetic Power Calculator (Purcell et al., 2003), assuming a PV prevalence of 2%. This showed that the dataset consisting of 363 patients and 2,313 controls could reveal disease associations with 80% power in the presence of allele frequencies as low as 0.10%, as long as the Genotype Relative Risk (GRR) was higher than 5 (Figure 3.2.2/B). Of note, the p.Ser113Leu variant has a minor allele frequency of 0.28% in the British population and has been associated with a GRR of 4.9 in pustular psoriasis (Setta-Kaffetzi et al., 2013). Thus, the study would have 80% power to detect an association with this change, which represents the most common GPP allele in European populations (Setta-Kaffetzi et al., 2013). Smaller effect sizes (GRR $\geq$2.75) could have been also detected, provided the frequency of the risk allele was higher than 0.5%, although those with lower frequencies might have been missed.

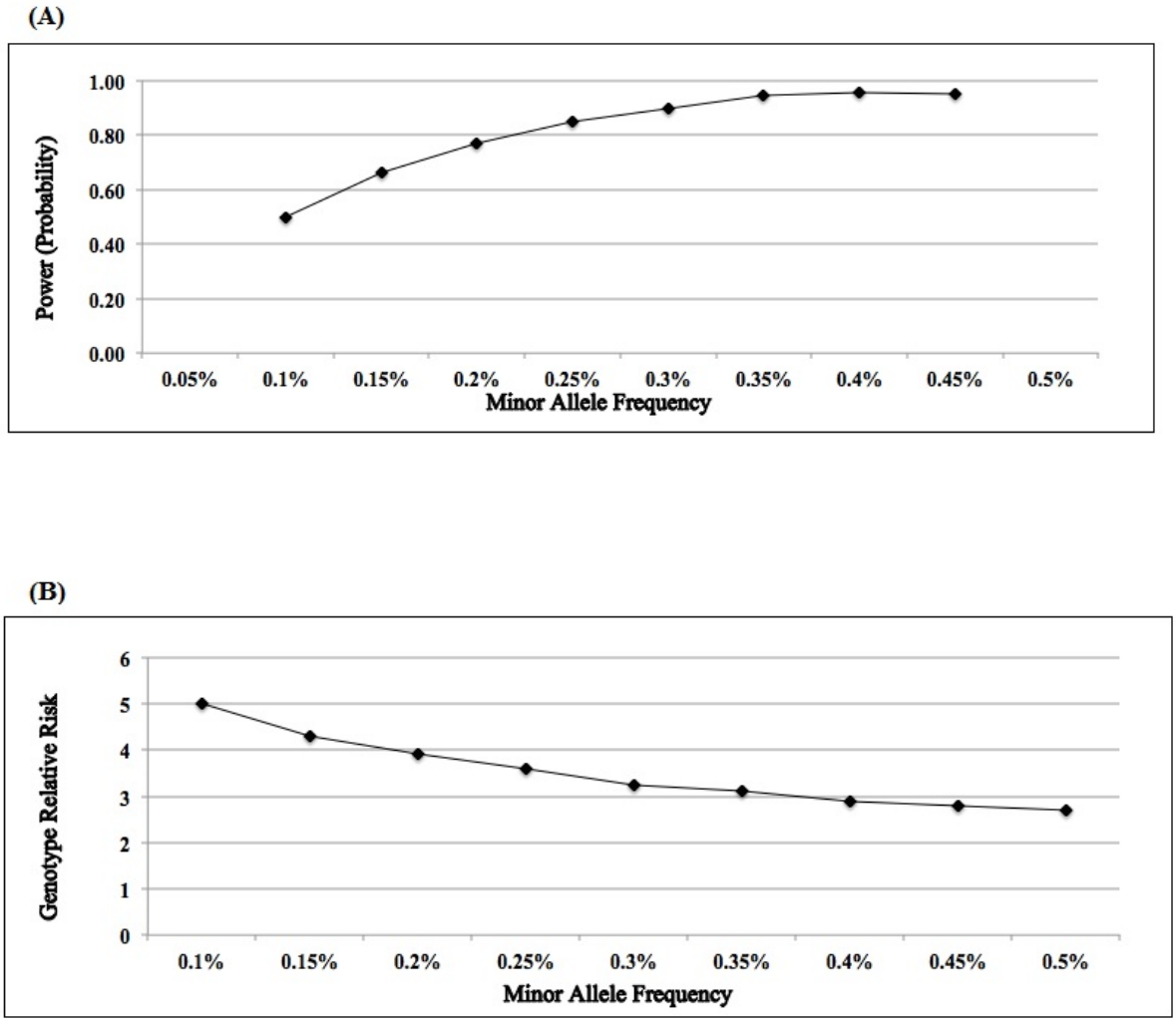

Figure 3.2.2. Power to identify rare disease alleles (A) and to detect disease associations (B) The power was estimated using the online binomial calculator (A) and the Genetic Power Calculator (B) (Appendix III; Purcell et al., 2003). The calculations were performed on 363 patients and 2,313 controls.

3.2.3 Sanger sequencing of *IL36RN* coding exons in familial psoriasis vulgaris

Sequencing of the *IL36RN* coding sequence (exons 2-5) and proximal promoter region (1,070 bp) did not identify any rare alleles in the homozygous or compound heterozygous state, indicating that bialleleic *IL36RN* mutations did not underlie the onset of PV or erythrodermic psoriasis, in the examined cases.

One PV patient harboured a Threonine to Isoleucine substitution (p.Thr77Ile). The change; however, was predicted to be tolerated by five different algorithms and as a result was not studied any further (Table 3.2.3.1). Two additional individuals with psoriasis vulgaris carried a copy of the p.Ser113Leu mutation, which is the most frequent pustular psoriasis allele in European populations (Setta-Kaffetzi et al., 2013). To further investigate the pathogenic potential of the Ser113Leu variant in these subjects, the segregation of the substitution was analysed in the relevant two pedigrees.

In one family (upper panel in Figure 3.2.3), the affected children inherited the mutation from their unaffected mother, while their affected father carried a wild-type allele. In the second pedigree (lower panel in Figure 3.2.3), two affected siblings harboured the p.Ser113Leu substitution, but a third brother did not. These observations demonstrate that p.Ser113Leu does not segregate with PV in the families.

To complement these findings, the frequency of the p.Ser113Leu in the PV cases was compared with that observed in 2,313 unrelated controls of British origin. This failed to identify any enrichment of the p.Ser113Leu allele among PV patients (Table 3.2.3.2).

Table 3.2.3.1. Pathogenicity predictions for the rare variants detected in the study

Variant	PROVEAN	SIFT	PolyPhen-2	Mutation Taster	CADD[1]
p.Thr77Ile	Tolerated	Neutral	Benign	Polymorphism	1.2

[1]The CADD algorithm returns a quantitative prediction, with scores above 15 considered pathogenic.

Table 3.2.3.2. Distribution of the p.Ser113Leu allele in PV cases and controls

Variant	Location	rs number	Allele frequencies (allele counts)		P value
			Cases	Controls	
p.Ser113Leu	Exon 5	rs144478519	0.003 (2/726)	0.0035 (16/4626)[1]	0.76

[1]2,222 controls exome-sequenced in house and 91 analysed by 1000 Genomes Consortium (GBR dataset).

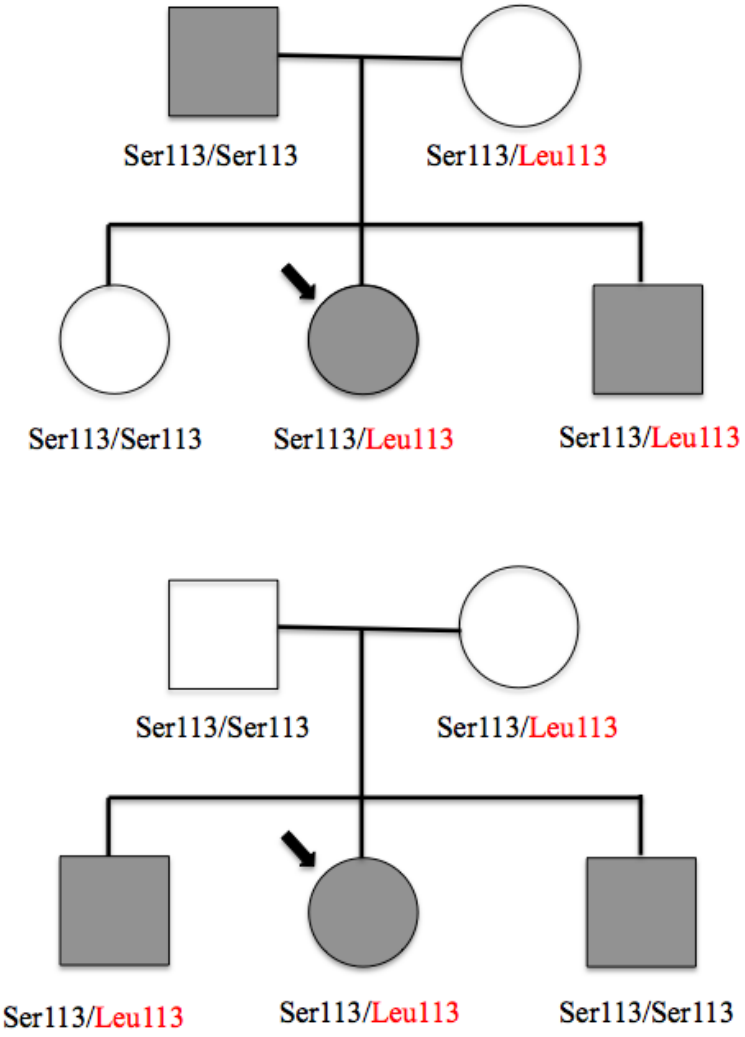

Figure 3.2.3. Segregation of the p.Ser113Leu variant in the families of the two patients who were originally Sanger sequenced. Grey symbols represent individuals affected by PV. Probands are highlighted by arrows.

3.2.4 Analysis of *IL36RN* genotypes from exome-wide association data

The study described in 3.2.3 had < 80% power to detect association with very rare variants (MAF<0.25%). Therefore, a larger resource was also examined. Data on *IL36RN* coding variants was extracted from a collaborative study of 11,801 PV cases and 27,233 controls (Table 3.2.4.1), which had been typed on Illumina's HumanExome Beadchip. Genotypes were available for six rare, single nucleotide changes lying within *IL36RN*. Three were known disease alleles (p.Pro27Leu, p.Arg48Trp, p.Ser113Leu) (Marrakchi et al., 2011; Onoufriadis et al., 2011), whereas the remaining three (p.Lys35Arg, p.Asn47Ser, p.Pro82Leu) were predicted to be benign by multiple algorithms (Table 3.2.4.2) and were therefore excluded from further analyses.

A comparison of allele counts between patients and controls detected no statistically significant differences for any of the three pathogenic alleles (Table 3.2.4.3). A burden test based on the combined frequency of deleterious alleles in each group was also undertaken, but did not generate any evidence for association.

Table 3.2.4.1. Participants in the study

Origin	Cases	Controls	Total
UK	2,431	5,892	8,323
Estonia	1,264	1,252	2,516
Germany	2,508	14,541	17,049
USA	5,598	5,548	11,146
All	**11,801**	**27,233**	**39,034**

Table 3.2.4.2. Changes with predicted neutral outcome

AA Change	Pathogenicity Predictions				
	PROVEAN	**SIFT**	**Polyphen-2**	**Mutation Taster**	**CADD[1]**
p.Lys35Arg	Neutral	Tolerated	Benign	Polymorphism	22.7
p.Asn47Ser	Neutral	Tolerated	Possibly damaging	Polymorphism	22
p.Pro82Leu	Neutral	Deleterious	Benign	Disease causing	23.2

[1]The CADD algorithm returns a quantitative prediction, with scores above 15 considered pathogenic. Variants that were deemed to be pathogenic are highlighted in bold. Abbreviation is as follows: AA, amino acid.

Table 3.2.4.3. Frequency of deleterious *IL36RN* alleles in cases vs. controls

AA change	Allele counts (%)		P values
	Cases	Controls	
p.Leu27Pro	1/23,600 (0.004%)	1/57,420 (0.001%)	0.26
p.Arg48Trp	6/23,600 (0.025%)	10 /57,424 (0.017%)	0.32
p.Ser113Leu	87/23,538 (0.370%)	238/57,394 (0.397%)	0.20
All changes	**94/23,538 (0.40%)**	**249/57,394 (0.43%)**	**0.26**

Abbreviation is as follows: AA, amino acid. The differences in total allele counts are due to slight variations in SNP genotyping rates. P values were calculated with Chi-square tests (Methods 2.10.2).

3.3 Analysis of *IL36RN* mutations in GPP patients with concurrent psoriasis vulgaris

To further investigate the pathogenic role of *IL36RN* in psoriasis vulgaris, the prevalence of disease alleles was compared in individuals affected by GPP only or GPP presenting with concomitant PV.

Data on *IL36RN* mutation status and PV concurrence was first collated by Safia Hussain through a thorough review of the literature, based on the terms "*IL36RN*" and "generalised pustular psoriasis". This generated a dataset including 177 unrelated patients of African, Asian, and European origin. A further 56 cases were screened in-house specifically for this study (the work was partly undertaken by Safia Hussain, under Dorottya Berki's direct supervision)-, so that genotype and phenotype information was available for a total of 233 GPP patients, 136 of which also had PV (Tables 3.3.1 and 3.3.2).

A total of fourteen rare *IL36RN* variants were detected in this resource. Four of these changes - p.Arg10X, p.Arg10Argfs*1, p.Leu27Pro, and p.Ser113Leu - have well established deleterious consequences (Farooq et al., 2013; Sugiura et al., 2012; Marrakchi et al., 2011; Onofriadis et al., 2011). The pathogenic potential of the remaining alleles was assessed by online tools, and six further rare variants were predicted to be damaging (Table 3.3.3).

Patients harbouring bi-allelic (homozygous or compound heterozygous, n=36) or single heterozygous *IL36RN* changes (n=15) were classified as *IL36RN*-positive, whereas individuals who had a wild-type gene sequence were labelled as *IL36RN*-negative. A comparison of these two groups revealed that the prevalence of PV was significantly lower in individuals carrying mutations in *IL36RN* (43.14% vs. 68.67%, P= 0.0009, Table 3.3.4), further supporting the notion that *IL36RN*-deficiency does not confer an increased risk of PV.

Table 3.3.1. Key demographics of patients included in the analysis of genotype phenotype correlations

Sex		**Ethnicity**		
Male	**Female**	**African**	**Asian**	**European**
92 (39.5%)	141 (60.5%)	12 (5.2%) 6 Male, 6 Female	172 (73.8%) 71 Male, 101 Female	49 (21%) 15 Male, 34 Female

Table 3.3.2. The resource underpinning genotype-phenotype correlations

Study	**Number of GPP patients (with concomitant PV)**
Abbas et al., 2013	1 (0)
Farooq et al., 2013	14 (5)
Kanazawa et al., 2013	1 (1)
Körber et al., 2013	17 (6)
Li et al., 2013	10 (1)
Marrakchi et al., 2011	9 (2)
Onoufriadis et al., 2011	5 (0)
Rossi-Semerano et al., 2013	1 (0)
Renert-Yuval et al., 2014	1 (0)
Setta-Kaffetzi et al., 2013	85 (65)
Song et al., 2014	1 (0)
Sugiura et al., 2013	28 (19)
Sugiura et al., 2014	4 (1)
This study	56 (36)
Total	**233 (136)**

Table 3.3.3. Pathogenic potential of rare *IL36RN* changes

Mutation	Pathogenicity Prediction				
	PROVEAN	**SIFT**	**PolyPhen-2**	**Mutation Taster**	**CADD[1]**
p.His32Arg	Neutral	Tolerated	Benign	Polymorphism	14.0
p.Lys35Arg	Neutral	Damaging	Benign	Polymorphism	21.5
p.Asn47Ser	Neutral	Damaging	Probably Damaging	Polymorphism	21.8
p.Arg48Trp	**Deleterious**	**Damaging**	**Possibly Damaging**	**Disease Causing**	**27.3**
p.Glu94X	**n/a**	**n/a**	**n/a**	**Disease Causing**	**37.0**
p.Arg102Gln	Neutral	Tolerated	Probably Damaging	Polymorphism	25.1
p.Arg102Trp	**Deleterious**	**Damaging**	**Possibly Damaging**	**Disease Causing**	**27.8**
p.Thr123Arg	**Deleterious**	**Damaging**	**Probably Damaging**	**Disease Causing**	**25.2**
p.Thr123Met	**Deleterious**	**Damaging**	**Possibly Damaging**	**Disease Causing**	4.0
p.Gly141Metfs*29	**n/a**	**n/a**	**n/a**	**Disease Causing**	**n/a**

[1]The CADD algorithm returns a quantitative prediction, with scores above 15 considered pathogenic. These varinats were collected from the literature; none of them were detected upon sequencing 56 cases in-house. Variants with at least two neutral predictions were deemed to be tolerated, the rest were deemed to be deleterious and highlighted in bold. Abbreviation is as follows: n/a not applicable.

Table 3.3.4. Prevalence of concomitant PV in *IL36RN* positive vs. *IL36RN* negative patients.

	Number of cases (%)	
Clinical Phenotype	***IL36RN* positive**[1]	***IL36RN* negative**
Isolated GPP	29 (56.86%)	52 (31.33%)
GPP with concomitant PV	22 (43.14%)	114 (68.67%)

[1]Homozygous, compound heterozygous, or heterozygous mutations

Participants with unknown PV status (n =16) were excluded from the analysis.

3.4 Discussion

The prevalence of PV among GPP patients markedly exceeds that observed in the general population, while no overlapping genetic factors have been identified between these disease phenotypes (Capon et al., 2012). However, experimental evidence - mostly obtained from animal studies - indicates that IL-36 cytokines contribute to the pathogenesis of PV. Blumberg et al. were the first to report that transgenic mice over-expressing *Il36a* in their keratinocytes show a psoriasis-like skin disorder, characterised by acanthosis, hyperkeratosis, and infiltration of inflammatory cells in the dermis and the epidermis. Importantly, the disease phenotype was more severe in animals that were deficient for *Il36rn*. Consistent with these results, Tortola et al. showed that *Il36rn* -/- mice experienced exacerbated symptoms of skin inflammation in an Imiquimod-induced model of psoriasis. Finally, a recent study by Milora et al. highlighted IL36α as a key driver of psoriasiform skin inflammation.

On the basis of the above observations, it was suggested that IL-36 blockade could be a novel therapeutic approach to the treatment of psoriasis (Tortola et al., 2012). This is not just a theoretical possibility, as an antibody targeting the IL-36 receptor had now been developed (Wolf and Ferris, 2014).

At the same time, it is important to bear in mind that the pathogenic role of IL-36 cytokines has not been investigated in human PV, as the only findings that are available are expression data indicating that the pathway agonists (IL-36α, IL-36β, IL-36γ) and antagonist (IL-36Ra) are up-regulated in psoriatic lesions (Blumberg et al., 2007; Carrier et al., 2011). Therefore, the goal of this study was to establish whether loss-of-function mutations of *IL36RN* confer PV susceptibility in humans.

This objective was pursued through case-control studies, which were specifically

designed to detect associations with common and rare variants.

The role of common alleles was investigated by re-examining the genotypes generated in a previous genome-wide association study of 2,600 PV patients and 5,700 controls. Despite evidence for adequate power and locus coverage, this analysis did not reveal any *IL36RN* changes that would confer risk for PV. Importantly, a number of GWAS have been carried out in recent years in various European and Asian populations (Yin et al., 2014; Tsoi et al., 2015), but none has generated evidence for association at the *IL36RN* locus. Thus, common *IL36RN* variants are unlikely to confer PV susceptibility.

The role of rare variants was initially examined in a re-sequencing study, where the coding and proximal promoter region of *IL36RN* were screened in 363 unrelated psoriasis cases, selected on the basis of a positive family history. No homozygous or compound heterozygous mutations were detected in any of these individuals. The p.Ser113Leu allele, which is the most frequent GPP mutation in Europeans, was the only deleterious change observed among the PV patients. It was found in the heterozygous state in two patients, but the allele frequency of the variant was not different in psoriasis cases compared to controls, nor was the change segregating with the disease in the relevant pedigrees. Therefore, it can be concluded that *IL36RN* mutations are not highly penetrant in PV. Importantly, the power calculations indicated that the lack of association between rare variants and PV was most likely not the consequence of limited sample size, although the possibility of coding changes with small GRR could not be excluded.

The issue of power was addressed by interrogating the results of a larger exome-wide study, including a total of 11,801 cases and 27,233 controls. When the frequency of rare *IL36RN* changes with pathogenic potential, was compared between PV cases and controls, no

significant differences were observed. While an association with variants that were not part of the genotyping platform cannot be formally ruled out, the likelihood that such markers were missed during the chip design is low, given that SNPs were selected based on the analysis of >12,000 exomes.

Of note, the association findings were complemented by a study of genotype-phenotype correlations, demonstrating that GPP patients with *IL36RN* mutations are at low risk of developing PV.

Taken together, the data presented in this chapter demonstrate that the most frequent disease gene for GPP is not associated with PV susceptibility. It is important to bear in mind, however, that the study only focused on *IL36RN* and was not designed to address the possibility that mutations in related genes (e.g. *IL36R*, encoding the IL-36 receptor) could be responsible for the up-regulation of IL-36 cytokines in psoriatic plaques. Alternatively, this phenomenon could be explained by the abnormal IL-23/Th17 signalling that underlies chronic inflammation in PV. In fact, IL-17 produced by Th17 cells can induce IL-36 secretion by keratinocytes (Carrier et al., 2011).

While the above hypotheses are both interesting, the current study shows that the mechanism whereby IL-36 signalling is disrupted in pustular psoriasis is specific to this disease. Further investigations will therefore be required to clarify whether IL-36 up-regulation contributes to the propagation of chronic skin inflammation in PV.

4 GENETIC ANALYSIS OF *CARD14* ALLELES IN DIFFERENT SUBTYPES OF PSORIASIS

A pathogenic role of *CARD14* has been demonstrated in familial PV by detecting mutations that segregated with the disease in two large pedigrees (Jordan et al., 2012). Deleterious changes within this locus were also found in patients with pityriasis rubra pilaris (PRP) (Fuchs-Talem et al., 2012), a skin disorder that has a similar presentation to PV (Fuchs-Talem et al., 2012). Finally, a small Japanese study revealed an association between generalised pustular psoriasis and a non-synonymous *CARD14* substitution (p.Asp176His) (Sugiura et al., 2014).

While these observations suggest the presence of an allelic series underlying the pathogenesis of various inflammatory dermatoses (Figure 4.1), most of the above findings had been subject to very limited follow-up at the time of the start of the study. Therefore, the aim was to systematically investigate the role of *CARD14* mutations in various psoriasis-related disorders.

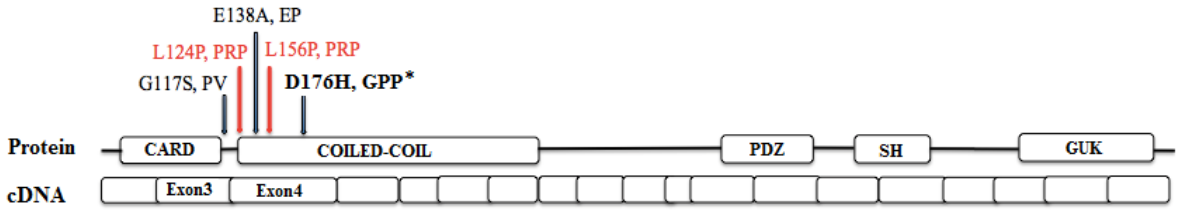

Figure 4.1. Localisation of the main *CARD14* mutations in the protein and cDNA sequence

Mutations were identified by Jordan et al., 2012; Fuchs-Telem et al., 2012; and Sugiura et al., 2014. The D176H mutation described in this chapter is indicated by an asterisk. The protein and cDNA sequences were obtained from Ensembl, while the diagram of the domain structure has been adapted from Scudiero et al., 2014.

Abbreviations are as follows: EP: erythrodermic psoriasis; GPP: Generalised Pustular Psoriasis; PRP: pityriasis rubra pilaris; PV: psoriasis vulgaris; G117S: p.Gly177Ser; E138A: p.Glu138Ala; L156P: p.Leu156Pro; D176H: p.Asp176His.

4.1 Case selection

A total of 416 unrelated patients were selected for the study. These individuals were affected by psoriasis vulgaris (n=159), pityriasis rubra pilaris (n=29), erythrodermic psoriasis (n=23), acral pustular psoriasis (Acrodermatitis Continua of Hallopeau, n=8; Palmar Plantar Pustulosis, n=92), or generalised pustular psoriasis (n=105) (Table 4.1.1). Importantly, all PV patients (Table 4.1.2) and six individuals with GPP (Methods section, Table 2.2.4) reported a positive family history of the disease. All the others were, to the best of our knowledge, isolated cases.

Table 4.1.1. Patient resource summary

Disease	N. of Cases screened	
	Exons 3 and 4	Entire coding region
Acral Pustular Psoriasis	100[1]	26[2]
Erythrodermic Psoriasis	23	20
Familial Psoriasis Vulgaris	159	16
Generalised Pustular Psoriasis	105	15
Pityriasis rubra pilaris	29	20
Total	**416**	**97**

[1]Including Palmar Plantar Pustulosis (n=92) and Acrodermatits continua of Hallopeau (n=8)

[2]Including Palmar Plantar Pustulosis (n=18) and Acrodermatits continua of Hallopeau (n=8)

Table 4.1.2. Familial PV cases screened for *CARD14* variants

	Number of affected individuals in the family					
	>5	5	4	3	2	**Total**
Number of families	12	10	29	58	50	159

4.2 Power calculations

Given that all published *CARD14* mutations map to exons 3 and 4 (Fuchs-Talem et al., 2012; Jordan et al., 2012), these genomic segments were screened in the entire study resource, while the rest of the coding region (exon 2, exons 5-23) was only examined in representative patient subsets (Table 4.1.1).

The power to detect rare sequence changes in the above datasets was estimated with an online binomial calculator. This demonstrated that in all patient resources, the analysis of exons 3 and 4 had sufficient power (>80%) to uncover mutations accounting for >5% of disease cases (Figure 4.2.1.A). Of note, power exceeded 95% in the acral pustular psoriasis, familial PV, and generalised pustular psoriasis datasets.

The samples screened for the entire *CARD14* coding region had sufficient power (>80% in erythrodermic psoriasis, generalised pustular psoriasis, psoriasis vulgaris, pityriasis rubra pilaris; >90% in acral pustular psoriasis) to detect changes presenting in >11% of disease cases (Figure 4.2.1.B).

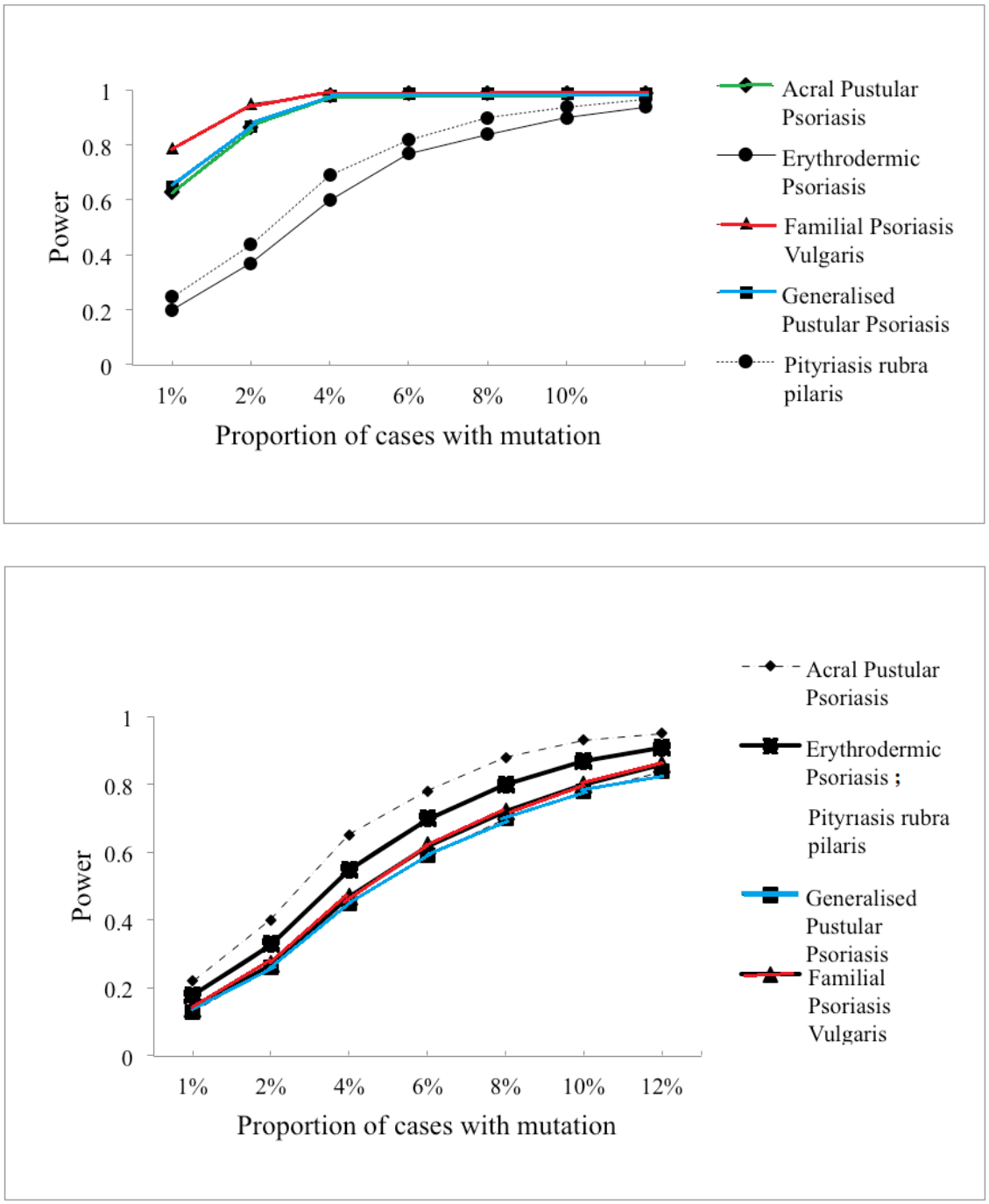

Figure 4.2.1. Power calculations for the analysis of exons 3-4 (top panel) or for the study of the whole coding region (lower panel)

4.3 Sanger sequencing of the *CARD14* coding region

4.3.1 Patients with familial PV, erythrodermic psoriasis, and pityriasis rubra pilaris

No bialellic (loss of function) mutations were detected in these patients, but three rare heterozygous variants were found (Table 4.3.1.1). The first was a novel p.Met119Arg substitution that was located just two amino acids away from the mutation (p.Gly117Ser) originally observed by Jordan et al. in familial PV. The second allele, a p.Ser200Asn change, was detected in four PV patients. Both amino acid changes however, were predicted to be tolerated by multiple algorithms (Table 4.3.1.1).

The third variant was a p.Gln136Lys substitution that was observed in one PRP patient and was predicted to have a pathogenic outcome (Table 4.3.1.1). A closer inspection of the case notes revealed that a differential diagnosis of erythrokeratoderma had been considered, and a p.Cys169Trp substitution had been detected in the *GJB4* gene (Common et al., 2005). Since the latter variant was also predicted to be deleterious (Table 4.3.1.2), it was not possible to draw any conclusion on the pathogenic role of the *CARD14* substitution.

Taken together, the above observations indicate that *CARD14* alleles are unlikely to account for a significant number of familial PV, pityriasis rubra pilaris or erythrodermic psoriasis cases.

Table 4.3.1.1. Rare non-synonymous *CARD14* variants detected in PRP and familial PV cases

Change (rs ID)	Patient phenotype	Pathogenicity prediction					
		SIFT	**Polyphen-2**	**PROVEAN**	**Mutation Taster**	**CADD [1]**	**CONSENSUS**
p.Met119Arg (novel)	PRP (n =1)	Tolerated	Benign	Neutral	Disease Causing	Damaging	NEUTRAL
p.Gln136Lys (novel)	PRP (n =1)	Damaging	Probably Damaging	Neutral	Disease Causing	Damaging	DAMAGING
p.Ser200Asn (rs114688446)	Familial PV (n =4)	Tolerated	Benign	Neutral	Polymorphism	Neutral	NEUTRAL

[1] CADD scores >15.0 are considered as evidence of pathogenicity. PRP: pityriasis rubra pilaris; PV: psoriasis vulgaris

Table 4.3.1.2. Pathogenicity prediction of the *GJB4* variant detected in a PRP patient

Change	**Pathogenicity prediction**					
	SIFT	**Polyphen-2**	**PROVEAN**	**Mutation Taster**	**CADD[1]**	**CONSENSUS**
p.Cys169Trp	Damaging	Probably damaging	Deleterious	Disease Causing	18.6	DAMAGING

[1] CADD scores >15.0 are considered as evidence of pathogenicity

4.3.2 Patients with pustular psoriasis

No bialellic mutations were detected in the patients with pustular phenotypes, but six rare heterozygous changes were observed (Table 4.3.2.1 and 4.3.2.2). These included two novel substitutions (p.Glu168Lys and p.Ala216Thr), two splice site variants (c.2283+11A>C and c.2569+4T>C), and the p.Ser200Asn allele that had been previously detected in the genome of four PV patients. Pathogenicity predictions however, indicated that all changes were likely to be neutral (Tables 4.3.2.1 and 4.3.2.2).

An Asparagine to Histidine substitution (c.526G>C; p.Asp176His) was detected in three unrelated cases of Chinese origin (Figure 4.3.2.1; Table 4.3.2.3). One of the patients (T014369) had a positive family history of the disease and the analysis of her maternal aunt (T014368), who was also affected by GPP, revealed that the variant was segregating with the phenotype. The frequency of the p.Asp176His allele was also increased in Chinese cases compared to population-matched controls (6.2% vs.1.0%; P=0.03).

Interestingly, the same p.Asp176His allele was described by Sugiura et al. in their analysis of a small GPP dataset ascertained in Japan. Thus, the association between p.Asp176His and generalised pustular psoriasis was further investigated in a meta-analysis of the Chinese sample examined here and the published Japanese resource. To increase the power of the study, *CARD14* sequence data was obtained for a further 322 Japanese healthy individuals (218 subjects analysed in house and 104 sequenced by the 1000 Genomes Consortium, JPT data set), which increased the size of the published control cohort by 4-fold.

The meta-analysis revealed that the Chinese and Japanese datasets were genetically similar (I^2=0%), and that *CARD14* mutations were associated with GPP in both samples

(P=8.4x10^{-5}; OR:6.4; 95% CI: 2.5-16.1) (Table 4.3.2.4).

In the Japanese population, the c.526G>C (p.Asp176His) base change occurs on the background of a specific *CARD14* ancestral haplotype (Sugiura et al., 2014). To investigate whether this also applied to the Chinese GPP cases described here, four *CARD14* tagging SNPs were typed in these patients (Methods 2.9.4). This showed that three of the subjects were homozygous, and one likely heterozygous for the same intragenic haplotype that was reported in the Japanese individuals with the p.Asp176His allele (Table 4.3.2.5). This suggests that the spread of the mutation in East Asia is likely the consequence of a founder effect.

Table 4.3.2.1. Rare non-synonymous *CARD14* variants detected in the pustular psoriasis study resource

Change (rs ID)	Patient phenotype	Pathogenicity prediction					
		SIFT	Polyphen-2	PROVEAN	Mutation Taster	CADD [1]	CONSENSUS
p.Glu168Lys (novel)	GPP (n =1)	Tolerated	Benign	Neutral	Polymorphism	Neutral	NEUTRAL
p.Asp176His (rs144475004)	GPP (n =3)	Damaging	Probably damaging	Neutral	Disease Causing	Damaging	DAMAGING
p.Ser200Asn (rs114688446)	PPP (n=2)	Tolerated	Benign	Neutral	Polymorphism	Neutral	NEUTRAL
p.Ala216Thr (novel)	GPP (n=1)	Tolerated	Benign	Neutral	Polymorphism	Neutral	NEUTRAL

[1] CADD scores >15.0 are considered as evidence of pathogenicity. GPP: generalised pustular psoriasis; PPP: palmar plantar pustulosis

Table 4.3.2.2. Rare *CARD14* splice site variants detected in the pustular psoriasis study resource

Change (rs ID)	**Patient phenotype**	**Pathogenicity prediction**					
		Max entropy	**Sroogle**	**Senepathy**	**MutationTaster**	**CADD score[1]**	**CONSENSUS**
c.2283+11A>C (rs9905662)	PPP (n=1)	Neutral	Neutral	Neutral	Polymorphism	Neutral	NEUTRAL
c.2569+4T>C (rs146678380)	PPP (n=1)	Neutral	Neutral	Neutral	Disease Causing	Neutral	NEUTRAL

[1] CADD scores >15.0 are considered as evidence of pathogenicity PPP: palmar plantar pustulosis

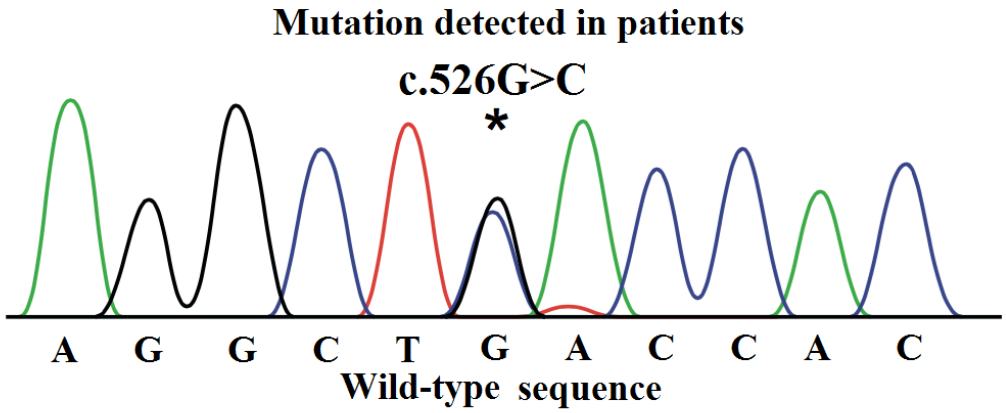

Figure 4.3.2.1. The NM_0204110.4:c.526G>C (NP_077015.2: p.Asp176His) change

The chromatogram was obtained after Sanger sequencing the coding region of *CARD14* in the DNA of case T014369. The Asp176His (c.526G>C) mutation is indicated by an asterisk, while the wild-type sequence can be seen below the chromatogram. The same change was detected in the heterozygous state in two further (unrelated) patients.

Table 4.3.2.3. Clinical features of GPP patients harbouring the p.Asp176His substitution

Patient ID	Sex	Age of onset	PV	PsA	Systemic involvement
T014368[1]	F	25	Yes	Yes	Fever >38C; neutrophil count >13x10^9/L
T014369	F	3	No	No	Fever >38C
T022932	F	13	No	No	-
T022956	M	38	Yes	Yes	CRP >100mg/L; neutrophil count >15x10^9/L

[1]Maternal aunt of T014369; abbreviations are as follows: PV, psoriasis vulgaris; PsA, Psoriatic Arthritis.

Table 4.3.2.4. Genetic analysis of the p.Asp176His variant

Ethnicity	**Allele counts (%)**		***P* value**
	Cases	**Controls**	
Japanese	4/42 (9.5%)	14/844 (1.7%)	0.008
Chinese	3/48 (6.2%)	4/400 (1.0%)	0.030
Meta-analysis			**8.4×10^{-5}**

P values were calculated with Chi-square test and meta-analysis (Methods 2.10.2).

Table 4.3.2.5. Intragenic SNP haplotypes of patients bearing the p.Asp176His allele

SNP ID	Patient ID							
	T014368[1]		T014369		T022932[2]		T022956	
rs4889991	**G**	G	**G**	G	**G**	A	**G**	G
rs2044103	**A**	A	**A**	A	**A**	G	**A**	A
rs3829612	**C**	C	**C**	C	**C**	T	**C**	C
rs8068433	**C**	C	**C**	C	**C**	T	**C**	C

[1]Maternal aunt of T014369; [2]genotypes are also compatible with an alternative haplotype configuration

4.4 *In-silico* characterization of the p.Asp176His allele

Prior to functional studies, the pathogenic potential of the p.Asp176His change was further assessed and compared with that of representative mutations, previously associated with familial PV (p.Gly117Ser), pityriasis rubra pilaris (p.Leu156Pro), and erythrodermic psoriasis (p.Glu138Ala) (Jordan et al., 2012; Fuchs-Telem et al., 2012).

An initial sequence alignment indicated that the evolutionary conservation of Asparagine 176 is comparable to that of other residues that are affected by deleterious changes (Figure 4.4.1).

Since exon 4 encodes the CARD14 coiled-coil (CC) domain, the NCOILS software was subsequently used to assess the potential effects of the various mutations. The amino acid change from a negatively charged Asparagine to a positively charged Histidine was predicted to decrease the likelihood of CC formation in the region surrounding residue 176 (Figure 4.4.2). Importantly a similar effect was observed for the p.Leu156Pro and p.Glu138Ala disease alleles (Figure 4.4.2).

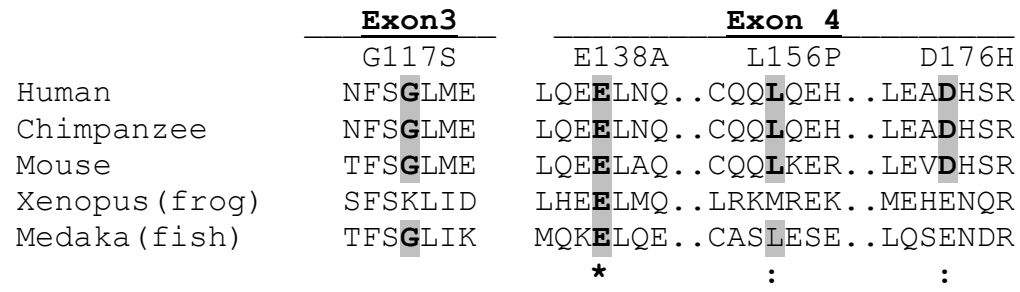

Figure 4.4.1. Evolutionary conservation of the p.Asp176His substitution and representative *CARD14* mutations

Conservation was assessed with ClustalW. Symbols are as follows: asterisks (*) indicate positions which have a single, fully conserved residue; colons (:) indicates conservation between groups of residues with strongly similar properties. G117S: p.Gly177Ser; E138A: p.Glu138Ala; L156P: p.Leu156Pro; D176H: p.Asp176His.

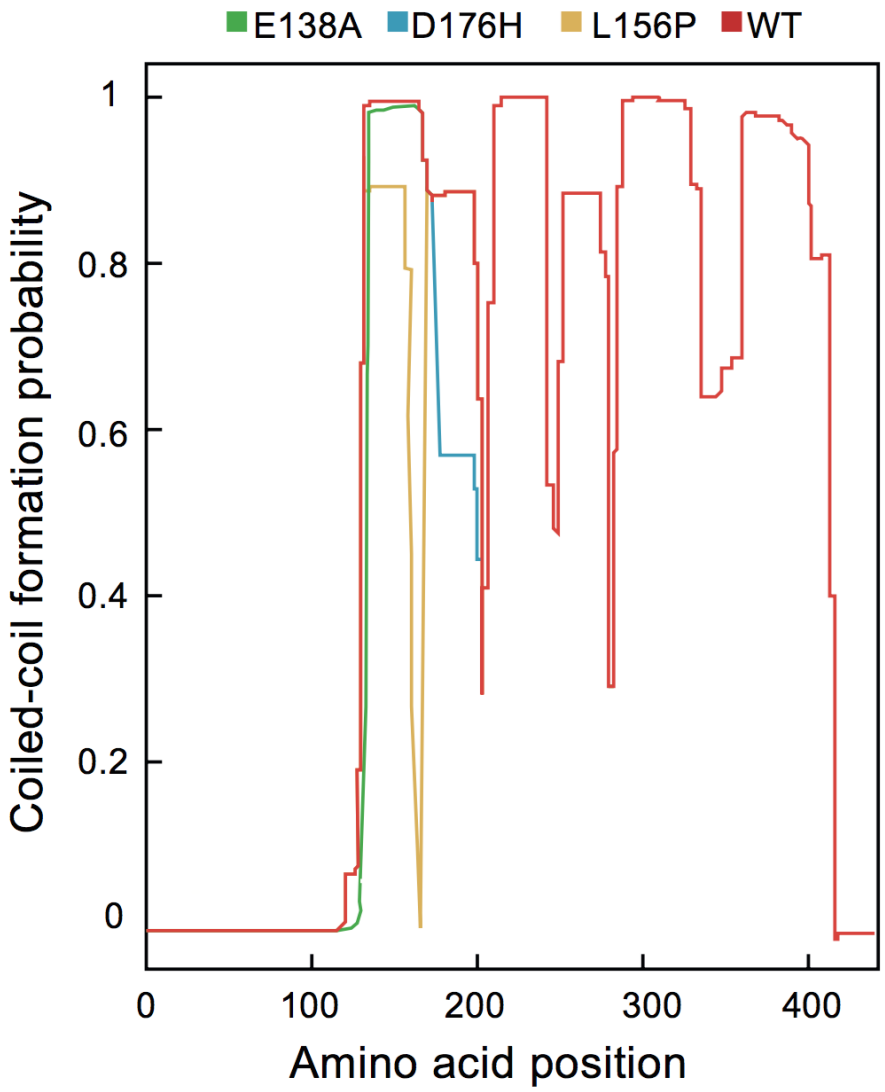

Figure 4.4.2. Predicted effects of *CARD14* mutations on coiled coil formation

Wild-type (WT) and mutant (E138A: p.Glu138Ala; L156P: p.Leu156Pro; D176H: p.Asp176His) CARD14 sequences were analysed with NCOILS to estimate the likelihood of CC formation along sliding windows of seven amino acids. This showed that all mutations were predicted to affect CC formation.

4.5 Experimental characterization of the p.Asp176His allele

4.5.1 Analysis of CARD14 aggregates by Western blotting

While it has been shown that *CARD14* mutations can up-regulate NF-κB signalling (Jordan et al., 2012), the mechanism whereby they result in such an outcome has not been investigated.

Of interest, gain-of-function mutations causing diffuse large B-cell lymphoma have been detected in the CC domain of *CARD11*, a *CARD14* paralogue (Lenz et al., 2008; Scudireo et al., 2013). Since these disease alleles cause spontaneous protein oligomerisation leading to constitutive NF-κB activation (Lenz et al., 2008), the possibility that *CARD14* mutations may act in a similar fashion was investigated.

Since the aim of the experiment was to investigate the aggregation of wild-type and mutant proteins (rather than dissecting the consequences of disease alleles on keratinocyte signalling), all the assays were carried out in HEK293 cells. Cultures were transfected with wild type and mutant FLAG-*CARD14* constructs and the accumulation of recombinant protein was measured by western blotting, using an anti-FLAG antibody. An initial assessment of whole-cell extracts confirmed that all constructs were expressed at comparable levels (Figure 4.5.1.1). After that, the soluble and insoluble factions of the cell lysates were examined in separate experiments. The analysis of soluble extracts showed that the p.Asp176His change was associated with a statistically significant decrease in the accumulation of free CARD14 (Figure 4.5.1.2). A similar effect was observed for the p.Leu156Pro and p.Glu138Ala mutations. Conversely, the analysis of the insoluble fraction demonstrated that the transfection of mutant cDNAs caused a marked increase in the accumulation of CARD14 aggregates, compared to the over-expression of wild type constructs (Figure 4.5.1.3).

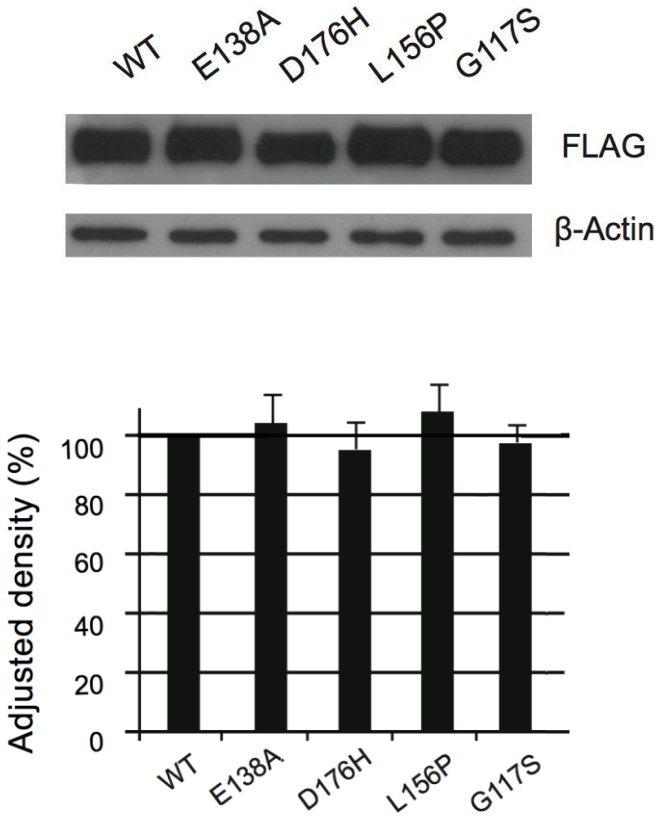

Figure 4.5.1.1. Western blotting of total cell lysates

HEK293 cells were transfected with wild-type or mutant FLAG-CARD14 constructs and the expression of recombinant proteins was visualised with an anti-FLAG antibody. The image is representative of the results obtained in two independent experiments. . The densitometry data (mean ±SD of measurements obtained in two independent experiments) were analysed using one-way ANOVA, followed by a Dunnett's post-test. WT: Wild-type; E138A: p.Glu138Ala; L156P: p.Leu156Pro; D176H: p.Asp176His.

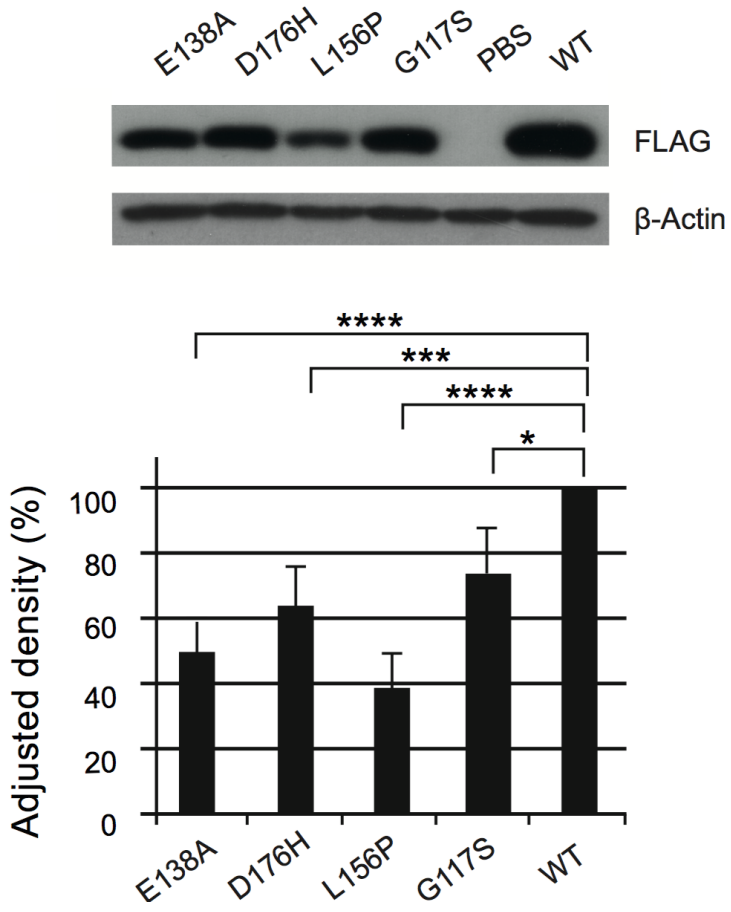

Figure 4.5.1.2. Western blotting of soluble proteins

HEK293 cells were transfected with wild-type and mutant FLAG-CARD14 constructs and the soluble fraction of whole-cell lysates was isolated by centrifugation. The accumulation of recombinant proteins was visualised with an anti-FLAG antibody and quantified by densitometry, normalising the intensity of each band to the expression of β-actin. The image is representative of the results obtained in four independent experiments. WT: Wild-type; E138A: p.Glu138Ala; L156P: p.Leu156Pro; D176H: p.Asp176His. Asterisks represent the following P values: *P≤0.05; **P≤0.01; ***P≤0.001; ****P≤0.0001 (one-way ANOVA, followed by Dunnett's post-test, error bars represent standard deviations).

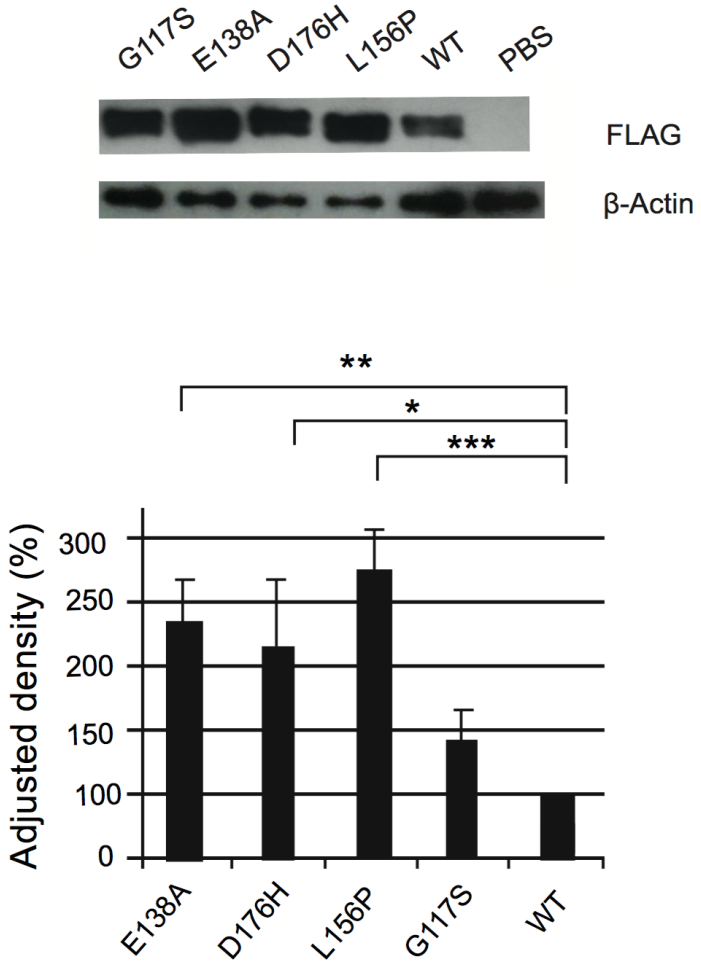

Figure 4.5.1.3. Western blotting of insoluble proteins

HEK293 cells were transfected with wild-type and mutant FLAG-CARD14 constructs an the insoluble fraction of whole-cell extracts was isolated by centrifugation. The accumulation of recombinant proteins was visualised with an anti-FLAG antibody and quantified by densitometry, normalising the intensity of each band to the expression of of β-actin. The image is representative of the results obtained in three independent experiments. WT: Wild-type; E138A: p.Glu138Ala; L156P: p.Leu156Pro; D176H: p.Asp176His. Asterisks represent the following P values: *P≤0.05; **P≤0.01; ***P≤0.001 (one-way ANOVA, followed by Dunnett's post-test, error bars represent standard deviations).

4.6 Discussion

CARD14 belongs to a family of three proteins: CARMA1/CARD11; CARMA2/CARD14 and CARMA3/CARD10 that promote NF-κB signalling downstream of TRAF2 (Scudiero et al., 2014). CARMAs show high sequence similarities given that they all consist of a caspase activation and recruitment domain **(**CARD), Coiled-coil domain, Post synaptic density Drosophila disc large tumor suppressor Zonula occludens-1 protein (PDZ), SRC Homology 3 (SH3), and guanylate kinases (GUK) domains (Scudiero et al., 2014). Although CARD14 is the least studied among the three CARMA proteins, the function of the above motifs has been investigated in CARMA1 and 3:

PDZ domains play an important role in organizing multiprotein signalling complexes, while the SH3, GUK, and CARD motifs are required for the oligomerisation of CARMA proteins (Baruch and Wendell, 2011; Hara et al., 2015; Scudiero et al., 2011; Scudiero et al., 2014). The Coiled-coil part is also of crutial importance for signal transduction given that it is involved in binding to downstream signalling molecules (Scudiero et al., 2014; Bertin et al., 2014; Lamason et al., 2011).

Inflammatory stimuli - e.g. TNF or T Cell Receptor engagement- cause the phosphorylation of these proteins by phospholipase C or protein kinase C, and their subsequent oligomerisation. Such modifications enable the recruitment of Bcl10, MALT1, and TRAF2/6 leading to the formation of a multi-protein complex that drives NF-κB signalling (Bertin et al., 2001; Scudeiro et al., 2011; Xie, 2013). Recent studies showed that the latter two molecules activate the pathway independently, through a distinct mechanism, likely upon different stimuli such as the yeast cell-wall derived zymosan in case of MALT1, and TNF-α in case of the TRAFs (Afonina et al., 2016; Scuediero et al., 2011). Of note, CARD14 and the complex described above also regulate the p38/JNK axis (Afonina et al.,

2016).

The association of common *CARD14* variants with PV is well established and was confirmed in several large-scale studies (Tsoi et al., 2012; Chen et al., 2014). Rare gain-of-function *CARD14* mutations were also detected in familial forms of PV and PRP (Jordan et al., 2012; Fuchs-Telem et al., 2012). Moreover, Sugiura et al. described a recurrent Asparagine to Histidine substitution (p.Asp176His) in a number of *IL36RN*-negative GPP patients. However, the size of the latter study was limited, and the observations made in PV and PRP datasets were only followed-up in small samples of non-European descent (Ammar et al., 2013; Eytan et al., 2014).

Hence, the aim of this study was to further assess the prevalence of *CARD14* mutations in the above phenotypes and in erythrodermic psoriasis, one of the most severe subtypes of the disease (Griffiths and Barker, 2008). Given that all previously described *CARD14* mutations map to exons 3 and 4 (Jordan et al., 2012; Fuchs-Telem et al., 2012), these coding regions were prioritised in the project. Importantly, Bertin et al. reported that the domains encoded by these exons (CARD region and coiled-coil) are necessary for cell signalling by CARMA proteins, unlike the C-terminal motifs, which are not required for NF-κB activation.

No disease alleles were detected in individuals affected by familial PV (n=159). Of note, these patients were not screened for HLA-Cw6, which is the major susceptibility determinant for psoriasis vulgaris (Nair et al., 2006). Given that the two mutation bearing families originally described by Jordan et al. were Cw6-negative, it is possible that the inclusion of Cw6-positive cases may have affected the outcome of this study. It is also theoretically possible that disease-causing mutations may reside outside of exons 3-4, in the regions that were only examined in a subset of cases. It has to be emphasised, however, that

even this smaller dataset had sufficient power (>80%) to detect changes accounting for more than 10% of cases.

The data presented here are in accordance with the results of a recent study, which also failed to detect an association between deleterious changes in *CARD14* and the progression of PV in European patients (Ammar et al., 2015). Of note, the same authors identified various *CARD14* mutations (p.Gly117Ser; p.Arg69Trp; p.Glu197Lys; p.Glu197Lys; c.1356+5G>A; p.Leu350Pro; p.Thr420Ala) in PV cases of Tunisian descent, suggesting that *CARD14*-driven familial psoriasis may be more prevalent in non-Caucasian populations (Ammar et al., 2015).

The mutation screen was also negative in Acral pustular psoriasis (APP), Erythrodermic psoris (EP), Pityriasis rubra pilaris (PRP), although it has to be emphasised that the patient resource was smaller in the latter two disease types (n=29 and n=23; respectively).

The PRP patients were all sporadic cases, so that the lack of disease alleles in this dataset is in keeping with the results of other studies (Eytan et al., 2014; Hong et al., 2014) and indicates that the gene is specifically mutated in familial forms of the disease.

The analysis of the generalised pustular psoriasis resource identified the same p.Asp176His substitution previously described in a small Japanese sample (Sugiura et al., 2014) and demonstrated that the change was significantly associated with the disease in Asian populations. The p.Asp176His allele was not found in any of the patients with acral pustular psoriasis, but these were all of European descent, so that the lack of association could simply reflect the very low allele frequency of the substitution (MAF=0.0006) among Caucasians. In fact, Mössner et al. recently described 2 out of 34 individuals with palmar plantar pustulosis,

who harboured the p.Asp176His mutation. Of note, these cases had all been recruited within the Estonian population, which is characterised by significant degree of Asian admixture (Kasperavicute et al., 2004). Thus, the association between *CARD14* and pustular disease would seem specific to the p.Asp176His allele, as it is only observed in those ethnic groups where this change is present.

The functional impact of the p.Asp176His allele was assessed in the subsequent phase of the study. Of note, the pathogenic potential of previously detected *CARD14* mutations has been extensively investigated. For instance, Jordan et al. showed that the transfection of *CARD14* mutant constructs into HEK293 cells caused an increase in the expression of several NF-κB driven, pro-inflammatory genes - e.g *CCL20, IL8* and *IL36G*. These observations were in keeping with those made in the keratinocytes of mutation bearing patients, where the same loci were found to be up-regulated (Jordan et al., 2012). Fuchs-Telem et al. also investigated *CARD14* mutations in PRP and reported that individuals harbouring deleterious changes showed up-regulation of *IL1B* and *CCL20* in their skin lesions. However, the mechanism whereby *CARD14* disease alleles lead to such consequences has not been studied. Thus, the additional aim of the project was to elucidate the nature of this process.

Since the other two CARMA proteins had been more thoroughly investigated, a working hypothesis was generated, based on observations obtained in the analysis of *CARD11* mutations. Lamason et al. showed that the coiled-coil (CC) and CARD domains of CARD11 keep the protein in a closed, inactive state through intra-molecular binding. Upon receptor signalling - e.g TCR or BCR engagement-, the protein is phosphorylated, which disrupts the CC-CARD interaction, and leads to a conformation change. The protein opens up, and becomes active by exposing the CARD and CC regions. While the CARD domain mediates the interaction with downstream signalling molecules such as Bcl10, the CC enables the

formation of protein oligomers. Most importantly, Lamason et al. showed that oncogenic mutations in the CC domain of CARD11 prevented intra-molecular interactions with the inhibitory region, leading to spontaneous protein oligomerisation and constitutive NF-κB activation. Given the high degree of structure homology between CARD14 and CARD11 (Scudiero et al., 2011), it was hypothesised that *CARD14* mutations may also result in abnormal protein oligomerisation.

This hypothesis was tested in western blot which demonstrated that the p.Asp176His, p.Leu156Pro and p.Glu138Ala mutations were all associated with increased accumulation of CARD14 aggregates, indicating that mutant CARD14 proteins tend to spontaneously oligomerise. The impact of the p.Asp176His substitution is also comparable to that of previously characterised mutations. Of note, this outcome was consistent with the results of bioinformatic predictions, which validates the accuracy of the NCOILS software and suggests that the pathogenic potential of further CARD14 mutations could be assessed *in-silico*, using this effective tool. In fact, Howes et al. also reported recently that disease causing *CARD14* mutations led to spontaneous NF-κB activation. Although the p.Asp176His change was not included in their, overall their findings supported the above observations.

What remains to be understood is how the various mutations can have the same immediate consequences – spontaneous protein oligomerisation leading to abnormal NF-κB signalling – but lead to different diseases. Further studies will be needed to uncover whether patients affected by clinically distinct conditions also harbour additional deleterious changes in their genomes – e.g. in genes encoding molecules that act downstream of CARD14.

The analysis of larger datasets will also be needed to investigate the correlation between *CARD14* mutations and PV concurrence in GPP, and more broadly to define

genotype-phenotype correlations, so that the analysis of *CARD14* alleles can aid the stratification of pustular psoriasis patient resources.

5 IDENTIFICATION OF NOVEL CANDIDATE GENES BY WHOLE-EXOME SEQUENCING

5.1 Case selection

In order to find additional genes – besides *IL36RN, AP1S3*, and *CARD14* – underlying pustular psoriasis, whole-exome sequencing was undertaken in a small number of patients who did not carry mutations in the aforementioned loci. To maximise the likelihood of identifying recurrent disease alleles, cases were selected to form a phenotypically homogeneous cohort. The foremost criterion was the presence of severe disease manifesting at an early age (<35 years old). Patients also had to satisfy at least one of the following conditions: a) originate from a consanguineous union; b) have a positive family history of GPP; c) demonstrate multiple episodes of systemic inflammation. Such criteria defined a panel of twelve individuals, including ten females and two males (Table 5.1.1), a composition that is consistent with a well-documented sex bias in the incidence of GPP (Griffiths and Barker, 2007; Naldi and Gambini, 2007). Two of the selected patients were born into consanguineous marriages (Figure 5.1.1), while eight had a positive family history of GPP (Figure 5.1.2).

All selected cases had concomitant PV or close relatives that were affected by the disease. Therefore, they were screened for the rs4406273-A allele, which is a surrogate of HLA-Cw6 (Stuart et al., 2015), the major genetic determinant of psoriasis vulgaris. All twelve individuals harboured the rs4406273-G variant in the homozygous state, which demonstrated that their disease was not associated with HLA-Cw6.

In the most informative pedigree (23GPP; Figure 5.1.2. b) the involvement of the MHC region was further excluded by genotyping a chromosome 6p21 microsatellite (D6S273; Figure 5.1.3).

Table 5.1.1. Cases selected for whole-exome sequencing

ID	Gender	Ethnicity	Age of onset	PV	PsA	Markers of systemic inflammation
T009425	Female	Romany	9	Yes	No	Fever>38°C; CRP>100mg/l; ESR> 50mm/hr
2GPP1	Male	Indian	28	Yes	No	Fever > 38°C; Neutrophilia[a]
T002229	Female	British	19	Yes	No	Fever>38°C; CRP>100mg/l; ESR> 50mm/hr; Neutrophilia[a]
T003673	Female	British	29	Yes	No	Fever>38°C; CRP>100mg/l; ESR> 50mm/hr; Neutrophilia[a]
8GPP1	Female	Chinese	30	Yes	Yes	ESR> 50mm/hr
8GPP2	Female	Chinese	21	No	Yes	none
41GPP1	Female	Malay	25	Yes	No	none
41GPP2	Female	Malay	35	No	No	Fever > 38°C; CRP>100mg/l; ESR> 50mm/hr
23GPP1	Female	Malay	31	Yes	Yes	Fever > 38°C; Neutrophilia[a]
23GPP2	Female	Malay	12	Yes	No	Fever > 38°C; CRP>100mg/l
38GPP1	Male	Malay	27	Yes	Yes	Fever > 38°C; Neutrophilia[a]
38GPP2	Female	Malay	25	Yes	No	Fever > 38°C; CRP > 100mg/l; ESR> 50mm/hr; Neutrophilia[a]

Abbreviations are as follows: CRP. C-Reactive Protein; ESR. Erythrocyte Sedimentation Rate; PsA. Psoriatic arthritis; PV. Psoriasis vulgaris. [a]Neutrophilia: neutrophil count >$15x10^9$/L.

a)

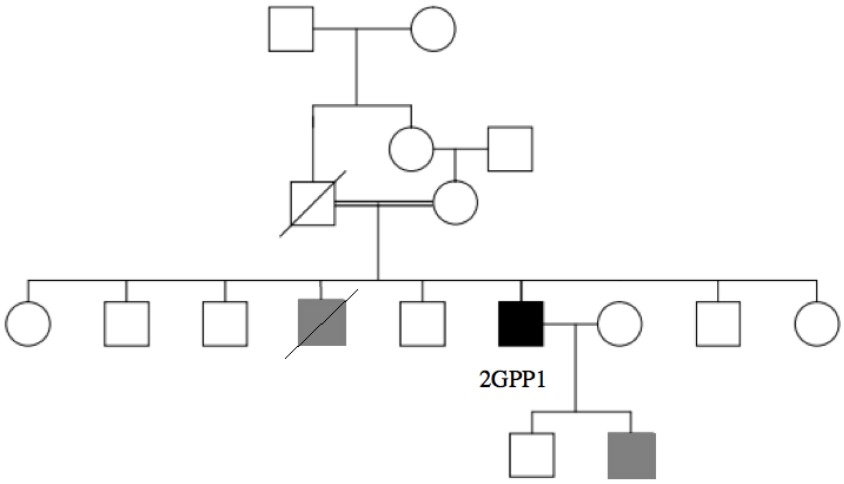

b)

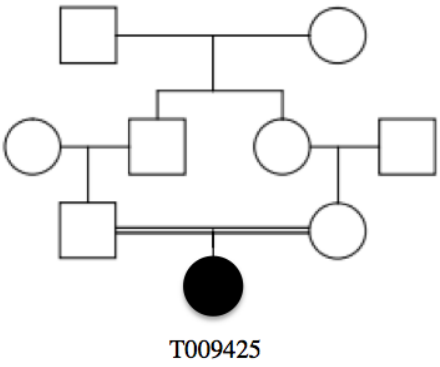

Figure 5.1.1. Pedigrees of patients born into consanguineous marriages

Individual 2GPP1 (a) and T009425 (b) were selected for whole-exome sequencing. Grey symbols refer to family members who were only affected by PV. DNA was only available for patients indicated with T numbers.

a)

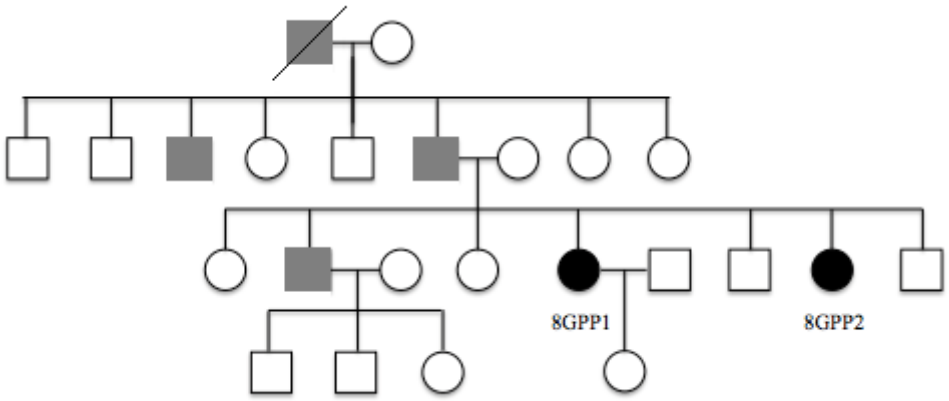
8GPP1
8GPP2

b)

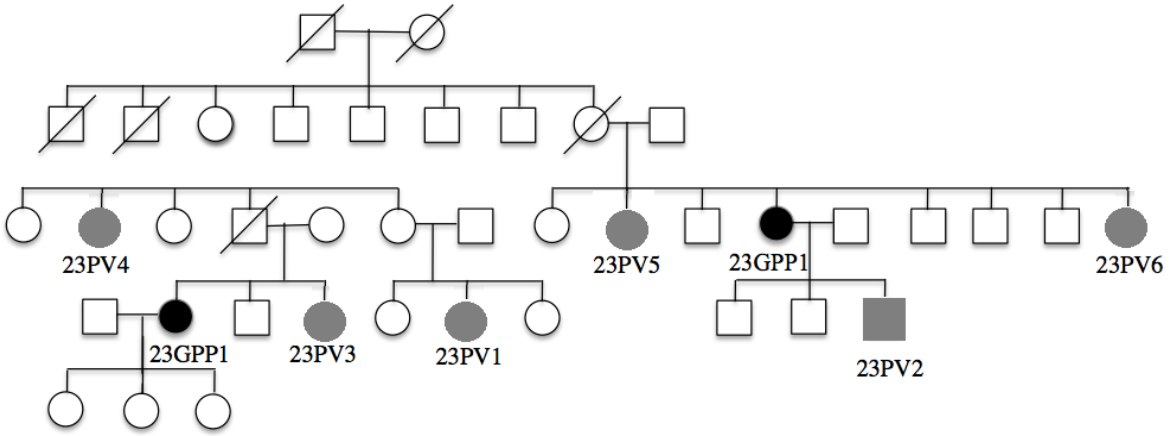
23PV4
23GPP1
23PV3
23PV1
23PV5
23GPP1
23PV2
23PV6

c)

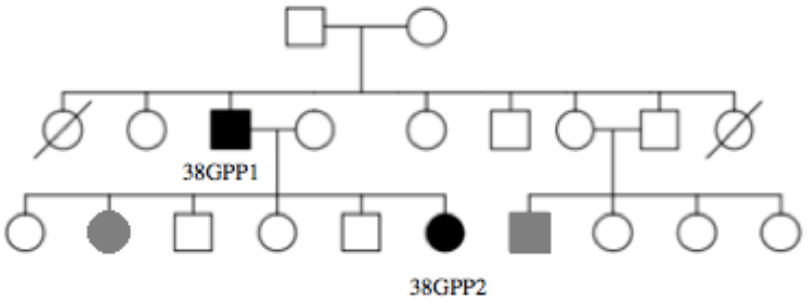

d)

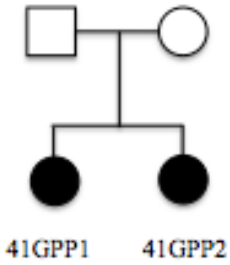

Figure 5.1.2. Pedigrees of patients with a family history of psoriasis

Individuals 8GPP1 and 8GPP2 (a), 23GPP1 and 23GPP2 (b), 38GPP1 and 38GPP2 (c), 41GPP1 and 41GPP2 (d) were selected for whole-exome sequencing. Grey symbols refer to family members who were only affected by PV. DNA was only available for patients indicated with PV or GPP numbers.

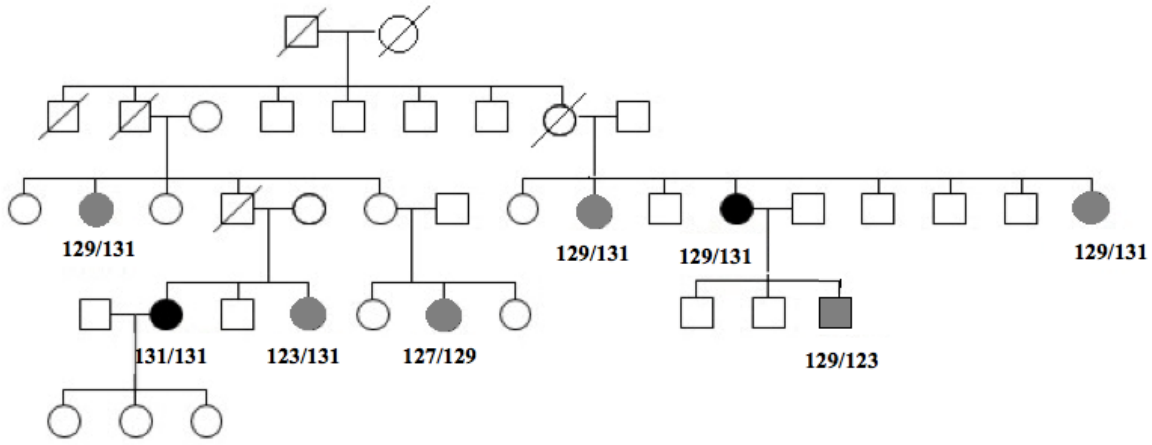

Figure 5.1.3. Family 23GPP is not linked to the Major Histocompatibility Complex

Marker D6S273 (AFM142xh6) does not segregate with the disease, as can be deduced by comparing the genotypes of the individuals from the fourth generation. Black symbols represent GPP, while grey symbols refer to family members who were only affected by PV. DNA was not available for healthy individuals.

To maximise the power, the study resource was expanded to include five severe cases of acrodermatitis continua of Hallopeau that had been whole-exome sequenced prior to the onset of the project (Table 5.1.2). These patients, who did not carry any deleterious changes at known disease genes, were analysed together with the generalised pustular psoriasis subjects, based on the well-documented genetic overlap between GPP and ACH (Setta-Kaffetzi et al., 2013; Setta-Kaffetzi et al., 2014).

Table 5.1.2. Previously whole-exome sequenced samples that were included in the analysis of variant profiles.

ID	Gender	Ethnicity	Age at onset	PV	PsA
S0655	F	Polish	57	Y	N
S0657	F	Swiss	82	N	N
S0658	M	Swiss	49	N	N
S0660	F	Swiss	56	N	Y
S0661	F	British	39	N	N

Abbreviations are as follows: PsA. Psoriatic arthritis; PV. Psoriasis vulgaris.

5.2 Coverage statistics

For the GPP cases, the mean sequence coverage across the exome ranged from 79.3x to 150.4x, with more than 85% of CCDS bases covered at a depth of at least 20x (Table 5.2.1). An average of 25,185 variants per sample (range: 24,169 to 25,861) were identified (Table 5.2.2).

In the previously sequenced ACH cases, the mean sequence coverage across the exome ranged from 115.8x to 175.3x, with more than 90% of CCDS bases covered at a depth of at least 20x (Setta-Kafetzi et al., 2014). The average number of variants was 24,446 per sample (range: 24,297-24,650, Table 5.2.3).

Table 5.2.1. Coverage of target exons

	2GPP1	T009425	T00229	T003673	8GPP1	8GPP2
Mean Coverage (%)	79.30	132.43	138.41	150.38	100.96	109.78
CCDS bases >1	98.08	98.3	98.4	98.44	98.9	98.92
CCDS bases >5	95.79	96.72	96.88	96.81	98.06	98.14
CCDS bases >10	92.92	95.3	95.6	95.45	97.11	97.28
CCDS bases >20	85.57	91.8	92.38	92.3	94.26	94.84
	23GPP1	**23GPP2**	**38GPP1**	**38GPP2**	**41GPP1**	**41GPP2**
Mean coverage (%)	127.45	94.63	107.48	100.74	112.85	112.9
CCDS bases >1	98.42	98.86	95.38	98.11	98.93	98.92
CCDS bases >5	96.8	97.98	100.03	96.27	98.15	98.15
CCDS bases >10	95.34	96.93	99.51	94.22	97.32	97.33
CCDS bases >20	91.69	93.78	99.39	89.02	94.98	94.98

Abbreviation: CCDS; Consensus coding sequences.

Table 5.2.2. Number of sequence variants detected in each GPP patinet

2GPP1		**T009425**		**T002229**		**T003673**		**8GPP1**		**8GPP2**	
All	24,169	*All*	24,336	*All*	24,670	*All*	24.928	*All*	25,767	*All*	25,729
HOM	10,316	*HOM*	10,341	*HOM*	9,634	*HOM*	9,665	*HOM*	10,499	*HOM*	10,667
rare NS	80	*rare NS*	80	*rare NS*	12	*rare NS*	19	*rare NS*	42	*rare NS*	49
HET	13,853	*HET*	13,995	*HET*	15,036	*HET*	15,263	*HET*	15,268	*HET*	15,062
rare NS	1,294	*rare NS*	1,063	*rare NS*	883	*rare NS*	911	*rare NS*	1,457	*rare NS*	1,444
rare CH	43	*rare CH*	44	*rare CH*	34	*rare CH*	36	*rare CH*	44	*rare CH*	40
23GPP1		**23GPP2**		**41GPP1**		**41GPP2**		**38GPP2**		**38GPP1**	
All	25,240	*All*	25,771	*All*	25,861	*All*	25,782	*All*	24,697	*All*	25,665
HOM	10,036	*HOM*	10,517	*HOM*	11,099	*HOM*	11,014	*HOM*	10,306	*HOM*	10,407
rare NS	33	*rare NS*	41	*rare NS*	31	*rare NS*	47	*rare NS*	34	*rare NS*	37
HET	15,204	*HET*	15,254	*HET*	14,762	*HET*	14,768	*HET*	14,191	*HET*	14,290
rare NS	1,359	*rare NS*	1,482	*rare NS*	1,323	*rare NS*	1,273	*rare NS*	1,347	*rare NS*	1,348
rare CH	42	*rare CH*	44	*rare CH*	47	*rare CH*	45	*rare CH*	40	*rare CH*	42

Abbreviations are as follows: HOM, homozygous; HET, heterozygous; CH, possible compound heterozygous; NS, not synonymous. The term “rare” refers to variants with a minor allele frequency< 0.015.

Table 5.2.3. Number of sequence variants detected in each ACH patient

S0655		**S0657**		**S0658**		**S0660**		**S0661**	
All	24,307	*All*	24,490	*All*	24,297	*All*	24,336	*All*	24,997
HOM	9,530	*HOM*	9,329	*HOM*	9,567	*HOM*	9,497	*HOM*	9,356
rare NS	16	*rare NS*	17	*rare NS*	15	*rare NS*	14	*rare NS*	17
HET	14,776	*HET*	15,160	*HET*	14,729	*HET*	15,006	*HET*	14,998
rare NS	632	*rare NS*	773	*rare NS*	690	*rare NS*	657	*rare NS*	679
rare CH	33	*rare CH*	31	*rare CH*	34	*rare CH*	30	*rare CH*	31

Abbreviations are as follows: HOM, homozygous; HET, heterozygous; CH, possible compound heterozygous; NS, not synonymous. The term “rare” refers to variants with a minor allele frequency< 0.015.

5.3 Allocation of samples to distinct analysis groups

The whole-exome sequenced samples were allocated to two analysis groups, dominant and recessive, based on disease recurrence and/or parental relatedness (Table 5.3).

The variant profiles of the two individuals born into consanguineous marriages were studied under a recessive model, based on the hypothesis that they harboured autozygous disease alleles. The four patients originating from families 23GPP and 38GPP were examined assuming dominant inheritance, which was inferred based on the pedigree structure. Conversely, the pattern of disease segregation in families 8GPP and 41GPP was compatible with recessive inheritance but also with the presence of a dominant allele showing reduced penetrance (Figure 5.1.2). Thus, the sequence data was analysed with both models. The same approach was applied to the isolated cases, which could have arisen as the result of recessive or dominant mutations (Table 5.3).

Table 5.3. Allocation of patients to the two analysis groups

Patient classification	ID	Analysis group	
		Recessive	Dominant
Offspring of a consanguineous union	T009425	✓	
	2GPP1	✓	
Isolated case	T002229	✓	✓
	T003673	✓	✓
	S0655	✓	✓
	S0657	✓	✓
	S0658	✓	✓
	S0660	✓	✓
	S0661	✓	✓
Familial case	8GPP1	✓	✓
	8GPP2	✓	✓
	41GPP1	✓	✓
	41GPP2	✓	✓
	23GPP1		✓
	23GPP2		✓
	38GPP1		✓
	38GPP2		✓

5.4 Analysis of recessive cases

5.4.1 Analysis of the entire dataset

The sequence variant profiles were filtered for rare (MAF ≤ 0.015), bialellic changes that were classified as deleterious by at least four out of five pathogenicity prediction tools. The haplotypes spanning homozygosity regions >2Mb were considered identical by descent (autosygous) as opposed to identical by status (Methods 2.9.6) (Alsalem et al., 2013; McQuillan et al., 2008). Hence, variants lying in such regions were further prioritised. The sequence changes that met these criteria were then compared across samples, searching for genes that were mutated in multiple individuals (Figure 5.4.1).

This process uncovered a variant in *ARHGAP11A* (rs140472511, p.Asp333His), which was found in the homozygous state in case T009425 and in the heterozygous state in S0658 (Table 5.4.1). The Asparagine to Histidine substitution was predicted to be deleterious by all online tools used in the study, and its frequency in the British control population was < 0.1%.

A closer inspection of the *ARHGAP11A* locus revealed that four of the coding exons were not covered by exome sequence reads, in any of the samples. Therefore, it was hypothesised that S0658 may harbour a second, as yet undetected mutation.

To explore this possibility and uncover additional pathogenic changes at this locus, exons 4-7 of *ARHGAP11A* were Sanger sequenced in all the samples from the recessive analysis group. No further mutations were observed in S0658, or in any of the other subjects, arguing against the notion that *ARHGAP11A* may be a recessive locus for the disease, although the possibility of a second mutation in non-coding regions cannot be excluded.

No other gene harboured bialellic mutations in more than one affected individual, indicating the presence of substantial genetic heterogeneity.

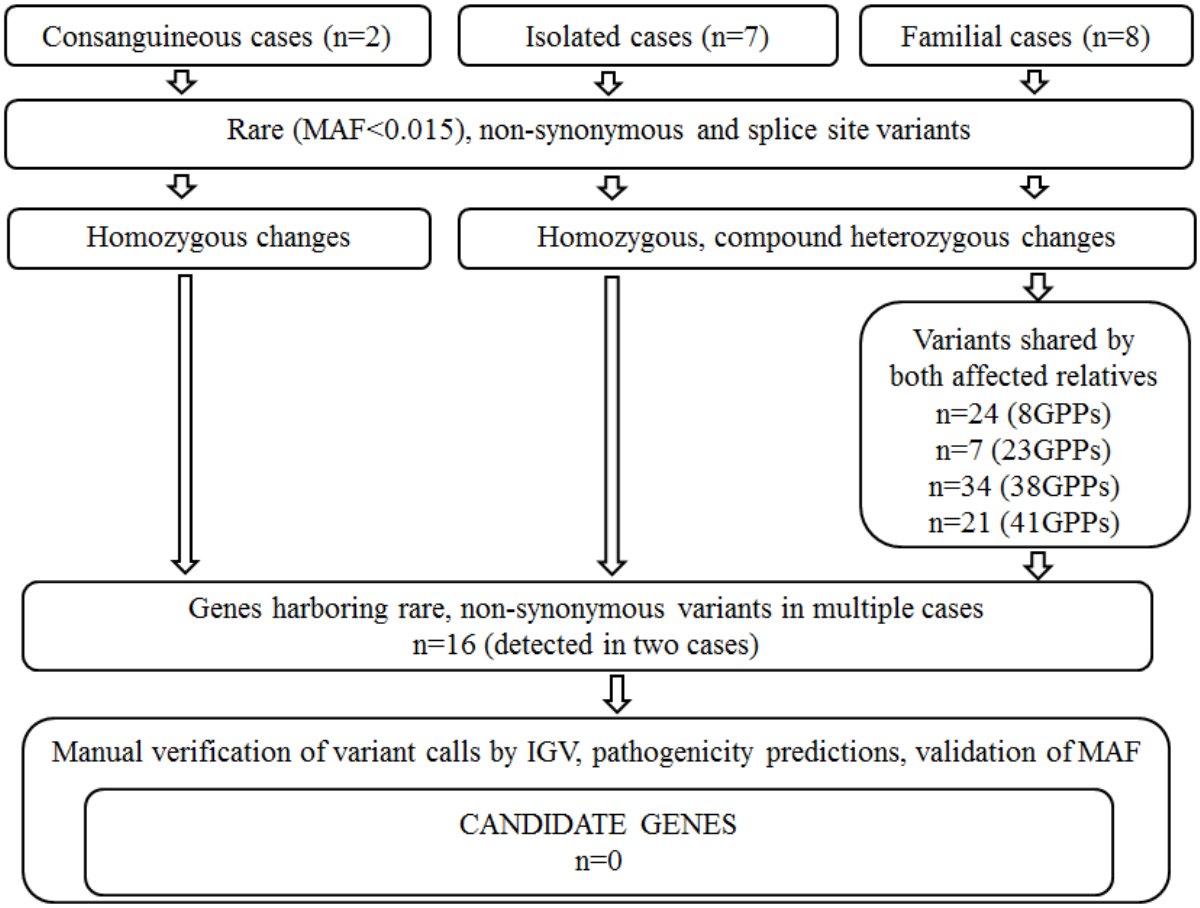

Figure 5.4.1. Filtering steps in the analysis of recessive cases

The filtering process is described in detail in section 2.9.6 of the Methods. The numbers of rare, biallelic changes detected in the patients are summarised in Tables 5.2.2 and 5.2.3.

Table 5.4.1. The *ARHGAP11A* variant emerging from the initial recessive analysis

Sample ID	Variant	Pathogenicity predictions					Outcome of follow-up
		SIFT	PROVEAN	PolyPhen-2	MutationTaster	CADD[1]	
T009425 (HOM)	p.Asp333His rs140472511	Deleterious	Damaging	Probably Damaging	Disease Causing	23.4	Locus Excluded
S0658(HET)							

[1]The CADD algorithm returns a quantitative prediction and scores above 15 are considered pathogenic. Abbreviations are as follows: HOM, homozygous; HET, heterozygous.

5.4.2 Analysis of patients born into consanguineous marriages

Given that no genes were found to harbour biallelic mutations in multiple cases, candidates were next selected from individual pedigrees. The power to detect disease alleles was highest in the offspring of consanguineous unions; therefore, individuals T009425 and 2GPP1 became the focus of these analyses.

Based on the hypothesis that the probands had inherited autozygous disease allele, an additional filtering step was introduced by prioritising variants that lie in regions of homozygosity.

In individual T009425, who originated from a Roma community where consanguineous unions were reported on many occasions, there were numerous homozygosity clusters. Thus the number of damaging changes lying in these regions was elevated (Table 5.4.2), making it difficult to prioritize any candidate for further examination.

The filtering strategy was more successful in individual 2GPP1, as rare variants with deleterious potential were only identified in *MAPKBP1, DOCK8,* and *STOX1* (Table 5.4.2). Importantly, all three genes are expressed in disease relevant cell types (skin and/or in immune cells) and participate in inflammatory processes. *STOX1* encodes a transcription factor regulating TNSF10/TRAIL (Rigourd et al., 2008), while *DOCK8* is a disease gene for the immune deficiency known as hyper-IgE syndrome (Aydin et al., 2015), and *MAPKBP1* contributes to JNK signaling (Arasa et al., 2015).

Table 5.4.2. Filtering of variant profiles in individuals born into consanguineous marriages

	Sample ID	
	2GPP1	**T009425**
Total n. of variants	24,169	24,336
Rare, non-synonymous/splice site variants	859	746
Homozygous changes	45	54
Located in homozygosity clusters > 2Mb	17	31
Predicted to be deleterious	3	6
Candidate Genes	*DOCK8, MAPKBP1, STOX1**	*ARHGAP11A, EVI5*, FMN1, GLI2, NR3C2*, SLC45A4**,

*Gene mapping to a homozygosity block larger than 10Mb

5.4.3 Candidate gene follow-up

Given that patient 2GPP1 was of Indian origin, the three candidate genes were followed up in an Asian patient cohort including 86 cases of Indian (n=17), Malay (n=48) and Chinese (n=21) descent (Table 2.2.5 in Methods).

The adopted strategy was to first check the recurrence of the variant detected by whole-exome sequencing. If the change was observed in additional samples, then the mutation screening was extended to include the whole coding region of the candidate gene. Since the majority of pustular psoriasis alleles are accounted for by recurrent mutations (Onoufriadis et al., 2012, Setta-Kaffetzi et al., 2013 Setta-Kaffetzi et al., 2014), this approach was deemed to be the most cost-effective.

While screening the p.Glu385Lys allele originally found in *STOX1*, two additional Indian patients were identified, who harboured the change in the heterozygous state. The remaining 3 coding exons of the gene were therefore screened in the Asian patient cohort. However, no further deleterious variants could be identified, excluding the possibility that the two p.Glu385Lys patients may have been compound heterozygotes. Of note, an analysis of Indian control datasets that have only recently become available (Table 2.2.5 in Methods) revealed an overall MAF of 5.6% for the p.Glu385Lys allele, arguing against the notion that this may be pathogenic mutation.

The follow-up of *DOCK8* and *MAPKBP1* uncovered no additional patients bearing the changes detected by whole-exome sequencing. Therefore, the rest of the genes were not sequenced.

Thus, the analysis of the recessive cases could not identify a strong candidate gene for the disease.

Table 5.4.3. Follow-up of candidate genes emerging from the analysis of consanguineous pedigrees

Sample ID	Gene (chr)	Variant	Pathogenicity Predictions					Outcome of follow-up
			SIFT	PROVEAN	PolyPhen-2	MutationTaster	CADD[1]	
2GPP1	***STOX1*** *(chr10)*	p.Glu385Lys (rs1341667)	Delterious	Damaging	Probably Damaging	Disease Causing	21	Locus excluded
	MAPKBP1 *(chr15)*	p.Glu259Lys	Delterious	Damaging	Probably Damaging	Disease Causing	31	Recurrent mutation excluded
	DOCK8 *(chr 9)*	p.Asp224His	Delterious	Damaging	Probably Damaging	Disease Causing	27	Recurrent mutation exlcuded

[1]The CADD algorithm returns a quantitative prediction, with scores above 15 considered pathogenic.

5.5 Analysis of dominant cases

The variant profiles were filtered for rare (MAF ≤ 0.015), heterozygous changes that were shared by affected relatives and classified as deleterious by at least four out of five pathogenicity prediction tools. The sequence changes that passed these criteria were then compared across samples, searching for genes that were mutated in multiple pedigrees or isolated cases (Figure 5.5.1). Finally, the candidate genes harbouring the changes with the highest CADD scores were prioritised for follow-up. The latter step was introduced, as the number of potential candidate genes was much larger than that observed in the recessive analysis.

Given that *AP1S3* and *CARD14* are only mutated in specific ethnic groups (Setta-Kaffetzi et al., 2014; Chapter 4 of this thesis), the Asian and European cases were initially analysed as separate datasets to maximise the power to detect population-specific disease genes (Figure 5.5.1).

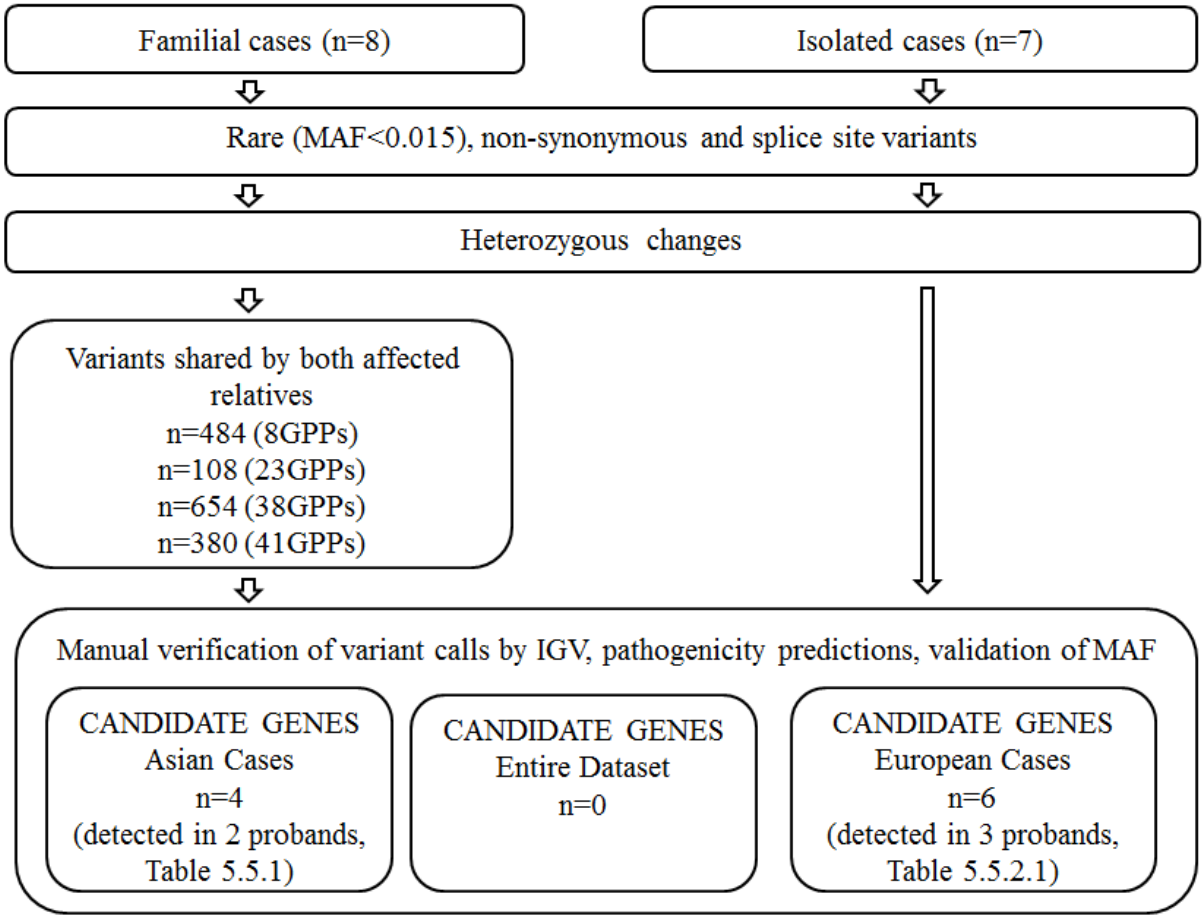

Figure 5.5.1. Filtering steps in the analysis of dominant cases

The filtering process is described in detail in section 2.9.6 of the Methods. The number of all and rare heterosygous changes detected in the patinets are summarised in Tables 5.2.2 and 5.2.3.

5.5.1 Analysis of the Asian cohort

5.5.1.1 Analysis of the entire dataset

The analysis of the eight Asian subjects uncovered four candidate genes, each harbouring rare deleterious changes in two affected relative pairs (Table 5.5.1.1). The variants with the strongest pathogenic potential (CADD>30) were found in *MEGF11*, a gene that regulates the spacing of different neuron subtypes in the retina (Kay et al., 2012). Deleterious changes were also observed in *HKR1*, which functions as a UV-light sensor in the retina (Luck M et al., 2012.), *FRAS1,* a disease gene for a developmental disorder known as Fraser syndrome and *F8,* which encodes coagulation factor VIII (Hoefele et al., 2013; Choi et al., 2015). Given that the function of these genes did not appear to be disease relevant, none of the above loci were prioritised for follow-up. The focus of the investigation moved to the individual families.

Table 5.5.1.1. Candidate genes emerging from the analysis of Asian dominant cases

Sample ID	Gene	Amino Acid Change	Gene size[1] [bp]	Pathogenicity Predictions				
				PolyPhen2	PROVEAN	SIFT	Mutation Taster	CADD[2]
38GPP1/2	***F8***	p.Lys399Glu	7053	Probably Damaging	Damaging	Deleterious	Polymorphism	17.7
41GPP1/2	*(chr X)*	p.Ser1974Pro		Probably Damaging	Damaging	Tolerated	Disease Causing	16.6
38GPP1/2	***HKR1***	p.Glu410Lys	1977	Possibly damaging	Damaging	Deleterious	Disease Causing	20.6
8GPP1/2	*(chr 19)*	p.Gly531Arg		Probably Damaging	Damaging	Deleterious	Disease Causing	15.3
23GPP1/2	***MEGF11***	p.Arg771His	3132	Probably Damaging	Neutral	Deleterious	Disease Causing	31
8GPP1/2	*(chr 15)*	p.Gly723Arg		Probably Damaging	Damaging	Deleterious	Disease Causing	33
38GPP1/2	***FRAS1***	p.His3347Gln	12024	Probably Damaging	Damaging	Deleterious	Disease Causing	18.8
23GPP1/2	*(chr 4)*	p.Thr2991Met		Probably Damaging	Damaging	Deleterious	Disease Causing	15.4

[1] Gene size refers to the length of the coding region [2]The CADD algorithm returns a quantitative prediction, and scores above 15 are considered pathogenic.

5.5.1.2 Analysis of pedigree 23GPP

While numerous deleterious changes emerged from the analysis of families 8GPP, 41GPP, and 38GPP, the list of candidate genes was much shorter in pedigree 23GPP, where the two affected cases were more distantly related (Table 5.5.1.2.1).

Based on the variants' pathogenic potential, the most promising candidate in family 23 was *CYP1A1* (Table 5.5.1.2.2). Of note, this gene codes for a monooxygenase which regulates the AhR pathway, a signalling cascade that has been implicated in the progression of psoriasis (Di Meglio et al., 2014).

To further investigate *CYP1A1* as a candidate gene, two lines of enquiry were pursued. First the p.Arg511Leu allele was screened in six additional members of family 23GPP (23PV1-6, Figure 5.5.1.2.1) who were affected by plaque psoriasis. In parallel, the entire coding region was screened in an Asian patient cohort including 86 cases of Indian (n=17), Malay (n=48), and Chinese (n=21) descent (Table 2.2.5 in Methods).

The analysis of family 23GPP did not detect p.Arg511Leu in any additional individuals. Meanwhile, screening of the Asian cohort identified four unrelated subjects carrying p.Arg511Leu, p.Arg455Gln, and p.Pro492Arg alleles (Table 5.5.1.2.3). However, a survey of the datasets recently released by the 1000 Genomes Consortium, revealed that the p.Arg511Leu change has an average frequency of 1.9% in Indian populations and is especially common among the Telegu (MAF: 2.9%), one of the ethnic groups that is genetically closer to the Indians who settled in Malaysia (Wong et al., 2014). Thus, the prevalence of the variant exceeds the 1.5% pathogenicity threshold that was used throughout the study. Moreover, a burden test indicated that there was no statistical difference in the representation of *CYP1A1* pathogenic variants between cases and controls (Table 5.5.1.2.4). Taken together, these findings indicated that *CYP1A1* is unlikely to be a disease causing gene.

Table 5.5.1.2.1. Number of rare, deleterious changes segregating in the Asian pedigrees.

8GPP			**41GPP**			**38GPP**			**23GPP**		
CADD>30	*CADD>20*	*CADD>15*	*CADD >30*	*CADD>20*	*CADD>15*	*CADD >30*	*CADD>20*	*CADD>15*	*CADD>30*	*CADD>20*	*CADD>15*
4	28	34	6	23	31	5	36	41	2	6	9

Table 5.5.1.2.2. Deleterious changes emerging from the analysis of pedigree 23GPP.

Gene	Size[1] [bp]	AA change	Pathogenicity Predictions				
			PolyPhen2	PROVEAN	SIFT	Mutation Taster	CADD[2]
CYP1A1 (chr15)	1536	p.Arg511L	Probably damaging	Damaging	Deleterious	Disease causing	32.0
ZNF516 (chr18)	3489	p.Pro117Ser	Probably damaging	Damaging	Deleterious	Disease causing	26.9
PLCH1 (chr3)	5079	p.Thr653Met	Probably damaging	Damaging	Deleterious	Disease causing	26.5
EPHA8 (chr1)	3015	p.Arg837W	Probably damaging	Damaging	Deleterious	Disease causing	22.4
TAS2R3 (chr7)	948	p.Asn24Ser	Probably damaging	Damaging	Deleterious	Disease causing	18.2
ARHGEF16 (chr1)	2127	p.Ile405Ser	Probably damaging	Damaging	Deleterious	Disease causing	16.7
IGSF10 (chr3)	7869	p.Arg1009Cys	Probably damaging	Damaging	Deleterious	Disease causing	15.5
FRAS1 (chr4)	12024	p.Thr2991Met	Probably damaging	Damaging	Deleterious	Disease causing	15.4
MEGF11 (chr15)	3132	p.Arg771H	Probably damaging	Neutral	Deleterious	Disease causing	31.0
OR51G1 (chr11)	963	p.Cys248Ser	Possibly damaging	Damaging	Tolerated	Disease causing	15.8

[1] Gene size refers to the length of the coding region [2]The CADD algorithm returns a quantitative prediction, and scores above 15 are considered pathogenic; AA, amino acid

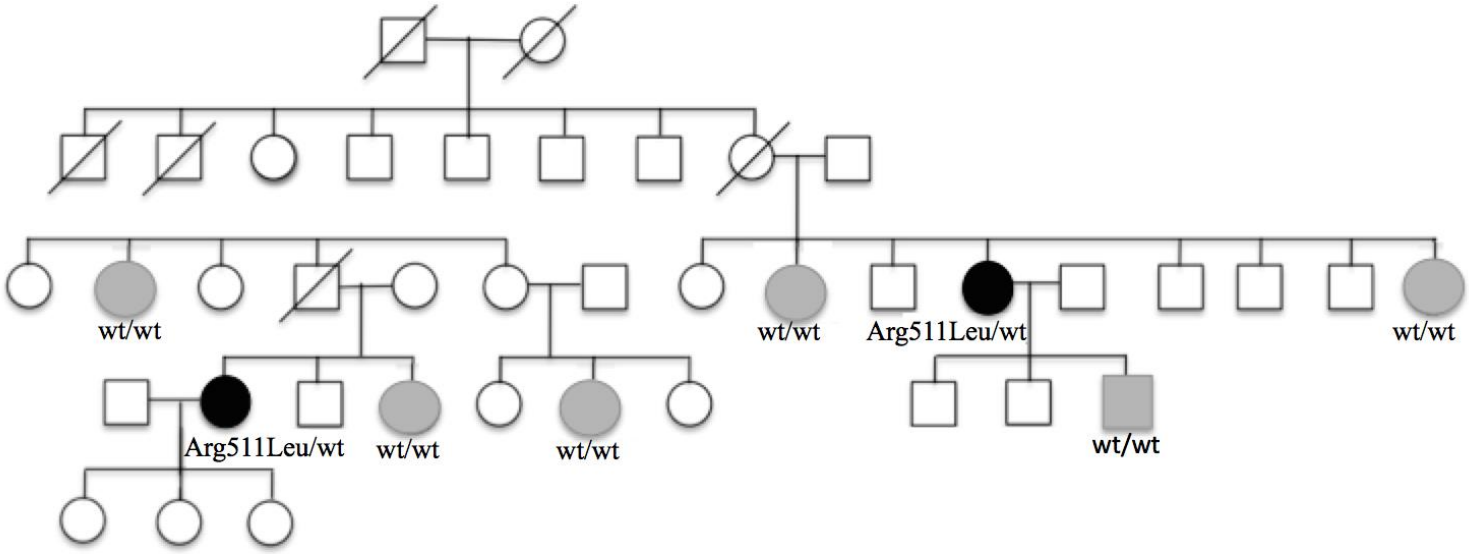

Figure 5.5.1.2.1. Screening of the p.Arg511Leu allele of *CYP1A1* in pedigree 23GPP. Black symbols represent GPP, while grey symbols refer to family members who were only affected by PV. Wt stands for wild type.

Table 5.5.1.2.3 Deleterious changes detected in *CYP1A1*

Sample ID	Ethnicity	Amino acid change	Pathogenicity Predictions				
			PolyPhen-2	SIFT	PROVEAN	Mutation Taster	CADD[2]
23GPP1 23GPP2 83GPP1 90GPP1	Malay Malay Indian Indian	p.Arg511Leu	Probably Damaging	Deleterious	Damaging	Disease Causing	32.0
60GPP1	Chinese	p.Arg455Gln	Probably Damaging	Deleterious	Damaging	Disease Causing	36.0
64GPP1	Chinese	p.Pro492Arg	Possibly Damaging	Deleterious	Damaging	Disease Causing	19.9

[1]The Control datasets used in the study are described in section 2.2.5 [2]The CADD algorithm returns a quantitative prediction, and scores above 15 are considered pathogenic.

Table 5.5.1.2.4. Frequency distribution of rare and deleterious *CYP1A1* alleles.

Ethnicity	Allele counts in Cases		Allele counts in Controls[2]		P value
	alt/all	%	alt/all	%	
Malay	1/96[1]	1.04	2/192	1.04	0.5
Chinese	2/42	4.8	7/416	1.68	0.22
Indian	2/34	5.9	17/878	1.94	0.15

[1]As the association analysis was performed on unrelated cases, only one of the GPP patients from family 23 was included in the dataset. [2]Details of the control cohorts can be found in section 2.2.5. Abbreviations are as follows: alt, alternative allele count; all, total allele count. P values were calculated with Chi-square tests (Methods 2.10.2).

5.5.2 Analysis of the European cohort

The analysis of European cases revealed six candidate genes, each harbouring rare deleterious alleles in three unrelated patients (Table 5.5.2.1). Among these, *DNAH12* and *ARFGAP2* were prioritised, because of the high CADD scores generated by the variants (Table 5.5.2.2).

The same deleterious change in *DNAH12* (p.Gly1895Ser; rs189965161) was found in three patients, affected by ACH (S0657, S0661) and GPP (T003673). Therefore, the locus was selected for follow-up in an extended cohort including 92 British pustular psoriasis cases (7 ACH, 4 GPP, and 81 PPP patients). However, no further individuals carrying p.Gly1895Ser were detected, arguing against the notion that the allele may be a recurring mutation.

Three variants with pathogenic potential (p.Asn103Ser, p.Val320Met, p.Gly519Ser) were detected in *ARFGAP2*. Interestingly, this gene has been implicated in protein transport between the Golgi complex and the endoplasmic reticulum, which is reminiscent of *AP1S3* function in vesicular trafficking (Setta-Kaffetzi, 2014).

Table 5.5.2.1. Genes harbouring mutations in multiple European cases

N. of cases	CADD>15	CADD>20
3	n=4	n=2
2	n=30	n=21

Table 5.5.2.2. Candidates emerging from the dominant analysis of European cases

Sample ID	Gene	Amino Acid Change	Gene size[1] (bp)	Pathogenicity Predictions				
				PolyPhen-2	PROVEAN	SIFT	Mutation Taster	CADD[2]
S0661	***DNAH12***	p.Gly1895Ser	12146	Probably Damaging	Deleterious	Damaging	Disease Causing	25.5
S0657	*(chr 3)*	p.Gly1895Ser		Probably Damaging	Deleterious	Damaging	Disease Causing	25.5
T003673		p.Gly1895Ser		Probably Damaging	Deleterious	Damaging	Disease Causing	25.5
S0655	***ARFGAP2***	p.Asn103Ser	2976	Benign	Deleterious	Damaging	Disease causing	21.8
S0658	*(chr 11)*	p.Val320Met		Possibly damaging	Tolerated	Damaging	Disease causing	22.4
S0660		p.Gly519Ser		Probably damaging	Tolerated	Damaging	Disease causing	22.3
S0657	***FBN3***	p.Asp2278His	8427	Probably damaging	Deleterious	Damaging	Disease causing	15.2
S0660	*(chr 19)*	p.Gly1311Ala		Probably damaging	Deleterious	Damaging	Disease causing	19.9
S0661		p.Cys1616Tyr		Probably damaging	Deleterious	Damaging	Disease causing	19.8
S0655	***MPEG1***	p.Thr73Ala	2148	Probably damaging	Deleterious	Damaging	Disease causing	19.0
S0660	*(chr 11)*	p.Thr73Ala		Probably damaging	Deleterious	Damaging	Disease causing	19.0
T002229		p.Pro405Thr		Probably damaging	Deleterious	Damaging	Disease causing	20.5

S0657	***MYOM2***	p.Gly1107Ala	4395	Probably damaging	Deleterious	Damaging	Disease causing	16.9
S0661	*(chr 8)*	p.Pro568Leu		Possibly damaging	Deleterious	Damaging	Disease causing	22.0
T003673		p.Arg537Cys		Probably damaging	Deleterious	Damaging	Disease causing	16.3
S0658	***RBMXL1***	p.Tyr234Cys	1170	Probably damaging	Deleterious	Damaging	Disease causing	19.0
S0660	*(chr 1)*	p.Tyr234Cys		Probably damaging	Deleterious	Damaging	Disease causing	19.0
T002229		p.Arg43Cys		Probably damaging	Deleterious	Damaging	Disease causing	20.0

[1]Size refers to the length of the coding region [2]The CADD algorithm returns a quantitative prediction and scores above 15 are considered pathogenic.

The *ARFGAP2* exons harbouring deleterious changes were screened in the British dataset mentioned above, which included the three individuals who had been originally whole-exome sequenced. The presence of the p.Asn103Ser, p.Val320Met and p.Gly519Ser variants was verified and the p.Gly519Ser allele was also detected in another 2 unrelated individuals. Next, the whole coding region of *ARFGAP2* (16 exons) was Sanger sequenced, and a further two changes with deleterious potential (p.Arg255Gly and p.Phe466Tyr) were uncovered (Table 5.5.2.3). Thus, a total of 5 mutations were observed in 7 unrelated individuals. Of note, all of these changes affected evolutionarily conserved residues (Figure 5.5.2.1). A burden test demonstrated that this was a significant finding, as the frequency of pathogenic alleles was markedly increased in cases compared to controls (3.80% vs. 0.76%; P = 1.8×10^{-5}) (Table 5.5.2.5).

Table 5.5.2.3. Deleterious *ARFGAP2* changes detected in cases

Disease Type	Sample ID	Amino Acid Change	Pathogenicity Predicitons					Cases	
			PROVEAN	SIFT	PolyPhen-2	Mutation Taster	CADD[1]	Alelle Counts	MAF (%)
PPP & ACH	T008999 T000991 S0660	p.Gly519Ser (rs142683966)	Deleterious	Tolerated	Probably damaging	Disease causing	22.3	3/184	1.63
PPP	T000989	p.Phe466Tyr	Deleterious	Deleterious	Probably damaging	Disease causing	22.2	1/184	0.54
ACH	S0658	p.Val320Met (rs373135315)	Neutral	Deleterious	Possibly damaging	Disease causing	22.4	1/184	0.54
PPP	T008962	p.Arg255Cys (rs138040761)	Deleterious	Deleterious	Possibly damaging	Disease causing	22.2	1/184	0.54
ACH	S0655	p.Asn103Ser (rs117324352)	Deleterious	Deleterious	Neutral	Disease causing	21.8	1/184	0.54

[1]The CADD algorithm returns a quantitative prediction and scores above 15 are considered pathogenic.

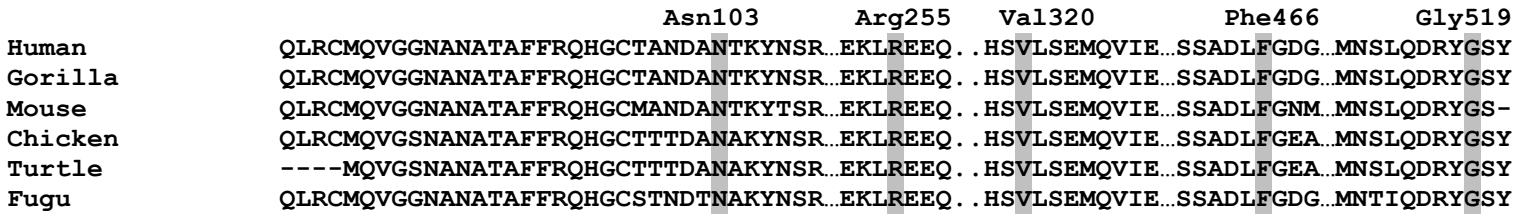

Figure 5.5.2.1. Conservation status of the deleterious *ARFGAP2* changes detected in cases

Table 5.5.2.4. Deleterious *ARFGAP2* changes detected in controls

AA Change	rs ID	Allele counts[1]		Pathogenicity prediction				
		ExAC	British exomes	SIFT	PolyPhen-2	PROVEAN	Mutation taster	CADD[2]
p.Gly519Ser	rs142683966	275	15	Tolerated	Probably damaging	Deleterious	Disease causing	22.3
p.Phe466Tyr	-	1	0	Damaging	Probably damaging	Deleterious	Disease causing	22.2
p.Met435Val	-	0	1	Damaging	Probably damaging	Deleterious	Disease causing	26.6
p.Arg406Gln	rs200794218	17	0	Damaging	Probably damaging	Neutral	Disease causing	35.0
p.Arg406Trp	rs35950498	58	1	Damaging	Probably damaging	Deleterious	Disease causing	35.0
p.Arg406Gly	rs35950498	20	0	Damaging	Probably damaging	Deleterious	Disease causing	26.8
p.Arg255Cys	rs138040761	2	0	Damaging	Probably damaging	Deleterious	Disease causing	22.2
p.Arg255Gly	rs138040761	1	0	Damaging	Possibly damaging	Deleterious	Disease causing	22.4
p.Asn103Ser	rs117324352	129	12	Damaging	Benign	Deleterious	Disease causing	21.8
p.Arg5Lys	-	1	1	Damaging	Benign	Deleterious	Disease causing	18.9
Total n. of changes		**504/66330** (0.76%)	**30/3570** (0.84%)					

[1]Details of the control cohorts can be found in section 2.2.5 [2]The CADD algorithm returns a quantitative prediction and scores above 15 are considered pathogenic. AA, amino acid; ExAC, Exome Aggregation Consortium. P values were calculated with Chi-square tests (Methods 2.10.2).

Table 5.5.2.5. Frequency distribution of rare and deleterious *ARFGAP2* changes

Allele counts in Cases		**Allele counts in Controls**		**P value**
alt/all	**%**	**alt/all**	**%**	
7/184	3.80	534/69,900	0.76	**1.8×10^{-5}**

P value was calculated with Chi-square test (Methods 2.10.2).

5.5.3 Comparison of the Asian and European datasets

In the final stage of the analysis, the list of rare alleles with pathogenic potential was compared across the European and Asian datasets. This failed to reveal any genes that was mutated in both population.

Given the association findings described in the previous section, the *ARFGAP2* gene was examined in more detail. A p.Asp346Asn substitution affecting a conserved residue was found in cases 38GPP1 and 38GPP2 (Figure 5.5.3.1; Table 5.5.3). The change did not meet our pathogenicity criteria, as it was only classified as deleterious by three out of five algorithms. However, an inspection of the *ARFGAP2* locus on the Ensembl genome browser revealed the presence of a shorter transcript isoform (ENST00000426335, Refseq ID: NM_001242832), which lacks exon 5 and encodes a protein that is likely to be adversely affected by the p.Asp210Asn variant (Table 5.5.3). To verify the expression profile of this shorter transcript, real-time PCR experiments were undertaken using isoform specific primers. These demonstrated that the shorter transcript was present in skin and immune cells. Thus, the p.Asp210Asn change is likely to have a deleterious effect on ARFGAP2 activity in disease relevant cell types.

Table 5.5.3. Effects of *ARFGAP2* changes on the proteins encoded by the two gene transcripts

Gene	Sample ID	Transcript[1]	AA Change	Pathogenicity Predictions				
				PROVEAN	SIFT	PolyPhen-2	Mutation Taster	CADD[2]
ARFGAP2	38GPP1/2	Full length	p.Asp346Asn	Neutral	Tolerated	Possibly damaging	Disease causing	22
		Short isoform	p.Asp210Asn	Deleterious	Deleterious	Possibly damaging	Disease causing	22
	S0660	Full length	p.Gly519Ser	Deleterious	Tolerated	Probably damaging	Disease causing	22.3
		Short isoform	p.Gly383Ser	Deleterious	Deleterious	Probably damaging	Disease causing	22.3
	S0658	Full l length	p.Val320Met	Neutral	Deleterious	Possibly damaging	Disease causing	22.4
		Short isoform	p.Val184Met	Neutral	Deleterious	Possibly damaging	Disease causing	22.4
	S0655	Full length	p.Asn103Ser	Deleterious	Deleterious	Neutral	Disease causing	21.8
		Short isoform	p.Asn103Ser	Deleterious	Deleterious	Neutral	Disease causing	21.8

[1]Refseq ID are as follow: full length transcript NM_032389 (protein: ENSP00000434442); isoform lacking exon 5 NM_001242832 (protein: ENSP00000400226); [2]The CADD algorithm returns a quantitative prediction and scores above 15 are considered pathogenic. AA, amino acid.

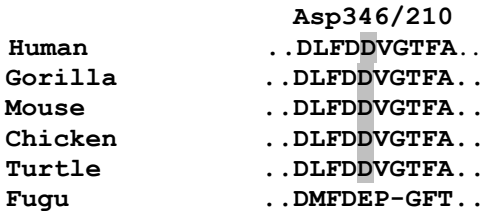

Figure 5.5.3.1. Conservation status of *ARFGAP2* Asp346 (ENSP00000434442) /Asp210 (ENSP00000400226)

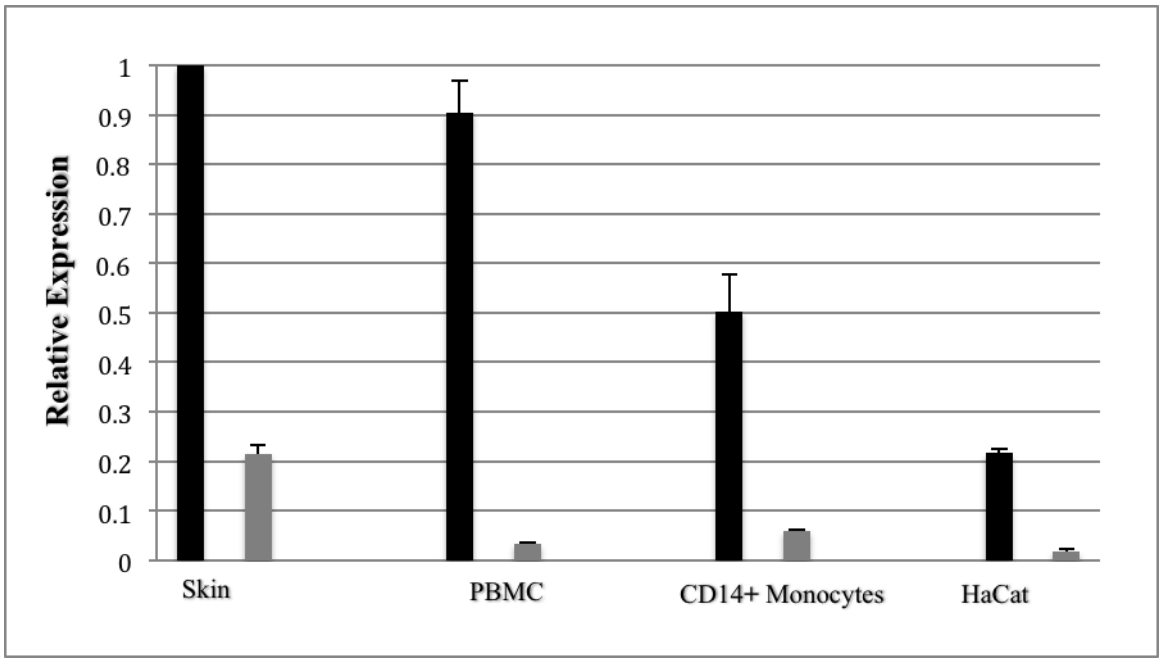

Figure 5.5.3.2. Relative expression of *ARFGAP2* full length transcript (NM_032389, indicated with black bars) and the isoform lacking exon 5 (NM_001242832, indicated with grey bars) in disease relevant cell types. All transcript levels are normalised to *PPIA* expression. Data are presented as mean ± SD obtained on two independent RNA samples.

5.6 Discussion

Despite the identification of disease alleles within *IL36RN*, *CARD14* and *AP1S3*, the majority of pustular psoriasis cases remain unaccounted for (Setta-Kaffetzi et al., 2014; Mahil et al., 2015; Sugiura et al., 2014). Thus, the aim of this study was to uncover additional genetic determinants for the disease, by means of whole-exome sequencing.

In order to maximise the likelihood of discovering novel genes, a homogeneous patient cohort was ascertained on the basis of severe disease presentation. In the absence of quantifiable markers, severity was assessed by surrogate measures such as age of onset and systemic involvement. To further reduce the confounding effect of genetic heterogeneity, the cases were allocated to different analysis groups, based on ethnicity and predicted mode of disease inheritance.

Despite these precautions, substantial genetic heterogeneity was observed, which complicated the design of follow-up studies.

5.6.1 Analysis of recessive cases

Patients born from consanguineous unions are likely to harbour autozygous disease alleles. This allows geneticists to prioritise homozygous variants during the filtering process and quickly exclude large portions of the genome. While this is undoubtedly a great advantage, ascertaining probands from communities with high rates of parental relatedness can cause other problems.

If the patient originates from an isolated population, their genome will be enriched for variants that are not found in reference datasets, which will confound the

identification of genuine mutations. The disease allele may also prove to be unique to the population in question, so that the inclusion of autozygous pedigrees in gene discovery studies may increase the heterogeneity of the study resource. Here, no genes showed recessive (homozygous or compound heterozygous) deleterious variants in more than one case. Of note, a number of assumptions were built in the filtering strategy that could have affected the identification of candidate genes.

First of all, it was postulated that the disease is caused by rare mutations, so that all variants with a MAF > 1.5% were filtered out. Given that the frequency of *IL36RN* mutations is nearly 2% in some Asian population (Hussain et al., 2015), other members of the lab have more recently repeated the analysis of the recessive group by increasing the MAF threshold to 5%. This still revealed no genetic overlaps between the pedigrees, indicating that the negative results were not due to an incorrect estimation of the mutation frequency.

Importantly, structural rearrangements were analyzed alongside nucleotide changes, but all the copy number variants (CNV) that appeared in multiple cases proved to be artifacts, which could not be verified upon manual inspection of reads with IGV. Moreover, no intersection was detected between CNVs and single base changes. Thus, it is unlikely that the disease was caused by the large genomic rearrangements detected in the examined cases. Of note, WES is less efficient as WGS in the detection of CNVs, (Singleton, 2011), so that we cannot exclude the possibility that a pathogenic structural change may have been missed.

In individuals that were the offspring of consanguineous marriages, it was further assumed that two copies of the disease allele were inherited alongside SNP haplotypes that were identical by descent. Although this is an entirely reasonable model,

other scenarios (e.g. the possibility of *de-novo* inheritance in one or both pedigrees) were not examined and cannot be discounted. It is also important to bear in mind that the analysis was limited to homozygous regions spanning at least 2Mb. While this threshold is consistent with that used in other studies of consanguineous pedigrees (Alsalem et al., 2013; McQuillan et al., 2008), the possibility that bialellic mutations may have been located in smaller regions cannot be excluded. It is interesting, however, that reducing the size of homozygous regions to 1.5Mb would not have revealed additional candidates in the Indian family.

Another critical factor to bear in mind is the sequencing depth, which in some cases (2GPP1 and 38GPP2, see Table 5.2.1), fell below our proposed benchmark of 20x coverage for 90% of CCDS transcripts. The issue of coverage is particularly important for two homozygosity blocks spanning 5 and 17 Mb on chromosome 10, which were shared by both patients born into consanguineous marriages. In fact, fifteen protein coding genes lying in these regions were not adequately covered in at least one of the two affected individuals. Of note, two of these loci are known to partake in immune-responses. *KIF5B* encodes a protein that is crucial for the polarization of lytic granules in Natural Killer cells, an immune cell type that has been detected in the inflammatory infiltrate of psoriatic lesions (Dunphy et al., 2011; Tuli et al., 2013). *MAP3K8* encodes a serine/threonine protein kinase that regulates NF-κB signalling as well as IL-1 and TLR-4 mediated activation of the Extracellular-regulated-kinase (ERK) pathway (Hedl et al., 2015). Of interest, a *MAP3K8* SNP associated with inflammatory bowel disease was shown to up-regulate IL-1 production in pattern-recognition receptor activated macrophages (Hedl et al., 2015). Thus, it will be important to Sanger sequence these two genes, to exclude the possibility that a shared disease allele may have been missed. In the subsequent phase of the analysis, the consanguineous pedigrees were individually

examined, looking for autozygous diseases alleles.

There was significant background consanguinity in the Roma pedigree, since the number of homosygous changes lying in homozygousity regions markedly exceeded that detected in the Indian case (31 vs. 17). Of note, six autozygous variants found in the Roma patient were predicted to be deleterious by multiple alogorithms. Most mapped to genes involved in cell cycle control (*ARHGAP11A* and *EVI5) (*Xu et al., 2013; Lim et al., 2013), cell motility (*FMN1*) (Dettenhofer et al., 2013), and metabolism (*SLC45A4*) (Bartölke et al., 2014), but two were in genes (*GLI2* and *NR3C2*) that partake in immune response. GLI2 is a hedgehog responsive transcription factor which attenuates T-cell receptor-signaling by inhibiting NF-κB and AP-1 activity (Furmanski et al., 2015). *NR3C2* encodes a mineralocorticoid hormone activated transcription factor, that regulates the activation of macrophages and NK-cells (Bene et al., 2014).

Overall, the high number of autozygous changes and the lack of detailed functional information for some of the mutated loci hindered the prioritisation of candidate genes. Thus none of the above loci was screened in further affected individuals.

As all relatives of the Roma patient refused to participate in the study, the only way to narrow down the candidate list in the future could be to generate additional sequence data from unrelated individuals who are likely to harbour recessive disease alleles. Of note, an agreement to share data has been reached with Dr Asma Smahi (Hospital Necker, Paris), who has exome sequenced a number of GPP patients born into consanguineous marriages. In parallel, the lab is working on ascertaining further recessive cases through international collaborations. Thus, the variant profile of the Roma case will be further analysed as soon as additional data is available.

In the Indian sample, the filtering of the variant profile narrowed down the list of possible candidates to three loci: *STOX1, DOCK8* and *MAPKBP1*.

STOX1 was excluded from the list of possible disease genes as the analysis of a recently released Indian dataset, indicated that the critical variant was in fact a common polymorphism. This demonstrated the importance of accessing frequency data for ethnicity-matched controls, to avoid the confounding effect of population-specific SNPs. Thus, resources such as the ExAC dataset (including >60,000 individuals sampled from multiple ethnic groups) or smaller population specific samples (e.g. the Dutch controls sequenced by Francioli et al., 2014), will be crucial to the identification of disease genes in whole genome/whole exome-sequencing studies.

The mutations originally observed in *DOCK8* and *MAPKBP1* were not detected in any other individual from the follow-up resource. Thus the screening of these candidates was not pursued any further. While this decision was based on the observation that the vast majority of GPP mutations are recurrent (Setta-Kafetzi et al., 2013; Setta-Kafetzi et al., 2014; Jordan et al., 2012), the possibility that disease-causing changes may reside elsewhere in *DOCK8* or *MAPKBP1* cannot be excluded, especially as the two genes have immune related functions. *DOCK8* encodes a guanine nucleotide exchange factor and is a disease gene for autosomal recessive hyper-IgE syndrome, an immune deficiency characterised by recurrent infections, eosinophilia and high incidence of allergic manifestations (Aydin et al., 2015). *MAPKBP1* encodes a scaffold protein, which down-regulates TRAF2- and NOD2 dependent NF-κB signaling in epithelial tissues (Yamaguchi et al., 2009; Lecat et al., 2012). It has to be emphasized, however, that the follow-up cohort for these two loci included almost a hundred pustular psoriasis cases, and that the DNA segments that were sequenced were over 400 base pair long. The fact that no damaging variants were found in these conditions

suggests that *DOCK8* and *MAPKBP1* are unlikely to be disease genes for pustular psoriasis.

5.6.2 Analysis of dominant cases

In the dominant group, the variant profiles were allocated to two different pools (Asian and European) based on the patient ethnicity.

The analysis of the Asian dataset identified four genes - *F8, HKR1, MEGF11, FRAS1-*, which harboured mutations in more than one pedigree. Of note, family 23GPP had the most power to uncover disease-causing changes, given that the two affected individuals were the farthest related. Since the best candidate for this pedigree (*CYP1A1)* was excluded because of the high allele frequency of the putative mutation, the four genes mentioned above could be ranked, based on whether they were mutated in pedigree 23GPP. This would suggest that the best candidates are *FRAS1* and *MEGF11,* where the latter could be further prioritised because of the higher CADD scores generated by putative mutations. *MEGF11* is involved in the mosaic arrangement of neurons in the retina; however, the possibility that it is also expressed in the skin or in immune cells cannot be excluded (Kay et al., 2015). Thus, the locus may be worthy of further consideration.

In the European cohort, 6 genes harboured deleterious changes in three unrelated cases. As the probands were all isolated cases, candidate genes were simply prioritised on the basis of the pathogenic potential and recurrence of putative mutations. On this basis, two loci (*DNAH12* and *ARFGAP2*) were selected for follow-up.

DNAH12 encodes a heavy chain dynein that participates both in axoneme motility and has been tentatively implicated in intracellular transport (Vaisberg et al.,

1996). Although three unrelated individuals were found to carry a p.Gly1895Ser substitution by exome sequencing, the screening of this change in a European dataset failed to uncover any further cases harbouring the same variant. Thus the *DNAH12* locus is unlikely to contribute to disease onset.

ARFGAP2 encodes a GTPase activating protein, which participates in the early secretory pathway by enhancing the enzymatic activity of ADP-ribosylation factor 1 (ARF1) (Kartberg et al., 2010). Most importantly, one of the mechanisms mediating the effect of ARF1 on intracellular transport is the activation of the AP-1 clathrin adaptor complex (Meyer et al., 2005). This is noteworthy, as the *AP1S3* gene encodes one of the AP-1 subunits (Setta-Kafetzi et al., 2014). Thus, the function of *ARFGAP2* in vesicular trafficking makes it an attractive candidate gene.

Here, the follow-up of the *ARFGAP2* locus generated some promising results. One of the three mutations captured by exome sequencing (p. Gly519Ser) proved to be recurrent, while two further deleterious variants were identified. A burden test showed that the combined frequency of deleterious alleles was significantly higher in European patients compared to controls ($P=1.8 \times 10^{-5}$). Of note, a sixth change with pathogenic potential was observed in pedigree 38GPP (p.Asp346Asn). Interestingly, this base change was only predicted to have an adverse effect on the protein encoded by an *ARFGAP2* isoform that lacks exon 5. Although, the presence of this transcript in disease relevant cell types was confirmed by real-time PCR, the isoform was much less abundant than the full-length transcript, so that the pathogenicity of the p.Asp346Asn allele will need to be validated with additional studies of protein conservation and three-dimensional structure homology modelling.

It also has to be noted, that the result of the *ARFGAP2* follow-up did not reach

exome-wide significance ($P<2.5*10^{-6}$, Kiezun et al., 2012), nor were functional studies performed to support the pathogenic potential of this locus. Further genetic investigations will now be undertaken by another member of the group, with the aim to validate the pathogenic role of the locus and lay the foundations for the functional characterization of disease alleles.

5.6.3 Conclusions

Overall, the present data highlights the difficulty of applying whole-exome sequencing to the study of a disease that is clinically and genetically heterogeneous. It also emphasizes the importance of accessing ethnically matched control data. In this context, the identification of *ARFGAP2* as a promising candidate gene seems to suggest that the analysis of unrelated but carefully selected cases could be more powerful than the characterisation of single, moderately informative pedigrees. Thus, the most important step in a contemporary gene identification study is the selection of patients for whole-exome sequencing, which requires thorough phenotyping by expert dermatologists. In the future, gathering information on possible disease triggers (e.g. infections or pregnancy), risk factors (e.g. smoking) and response to treatment will allow a better stratification of pustular psoriasis and facilitate the identification of new disease genes.

6 FINAL DISCUSSION

6.1 The genetic overlap between plaque and pustular psoriasis

Autoimmune diseases are caused by the abnormal activation of the immune system, which can result in systemic or organ-specific inflammation.

Psoriasis is an example of this phenomenon. Although it is primarily a skin disorder, it is mediated by abnormal activation of innate and adaptive responses, with a clear pathogenic involvement of Th17 lymphocytes (Lynde et al., 2014).

Psoriasis vulgaris, the most common subtype of the disease, is a complex, multifactorial disorder, which affects 2 % of the population worldwide. Conversely generalized pustular psoriasis is a rare, but very severe clinical variant (Mahil et al., 2015). Given that the frequency of PV among GPP patients (~50%) highly exceeds that in the general population (Mahil et al., 2015), the question has been raised as to whether the two conditions share common genetic determinants.

While the major susceptibility locus for PV (*HLA-Cw*0602*) is not associated with pustular forms of the disease (Mahil et al., 2015), this study demonstrated that *IL36RN* alleles do not confer an increased risk of plaque psoriasis. This conclusion, which was reached through the Sanger sequencing of >200 disease cases and the re-analysis of two large-scale studies, is unlikely to be confounded by lack of statistical power.

Thus, it would appear that the major genetic determinants of PV and GPP show mutual exclusion, which argues against the notion that the same genes could underlie both phenotypes.

Interestingly, these differences in genetic architecture point to distinctive

pathogenic pathways. HLA-C is an important mediator of antigen presentation, so that the association with *HLA-Cw*0602* is in keeping with the notion that PV is mainly a T-cell mediated disorder (Harden et al., 2015). Conversely, *IL36RN* encodes an anti-inflammatory molecule that is highly expressed in keratinocytes, where it regulates the activity of three innate cytokines (IL-36α/β/γ) (Gabay and Towne, 2015). Generalised pustular psoriasis is therefore more likely to be an autoinflammatory condition, caused by the abnormal activation of innate, rather than adaptive immunity. In fact, the acute and episodic presentation of GPP is reminiscent of autoinflammatory disorders such as the cryopyrin associated syndromes, which manifest with recurrent fevers accompanied by flares of neutrophilic skin inflammation (Holzinger et al., 2015).

The distinction between GPP and PV is also in keeping with the results of recent studies, indicating that IL-1 and IL-36, rather than IL-17 and IL-23, are the dominant cytokines in the GPP transcriptome (Johnston et al., 2015). Thus it would be tempting to propose that GPP is an IL-1/IL-36 mediated autoinflammatory disease while PV is an IL-23/IL-17 driven autoimmune disorder. While this is an attractive dichotomy, other experimental data suggest that the distinction may not be as clear cut and indicate a degree of overlap in the pathogenic pathways underlying the two conditions (Figure 6.1.1 and Figure 6.1.2).

For instance, it is well known that IL-36γ and IL-36α are markedly over-expressed in the skin lesions of psoriatic patients (Carrier et al., 2011; Gabay and Towne, 2015), where they are upregulated by IL-17, rather than IL-36Ra deficiency (Carrier et al., 2011; D'Erme et al., 2015). In fact, a recent study has identified IL-36γ as a biomarker of disease activity and response to treatment in plaque psoriasis (D'Erme et al., 2015).

The analysis of *CARD14* reported in this study also suggests an overlap between the pathogenesis of PV and GPP. Although the data presented in Chapter 4 showed that penetrant *CARD14* mutations are rare in PV, this does not detract from the fact that common *CARD14* alleles have been repeatedly associated with the disease (Mahil et al., 2015). As my work identified an association between the p.Asp176His allele and GPP, the abnormal activation of NF-κB downstream of *CARD14* would appear to be another pathway underlying the pathogenesis of plaque and pustular psoriasis.

More broadly, these results indicate that further studies of PV susceptibility genes may be warranted in GPP, to fully dissect the genetic and pathogenic overlap between the two disorders.

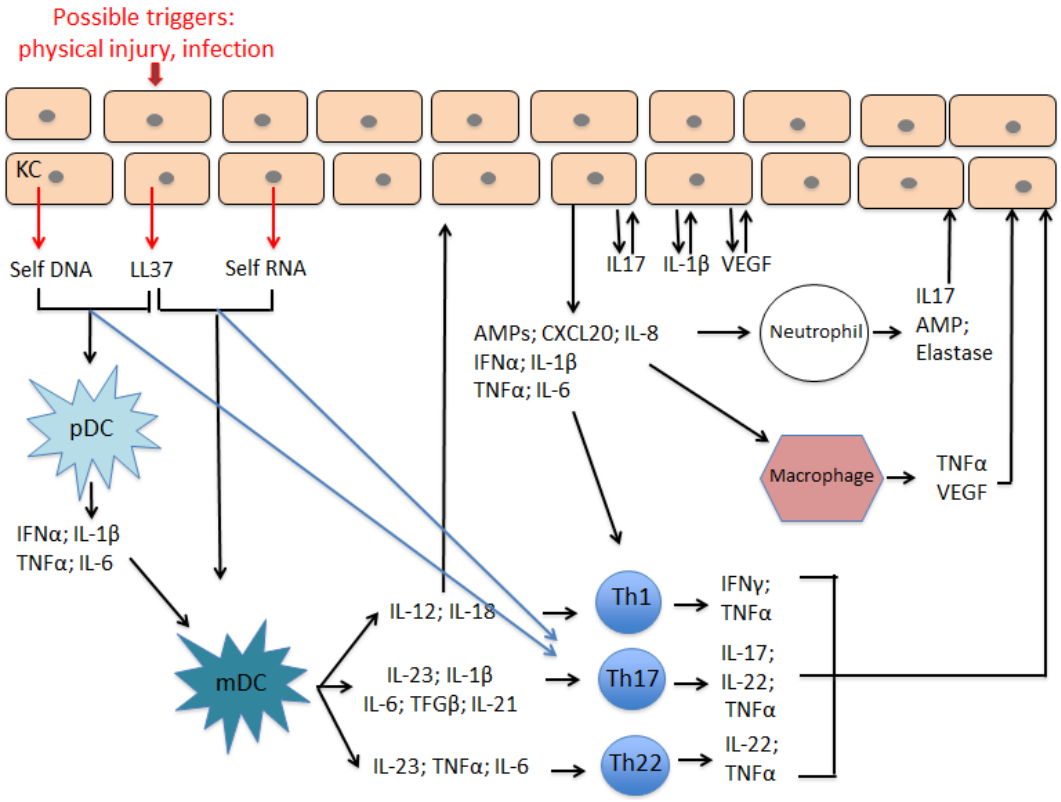

Figure 6.1.1. Current understanding of the pathogenesis of psoriasis vulgaris

When exposed to injury or infection, keratinocytes release DNA and/or RNA, as well as the antimicrobial peptide LL37. LL37-self nucleic acid complexes are then recognized by pDCs through TLR9 and by mDCs through TLR7/8, mDC cells migrate to the lymph nodes and activate Th1, Th17, and Th22 lymphocytes. Indeed, polymorphisms that affect antigen presentation to T cells (HLA-Cw6) and Th17 cell activation are strongly associated with PV susceptibility. T-lymphocyte subsets re-circulate to the skin, and the cytokines they release further activate keratinocytes, generating a feedback-loop between innate and adaptive immunity. These events are supported by neutrophils and macrophages, attracted towards the epidermis though KC derived chemokines. This further highlights the role of KC in psoriasis. KC, keratinocyte; pDC, plasmacytoid dendridic cell; mDC, myeloid dendridic cell; AMP, antimicrobial peptide.

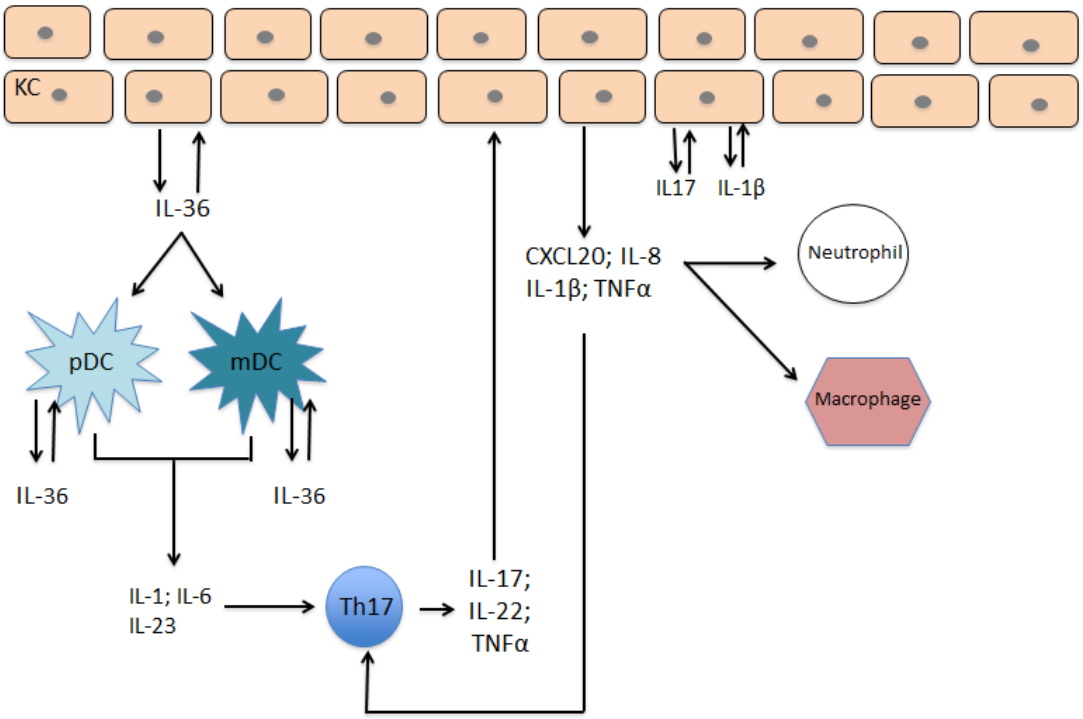

Figure 6.1.2. Current understanding of the pathogenesis of generalised pustular psoriasis

Following exposure to inflammatory stimuli (e.g. infections), mutation in *IL36RN*, *AP1S3* or *CARD14* up-regulate IL-36 secretion by keratinocytes. IL-36 molecules act both in an autocrine and paracrine fashion on KC and dendridic cells. Activated KC release chemokines that attract both neutrophils and macrophages towards the epidermis while DCs activate Th17 cell subsets, driving a positive feedback-loop between keratinocytes and T-cells. Abbreviations are as follows: KC, keratinocyte; pDC, plasmacytoid dendridic cell; mDC, myeloid dendridic cell; AMP, antimicrobial peptide.

6.2 Identification of pustular psoriasis susceptibility genes

Whole-exome sequencing of patients with pustular psoriasis revealed the presence of substantial genetic heterogeneity. This was observed even though the cases had been carefully selected, so as to be as homogeneous as possible in terms of their clinical phenotype.

The analysis of likely dominant cases highlighted *ARFGAP2* as a possible disease gene. After the completion of this study, the locus was followed-up by other members of the Capon lab. This revealed *ARFGAP2* alleles with deleterious potential in a total of five unrelated cases of Malay descent. While this is an interesting observation, the enrichment of damaging alleles in cases vs. controls was not statistically significant, possibly owing to the small size of the control Malay resource. Thus, the status of *ARFGAP2* as a pustular psoriasis gene remains to be validated.

The analysis of the recessive cases was confounded by suboptimal coverage of the target exome, in one of the two individuals who were examined by next generation sequencing. This issue is currently being addressed by the group through a careful examination of the sequence gaps, with a special focus on a block of homozygosity on chromosome 10, which was shared by the two individuals who were exome-sequenced.

This re-analysis has revealed an interesting candidate among the genes that were poorly covered. cAMP response element modulator (*CREM*) encodes a transcription factor that is highly expressed in T cells and has been implicated in both innate and adaptive immune regulation (Rauen et al., 2011; Verjans et al., 2015). The gene is currently being Sanger sequenced to explore the possibility that mutations at this locus may have been missed.

For the future, the group is committed to further exome sequencing studies, with

the expectation that the analysis of larger patient numbers will enhance the likelihood of detecting novel disease genes, despite the presence of genetic heterogeneity. Of note, Generalised Pustular Psoriasis has been successfully nominated for inclusion in the 100,000 genomes project (McGrath, 2016). Thus it, is anticipated that sequence data will be available for at least 30 unrelated cases by the end of 2018. Of note this will be generated by whole-genome, rather than whole-exome sequencing, which will resolve the issue of uneven coverage of target regions.

In the meantime, there is scope for re-analysing the available data at selected candidate regions, where mutations would be worthy of follow-up even if they had been observed in one or two cases. Thus, the variant profiles are currently been filtered for mutations that affect genes implicated in other autoinflammatory disorders.

Of note, current research in our lab indicates that *AP1S3* mutations affect IL-36α production, by disrupting the immune regulatory function of autophagy. These interesting results highlight IL-36α as a key player in the pathogenesis of pustular psoriasis and suggest that future studies could focus on genes that regulate the production and biological activity of this cytokine. Thus, genetic screens of IL-36 signalling modulators would shed new light on IL-36 biology, while also identifying an important set of candidate genes for generalised pustular psoriasis.

REFERENCES

Abbas, O., Itani, S., Ghosn, S., Kibbi, A.G, Fidawi, G., Farooq, M,, Shimomura, Y., Kurban M. (2013) Acrodermatitis continua of Hallopeau is a clinical phenotype of DITRA: evidence that it is a variant of pustular psoriasis. Dermatology. 2013;226(1):28-31.

Aebersold, R., & Malmstroem, L. (n.d.). Faculty of 1000 evaluation for An integrated map of genetic variation from 1,092 human genomes. *F1000 - Post-publication Peer Review of the Biomedical Literature*.

Afonina IS, Van Nuffel E, Baudelet G, Driege Y, Kreike M, Staal J, Beyaert R. (2016). The paracaspase MALT1 mediates CARD14-induced signaling in keratinocytes. *EMBO reports,17*(6): 914-27.

Alsalem, A. B., Halees, A. S., Anazi, S., Alshamekh, S., & Alkuraya, F. S. (2013). Autozygome Sequencing Expands the Horizon of Human Knockout Research and Provides Novel Insights into Human Phenotypic Variation. *PLoS Genetics PLoS Genet, 9*(12).

Ammar, M., Bouchlaka-Souissi, C., Helms, C., Zaraa, I., Jordan, C., Anbunathan, H., Bouhaha, R., Kouidhi, S., Doss, N., Dhaoui, R., Ben Osman., A, Ben Ammar El Gaied, A., Marrakchi, R., Mokni, M., Bowcock, AM. (2013). Genome-wide linkage scan for psoriasis susceptibility loci in multiplex Tunisian families. *British Journal of Dermatology, 168*(3), 583-587.

Ammar, M., Jordan, C., Cao, L., Lim, E., Souissi, C. B., Jrad, A., Omrane, I., Kouidhi, S., Zaraa, I., Anbunathan, H., Mokni, M., Doss, N., Guttman-Yassky, E., Gaaied, A., Menter, A., Bowcock, AM. (2015). CARD14 alterations in Tunisian patients with psoriasis and further characterization in European

cohorts. *British Journal of Dermatology, 174*(2), 330-337.

Arasa, J., Terencio, M. C., Andrés, R. M., Valcuende-Cavero, F., & Montesinos, M. C. (2015). Decreased SAPK/JNK signalling affects cytokine release and STAT3 activation in psoriatic fibroblasts. *Experimental Dermatology, 24*(10), 800-802.

Asumalahti, K., Ameen, M., Suomela, S., Hagforsen, E., Michaëlsson, G., Evans, J., Munro, M., Veal, C., Allen, M., Leman, J., David Burden, A,, Kirby B, Connolly, M, Griffiths, CE., Trembath, RC., Kere, J., Saarialho-Kere, U., Barker, J. N. (2003). Genetic Analysis of PSORS1 Distinguishes Guttate Psoriasis and Palmoplantar Pustulosis. *Journal of Investigative Dermatology, 120*(4), 627-632.

Augey, F., Renaudier, P., & Nicolas JF. (2006). Generalized pustular psoriasis (Zumbusch): a French epidemiological survey. *European Journal of Dermatology*, 16(6):669-73.

Aydin, S. E., Kilic, S. S., Aytekin, C., Kumar, A., Porras, O., Kainulainen, L., Kostyuchenko, L., Genel, F., Kütükcüler, N,. Karaca, N., Gonzalez-Granado, L., Abbott, J., Al-Zahrani, D., Rezaei, N., Baz, Z., Thiel, J., Ehl, S., Marodi, L., Orange, JS., Sawalle-Belohradsky, J., Keles, S., Holland, SM., Sanal, Ö., Ayvaz, DC., Tezcan, I., Al-Mousa, H., Alsum, Z., Hawwari, A., Metin, A., Matthes-Martin, S., Hönig, M,. Schulz, A., Picard, C., Barlogis, V., Gennery, A., Ifversen, M., van Montfrans, J., Kuijpers, T., Bredius, R., Dückers, G., Al-Herz, W., Pai, SY., Geha, R., Notheis, G., Schwarze, CP., Tavil, B., Azik, F., Bienemann, K., Grimbacher, B., Heinz, V., Gaspar, HB., Aydin, R., Hagl, B., Gathmann, B., Belohradsky, BH.,

Ochs, HD., Chatila, T., Renner, ED., Su, H., Freeman, AF., Engelhardt, K., Albert, M. H. (2015). DOCK8 Deficiency: Clinical and Immunological Phenotype and Treatment Options - a Review of 136 Patients. *Journal of Clinical Immunology, 35*(2), 189-198.

Bailey, S. R., Nelson, M. H., Himes, R. A., Li, Z., Mehrotra, S., & Paulos, C. M. (2014). Th17 Cells in Cancer: The Ultimate Identity Crisis. *Frontiers in Immunology, 5*.

Barrett, J. C., Fry, B., Maller, J., & Daly, M. J. (2004). Haploview: Analysis and visualization of LD and haplotype maps. *Bioinformatics, 21*(2), 263-265.

Bartölke, R., Heinisch, J., Wieczorek, H., & Vitavska, O. (2014). Proton-associated sucrose transport of mammalian solute carrier family 45: An analysis in Saccharomyces cerevisiae. *Biochemical Journal, 464*(2), 193-201.

Bendke, J., Stenzl, A. (2010). Immunologic mechanisms in RCC and allogeneic renal transplant rejection. *Nature reviews Urology*, 7(6):339-47.

Bene, N. C., Alcaide, P., Wortis, H. H., & Jaffe, I. Z. (2014). Mineralocorticoid receptors in immune cells: Emerging role in cardiovascular disease. *Steroids, 91*, 38-45.

Berger, B., Wilson, D. B., Wolf, E., Tonchev, T., Milla, M., & Kim, P. S. (1995). Predicting coiled coils by use of pairwise residue correlations. *Proceedings of the National Academy of Sciences, 92*(18), 8259-8263.

Bertin, J., Wang, L., Guo, Y., Jacobson, M. D., Poyet, J., Srinivasula, S. M., Merriam, S., DiStefano, PS., Alnemri, E. S. (2001). CARD11 and CARD14 Are Novel Caspase Recruitment Domain (CARD)/Membrane-associated Guanylate

Kinase (MAGUK) Family Members that Interact with BCL10 and Activate NF-kappa B. *Journal of Biological Chemistry, 276*(15), 11877-11882.

Blumberg, H., Dinh, H., Dean, C., Trueblood, E. S., Bailey, K., Shows, D., Bhagavathula, N., Aslam, MN., Varani, J., Towne, JE., Sims, J. E. (2010). IL-1RL2 and Its Ligands Contribute to the Cytokine Network in Psoriasis. *The Journal of Immunology, 185*(7), 4354-4362.

Blumberg, H., Dinh, H., Trueblood, E. S., Pretorius, J., Kugler, D., Weng, N., Kanaly, ST., Towne, JE., Willis, CR., Kuechle, MK., Sims, JE., Peschon, J. J. (2007). Opposing activities of two novel members of the IL-1 ligand family regulate skin inflammation. *The Journal of Experimental Medicine, 204*(11), 2603-2614.

Boehncke, W., & Schön, M. P. (2015). Psoriasis. *The Lancet, 386*(9997), 983-994.

Brubaker, S. W., Bonham, K. S., Zanoni, I., & Kagan, J. C. (2015). Innate Immune Pattern Recognition: A Cell Biological Perspective. *Annual Review of Immunology, 33*(1), 257-290.

Buermans, H., & Dunnen, J. D. (2014). Next generation sequencing technology: Advances and applications. *Biophysica Acta (BBA) - Molecular Basis of Disease, 1842*(10), 1932-1941.

Burns, T., Breathnach, S. (2010). Rook's Textbook of Dermatology, Eighth Edition. Chichester, UK, Wiley-Blackwell.

Capon, F., Burden, A. D., Trembath, R. C., & Barker, J. N. (2012). Psoriasis and Other Complex Trait Dermatoses: From Loci to Functional Pathways. *Journal of*

Investigative Dermatology, *132*(3), 915-922.

Capon, F. (2013). IL36RN Mutations in Generalized Pustular Psoriasis: Just the Tip of the Iceberg? *Journal of Investigative Dermatology, 133*(11), 2503-2504.

Carrier, Y., Ma, H., Ramon, H. E., Napierata, L., Small, C., O'toole, M., Young, DA., Fouser, LA., Nickerson-Nutter, C., Collins, M., Dunussi-Joannopoulos, K., Medley, Q. G. (2011). Inter-Regulation of Th17 Cytokines and the IL-36 Cytokines In Vitro and In Vivo: Implications in Psoriasis Pathogenesis. *Journal of Investigative Dermatology, 131*(12), 2428-2437.

Cesare, A. D., Meglio, P. D., & Nestle, F. O. (2009). The IL-23/Th17 Axis in the Immunopathogenesis of Psoriasis. *Journal of Investigative Dermatology, 129*(6), 1339-1350.

Cheng, H., Li, Y., Zuo, X., Tang, H., Tang, X., Gao, J., Sheng, YJ., Yin, XY.,, Zhou, F., Zhang, C., Chen, G., Zhu, J., Pan, Q., Liang, B., Zheng, X., Li, P., Ding YT1, Cheng F1, Luo J1, Chang RX1, Pan GB1, Fan X1, Wang ZX1, Zhang, A., Liu, J., Yang, S., Sun, LD., Zhang, X. (2014). Identification of a Missense Variant in LNPEP that Confers Psoriasis Risk. *Journal of Investigative Dermatology, 134*(2), 359-365.

Chin, C., Alexander, D. H., Marks, P., Klammer, A. A., Drake, J., Heiner, C., Clum, A., Copeland, A., Huddleston, J,. Eichler, EE., Turner, SW., Korlach, J. (2013). Nonhybrid, finished microbial genome assemblies from long-read SMRT sequencing data. *Nature Methods Nat Meth, 10*(6), 563-569.

Choi, S. J., Jang, K. J., Lim, J., & Kim, H. S. (2015). Human coagulation factor VIII domain-specific recombinant polypeptide expression. *Blood Research,*

50(2), 103.

Clark, M. J., Chen, R., Lam, H. Y., Karczewski, K. J., Chen, R., Euskirchen, G., Butte, AJ., Snyder, M. (2011). Performance comparison of exome DNA sequencing technologies. *Nature Biotechnology, 29*(10), 908-914.

Clop, A., Bertoni, A., Spain, S. L., Simpson, M. A., Pullabhatla, V., Tonda, R., Hundhausen, C., Di Meglio, P., De Jong, P., Hayday, AC., Nestle, FO., Barker, JN., Bell, RJ, Capon. F., Trembath, R. C. (2013). An In-Depth Characterization of the Major Psoriasis Susceptibility Locus Identifies Candidate Susceptibility Alleles within an HLA-C Enhancer Element. *PLoS ONE, 8*(8).

Common, J. E., O'toole, E. A., Leigh, I. M., Thomas, A., Griffiths, W. A., Venning, V., Grabczynska, S., Peris Z, Kansky, A., Kelsell, D. P. (2005). Clinical and Genetic Heterogeneity of Erythrokeratoderma Variabilis. *Journal of Investigative Dermatology*, *125*(5), 920-927.

Crow, J. M. (2012). Psoriasis uncovered. *Nature, 492*(7429).

Cutting, G. R. (2014). Cystic fibrosis genetics: From molecular understanding to clinical application. *Nature Reviews Genetics*, *16*(1), 45-56.

D'erme, A. M., Wilsmann-Theis, D., Wagenpfeil, J., Hölzel, M., Ferring-Schmitt, S., Sternberg, S., Wittmann, M., Peters, B., Bosio, A., Bieber, T.,Wenzel, J. (2015). IL-36γ (IL-1F9) Is a Biomarker for Psoriasis Skin Lesions. *Journal of Investigative Dermatology, 135*(4), 1025-1032.

Dettenhofer, M., Zhou, F., & Leder, P. (2008). Formin 1-Isoform IV Deficient Cells Exhibit Defects in Cell Spreading and Focal Adhesion Formation. *PLoS*

ONE, 3(6):e2497.

Di Meglio, P., Duarte, J., Ahlfors, H., Owens, N., Li, Y., Villanova, F., Tosi, I., Hirota, K., Nestle, F., Mrowietz, U., Gilchrist, MJ., Stockinger, B. (2014). Activation of the Aryl Hydrocarbon Receptor Dampens the Severity of Inflammatory Skin Conditions. *Immunity, 40*(6), 989-1001.

Dranoff, G. (2004). Cytokines in cancer pathogenesis and cancer therapy. *Nature Reviews Cancer Nat Rev Cancer, 4*(1), 11-22.

Dunphy, S., & Gardiner, C. M. (2011). NK Cells and Psoriasis. *Journal of Biomedicine and Biotechnology, 2011*, 1-10.

Egbuniwe, I. U., Karagiannis, S. N., Nestle, F. O., & Lacy, K. E. (2015). Revisiting the role of B cells in skin immune surveillance. *Trends in Immunology, 36*(2), 102-111.

Eytan, O., Qiaoli, L., Nousbeck, J., Steensel, M. V., Burger, B., Hohl, D., Taïeb, A., Prey, S., Bachmann, D., Avitan-Hersh, E., Jin Chung, H., Shemer, A., Trau, H., Bergman, R., Fuchs-Telem, D., Warshauer, E., Israeli, S., Itin, PH., Sarig, O., Uitto, J., Sprecher, E. (2014). Increased epidermal expression and absence of mutations in CARD14 in a series of patients with sporadic pityriasis rubra pilaris. *British Journal of Dermatology, 170*(5), 1196-1198.

Farooq, M., Nakai, H., Fujimoto, A., Fujikawa, H., Matsuyama, A., Kariya, N., Aizawa, A., Fujiwara, H., Ito, M., Shimomura, Y. (2012). Mutation Analysis of the IL 36 RN Gene in 14 Japanese Patients with Generalized Pustular Psoriasis. *Human Mutation, 34*(1), 176-183.

Feng, C., Wang, T., Li, S., Fan, Y., Shi, G., & Zhu, K. (2015). CARD14 gene

polymorphism c.C2458T (p.Arg820Trp) is associated with clinical features of psoriasis vulgaris in a Chinese cohort. *The Journal of Dermatology, 43*(3), 294-297.

Ferreira, T., & Marchini, J. (2010). Modeling interactions with known risk loci-a Bayesian model averaging approach. *Annals of Human Genetics, 75*(1), 1-9.

Flicek, P., Amode, M. R., Barrell, D., Beal, K., Billis, K., Brent, S., Carvalho-Silva, D., Clapham, P., Coates, G., Fitzgerald, S., Gil, L., Girón, CG., Gordon, L., Hourlier, T., Hunt, S., Johnson, N., Juettemann, T., Kähäri, AK., Keenan, S, Kulesha, E., Martin, FJ., Maurel, T., McLaren, WM., Murphy, DN., Nag, R., Overduin, B., Pignatelli, M., Pritchard, B., Pritchard, E., Riat, HS., Ruffier, M., Sheppard, D., Taylor, K., Thormann, A., Trevanion, SJ., Vullo, A., Wilder, SP., Wilson, M., Zadissa, A., Aken, BL., Birney, E., Cunningham, F., Harrow, J., Herrero, J., Hubbard, TJ., Kinsella, R., Muffato, M., Parker, A., Spudich, G., Yates, A., Zerbino, DR.,Searle, S. M. (2013). Ensembl 2014. *Nucleic Acids Research Nucl. Acids Res., 42*(D1)

Foss, D.L. Zilliox, M.J., Murtaugh, M.P. (1999). Differential regulation of macrophage interleukin-1 (IL-1), IL-12, and CD80-CD86 by two bacterial toxins. *Infection and Immunity*, 67(10):5275-81

Francioli, L. C., Menelaou, A., Pulit, S. L., Dijk, F. V., Palamara, P. F., Elbers, C. C., . . . Wijmenga, C. (2014). Whole-genome sequence variation, population structure and demographic history of the Dutch population. *Nature Genetics Nat Genet, 46*(8), 818-825.

Fuchs-Telem, D., Sarig, O., Van Steensel, M., Isakov, O., Israeli, S., Nousbeck, J.,

Richard, K,. Winnepenninckx, V., Vernooij, M., Shomron, N., Uitto, J,. Fleckman, P., Richard, G., Sprecher, E. (2012). Familial Pityriasis Rubra Pilaris Is Caused by Mutations in CARD14. *The American Journal of Human Genetics, 91*(1), 163-170.

Furmanski, A. L., & Crompton, T. (2015). Gli2, hedgehog and TCR signalling. *Oncotarget, 6*(28), 24592-24593.

Fukata, M., Vamadevan, A.S., Abreu, M.T., (2009). Toll-like receptors (TLRs) and Nod-like receptors (NLRs) in inflammatory disorders. *Seminars in Immunology*. ;21(4):242–253

Gabay, C., & Towne, J. E. (2015). Regulation and function of interleukin-36 cytokines in homeostasis and pathological conditions. *Journal of Leukocyte Biology, 97*(4), 645-652.

Ganguly, D., Chamilos, G., Lande, R., Gregorio, J., Meller, S., Facchinetti, V., Homey, B., Barrat, FJ., Zal, T., Gilliet, M. (2009). Self-RNA–antimicrobial peptide complexes activate human dendritic cells through TLR7 and TLR8. *The Journal of Experimental Medicine, 206*(9), 1983-1994.

Gille, C., Fahling, M., Weyand, B., Wieland, T., & Gille, A. (2014). Alignment-Annotator web server: Rendering and annotating sequence alignments. *Nucleic Acids Research, 42*(W1).

Griffiths, C. E., & Barker, J. N. (2007). Pathogenesis and clinical features of psoriasis. *The Lancet, 370*(9583), 263-271.

Griffiths, W. (1980). Pityriasis rubra pilaris. *Clinical and Experimental Dermatology,*

5(1), 105-112.

Harden, J. L., Krueger, J. G., & Bowcock, A. M. (2015). The immunogenetics of Psoriasis: A comprehensive review. *Journal of Autoimmunity, 64*, 66-73.

Hara H, Yokosuka T, Hirakawa H, Ishihara C, Yasukawa S, Yamazaki M, Koseki H, Yoshida H, Saito T (2015). Clustering of CARMA1 through SH3-GUK domain interactions is required for its activation of NF-κB signalling. *Nature Communications, 6*(15):5555.

Hayashi, M., Hirota, T., Saeki, H., Nakagawa, H., Ishiuji, Y., Matsuzaki, H., Tsunemi, Y., Kato, T., Shibata, S., Sugaya, M., Sato, S., Tada ,Y., Doi, S., Miyatake, A., Ebe K., Noguchi, E., Ebihara, T., Amagai, M., Esaki, H., Takeuchi ,S., Furue, M.,Tamari, M. (2014). Genetic polymorphism in the TRAF3IP2 gene is associated with psoriasis vulgaris in a Japanese population. *Journal of Dermatological Science, 73*(3), 264-265.

Heath, W. R., & Carbone, F. R. (2013). The skin-resident and migratory immune system in steady state and memory: Innate lymphocytes, dendritic cells and T cells. *Nature Immunology Nat Immunol, 14*(10), 978-985.

Hedl, M., & Abraham, C. (2015). A TPL2 (MAP3K8) disease-risk polymorphism increases TPL2 expression thereby leading to increased pattern recognition receptor-initiated caspase-1 and caspase-8 activation, signalling and cytokine secretion. *Gut*, [Epub ahead of print]

Hoefele, J., Wilhelm, C., Schiesser, M., Mack, R., Heinrich, U., Weber, L. T., Biskup, S., Daumer-Haas, C., Klein, HG., Rost, I. (2013). Expanding the mutation spectrum for Fraser syndrome: Identification of a novel heterozygous

deletion in FRAS1. *Gene, 520*(2), 194-197.

Holzinger, D., Kessel, C., Omenetti, A., & Gattorno, M. (2015). From bench to bedside and back again: Translational research in autoinflammation. *Nature Reviews Rheumatology, 11*(10), 573-585.

Hong, J., Chen, P., Chen, Y., & Tsai, T. (2014). Genetic Analysis of CARD14 in Non-familial Pityriasis Rubra Pilaris: A Case Series. *Acta Dermato Venereologica, 94*(5), 587-588.

Howes A, O'Sullivan PA, Breyer F, Ghose A, Cao L, Krappmann D, Bowcock AM, Ley SC (2016).Psoriasis mutations disrupt CARD14 autoinhibition promoting BCL10-MALT1-dependent NF-κB activation. *The Biochemical Journal,* 15;473(12):1759-68.

Howie, B. N., Donnelly, P., & Marchini, J. (2009). A Flexible and Accurate Genotype Imputation Method for the Next Generation of Genome-Wide Association Studies. *PLoS Genetics, 5*(6).

Hüffmeier, U., Wätzold, M., Mohr, J., Schön, M., & Mössner, R. (2014). Successful therapy with anakinra in a patient with generalized pustular psoriasis carrying IL36RN mutations. *British Journal of Dermatology, 170*(1), 202-204.

Baruch, HA., & Wendell, AL (2011). Mechanism and role of PDZ domains in signaling complex assembly. *Journal of Cell Science, 114* (18): 3219-3231.

Johnston, J. J., & Biesecker, L. G. (2013). Databases of genomic variation and

phenotypes: Existing resources and future needs. *Human Molecular Genetics, 22*(R1).

Johnston, A., Xianying, X., Wolternik, L., & Arbor, M. (2015). IL-1 and IL-36 are the dominant cytokines in generalized pustular psoriasis. Ann Arbor, MI. 3:36 pm, Post 2015 meeting of the Society of Investigative Dermatology (SID).

Johnston A, Xing X, Guzman AM, Riblett M, Loyd CM, Ward NL, *et al.* (2011) IL-1F5, -F6, -F8, and -F9: a novel IL-1 family signaling system that is active in psoriasis and promotes keratinocyte antimicrobial peptide expression. *Journal of Immunology* 186:2613-22.

Jordan, C., Cao, L., Roberson, E., Pierson, K., Yang, C., Joyce, C., Ryan, C., Duan, S., Helms, CA., Liu, Y., Chen, Y., McBride, AA., Hwu, WL., Wu, JY., Chen, YT., Menter, A., Goldbach-Mansky, R., Lowes, MA.,Bowcock, A. (2012). PSORS2 Is Due to Mutations in CARD14. *The American Journal of Human Genetics, 90*(5), 784-795.

Jordan, C., Cao, L., Roberson, E., Duan, S., Helms, C., Nair, R., Liu, Y., Chen, Y., McBride, AA., Hwu, WL., Wu, JY., Chen, YT., Menter, A., Goldbach-Mansky, R Bowcock, A. (2012). Rare and Common Variants in CARD14, Encoding an Epidermal Regulator of NF-kappaB, in Psoriasis. *The American Journal of Human Genetics, 90*(5), 796-808.

Kanazawa, N., Nakamura, T., Mikita, N., Furukawa, F. (2013). Novel IL36RN mutation in a Japanese case of early onset generalized pustular psoriasis. *Jornal of Investigative Dermatology*, 40(9):749-51.

Kartberg, F., Asp, L., Dejgaard, S.Y., Smedh, M., Fernandez-Rodriguez, J., Nilsson, T., & Presley JF. (2010). ARFGAP2 and ARFGAP3 are essential for COPI

coat assembly on the Golgi membrane of living cells *The Journal of Biological Chemistry.*,285(47):36709-20

Kasperavičiūtė, D., Kučinskas, V., & Stoneking, M. (2004). Y Chromosome and Mitochondrial DNA Variation in Lithuanians. *Annals of Human Genetics, 68*(5), 438-452.

Kay, J. N., Chu, M. W., & Sanes, J. R. (2012). MEGF10 and MEGF11 mediate homotypic interactions required for mosaic spacing of retinal neurons. *Nature, 483*(7390), 465-469.

Kiezun, A., Garimella, K., Do, R., Stitziel, N.O., Neale, B.M., McLaren, PJ., Gupta, N., Sklar, P., Sullivan, PF., Moran, JL., Hultman, CM., Lichtenstein, P., Magnusson, P., Lehner, T., Shugart, YY., Price, AL., de Bakker, PI., Purcell, SM., Sunyaevm, SR. (2012). Exome sequencing and the genetic basis of complex traits. *Nature Genetics*, 29;44(6):623-30

Kircher, M., Witten, D. M., Jain, P., O'roak, B. J., Cooper, G. M., & Shendure, J. (2014). A general framework for estimating the relative pathogenicity of human genetic variants. *Nature Genetics, 46*(3), 310-315.

Knight, J., Spain, S. L., Capon, F., Hayday, A., Nestle, F. O., Clop, A., Barker, JM., Weale, ME., Trembath, R. C. (2012). Conditional analysis identifies three novel major histocompatibility complex loci associated with psoriasis. *Human Molecular Genetics*. 21:5185–5192.

Körber, A., Mössner, R., Renner, R., Sticht, H., Wilsmann-Theis, D., Schulz, P., Sticherling, M., Traupe, H., & Hüffmeier U. Mutations in IL36RN in patients with generalized pustular psoriasis. *Journal of Investigative*

Dermatology, 133(11):2634-7.

Lamason, R. L., Mccully, R. R., Lew, S. M., & Pomerantz, J. L. (2010). Oncogenic CARD11 Mutations Induce Hyperactive Signaling by Disrupting Autoinhibition by the PKC-Responsive Inhibitory Domain. *Biochemistry, 49*(38), 8240-8250.

Lecat, A., Valentin, E. D., Somja, J., Jourdan, S., Fillet, M., Kufer, T. A Habraken, Y., Sadzot, C., Louis, E., Delvenne, P., Piette, J., Legrand-Poels, S. (2012). The c-Jun N-terminal Kinase (JNK)-binding Protein (JNKBP1) Acts as a Negative Regulator of NOD2 Protein Signaling by Inhibiting Its Oligomerization Process. *Journal of Biological Chemistry, 287*(35), 29213-29226.

Lande, R., Gregorio, J., Facchinetti, V., Chatterjee, B., Wang, YH., Homey, B., Cao, W/, Wang, YH., Su, B., Nestle, FO., Zal, T., Mellman, I., Schröder, JM., Liu, YJ., Gilliet, M. (2007). Plasmacytoid dendritic cells sense self-DNA coupled with antimicrobial peptide. *Nature*, 449(7162):564-569.

Lenz, G., Davis, R. E., Ngo, V. N., Lam, L., George, T. C., Wright, G. W., Dave, SS., Zhao, H., Xu, W., Rosenwald, A., Ott ,G., Muller-Hermelink, HK., Gascoyne, RD., Connors, JM., Rimsza, LM., Campo, E., Jaffe, ES., Delabie, J., Smeland, EB., Fisher, RI., Chan, WC., Staudt, L. M. (2008). Oncogenic CARD11 Mutations in Human Diffuse Large B Cell Lymphoma. *Science, 319*(5870), 1676-1679.

Li, H., Handsaker, B., Wysoker, A., Fennell, T., Ruan, J., Homer, N., Marth, G., Abecasis, G., Durbin, R. (2009). The Sequence Alignment/Map format and

SAMtools. *Bioinformatics, 25*(16), 2078-2079.

Lim, Y. S., & Tang, B. L. (2013). The Evi5 family in cellular physiology and pathology. *FEBS Letters, 587*(12), 1703-1710.

Liu, L., Li, Y., Li, S., Hu, N., He, Y., Pong, R., Lin, D., Lihua, L., Law, M. (2014). Comparison of Next-Generation Sequencing Systems. *The Role of Bioinformatics in Agriculture,* 1-25.

Livak, K. J., & Schmittgen, T. D. (2001). Analysis of Relative Gene Expression Data Using Real-Time Quantitative PCR and the 2−ΔΔCT Method. *Methods, 25*(4), 402-408.

Luck, M., Mathes, T., Bruun, S., Fudim, R., Hagedorn, R., Nguyen, T. M., Kateriya, S., Kennis, JT., Hildebrandt, P., Hegemann, P. (2012). A Photochromic Histidine Kinase Rhodopsin (HKR1) That Is Bimodally Switched by Ultraviolet and Blue Light. *Journal of Biological Chemistry*, *287*(47), 40083-40090.

Luckheeram, R. V., Zhou, R., Verma, A. D., & Xia, B. (2012). CD4 T Cells: Differentiation and Functions. *Clinical and Developmental Immunology, 2012*, 1-12.

Lupas, A. (1996). Coiled coils: New structures and new functions. *Trends in Biochemical Sciences, 21*(10), 375-382.

Lupas, A., Dyke, M. V., & Stock, J. (1991). Predicting coiled coils from protein sequences. *Science, 252*(5009), 1162-1164.

Lynde, C. W., Poulin, Y., Vender, R., Bourcier, M., & Khalil, S. (2014). Interleukin

17A: Toward a new understanding of psoriasis pathogenesis. *Journal of the American Academy of Dermatology, 71*(1), 141-150.

Mackenroth, L., Fischer-Zirnsak, B., Egerer, J., Hecht, J., Kallinich, T., Stenzel, W., Kallinich, T., Stenzel, W., Spors, B., von Moers, A., Mundlos S., Kornak, U.3, Gerhold, K., Horn, D. (2016). An overlapping phenotype of Osteogenesis imperfecta and Ehlers-Danlos syndrome due to a heterozygous mutation in COL1A1 and biallelic missense variants in TNXB identified by whole exome sequencing. *American Journal of Medical Genetics Part A*.

Mahil, S. K., Capon, F., & Barker, J. N. (2015). Genetics of Psoriasis. *Dermatologic Clinics, 33*(1), 1-11.

Marrakchi, S., Guigue, P., Renshaw, B. R., Puel, A., Pei, X., Fraitag, S., Zribi, J., Bal ,E., Cluzeau, C., Chrabieh, M., Towne, JE., Douangpanya, J., Pons, C., Mansour, S., Serre, V., Makni, H., Mahfoudh, N., Fakhfakh, F,. Bodemer, C., Feingold, J., Hadj-Rabia, S., Favre, M., Genin, E., Sahbatou, M., Munnich, A., Casanova, JL., Sims, JE., Turki, H., Bachelez, H., Smahi, A. (2011). Interleukin-36–Receptor Antagonist Deficiency and Generalized Pustular Psoriasis. *New England Journal of Medicine, 365*(7), 620-628.

Marsland, A.M., Chalmers, R.J., Hollis, S., Leonardi-Bee, J., & Griffiths, C.E. (2006). Interventions for chronic palmoplantar pustulosis. *Cochrane Database of Systematic Reviews* 25;(1):CD001433

Mathews, R. J., Sprakes, M. B., & Mcdermott, M. F. (2008). NOD-like receptors and inflammation. *Arthritis Res Ther Arthritis Research & Therapy, 10*(6), 228.

Mcgrath, J. (2016). Rare inherited skin diseases and the Genomics England 100 000

Genome Project. *Br J Dermatol British Journal of Dermatology, 174*(2), 257-258.

Mcquillan, R., Leutenegger, A., Abdel-Rahman, R., Franklin, C. S., Pericic, M., Barac-Lauc, Smolej-Narancic, N., Janicijevic, B., Polasek, O., Tenesa, A., Macleod, AK., Farrington, SM., Rudan, P., Hayward, C., Vitart, V., Rudan, I., Wild, SH., Dunlop, MG., Wright, AF., Campbell, H.,Wilson, J. F. (2008). Runs of Homozygosity in European Populations. *The American Journal of Human Genetics, 83*(3), 359-372.

Mössner R, Frambach Y, Wilsmann-Theis D, Löhr S, Jacobi A, Weyergraf A, Müller M, Philipp S, Renner R, Traupe H, Burkhardt H, Kingo K, Kõks S, Uebe S, Sticherling M, Sticht H, Oji V, Hüffmeier U (2015). *The Journal of Investigative Dermatology,* 135(10):2538-41. Palmoplantar Pustular Psoriasis Is Associated with Missense Variants in CARD14, but Not with Loss-of-Function Mutations in IL36RN in European Patients.

Abecasis, G. R., Bentley, D. R., Chakravarti, A., Handsaker, RE., Kang, HM., Marth, GT., Mcvean, G. A. (2012). An integrated map of genetic variation from 1,092 human genomes. *Nature, 491*(7422), 56-65.

Mease, P.J. (2015). Inhibition of interleukin-17, interleukin-23 and the TH17 cell pathway in the treatment of psoriatic arthritis and psoriasis. *Current Opinion in Rheumatology*, 27(2):127-33

Meyer, D. M. (2005). Oligomerization and Dissociation of AP-1 Adaptors Are Regulated by Cargo Signals and by ArfGAP1-induced GTP Hydrolysis. *Molecular Biology of the Cell, 16*(10), 4745-4754.

Miller, S., Dykes, D., & Polesky, H. (1988). A simple salting out procedure for extracting DNA from human nucleated cells. *Nucleic Acids Research, 16*(3), 1215-1215.

Milora, K. A., Fu, H., Dubaz, O., & Jensen, L. E. (2015). Unprocessed Interleukin-36α Regulates Psoriasis-Like Skin Inflammation in Cooperation With Interleukin-1. *Journal of Investigative Dermatology, 135*(12), 2992-3000.

Miosge, L. A., Field, M. A., Sontani, Y., Cho, V., Johnson, S., Palkova, A., Balakishnan, B., Liang, R., Zhang, Y., Lyon, S., Beutler, B., Whittle, B., Bertram, EM., Enders, A., Goodnow, CC., Andrews, T. D. (2015). Comparison of predicted and actual consequences of missense mutations. *Proceedings of the National Academy of Sciences Proc Natl Acad Sci USA, 112*(37).

Morizane, S., Yamasaki, K., Mühleisen, B., Kotol, P. F., Murakami, M., Aoyama, Y., Murakami, M., Aoyama, Y., Iwatsuki, K., Hata, T,. Gallo, R. L. (2012). Cathelicidin Antimicrobial Peptide LL-37 in Psoriasis Enables Keratinocyte Reactivity against TLR9 Ligands. *Journal of Investigative Dermatology, 132*(1), 135-143.

Mössner, R., Frambach, Y., Wilsmann-Theis, D., Löhr, S., Jacobi, A., Weyergraf, A., Müller ,M., Philipp, S., Renner ,R., Traupe, H., Burkhardt, H., Kingo, K., Kõks, S., Uebe, S., Sticherling, M., Sticht, H., Oji, V., Hüffmeier, U. (2015). Palmoplantar Pustular Psoriasis Is Associated with Missense Variants in CARD14, but Not with Loss-of-Function Mutations in IL36RN in European Patients. *Journal of Investigative Dermatology, 135*(10), 2538-2541.

Nair, R. P., Stuart, P. E., Nistor, I., Hiremagalore, R., Chia, N. V., Jenisch, S., Weichenthal, M., Abecasis, GR., Lim, HW., Christophers, E., Voorhees, JJ., Elder, J. T. (2006). Sequence and Haplotype Analysis Supports HLA-C as the Psoriasis Susceptibility 1 Gene. *The American Journal of Human Genetics, 78*(5), 827-851.

Naldi, L., & Gambini, D. (2007). The clinical spectrum of psoriasis. *Clinics in Dermatology, 25*(6), 510-518.

Nestle, F. O., Kaplan, D. H., & Barker, J. (2009). Psoriasis. *New England Journal of Medicine, 361*(5), 496-509.

Ng, S. B., Buckingham, K. J., Lee, C., Bigham, A. W., Tabor, H. K., Dent, K. M., Huff ,CD,. Shannon, PT., Jabs, EW., Nickerson, DA., Shendure, J., Bamshad, M. J. (2009). Exome sequencing identifies the cause of a mendelian disorder. *Nature Genetics, 42*(1), 30-35.

Okada, Y., Han, B., Tsoi, L., Stuart, P., Ellinghaus, E., Tejasvi, T., Chandran, V., Pellett, F., Pollock R7, Bowcock, AM., Krueger, GG., Weichenthal, M., Voorhees, JJ., Rahman, P., Gregersen, PK., Franke, A., Nair, RP., Abecasis, G., Gladman, D., Elder, JT., de Bakker PI,Raychaudhuri, S. (2014). Fine Mapping Major Histocompatibility Complex Associations in Psoriasis and Its Clinical Subtypes. *The American Journal of Human Genetics, 95*(2), 162-172.

Olson, N. D., Lund, S. P., Colman, R. E., Foster, J. T., Sahl, J. W., Schupp, J. M., Keim, P., Morrow, JB., Salit, ML.,Zook, J. M. (2015). Best practices for evaluating single nucleotide variant calling methods for microbial genomics. *Front.*

Genet. Frontiers in Genetics, 6.

Onoufriadis, A., Simpson, M., Pink, A., Di Meglio, P., Smith, C., Pullabhatla, V., Knight, J., Spain, SL., Nestle, FO., Burden, AD., Capon, F., Trembath, RC., Barker, J. (2011). Mutations in IL36RN/IL1F5 Are Associated with the Severe Episodic Inflammatory Skin Disease Known as Generalized Pustular Psoriasis. *The American Journal of Human Genetics, 89*(3), 432-437.

Pabinger, S., Dander, A., Fischer, M., Snajder, R., Sperk, M., Efremova, M., Snajder, R., Sperk, M., Efremova, M., Krabichler, B., Speicher, MR., Zschocke, J., Trajanoski, Z. (2013). A survey of tools for variant analysis of next-generation genome sequencing data. *Briefings in Bioinformatics, 15*(2), 256-278.

Pasparakis, M., Haase, I., & Nestle, F. O. (2014). Mechanisms regulating skin immunity and inflammation. *Nature Reviews Immunology, 14*(5), 289-301.

Pepper, R. J., & Lachmann, H. J. (2016). Autoinflammatory Syndromes in Children. *Indian J Pediatr The Indian Journal of Pediatrics, 83*(3), 242-247.

Polcari, I., Becker, L., Stein, S. L., Smith, M. S., & Paller, A. S. (2014). Filaggrin Gene Mutations in African Americans with Both Ichthyosis Vulgaris and Atopic Dermatitis. *Pediatric Dermatology, 31*(4), 489-492.

Purcell, S., Cherny, S. S., & Sham, P. C. (2003). Genetic Power Calculator: Design of linkage and association genetic mapping studies of complex traits. *Bioinformatics, 19*(1), 149-150.

Quinlan, A. R., & Hall, I. M. (2010). BEDTools: A flexible suite of utilities for

comparing genomic features. *Bioinformatics, 26*(6), 841-842.

Rauen, T., Benedyk, K., Juang, Y., Kerkhoff, C., Kyttaris, V. C., Roth, J., Snajder. R, Krabichler, B., Speicher, MR., Zschocke, J., Tenbrock, K. (2011). A Novel Intronic cAMP Response Element Modulator (CREM) Promoter Is Regulated by Activator Protein-1 (AP-1) and Accounts for Altered Activation-induced CREM Expression in T Cells from Patients with Systemic Lupus Erythematosus. *Journal of Biological Chemistry, 286*(37), 32366-32372.

Rehm, H. L. (2013). Disease-targeted sequencing: A cornerstone in the clinic. *Nat Rev Genet Nature Reviews Genetics, 14*(4), 295-300.

Reis, A., Hennies, H., Langbein, L., Digweed, M., Mischke, D., Drechsler, M., McGrath, JA., Smith, FJ., McLean, WH., Küster, W. (1994). Keratin 9 gene mutations in epidermolytic palmoplantar keratoderma (EPPK). *Nature Genetics Nat Genet, 6*(2), 174-179.

Renert-Yuval, Y., Horev, L., Babay, S., Tams, S., Ramot, Y., Zlotogorski, A., & Molho-Pessach, V. (2014). IL36RN mutation causing generalized pustular psoriasis in a Palestinian patient. *International Journal of Dermatology, 53*(7), 866-868.

Rigourd, V., Chauvet, C., Chelbi, S. T., Rebourcet, R., Mondon, F., Letourneur, F Mignot, TM., Barbaux, S., Vaiman, D. (2008). STOX1 Overexpression in Choriocarcinoma Cells Mimics Transcriptional Alterations Observed in Preeclamptic Placentas. *PLoS ONE, 3*(12).

Robinson, J. T., Thorvaldsdóttir, H., Winckler, W., Guttman, M., Lander, E. S., Getz,

G., & Mesirov, J. P. (2011). Integrative genomics viewer. *Nat Biotechnol Nature Biotechnology, 29*(1), 24-26.

Rossi-Semerano, L., Fautrel, B., Wendling, D., Hachulla, E., Galeotti, C., Semerano, L., Touitoui, I., Koné-Paut, I. (2015). Tolerance and efficacy of off-label anti-interleukin-1 treatments in France: A nationwide survey. *Orphanet Journal of Rare Diseases, 10*(1),19.

Rossi-Semerano, L., Piram, M., Chiaverini, C., Ricaud, D. D., Smahi, A., & Kone-Paut, I. (2013). First Clinical Description of an Infant With Interleukin-36-Receptor Antagonist Deficiency Successfully Treated With Anakinra. *Pediatrics, 132*(4), e1043-1047.

Ryan, C., & Kirby, B. (2015). Psoriasis Is a Systemic Disease with Multiple Cardiovascular and Metabolic Comorbidities. *Dermatologic Clinics, 33*(1), 41-55.

Sandgren, S., Wittrup, A., Cheng, F., Jonsson, M., Eklund, E., Busch, S., & Belting, M. (2004). The Human Antimicrobial Peptide LL-37 Transfers Extracellular DNA Plasmid to the Nuclear Compartment of Mammalian Cells via Lipid Rafts and Proteoglycan-dependent Endocytosis. *Journal of Biological Chemistry*, *279*(17), 17951-17956.

Schmidt, J. (2016). Membrane platforms for biological nanopore sensing and sequencing. *Current Opinion in Biotechnology, 39*, 17-27.

Schwartz, S., Hall, E., & Ast, G. (2009). SROOGLE: Webserver for integrative, user-friendly visualization of splicing signals. *Nucleic Acids Research, 37*(Web Server).

Schwarz, J. M., Cooper, D. N., Schuelke, M., & Seelow, D. (2014). MutationTaster2: Mutation prediction for the deep-sequencing age. *Nature Methods, 11*(4), 361-362.

Scudiero, I., Zotti, T., Ferravante, A., Vessichelli, M., Vito, P., & Stilo, R. (2011). Alternative splicing of CARMA2/CARD14 transcripts generates protein variants with differential effect on NF-κB activation and endoplasmic reticulum stress-induced cell death. *Journal of Cellular Physiology, 226*(12), 3121-3131.

Scudiero, I., Vito, P., & Stilo, R. (2014). The Three CARMA Sisters: So Different, So Similar: A Portrait of the Three CARMA Proteins and Their Involvement in Human Disorders. *Journal of Cellular Physiology, 229*(8), 990-997.

Setta-Kaffetzi, N., Navarini, A. A., Patel, V. M., Pullabhatla, V., Pink, A. E., Choon, S., Capon, F., Barker, J. N. (2013). Rare Pathogenic Variants in IL36RN Underlie a Spectrum of Psoriasis-Associated Pustular Phenotypes. *Journal of Investigative Dermatology, 133*(5), 1366-1369.

Setta-Kaffetzi, N., Simpson, M., Navarini, A., Patel, V., Lu, H., Allen, M, Barker, JN., Thrembath, RC, Capon, F. (2014). AP1S3 Mutations Are Associated with Pustular Psoriasis and Impaired Toll-like Receptor 3 Trafficking. *The American Journal of Human Genetics, 94*(5), 790-797.

Singleton, A. B. (2011). Exome sequencing: A transformative technology. *The Lancet Neurology, 10*(10), 942-946.

Song, H. S., Yun, S. J., Park, S., & Lee, E. (2014). Gene Mutation Analysis in a Korean Patient with Early-Onset and Recalcitrant Generalized Pustular Psoriasis.

Annals of Dermatology, *26*(3), 424.

Strange, A., Capon, F., Spencer, C. C., Knight, J., Weale, M. E., Allen, MH., Trembath, RC. (2010). A genome-wide association study identifies new psoriasis susceptibility loci and an interaction between HLA-C and ERAP1. *Nature Genetics Nat Genet, 42*(11), 985-990.

Stuart, P. E., Tejasvi, T., Shaiq, P. A., Kullavanijaya, P., Qamar, R., Raja, G. K., Li, Y., Voorhees, JJ., Abecacis, GR., Elder, JJ., Nair, R. P. (2015). A Single SNP Surrogate for Genotyping HLA-C*06:02 in Diverse Populations. *Journal of Investigative Dermatology*, *135*(4), 1177-1180.

Sugiura, K., Takeichi, T., Kono, M., Ogawa, Y., Shimoyama, Y., Muro, Y., & Akiyama, M. (2012). A novel IL36RN/IL1F5 homozygous nonsense mutation, p.Arg10X, in a Japanese patient with adult-onset generalized pustular psoriasis. *British Journal of Dermatology, 167*(3), 699-701.

Sugiura, K., Takemoto, A., Yamaguchi, M., Takahashi, H., Shoda, Y., Mitsuma, T., Tsuda, K., Nishida, E., Togawa, Y., Nakajima, K., Sakakibara, A., Kawachi, S., Shimizu, M., Ito, Y, Takeichi, T., Kono, M., Ogawa, Y., Muro, Y., Ishida-Yamamoto, A., Sano, S., Matsue, H., Morita, A., Mizutani, H., Iizuka, H., Muto, M., Akiyama, M. (2013). The Majority of Generalized Pustular Psoriasis without Psoriasis Vulgaris Is Caused by Deficiency of Interleukin-36 Receptor Antagonist. *Journal of Investigative Dermatology*, *133*(11), 2514-2521.

Sugiura, K., Muto, M., & Akiyama, M. (2014). CARD14 c.526GC (p.Asp176His) Is a Significant Risk Factor for Generalized Pustular Psoriasis with Psoriasis

Vulgaris in the Japanese Cohort. *Journal of Investigative Dermatology, 134*(6), 1755-1757.

Swindell, W. R., Stuart, P. E., Sarkar, M. K., Voorhees, J. J., Elder, J. T., Johnston, A., & Gudjonsson, J. E. (2014). Cellular dissection of psoriasis for transcriptome analyses and the post-GWAS era. *BMC Medical Genomics, 7*(1), 27.

Szun, S.T., Roediger, B., Tong, P. L., Tikoo, S., & Weninger, W. (2014) The skin-resident immune network. *Current Dermatology Reports,* 3:13-22.

Takeuchi, O., & Akira, S. (2010). Pattern Recognition Receptors and Inflammation. *Cell, 140*(6), 805-820.

Tavtigian, S. V., Greenblatt, M. S., Lesueur, F., & Byrnes, G. B. (2008). In silico analysis of missense substitutions using sequence-alignment based methods. *Human Mutation; 29*(11), 1327-1336.

Thomas, J., Kumar, P., & Balaji, S. R. (n.d.) (2014). *Psoriasis: A closer look.*

Thompson, J. D., Higgins, D. G., & Gibson, T. J. (1994). CLUSTAL W: Improving the sensitivity of progressive multiple sequence alignment through sequence weighting, position-specific gap penalties and weight matrix choice. *Nucleic Acids Research, 22*(22), 4673-4680.

Thorvaldsdottir, H., Robinson, J. T., & Mesirov, J. P. (2012). Integrative Genomics Viewer (IGV): High-performance genomics data visualization and exploration. *Briefings in Bioinformatics, 14*(2), 178-192.

Tortola, L., Rosenwald, E., Abel, B., Blumberg, H., Schäfer, M., Coyle, A. J., Renauld,

JC., Werner, S., Kisielow, J., Kopf, M. (2012). Psoriasiform dermatitis is driven by IL-36–mediated DC-keratinocyte crosstalk. *Journal of Clinical Investigation J. Clin. Invest., 122*(11), 3965-3976.

Tsoi, L. C., Spain, S. L., Knight, J., Ellinghaus, E., Stuart, P. E., Capon, F., Ding J, Li, Y., Tejasvi, T., Gudjonsson, JE., Kang, HM., Allen, MH., McManus, R., Novelli, G., Samuelsson, L., Schalkwijk, J., Ståhle, M., Burden, AD., Smith, CH., Cork, MJ., Estivill, X., Bowcock, AM., Krueger, GG., Weger, W., Worthington, J., Tazi-Ahnini, R., Nestle, FO., Hayday, A., Hoffmann, P., Winkelmann, J., Wijmenga, C., Langford, C., Edkins, S., Andrews, R., Blackburn, H., Strange, A., Band, G., Pearson, RD., Vukcevic, D., Spencer, CC., Deloukas, P., Mrowietz, U., Schreiber ,S., Weidinger, S., Koks, S., Kingo, K., Esko, T., Metspalu, A., Lim, HW., Voorhees, JJ., Weichenthal, M., Wichmann, HE., Chandran, V., Rosen, CF., Rahman, P., Gladman, DD., Griffiths, CE., Reis, A., Kere, J. Trembath, R. C. (2012). Identification of 15 new psoriasis susceptibility loci highlights the role of innate immunity. *Nature Genetics Nat Genet, 44*(12), 1341-1348.

Tsoi, L. C., Spain, S. L., Ellinghaus, E., Stuart, P. E., Capon, F., Knight, J., Stuart, P. E., Capon, F., Ding J, Li, Y., Tejasvi, T., Gudjonsson, JE., Kang, HM., Allen, MH., McManus, R., Novelli, G., Samuelsson, L., Schalkwijk, J., Ståhle, M., Burden, AD., Smith, CH., Cork, MJ., Estivill, X., Bowcock, AM., Elder, J. T. (2015). Enhanced meta-analysis and replication studies identify five new psoriasis susceptibility loci. *Nature Communications Nat Comms, 6,* 7001.

The 1000 Genomes Project Consortium (2012). An integrated map of genetic variation from 1,092 human genomes. Nature, 491(77422):56-65.

Tuli, A., Thiery, J., James, A. M., Michelet, X., Sharma, M., Garg, S., Sanborn, KB., Orange, JS., Lieberman, J., Brenner, M. B. (2013). Arf-like GTPase Arl8b regulates lytic granule polarization and natural killer cell-mediated cytotoxicity. *Molecular Biology of the Cell, 24*(23), 3721-3735.

Untergasser, A., Cutcutache, I., Koressaar, T., Ye, J., Faircloth, B. C., Remm, M., & Rozen, S. G. (2012). Primer3--new capabilities and interfaces. *Nucleic Acids Research, 40*(15).

Vaisberg, E.A., Grissom, P.M., & McIntosh, J.R. (1996). Mammalian cells express three distinct dynein heavy chains that are localized to different cytoplasmic organelles. *The Journal of Cell Biology*, 133(4):831-42.

Verjans, E., Ohl, K., Reiss, L., K., Wijk, F., Toncheva, A., Knol, E., Kabesch, M.7, Wagner, N., Tenbrock, K. (2015). The cAMP response element modulator (CREM) regulates TH2 mediated inflammation. *Oncotarget*., 6(36):38538-38551.

Venter, J. C. (2001). The Sequence of the Human Genome. *Science, 291*(5507), 1304-1351.

Wang, K., Li, M., & Hakonarson, H. (2010). ANNOVAR: Functional annotation of genetic variants from high-throughput sequencing data. *Nucleic Acids Research, 38*(16).

Wolf, J., & Ferris, L. K. (2014). Anti-IL-36R antibodies, potentially useful for the treatment of psoriasis: A patent evaluation of WO2013074569. *Expert Opinion on Therapeutic Patents, 24*(4), 477-479.

Wolf, E., Kim, P. S., & Berger, B. (1997). MultiCoil: A program for predicting two-and three-stranded coiled coils. *Protein Science, 6*(6), 1179-1189.

Wong, L., Ong, R., Poh, W., Liu, X., Chen, P., Li, R Lam, KK., Pillai, NE., Sim, KS., Xu, H., Sim, NL., Teo, SM., Foo, JN., Tan, LW., Lim, Y., Koo, SH., Gan, LS., Cheng , CY., Wee, S., Yap, EP., Ng, PC., Lim, WY., Soong, R., Wenk, MR., Aung, T., Wong, TY., Khor, CC., Little ,P., Chia, KS., Teo, Y. (2013). Deep Whole-Genome Sequencing of 100 Southeast Asian Malays. *The American Journal of Human Genetics, 92*(1), 52-66.

Wong, L., Lai, J. K., Saw, W., Ong, R. T., Cheng, A. Y., Pillai, N. E., Pillai, NE., Sim, KS., Xu, H., Sim, NL., Teo, SM., Foo, JN., Tan, LW., Lim, Y., Koo, SH., Gan, LS., Cheng , CY., Wee, S., Yap, EP., Ng, PC., Lim, WY., Soong, R Teo, Y. (2014). Insights into the Genetic Structure and Diversity of 38 South Asian Indians from Deep Whole-Genome Sequencing. *PLoS Genetics, 10*(5).

Wu, J., & Chen, Z. J. (2014). Innate Immune Sensing and Signaling of Cytosolic Nucleic Acids. *Annual Review of Immunology, 32*(1), 461-488.

Xie, P. (2013). TRAF molecules in cell signaling and in human diseases. *Journal of Molecular Signaling, 8(2):* 7.

Xu, J., Zhou, X., Wang, J., Li, Z., Kong, X., Qian, J., Hu, Y., Fang, J. (2013). RhoGAPs Attenuate Cell Proliferation by Direct Interaction with p53 Tetramerization Domain. *Cell Reports, 3*(5), 1526-1538.

Yamaguchi, T., Miyashita, C., Koyano, S., Kanda, H., Yoshioka, K., Shiba, T., Takamatsu, N., Ito, M. (2009). JNK-binding protein 1 regulates NF-κB

activation through TRAF2 and TAK1. *Cell Biology International, 33*(3), 364-368.

Yeo, G., & Burge, C. B. (2003). Maximum entropy modeling of short sequence motifs with applications to RNA splicing signals. *Proceedings of the Seventh Annual International Conference on Computational Molecular Biology - RECOMB '03*.

Yin, X., Cheng, H., Lin, Y., Fan, X., Cui, Y., Zhou, F., Yang, S., Zhang, X. (2014). Five regulatory genes detected by matching signatures of eQTL and GWAS in psoriasis. *Journal of Dermatological Science, 76*(2), 139-142.

Zhang, Z., Schwartz, S., Wagner, L., & Miller, W. (2000). A Greedy Algorithm for Aligning DNA Sequences. *Journal of Computational Biology, 7*(1-2), 203-214.

Zhang, X. (2015). Whole-exome SNP array identifies 15 new susceptibility loci for psoriasis. *Nature Communications Nat Comms, 6*, 6793.

APPENDIX

Appendix I: Case Report Form

Date of Collection: 27/09/12

Collected by: DR [redacted]

Institution: HOSPITAL SULTANAH AMINAH JOHOR BAHRU, JOHOR

Country: MALAYSIA

Patient Details

Subject no.	[redacted]	NHS No.	☐ Unknown
Forename	[redacted]	GSTT No.	☐ Unknown
Date of Birth	[redacted]	Sex: FEMALE	Consultant: DR [redacted]

Ethnicity/Family History

Ethnicity: White ☐ Black - African ☐ Black - Caribbean ☐ Black - Other ☐ Indian ☐ Bangladeshi ☐ **Chinese** ☑ Asian - Other ☐ Other ☐

If Other, Please Specify: CHINESE

Family History of Psoriasis: ☐ Yes ☑ No ☐ Unknown

If Yes, who else is affected: ____ (Please draw family tree **and highlight any consanguinity**)

Diagnostic & Phenotypic Data

Year of Diagnosis: 2005

Year first seen by specialist: 2005

Age of onset: 13

	Past	Present	No	
Generalised Pustular Psoriasis	☑	☐	☐	(Involvement of the flexures ☐)
Localised Pustular Psoriasis	☐	☐	☑	(Sites involved ____)
Chronic Plaque Psoriasis	☑	☐	☐	
Psoriatic Arthritis	☐	☐	☑	
Confirmed by Rheumatologist	☐	☐	☑	
Palms/Soles (Non Pustular)	☐	☐	☑	
Palmoplantar pustulosis	☐	☐	☑	
Acrodermatitis of Hallopeau	☐	☐	☑	
Nail Involvement	☐	☑	☐	
Pitting	☐	☑	☐	
Onycholysis	☐	☑	☐	
Subungual Hyperkeratosis	☐	☑	☐	
Number of Nails Affected	20 / 20			
Flex/Intertriginous	☐	☐	☑	
Seborrhoeic Psoriasis	☐	☐	☑	
Scalp involvement	☑	☑	☐	

Exacerbating factors:

Stress	☑	
Medication	☐	Please state ____
Pregnancy	☐	

Infections		Please state	
Other	☑	Please state	MENSTRUATION

Features associated with flares (state if ever had): NONE

Fever > 38 ºC	☐
Malaise	☐
CRP > 100	☐
ESR >50	☐
Neutrophilia > 15	☐

Clinical Assessment:

Date of Assessment	27/09//2012	Weight (kg)	44
PASI Score		Height (cm)	163
DLQI	12	Waist (cm)	68

Psoriasis Treatment –

Past Treatment – including UV

						Responder
TABLET DOXYCYLINE	100	OD	07/05/2009	Y/N	07/08/2009	**Y**

Current systemic psoriasis Treatment: (Including phototherapy)

Treatment week	Dose		Route	Start date		End Date	Responder
					Y/N	DD/MM/YY	Y/N

Sample collection

Date of collection	27/09/12

Blood for DNA extraction (need a minimum of 2 full EDTA containing blood tubes)	☑
DNA extracted from samples	☐

Appendix II: Primers used in the study

Table II a: Primers used for PCR and Sanger sequencing

Primer ID	Target Region	Sequence 5' to 3'	$T_{annealing}$ [°C]
ARFGAP2 Ex1-2 F	*ARFGAP2*	AGATCGGACTCCAATCACCC	66
ARFGAP2 Ex1-2 R	*Exon1-2*	GAATTCAGAGCGGCCCAAG	
ARFGAP2 Ex3 F	*ARFGAP2*	GACAGGTATCCGGGTTGC	56
ARFGAP2 Ex3 R	*Exon3*	TGACCAGTTTCGAAGTTTTCAG	
ARFGAP2 Ex4-5 F	*ARFGAP2*	AACCGGTGTCAGTAGCGTGT	62
ARFGAP2 Ex4-5 R	*Exon4-5*	CTAGGCCTACCCAGCAGGA	
ARFGAP2 Ex6-7 F	*ARFGAP2*	TGATTTCTTGTCCACAAGGTG	56
ARFGAP2 Ex 6-7 R	*Exon6-7*	CAGGCAGTAGGACCTCTGAA	
ARFGAP2 Ex8 F	*ARFGAP2*	CCTTGCCTGAAGCTGTTCTT	56
ARFGAP2 Ex8 R	*Exon8*	GGTAAGTGGTAAGGTCAAGGAGT	
ARFGAP2 Ex9-10F	*ARFGAP2*	AGAAGGGCCTTTTCCTTGTG	56
ARFGAP2 Ex9-10R	*Exon9-10*	GCATCCCAAACTGCTAGGAA	
ARFGAP2 Ex11 F	*ARFGAP2*	TGGGTAAGGACAGAAGGCTC	60
ARFGAP2 Ex11R	*Exon11*	TTGTCCTTGTACCTAGGGAGA	
ARFGAP2 Ex12F	*ARFGAP2*	TTGGTACTTTCGCCTCTGGA	60
ARFGAP2 Ex12R	*Exon12*	GTTCTTCTAGACAGTGCTGCC	
ARFGAP2 Ex13F	*ARFGAP2*	AATGCTGACGAAGCTGTGTG	56
ARFGAP2 Ex13R	*Exon13*	CTGGCCTCATACTGTGGTGA	
ARFGAP2 Ex14-15F	*ARFGAP2* *Exon14-15*	CTGTGTGAGTCCTTGGGTCA	62
ARFGAP2 Ex14-15R		AAATGCTCTTAAGGCTCAGAGG	

ARFGAP2 Ex 16F	*ARFGAP2*	CAGCTCTCACCGTGGACTC	62
ARFGAP2 Ex16R	*Exon16*	CAAGGGCTGGTACTGACCAT	
ARHGAP11A Ex4F	*ARHGAP11A*	CCACATAGTCTGTGCCACATT	56
ARHGAP11A Ex4R	*Exon 4*	TTGGAGTATACTCCTCATAG	
ARHGAP11A Ex5F	*ARHGAP11A*	GCCAATCATGTAGATGAAGGGTAA	56
ARHGAP11A Ex5R	*Exon 5*	CCAACTTTCTAACAGTTGCC	
ARHGAP11A Ex6F	*ARHGAP11A*	GTTGGTATATTACTGACCTCACCC	56
ARHGAP11A Ex6R	*Exon 6*	CCAAAAAGGCACATACCACA	
ARHGAP11A Ex7F	*ARHGAP11A*	TGGAAGTATAAGTGGGGAATGG	56
ARHGAP11A Ex7R	*Exon 7*	TGCCTACAATTTTGGGTTCA	
ARHGAP11A Ex8F	*ARHGAP11A*	GTAATTGCAGAGTGTTTTAG	56
ARHGAP11A Ex8R	*Exon 8*	AATTGCACTGTGCCCAGAA	
ARHGAP11AE12F	*ARHGAP11A*	CATGACCAAAGAGACTTTGG	56
ARHGAP11A E12R	*Exon 8*	GTTACAACACATGTACTCTGC	
ARHGEF16 F	*ARHGEF16*	GGTCTCCCAAAGCACATTCC	62
ARHGEF16 R	*Exon 8*	GGAGGAGAAGGTCACAAGCA	
CARD14 Ex 2	*CARD14 Exon 2*	ATG GCC ACT GGA ATG CTT C	63
CARD14 Ex 2		CAG GAC GAG AAG AGA CCC C	
CARD14 Ex 3	*CARD14 Exon 3*	ACC CAG CAG AAC CCA GAA A	64
CARD14 Ex 3		AAG GGG GAG TAG GGC AAA T	
CARD14 Ex 4	*CARD14 Exon 4*	TGC TCA CCT GCT CAC CTA C	66
CARD14 Ex 4		AAG GAG TTC CAG GGA GAT GG	
CARD14 Ex 5	*CARD14 Exon 5*	TTC AGT CTC GAG GCA GGA AG	63
CARD14 Ex 5		AAC CAC CTG TCA GAA ACC CC	
CARD14 Ex 6	*CARD14 Exon 6*	AAG ACT GCA TCC GTC CAC A	63
CARD14 Ex 6		AAT TAT GTG AGC TCG GCG TG	
CARD14 Ex 7	*CARD14 Exon 7*	AGA ACT GTC TCC CTC CCT C	66

CARD14 Ex 7		TGT GGA CCG AGG AAA GAG AC	
CARD14 Ex 8	*CARD14 Exon 8*	CAC TGC ACA TGT GAA CAC GA	63
CARD14 Ex 8		TCG CTC ATC ACA GTG ACA CT	
CARD14 Ex 9	*CARD14 Exon 9*	CTG GAA GCT GAC GAG AGG AA	63
CARD14 Ex 9		CGT ACC AAC CTC TTC CCT GT	
CARD14 Ex 10-11	*CARD14 Exon 10-11*	TGT GTC CTT CTT TCC CCT CC	65
CARD14 Ex 10-11		TAT CTG CCC TTT CCC TGG AG	
CARD14 Ex 12-13	*CARD14 Exon 12-13*	AGA TCT GTG AAG AAG GGG CT	66
CARD14 Ex 12-13		TGA AGT CTG CCT GGG TCA C	
CARD14 Ex 14-15	*CARD14 Exon 14-15*	TGC AGG CAG TGG TCC TAC	63
CARD14 Ex 15-15		CGC CCA CCC TCT ATT GCT	
CARD14 Ex 16-17	*CARD14 Exon 16-17*	AAA GCT CTG GAG ACT GGC AT	63
CARD14 Ex 16-17		TTT GAA GGG GTG CAG AGG AG	
CARD14 Ex 18-19	*CARD14 Exon 18-19*	ACA CAC CTC AGG CTG TTC TC	63
CARD14 Ex 18-19		CCC AGC CCC ATG ATT CTT GA	
CARD14 Ex 20-21	*CARD14 Exon 20-21*	TGG AAT TCTAGG TGCTGG GG	64
CARD14 Ex 20-21		GGT CGG TCCCTG TAC CTTTA	
CARD14 Ex 22	*CARD14 Exon 22*	AAATTCAGC TCTGCC CAGCTCC	63
CARD14 Ex 22		TCC CAA AGT TGT GCG GAA AC	
CARD14 Ex 23	*CARD14 Exon 23*	TGT CAT CAC TAC CCT AGC CA	63
CARD14 Ex 23		GCC TCA TGT GCC AAG GAG	
CYP1A1Ex2/1F	*CYP1A1Exon 2*	GTTTCCCCTTTCCCTGACAC	64
CYP1A1Ex2/1R		TGCCATCAGCTCCTGCAA	
CYP1A1Ex2/2F	*CYP1A1Exon 2*	CCAGAATGGCCTGAAAAGTT	62
CYP1A1Ex2/2R		CAGGTTGAAGCCTTCCTGAG	
CYP1A1Ex3-4F	*CYP1A1Exon 3-*	AGAGAAGCTGGGACAACAGC	67

CYP1A1Ex3-4R	*4*	GTCTGCAGAACACAGGGACA	
CYP1A1Ex5F	*CYP1A1 Exon 5*	TGAACCCCAGGGTACAGAGA	66
CYP1A1Ex5R		AGGAAGCTCAGTCAGGCTCA	
CYP1A1Ex6F	*CYP1A1 Exon6*	ATGGAGCCACTGCTGTCTGT	64
CYP1A1Ex6R		AGCCCCAAAGGATAGAGGAC	
CYP1A1Ex7F	*CYP1A1 Exon 7*	GCCTGTCCTCTATCCTTTGG	65
CYP1A1Ex7R		ACTGCAGCCAGATCAGTGTC	
DNAH12 varEx38F	*DNAH12 Exon 38*	TGAGTTTTTAATGAAGATGATTTG	58
DNAH12 varEx38R		TGTACAATTTTAAACACTGAGCA	
DOCK8e8F	*DOCK8 Exon 8*	TGTCCACCATGATCTCAAATGA	63
DOCK8e8R		CTCCAGTAGCCTCTCCCTCT	
EPHA8 F	*EPHA8 Exon 18*	GTTGTCCCTCTGGACTGGAA	62
EPHA8 R		TCCACAGAGCTGATGACCTG	
HLA-C S F	*HLA-C*	TACTACAACCAGAGCGAGGA	65
HLA-C S R		GGTCGCAGCCATACATCCA	
IL36RN- Exon1-F	*IL36RN- Exon1*	GCTCCGTGGAGGCTGTTC	52
IL36RN- Exon1-R		CACAATTTCCCAGCTGCAAT	
IL36RN- Exon2-F	*IL36RN- Exon2*	GGAGACAAGGCTGTGCTGTT	59
IL36RN- Exon2-R		GCTTAGAGCCTGGTTTGTGC	
IL36RN- Exon3-F	*IL36RN- Exon3*	CTGCTGAGAAGCCTCCCTTC	59
IL36RN- Exon3-R		CAAAGCTGCCATCAACAGAA	
IL36RN- Exon4-F	*IL36RN- Exon4*	TTCTGTTGATGGCAGCTTTG	59
IL36RN- Exon4-R		GGTCAGGTGCCCACTAAGTC	
IL36RN- promoter1-F	*IL36RN-promoter*	TTTTCTGTGTTTTGAACAACTTGA	59

IL36RN- promoter1-R		GCTATTGAAAACCATGTTGTGAC	
IL36RN- promoter2-F	*IL36RN-promoter*	AACCAGATACATGAGCAAAGATG	59
IL36RN- promoter2-R		TCCCCTATTCCCTTTCTTCC	
IGSF10 F	*IGSF10 Exon 4*	AGTAGCACCACCAACAAACT	62
IGSF10 R		CATTGAGCACTGTGGCTGAG	
IQGAP2 F	*IQGAP2 Exon 13*	TGCTTGCATCTTGCATCCTA	59
IQGAP2 R		GGGTCAAATCCTCCTCCTTC	
MAPKBP1e8F	*MAPKBP1 Exon 8*	CTGTCTGGGCTGAGGAGTAG	65
MAPKBP1e8R		GGAAATGGGCCAAGCTCTAG	
FRAS1 F	*FRAS1 Exon 60*	TGTGGGAAAGCACACAGATG	62
FRAS1 R		TCTGTAGAGGGAGATCATTTGC	
PLCH1 F	*PLCH1 Exon 15*	TGTGCGTGGTGTTTTCTTTG	60
PLCH1 R		CAAGATGGTGGCATAGTGAGA	
RELT F	*RELT Exon 11*	GCCACTTTCCTGGAGCCA	59
RELT R		ATCCTTCAGGGGAGCAACAT	
RNF207F	*RNF207 Exon 1*	CCACGTACTTCTGCAACACG	62
RNF207 R		CAAGAGGTAGGGCTCTGCG	
STOX1 F	*STOX1 Exon 3*	TTGGGTACAGAATGGGGCA	59
STOX1 R		GCCTTTTCTTAACCCCCTCTT	
TAS2R3 F	*TAS2R3 Exon 1*	CAGTGAAGCAACAGGTAGAGGA	62
TAS2R3 R		CCCTGAATCATGTGTGTTGG	
VNN2 F	*VNN2 Exon 4*	GATTCCCTGCAGTTGACCAT	62
VNN2 R		GAGGCATTCATTTCTCTGCACT	
ZNF516 F	*ZNF516 Exon 3*	GAAGCCCTACAAGTGTCCCT	58.5 (10%

ZNF516 R		CTTCTTACGCTCGAACTGGC	DMSO)

All primers were purchased from Eurofin Genomics.

Table II b: Primers used for Sanger Sequencing only

Primer ID	Target Region	Sequence 5' to 3'
CARD14s 1F / T7F	T7	AATACGACTCACTATAGGG
CARD14s 1R	*CARD14sh* in pcDNA 3.1	TCCAGAATGTCCTTCTCC
CARD14s 1ibF	*CARD14sh* in pcDNA 3.1	ACTTGCTGGATTTGCTGAA
CARD14s 1ibR	*CARD14sh* in pcDNA 3.1	TCAGCAAATCCAGCAAGT
CARD14s 2F	*CARD14sh* in pcDNA 3.1	TCCTGTGAGCTGGAATTG
CARD14s 2R	*CARD14sh* in pcDNA 3.1	TAATCCAGGTGTGGGTCG
CARD14s 3F	*CARD14sh* in pcDNA 3.1	GAGCTGGTGGACAGCTTC
CARD14s 3R/BGH R	*CARD14sh* in pcDNA 3.1	TAGAAGGCACAGTCGAGG
CMVextra1	*pCMV promoter in* pcDNA 3.1	GACTTTCCTACTTGGCAGT
BGHextra1	*BGH site in* pcDNA 3.1	CTTCTAGTTGCCAGCCATC

All primers were purchased from Eurofin Genomics.

Table II c: Primers used for real-time PCR

Primer ID	Target gene	Sequence 5' to 3'
ARFGAP2 Q F main	*ARFGAP2* full length transcript	TCACTCCCCAGAGAAGAAGG
ARFGAP2 Q R main	*ARFGAP2* full length transcript	CAGGCCACTGCTCTCTGTAGA
ARFGAP2 Q F 2nd	*ARFGAP2* isoform lacking exon 5	ATGGCACTGATCCCCCTGC

ARFGAP2 Q F 2nd	*ARFGAP2* isoform lacking exon 5	TCTGTGTTGGGGCCATGCT

All primers were purchased from Eurofin Genomics.

Table II d: Primers used for microsatellite genotyping

Primer ID	Target	Sequence 5' to 3'
Chr6 Micros F	AFM142xh6 (D6S273)	5'FAM-GCAACTTTTCTGTCAATCCA
Chr6 Micros R		ACCAAACTTCAAATTTTCGG

Appendix III: Web resources

Application	Website
Basic Local Alignment Search Tool (BLAST)	http://blast.ncbi.nlm.nih.gov/Blast.cgi
Beijing Meidi TCM Skin Disease Hospital	http://www.skindiseasehospital.org
British Association of Dermatologists	http://www.bad.org.uk
Clustalw2	http://www.ebi.ac.uk/Tools/msa/clustalw2/
COILs	http://embnet.vital-it.ch/software/COILS_form.html
Combined Annotation Dependent Depletion (CADD)	http://cadd.gs.washington.edu/
dbSNP	http://www.ncbi.nlm.nih.gov/SNP/
Ensembl	http://www.ensembl.org/index.html

Exome Sequencing in the Clinic	http://www.slideshare.net/informaoz/michael-buckley-seals
Genetic Power Calculator	http://pngu.mgh.harvard.edu/~purcell/gpc
Graphpad	http://graphpad.com/quickcalcs/contingency1.cfm
ImageJ	http://imagej.nih.gov/ij/
Integrative Genomics Viewer (IGV)	http://www.broadinstitute.org/igv/
HaploView	https://www.broadinstitute.org/scientific-community/science/programs/medical-and-population-genetics/haploview/haploview
MaxEntScan	http://genes.mit.edu/burgelab/maxent/Xmaxentscan_scoreseq.html
MultiCoil	http://groups.csail.mit.edu/cb/multicoil/cgi-bin/multicoil.cgi
Mutation Taster	http://www.mutationtaster.org/
Ncoils	http://manpages.ubuntu.com/manpages/precise/man1/ncoils
Online Binomial Calculator	http://stattrek.com/online-calculator/binomial.aspx
PolyPhen-2	http://genetics.bwh.harvard.edu/pph2/
Primer3	http://bioinfo.ut.ee/primer3-0.4.0/
Prism	http://www.graphpad.com/scientific-software/prism
Psoriasis Medication	http://psoriasismedication.org
Sanger Method sequencing	http://www.slideshare.net/suryasaha/sequencing-the-next-generation

SIFT/PROVEAN	http://sift.jcvi.org/
Singapore Sequencing Indian Project (SSIP)	http://www.statgen.nus.edu.sg/~SSIP/
Sroogle	http://sroogle.tau.ac.il/
STRAP	http://www.bioinformatics.org/strap/
The Exome Aggregation Consortium (ExAC) Browser	http://exac.broadinstitute.org/
QuikChange Primer Design tool	http://www.genomics.agilent.com/primerDesignProgram.jsp
1000 Genomes Browser	http://browser.1000genomes.org/index.html

PUBLICATIONS ARISING FROM THIS THESIS

impact on the ability of these cells to sense the local antigenic microenvironment and regulate cutaneous immune responses. It is also not clear why certain therapeutic interventions, but not others, are associated with a restoration of LC motility. It may be that anti-TNF and anti-IL-12/23 therapies result in a resetting of normal epidermal function, including LC mobilization. These data demonstrate the utility of the *ex vivo* explant model and provide evidence that aberrant LC mobilization is a function of the psoriatic process, rather than a predisposing phenotype.

CONFLICT OF INTEREST

CEMG has received honoraria, speaker's fees, and/or research grants from AbbVie, Actellion, Celgene, Janssen, LEO Pharma, Merck Sharpe Dohme, Novartis, Pfizer, Sandoz, and Trident. IK and RJD are currently in receipt of research grants from Novartis. The remaining authors state no conflict of interest.

ACKNOWLEDGMENTS

We are grateful to Mr Jean Bastrilles for subject recruitment and sample collection, and to our volunteers for their participation. We would also like to thank Ms Rummana Begum and Dr Laura Eaton for their technical help. This research was funded in part by the Medical Research Council (grant reference G0700292). Christopher Griffiths is an NIHR Senior Investigator.

***Frances L. Shaw*[1,3], *Kieran T. Mellody*[1,3], *Stephanie Ogden*[1,2], *Rebecca J. Dearman*[1], *Ian Kimber*[1] and *Christopher E.M. Griffiths*[2]**

[1]*Faculty of Life Sciences, University of Manchester, Manchester, UK and* [2]*Dermatology Research Centre, University of Manchester, Manchester Academic Health Science Centre, Manchester, UK*
E-mail: frances.shaw@manchester.ac.uk
[3]*The first two authors contributed equally to this work and have joint first authorship.*

REFERENCES

Bond E, Adams WC, Smed-Sörensen A *et al.* (1999) Techniques for time-efficient isolation of human skin dendritic cell subsets and assessment of their antigen uptake capacity. *J Immunol Methods* 348:42–56

Cumberbatch M, Dearman RJ, Kimber I (1997) Langerhans cells require signals from both tumour necrosis factor-alpha and interleukin-1 beta for migration. *Immunology* 92: 388–95

Cumberbatch M, Bhushan M, Dearman RJ *et al.* (2003) IL-1beta-induced Langerhans' cell migration and TNF-alpha production in human skin: regulation by lactoferrin. *Clin Exp Immunol* 132:352–9

Cumberbatch M, Singh M, Dearman RJ *et al.* (2006) Impaired Langerhans cell migration in psoriasis. *J Exp Med* 203:953–60

de Gruijl TD, Sombroek CC, Lougheed SM *et al.* (2006) A postmigrational switch among skin-derived dendritic cells to a macrophage-like phenotype is predetermined by the intracutaneous cytokine balance. *J Immunol* 176:7232–42

Ghoreschi K, Bruck J, Kellerer C *et al.* (2011) Fumarates improve psoriasis and multiple sclerosis by inducing type II dendritic cells. *J Exp Med* 208:2291–303

Gordon KB, Bonish BK, Patel T *et al.* (2005) The tumour necrosis factor-alpha inhibitor adalimumab rapidly reverses the decrease in epidermal Langerhans cell density in psoriatic plaques. *Br J Dermatol* 153:945–53

Griffiths CEM, Dearman RJ, Cumberbatch M *et al.* (2005) Cytokines and Langerhans cell mobilisation in mouse and man. *Cytokine* 32: 67–70

Gupta AK, Baadsgaard O, Ellis CN *et al.* (1989) Lymphocytes and macrophages of the epidermis and dermis in lesional psoriatic skin, but not epidermal Langerhans cells, are depleted by treatment with cyclosporin A. *Arch Dermatol Res* 281:219–26

Menter A, Griffiths CEM (2007) Current and future management of psoriasis. *Lancet* 370:272–84

Nestle FO, Kaplan DH, JNWN Barker (2009) Psoriasis. *N Engl J Med* 361:496–509

Ratzinger G, Stoitzner P, Ebner S *et al.* (2002) Matrix metalloproteinases 9 and 2 are necessary for the migration of Langerhans cells and dermal dendritic cells from human and murine skin. *J Immunol* 168:4361–71

Shaw FL, Cumberbatch M, Kleyn CE *et al.* (2010) Langerhans cell mobilization distinguishes between early-onset and late-onset psoriasis. *J Invest Dermatol* 130:1940–2

Wain EM, Darling MI, Pleass RD *et al.* (2010) Treatment of severe, recalcitrant, chronic plaque psoriasis with fumaric acid esters: a prospective study. *Br J Dermatol* 162: 427–34

Loss of *IL36RN* Function Does Not Confer Susceptibility to Psoriasis Vulgaris

Journal of Investigative Dermatology (2014) **134,** 271–273; doi:10.1038/jid.2013.285; published online 18 July 2013

TO THE EDITOR

Recessive mutations of the gene encoding the interleukin-36 receptor antagonist (*IL36RN)* have been associated with generalized pustular psoriasis, palmar-plantar pustulosis, and acrodermatitis continua of Hallopeau (Marrakchi *et al.*, 2011; Onoufriadis *et al.*, 2011; Setta-Kaffetzi *et al.*, 2013). As patients suffering from these pustular conditions often present with concomitant psoriasis vulgaris (PV), it has been proposed that *IL36RN* deficiency may also contribute to PV susceptibility (Marrakchi *et al.*, 2011). This hypothesis is supported by the observation that mice lacking *il36rn* show exacerbated symptoms of imiquimod-induced psoriasiform dermatitis and enhanced infiltration of inflammatory cells in the dermis and the epidermis (Tortola *et al.*, 2012). The elevated expression of IL-36 cytokines in psoriatic skin (Carrier *et al.*, 2011; Johnston *et al.*, 2011) is also consistent with the notion that abnormal IL-36 signaling has an important role in the establishment of cutaneous inflammation (Supplementary Figure 1 online).

On the basis of the above findings, it has recently been suggested that IL-36 blockade could be an innovative

Abbreviations: IL36RN, interleukin-36 receptor antagonist gene; PV, psoriasis vulgaris

Accepted article preview online 21 June 2013; published online 18 July 2013

Table 1. Disease recurrence in the familial PV resource

	Number of affected individuals in the pedigree					
	>5	5	4	3	2	Total
No. of families	15	11	33	121	169	349

Abbreviation: PV, psoriasis vulgaris.

approach for the treatment of PV (Tortola *et al.*, 2012). However, the pathogenic role of IL-36 cytokines has mostly been investigated in the context of animal models (Blumberg *et al.*, 2010; Carrier *et al.*, 2011; Tortola *et al.*, 2012), and the notion that *IL36RN* deficiency contributes to the onset of human PV has yet to be demonstrated. Here, we have explored this hypothesis by investigating whether *IL36RN* loss-of-function alleles are associated with PV.

We reasoned that the segregation of deleterious sequence variants would result in familial recurrence of PV and ascertained 349 unrelated patients with a positive family history of the disease (174 male and 175 female individuals; see also Table 1). We also examined 14 independent cases of erythrodermic psoriasis (10 male and 4 female individuals), based on the hypothesis that penetrant mutations would more likely result in a severe clinical presentation. All patients were recruited through St John's Institute of Dermatology and Glasgow Western Infirmary. The study was conducted in accordance with the declaration of Helsinki, and ethical approval was obtained from Guy's and St Thomas Local Research Ethics committee. All participants granted their written informed consent.

The four *IL36RN* coding exons and proximal promoter region were sequenced using primers and cycling conditions described elsewhere (Onoufriadis *et al.*, 2011; Setta-Kaffetzi *et al.*, 2013). Nucleotide changes were identified using the Sequencher software (Genecodes).

Sanger sequencing identified six common polymorphisms with minor allele frequencies exceeding 5%. None of these changes resulted in an amino-acid substitution and none of the variants was significantly overrepresented in cases compared with controls (Supplementary Table 1 online). To exclude the possibility that these findings may be due to lack of statistical power, we reexamined the *IL36RN* markers analyzed in a previous genome-wide association study of 2,600 psoriatic cases and 5,700 controls (Strange *et al.*, 2010). By integrating experimental and imputed data (see Supplementary Methods online), we obtained genotypes for 130 single-nucleotide polymorphisms spanning the *IL36RN* locus and 10 kb of flanking regions. None of these markers generated a *P*-value <0.05, indicating that common *IL36RN* variants are unlikely to confer significant increases in disease risk.

None of the examined patients harbored recessive alleles with pathogenic potential (i.e., homozygous or compound heterozygous changes resulting in non-synonymous substitutions or protein truncation). Three affected individuals were heterozygous for rare non-synonymous substitutions. Two carried a known p.Ser113Leu (rs144478519) change and one previously unreported p.Thr77Ile variant. The latter substitution was classified as benign by the SIFT (Kumar *et al.*, 2009) and PolyPhen-2 (Adzhubei *et al.*, 2010) pathogenicity prediction tools and therefore was not analyzed any further. Conversely, the p.Ser113Leu allele is known to be damaging, as it has been repeatedly detected in patients with pustular psoriasis (Onoufriadis *et al.*, 2011; Setta-Kaffetzi *et al.*, 2013). As data previously generated by our group suggested that this mutation may have a pathogenic effect even in the heterozygous state (Navarini *et al.*, 2013; Setta-Kaffetzi *et al.*, 2013), we investigated its segregation in the families of the two critical patients. In both cases, we found that the p.Ser113Leu substitution was not co-inherited with the disease (Supplementary Figure 2 online). We also observed that the frequency of p.Ser113Leu in our patient resource (2/726 chromosomes or 0.27%) was comparable to that seen in 2,222 exomes sequenced in-house (15/4,444 chromosomes or 0.34%). Thus, the p.Ser113Leu change is unlikely to contribute to PV susceptibility.

Data generated in animal models indicate that IL-36 cytokines are likely to have a pathogenic role in the establishment of skin inflammation. Transgenic mice overexpressing *il36a* in basal keratinocytes present with a psoriasiform phenotype (IL-23-dependent hyperkeratosis accompanied by infiltration of neutrophils and lymphocytes into the dermis) that is exacerbated by *il36rn* knockout (Blumberg *et al.*, 2007). It has also been demonstrated that IL-36R blockade resolves the inflammatory changes of human psoriatic skin transplanted onto immune-deficient mice (Blumberg *et al.*, 2010), whereas loss of *il36rn* exacerbates the pathology of imiquimod-induced psoriasiform dermatitis (Tortola *et al.*, 2012).

Despite the interest generated by these findings, the effect of *IL36RN* deficiency on the establishment of PV has not been investigated. Here, we addressed this issue through the genetic analysis of an extended clinical resource including 363 patients affected by familial and/or severe disease. We found that none of the examined cases harbored recessive *IL36RN* mutations. Although two patients were heterozygous for the pathogenic p.Ser113Leu mutation, this change did not segregate with the disease in the relevant families and was not overrepresented among case chromosomes. Our patient resource was sufficiently powered to uncover variants occurring at a frequency >0.25% and detect associations with alleles of moderate to strong effect (Supplementary Figure 3 online). Although the prevalence and the odds ratios documented for the p.Ser113Leu allele are within these parameters (Navarini *et al.*, 2013; Setta-Kaffetzi *et al.*, 2013), our analysis might have missed the pathogenic contribution of rarer alleles of modest effect. Nonetheless, it is reasonable to conclude that in the British population

loss of *IL36RN* activity is not associated with a significant increase of PV risk. As our study was focused on *IL36RN*, we cannot exclude the possibility that mutations in functionally related genes (e.g., *IL36A*, *IL36B*, and *IL36G*) may be associated with the disease. Thus, our findings warrant further genetic investigations into the role of IL-36 cytokines in human PV.

CONFLICT OF INTEREST

The authors state no conflict of interest.

ACKNOWLEDGMENTS

We acknowledge support from the Department of Health via the NIHR comprehensive Biomedical Research Centre award to GSTT NHS Foundation Trust in partnership with King's College London and KCH NHS Foundation Trust. This work was supported by the National Psoriasis Foundation, USA (Discovery Grant to FC) and the Medical Research Council (grant G0601387 to RCT and JNB). DB's PhD studentship is funded by the Psoriasis Association. SKM is supported by the NIHR through the Academic Clinical Fellowship scheme.

Dorottya M. Berki[1], Satveer K. Mahil[1], A. David Burden[2], Richard C. Trembath[1,3], Catherine H. Smith[1], Francesca Capon[1,4] and Jonathan N. Barker[1,4]

[1]Division of Genetics and Molecular Medicine, King's College London, London, UK; [2]Department of Dermatology, University of Glasgow, Glasgow, UK and [3]Queen Mary, University of London, Barts and The London School of Medicine and Dentistry, London, UK
[4]These authors contributed equally to this work
E-mail: francesca.capon@kcl.ac.uk or jonathan.barker@kcl.ac.uk

SUPPLEMENTARY MATERIAL

Supplementary material is linked to the online version of the paper at http://www.nature.com/jid

REFERENCES

Adzhubei IA, Schmidt S, Peshkin L *et al.* (2010) A method and server for predicting damaging missense mutations. *Nat Methods* 7:248–9

Blumberg H, Dinh H, Dean C Jr *et al.* (2010) IL-1RL2 and its ligands contribute to the cytokine network in psoriasis. *J Immunol* 185:4354–62

Blumberg H, Dinh H, Trueblood ES *et al.* (2007) Opposing activities of two novel members of the IL-1 ligand family regulate skin inflammation. *J Exp Med* 204:2603–14

Carrier Y, Ma HL, Ramon HE *et al.* (2011) Inter-regulation of Th17 cytokines and the IL-36 cytokines in vitro and in vivo: implications in psoriasis pathogenesis. *J Invest Dermatol* 131: 2428–37

Johnston A, Xing X, Guzman AM *et al.* (2011) IL-1F5, -F6, -F8, and -F9: a novel IL-1 family signaling system that is active in psoriasis and promotes keratinocyte antimicrobial peptide expression. *J Immunol* 186:2613–22

Kumar P, Henikoff S, Ng PC (2009) Predicting the effects of coding non-synonymous variants on protein function using the SIFT algorithm. *Nat Protocols* 4:1073–81

Marrakchi S, Guigue P, Renshaw BR *et al.* (2011) Interleukin-36-receptor antagonist deficiency and generalized pustular psoriasis. *N Engl J Med* 365:620–8

Navarini AA, Valeyrie-Allanore L, Setta-Kaffetzi N *et al.* (2013) Rare variations in IL36RN in severe adverse drug reactions manifesting as acute generalized exanthematous pustulosis. *J Invest Dermatol* 133:1904–7

Onoufriadis A, Simpson MA, Pink AE *et al.* (2011) Mutations in IL36RN/IL1F5 are associated with the severe episodic inflammatory skin disease known as generalized pustular psoriasis. *Am J Hum Genet* 89:432–7

Setta-Kaffetzi N, Navarini AA, Patel VM *et al.* (2013) Rare pathogenic variants in IL36RN underlie a spectrum of psoriasis-associated pustular phenotypes. *J Invest Dermatol* 133: 1366–9

Strange A, Capon F, Spencer CC *et al.* (2010) A genome-wide association study identifies new psoriasis susceptibility loci and an interaction between HLA-C and ERAP1. *Nat Genet* 42:985–90

Tortola L, Rosenwald E, Abel B *et al.* (2012) Psoriasiform dermatitis is driven by IL-36-mediated DC-keratinocyte crosstalk. *J Clin Invest* 122:3965–76

Plectin Mutations Underlie Epidermolysis Bullosa Simplex in 8% of Patients

Journal of Investigative Dermatology (2014) **134,** 273–276; doi:10.1038/jid.2013.277; published online 18 July 2013

TO THE EDITOR

Epidermolysis bullosa simplex (EBS) is a mechanobullous genodermatosis characterized by an intraepidermal split through the cytoplasm of basal keratinocytes, which is mainly caused by dominant-negative mutations in the genes encoding keratins 5 and 14 (Coulombe *et al.*, 1991; Lane *et al.*, 1992). Mutation analysis of *KRT5* and *KRT14* in a large biopsy-confirmed EBS population in the Netherlands, however, revealed that in 25% of unrelated cases no mutations could be identified in these genes (Bolling *et al.*, 2011). A similar percentage of EBS cases with wild-type *KRT5* and *KRT14* genes was reported for the EBS population in the United Kingdom (Rugg *et al.*, 2007). A missense mutation, Arg2000Trp, in *PLEC*, encoding the hemidesmosomal protein plectin, which connects the basal keratins to the hemidesmosomal plaque, was associated in cases with dominant EBS of hands and feet (EBS-Ogna) (Koss-Harnes *et al.*, 2002; Kiritsi *et al.*, 2013).

In this study, we investigated the frequency of *PLEC* mutations in biopsy-proven EBS probands that lacked mutations in *KRT5* and *KRT14*. The study was performed according to the Declaration of Helsinki principles, and informed consent was obtained from the patients. *PLEC* mutation analysis was performed in 16 Dutch probands with a biopsy-proven EBS in which mutations in *KRT5* and *KRT14* had been excluded. PCR amplification of all exons and adjacent intronic sequences of *PLEC* (GenBank NM_000445) was performed using primers located in the flanking introns. Primers resulting in overlapping PCR products were used for the large exons

Abbreviation: EBS, epidermolysis bullosa simplex

Accepted article preview online 17 June 2013; published online 18 July 2013

TABLE I. Results of allergy workup in our leucovorin-reactive patients

Patients	ST to oxaliplatin/ irinotecan	ST to both leucovorin and L-isomer calcium folinate	DPT with leucovorin	Tryptase levels during DPT with leucovorin (60 min after reaction) (ng/mL)	DPT with L-isomer calcium folinate	DPT with oxaliplatin/ irinotecan
Case 1	Negative	Negative	Positive: urticaria	1.87	Positive: urticaria	Negative
Case 2	Negative	Negative	Positive: general urticaria, rhinoconjunctivitis	3.04	Positive: general urticaria, rhinoconjunctivitis, shortness of breath	Negative
Case 3	Negative	Negative	Positive: chills, back pain, elevated blood pressures, fever	2.46	Not performed	Negative
Case 4	Negative	Negative	Positive: general urticaria, eyelid angioedema	4.85	Not performed	Negative
Case 5	Negative	Negative	Positive: chills, chest pain, facial erythema	1.23	Positive: chills, facial erythema	Negative

ST concentrations used for oxaliplatin were 5 mg/mL and 0.5 mg/mL.[1] For irinotecan (20 mg/mL; 2 mg/mL), leucovorin (10 mg/mL; 1 mg/mL), and calcium levolinate (10 mg/mL; 1 mg/mL) were empirically obtained: full-strength solution according to manufacturer instructions and diluted further in normal saline to 1:10, and these concentrations were tested in 10 control patients to prove them nonirritant.
ST, Skin test.

Our patients could continue their therapy either by avoiding leucovorin or by rapid desensitization (with adequate installations, standardized protocols, and expert personnel).

Up to 3 patients suffered overlooked milder symptoms during previous administrations. Helping patients identify and communicate these symptoms may prevent unnecessary risks.

In conclusion, we describe an important number of confirmed HSRs to leucovorin during a 1-year period. We show how patients reacting to leucovorin may also react to L-isomer calcium folinate. We believe that protocols studying FOLFOX/FOLFIRI HSRs should be undergone by drug allergy experts, and include systematic skin testing and DPT with folinic acid, to avoid infradiagnosis and its resulting risks. Moreover, we report the first intravenous rapid desensitization to leucovorin in a reactive patient (confirmed by DPT).

We are indebted to Dr Federico Longo-Muñoz and Dr Reyes Ferreiro-Monteagudo, from the Medical Oncology Department, and Dr Marina Sanchez-Cuervo, from the Pharmacy Department, for their colaboration and clinical expertise. We thank all the participants in the multidisciplinary Desensitization Program of the Ramon & Cajal University Hospital Allergy Division.

*Alicia Ureña-Tavera, MD**
*Miriam Zamora-Verduga, MD**
Ricardo Madrigal-Burgaleta, MD
Denisse Angel-Pereira, MD
Maria Pilar Berges-Gimeno, MD, PhD
Emilio Alvarez-Cuesta, MD, PhD

From the Allergy Division, Ramon & Cajal University Hospital, Madrid, Spain. E-mail: rmadbur@hotmail.com.
*These authors share first-author credit.
Disclosure of potential conflict of interest: The authors declare that they have no relevant conflicts of interest.

REFERENCES

1. Madrigal-Burgaleta R, Berges-Gimeno MP, Angel-Pereira D, Ferreiro-Monteagudo R, Guillen-Ponce C, Alvarez-Cuesta E, et al. Hypersensitivity and desensitization to antineoplastic agents: outcomes of 189 procedures with a new short protocol and novel diagnostic tools assessment. Allergy 2013;68:853-61.
2. Damaske A, Ma N, Williams R. Leucovorin-induced hypersensitivity reaction. J Oncol Pharm Pract 2012;18:136-9.
3. Kovoor PA, Karim SM, Marshall JL. Is levoleucovorin an alternative to racemic leucovorin? A literature review. Clin Colorectal Cancer 2009;8:200-6.
4. Vermeulen C, Mathelier-Fusade P, Gaouar H, Leynadier F. Two cases of allergy to leucovorin. Rev fr'allergol 2003;43:342-3.
5. Liu A, Fanning L, Chong H, Fernandez J, Sloane D, Sancho-Serra M, et al. Desensitization regimens for drug allergy: state of the art in the 21st century. Clin Exp Allergy 2011;41:1679-89.
6. Angel-Pereira D, Berges-Gimeno MP, Madrigal-Burgaleta R, Ureña-Tavera MA, Zamora-Verduga M, Alvarez-Cuesta E. Successful rapid desensitization to methylprednisolone sodium hemisuccinate: a case report. J Allergy Clin Immunol Pract 2014;2:346-8.
7. Madrigal-Burgaleta R, Berges-Gimeno MP, Angel-Pereira D, Guillen-Ponce C, Sanz ML, Alvarez-Cuesta E. Desensitizing oxaliplatin-induced fever: a case report. J Investig Allergol Clin Immunol 2013;23:435-6.
8. Dykewicz MS, Orfan NA, Sun W. In vitro demonstration of IgE antibody to folate-albumin in anaphylaxis from folic acid. J Allergy Clin Immunol 2000;106:386-9.

Available online November 7, 2014.
http://dx.doi.org/10.1016/j.jaci.2014.09.045

IL36RN mutations define a severe autoinflammatory phenotype of generalized pustular psoriasis

To the Editor:

Autoinflammatory diseases are a heterogeneous group of disorders mediated by abnormal activation of the innate immune system, resulting in recurrent episodes of systemic and organ-specific inflammation.[1] In recent years, the pace of autoinflammatory disease gene discovery has undergone a dramatic acceleration with the emergence of novel autoinflammatory phenotypes, highlighting the need to establish reliable diagnostic criteria through the analysis of extended case series.[1]

Generalized pustular psoriasis (GPP) is a rare autoinflammatory condition presenting with recurrent episodes of skin pustulation that are often accompanied by systemic inflammation (acute-phase response with neutrophilia) and concurrent psoriasis vulgaris (PV).[2] We and others demonstrated that a proportion of GPP cases carry recessive mutations of *IL36RN*, the gene encoding the IL-36 receptor antagonist.[3,4] This anti-inflammatory protein modulates the activity of IL-36 α, β, and γ, a group of IL-1 family cytokines that have repeatedly been shown to be overexpressed in psoriatic lesions. Importantly, studies of animal models and human primary

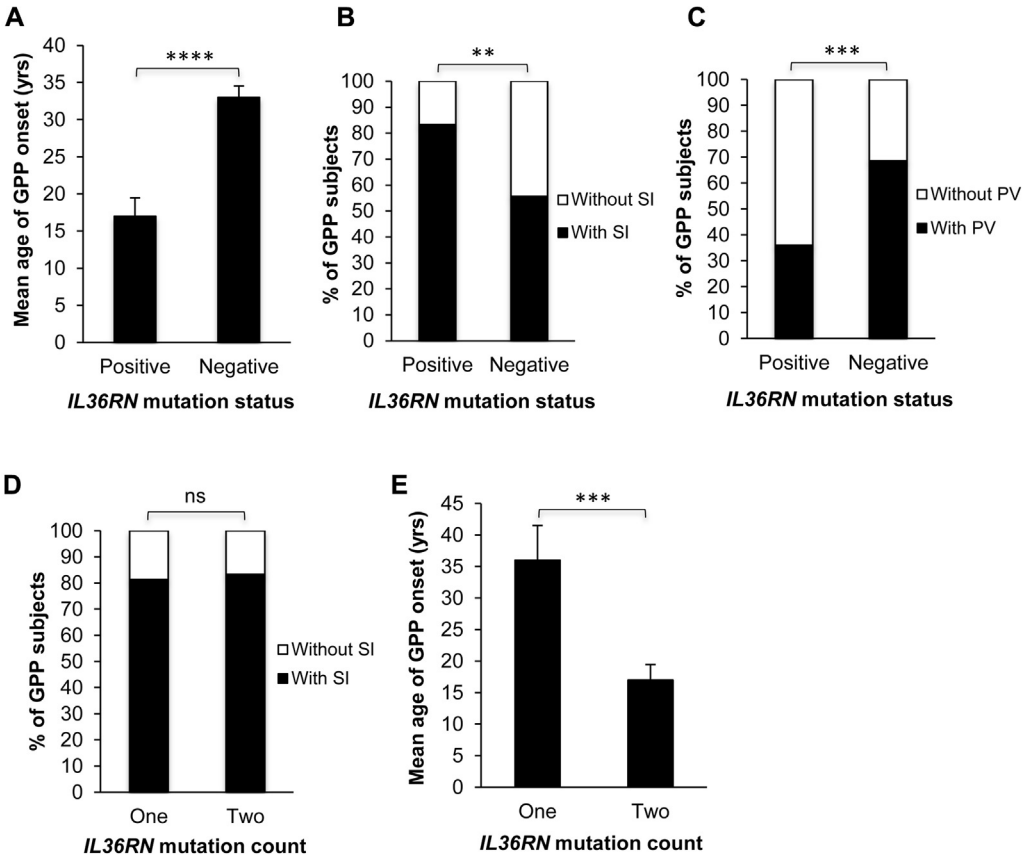

FIG 1. A-C, Subjects with recessive *IL36RN* alleles have earlier disease onset (Fig 1, *A*), more frequently have systemic inflammation (Fig 1, *B*), and less frequently have PV (Fig 1, *C*) compared with *IL36RN*-negative subjects. **D** and **E,** Although the prevalence of systemic inflammation remains high among cases with a single mutation (Fig 1, *D*), these subjects present with significantly delayed disease onset compared with those with recessive alleles (Fig 1, *E*). *ns,* Not significant; *SI,* systemic inflammation, which was defined according to the American College of Chest Physicians criteria (leukocyte count >12 × 10^9/L and fever >38°C)[6]. $^{**}P < .01$, $^{***}P < .001$, and $^{****}P < 10^{-6}$.

TABLE I. Frequency distribution of heterozygous *IL36RN* alleles

Origin	Allele counts (%)		*P* value	OR
	Cases	Control subjects		
British	2/22 (9.1%)	2/568 (0.3%)	.008	28.3
Chinese	4/72 (5.6%)	8/394 (2.0%)	.10	2.8
Japanese	3/66 (4.5%)	0/178 (0%)	.019	19.7
Malay	5/110 (4.5%)	0/192 (0%)	.006	20.1

OR, Odds ratio.

cell cultures indicate that IL-36 molecules induce the activation of keratinocytes and antigen-presenting cells, thus propagating skin inflammation in patients with psoriasis.[5]

Although these discoveries have shed new light on the pathogenesis of GPP, the rarity of the disease has thus far hindered a robust definition of the symptoms associated with deficiency of IL-36 receptor antagonist (DITRA), so that reliable indications for *IL36RN* screening are still lacking. Here we sought to address this issue by ascertaining an extended patient resource. We examined 233 cases (see Tables E1-E3 in this article's Online Repository at www.jacionline.org) recruited in accordance with the principles of the Declaration of Helsinki and with ethical approval from the relevant committees of participating institutions. This data set originated from 3 sources: (1) 177 cases were ascertained through a systematic literature search based on the terms "*IL36RN*" and "generalized pustular psoriasis" (see Fig E1 in this article's Online Repository at www.jacionline.org); (2) 45 patients received diagnoses from the coauthors of this study, according to established criteria[2]; and (3) 11 cases were initially ascertained by the International Registry of Severe Cutaneous Adverse Reaction Consortium. After an in-depth case review, the consortium expert committee proposed the presentation to be consistent with GPP. Thus the key inclusion criterion underlying the 3 ascertainment streams was a clinical diagnosis of GPP. The subsequent identification of patients with systemic flares was based on the criteria established by the American College of Chest Physicians (leukocytosis and fever >38°C).[6]

To delineate the phenotypic spectrum associated with DITRA, we first determined the frequency of *IL36RN* mutations in our cohort. We found that 49 (21.0%) of 233 cases carried recessive *IL36RN* alleles (see Table E1). Because information on age of onset, systemic involvement, and PV concurrence was available for 99.6%, 72.1%, and 86.7% of cases, we compared these features in patients bearing recessive *IL36RN* mutations (n = 49) and in those without pathogenic alleles at this locus (n = 166, see Table E1 and the Methods section in this article's Online

Repository at www.jacionline.org). We found that *IL36RN*-positive subjects manifested a strikingly more severe clinical phenotype characterized by an earlier age of onset (17 ± 2.4 vs 33 ± 1.5 years, $P = 5.9 \times 10^{-7}$) and a markedly increased risk of systemic inflammation (83.3% vs 55.6%, $P = 1.5 \times 10^{-3}$; Fig 1, *A* and *B*). We also observed a very significant reduction in the prevalence of PV in the *IL36RN*-positive cohort (36.1% vs 68.7%, $P = 5.0 \times 10^{-4}$; Fig 1, *C*), validating the results of a small Japanese study.[7]

We previously reported 6 patients with GPP bearing single heterozygous *IL36RN* mutations.[8] In keeping with this observation, we observed 18 cases (including the subjects we had originally described) with a single disease allele. To validate the significance of these findings, we compared the frequency of monoallelic *IL36RN* mutations in cases versus population-matched control subjects. We found that heterozygous disease alleles were consistently enriched among cases, with statistically significant *P* values ($P < .02$; false discovery rate < 0.05) observed in most ethnic groups (Table I). We also performed a meta-analysis of our case-control resources, which demonstrated that monoallelic *IL36RN* mutations confer a very substantial increase in disease risk (weighted pooled odds ratio, 7.32; 95% CI, 3.02-17.7; $P = 1.1 \times 10^{-5}$).

We next compared disease severity in subjects carrying 1 or 2 mutations. We focused our analysis on age of onset and systemic inflammation because PV concurrence is not considered a reliable indicator of GPP severity.[2] We observed a high prevalence of systemic inflammation (>80%) in both patient groups (Fig 1, *D*), but we noted that the mean age of onset in *IL36RN* heterozygotes exceeded by 2-fold that of patients with biallelic mutations (36 ± 5.5 vs 17 ± 2.4; $P = 6.0 \times 10^{-4}$; Fig 1, *E*).

The aim of our study was to investigate the correlation between *IL36RN* mutation status and the clinical presentation of GPP to aid the definition of diagnostic criteria for the stratification of patient cohorts. We found that *IL36RN* alleles define a GPP phenotype characterized by early onset, high risk of systemic inflammation, and low prevalence of PV. Of note, these conclusions were drawn by comparing the *IL36RN*-positive data set with a heterogeneous cohort that was solely defined by the lack of *IL36RN* mutations. As further disease genes are identified and systematically genotyped, the designation of more homogeneous patient subgroups will become possible, allowing the development of formal diagnostic algorithms.

We recognize that our study design, which combined the analysis of newly recruited cases with a literature review, might have been vulnerable to ascertainment bias. However, we note there was no significant variability in the frequency of *IL36RN* mutations across data sets (see Table E4 in this article's Online Repository at www.jacionline.org), indicating that our inclusion criteria were sufficiently robust to allow the ascertainment of a reasonably homogeneous resource.

Our analysis demonstrated a gene dosage effect whereby GPP onset is significantly delayed in subjects with monoallelic mutations. Intriguingly, we found that these subjects were still at high risk of systemic inflammation. Thus heterozygous patients might require a longer or more intense exposure to environmental triggers to manifest overt disease. Once an abnormal immune response is initiated, however, the presence of a wild-type *IL36RN* allele does not appear sufficient to prevent the onset of systemic inflammation. This suggests that abnormal cytokine signaling might be propagated by molecules acting downstream of *IL36RN*. Further *ex vivo* analyses will be required to validate this model and define the cytokines that sustain abnormal inflammatory responses in patients with GPP.

In conclusion, we have defined a clinical triad (early onset, systemic inflammation, and absence of concurrent PV) that could be used to prioritize patients with GPP for *IL36RN* screening. Importantly, pilot studies indicate that a proportion of patients with *IL36RN* mutations could be treated with the IL-1 antagonist anakinra.[9,10] Therapeutic agents that specifically target the IL-36 receptor are also being developed.[11] Thus our work is expected to facilitate the identification of patients who might benefit from personalized treatment with IL-1 or IL-36 blockers.

Safia Hussain, BSc[a]
Dorottya M. Berki, BSc[a]
Siew-Eng Choon, MRCP[b]
A. David Burden, MD, FRCP[c]
Michael H. Allen, PhD[a]
Juan I. Arostegui, MD, PhD[d]
Antonio Chaves, MD[e]
Michael Duckworth[a]
Alan D. Irvine, MD[f,g]
Maja Mockenhaupt, MD, PhD[h]
Alexander A. Navarini, MD, PhD[a,i]
Marieke M. B. Seyger, MD, PhD[j]
Pere Soler-Palacin, MD, PhD[k]
Christa Prins, MD[l]
Laurence Valeyrie-Allanore, MD[m]
M. Asuncion Vicente, MD[n]
Richard C. Trembath, FMedSci[o]
Catherine H. Smith, MD, FRCP[a]
Jonathan N. Barker, MD, FRCP[a]*
Francesca Capon, PhD[a]*

From [a]the Division of Genetics and Molecular Medicine, King's College London, London, United Kingdom; [b]the Department of Dermatology, Hospital Sultanah Aminah, Johor Bahru, Malaysia; [c]the Department of Dermatology, University of Glasgow, Glasgow, United Kingdom; [d]the Department of Immunology-CDB, Hospital Clinic, Barcelona, Spain; [e]the Department of Dermatology, Hospital Infanta Cristina, Badajoz, Spain; [f]Paediatric Dermatology, Our Lady's Children's Hospital, Dublin, Ireland; [g]Clinical Medicine, Trinity College Dublin, Dublin, Ireland; [h]the Department of Dermatology, Dokumentationszentrum Schwerer Hautreaktionen (dZh), Universitäts-Hautklinik, Freiburg, Germany; [i]the Department of Dermatology, Zurich University Hospital, Zurich, Switzerland; [j]the Department of Dermatology, Radboud University Nijmegen Medical Centre, Nijmegen, The Netherlands; [k]the Pediatric Infectious Diseases and Immunodeficiencies Unit, Hospital Universitari Vall d'Hebron, Barcelona, Spain; [l]the Dermatology Service, Geneva University Hospital, Geneva, Switzerland; [m]the Department of Dermatology, Henri Mondor Hospital, Paris, France; [n]the Department of Dermatology, Hospital Sant Joan de Deu, Esplugues, Spain; and [o]Queen Mary University of London, Barts and The London School of Medicine and Dentistry, London, United Kingdom. E-mail: francesca.capon@kcl.ac.uk, Or: jonathan.barker@kcl.ac.uk.

*These authors contributed equally to this work.

Supported by the Department of Health via the NIHR BioResource Clinical Research Facility and comprehensive Biomedical Research Centre award to Guy's and St Thomas' NHS Foundation Trust in partnership with King's College London and King's College Hospital NHS Foundation Trust. This work was funded by a Medical Research Council Stratified Medicine award (MR/L011808/1; to F.C., C.H.S., and J.N.B.). The exome sequencing of the TwinsUK cohort was funded by Wellcome Trust and European Community's Seventh Framework Programme (FP7/2007-2013) grants. The International Registry of Severe Cutaneous Adverse Reaction (RegiSCAR) Consortium was funded by unrestricted grants from the European Commission (QLRT-2002-01738), GIS-Institut des Maladies Rares and INSERM (4CH09G) in France, and a consortium of pharmaceutical companies (Bayer Vital, Boehringer Ingelheim, Cephalon, GlaxoSmithKline, MSD Sharp and Dohme, Merck, Novartis, Pfizer, Roche, Sanofi-Aventis, and Servier). S.H. is supported by the Genetics Society and D.M.B.'s studentship is funded by the Psoriasis Association.

Disclosure of potential conflict of interest: S. Hussain is supported by the Genetics Society. D. Berki has received funding from the Psoriasis Association. J. I. Arostegui's institution has received or has grants pending from Novartis and he has received payment for delivering lectures from Novartis, and Swedish Orphan Biovitrum. L. Valeyrie-Allanore has received compensation for board membership from Jansen,

MedImmune, and Boehringer Ingelheim. P. Soler-Palacin has received consultancy fees, fees for supplying expert testimony, payment for the development of educational presentations, and payment for delivering lectures from CSL Behring, and Baxter and has received or has grants pending from CSL Behring and has received compensation for travel and other meeting-related expenses from CSL Behring and Baxter. M. M. B. Seyger's institution receives compensation for board membership from Pfizer, has received or has grants pending from Pfizer, and has received payment for delivering lectures from Pfizer, as well as consultancy fees from Boehringer Ingelheim, Allmiral, and Pfizer and compensation for travel and other meeting-related expenses from Pfizer. M. Mockenhaupt receives royalties from UpToDate. J. N. Barker's institution has received funding from the National Institute for Health Research. F. Capon has grants pending from the British Skin Foundation. The rest of the authors declare that they have no relevant conflicts of interest.

REFERENCES

1. Aksentijevich I, Kastner DL. Genetics of monogenic autoinflammatory diseases: past successes, future challenges. Nat Rev Rheumatol 2011;7:469-78.
2. Griffiths CEM, Barker JN. Psoriasis. In: Burns T, Breathnach S, Cox N, Griffiths CEM, editors. Rook's textbook of dermatology. Chichester: Wiley-Blackwell; 2010. p. 20.1-20.60.
3. Marrakchi S, Guigue P, Renshaw BR, Puel A, Pei XY, Fraitag S, et al. Interleukin-36-receptor antagonist deficiency and generalized pustular psoriasis. N Engl J Med 2011;365:620-8.
4. Onoufriadis A, Simpson MA, Pink AE, Di Meglio P, Smith CH, Pullabhatla V, et al. Mutations in IL36RN/IL1F5 are associated with the severe episodic inflammatory skin disease known as generalized pustular psoriasis. Am J Hum Genet 2011;89:432-7.
5. Dietrich D, Gabay C. Inflammation: IL-36 has proinflammatory effects in skin but not in joints. Nat Rev Rheumatol 2014 [Epub ahead of print].
6. Bone RC, Balk RA, Cerra FB, Dellinger RP, Fein AM, Knaus WA, et al. Definitions for sepsis and organ failure and guidelines for the use of innovative therapies in sepsis. The ACCP/SCCM Consensus Conference Committee. American College of Chest Physicians/Society of Critical Care Medicine. Chest 1992;101:1644-55.
7. Sugiura K, Takemoto A, Yamaguchi M, Takahashi H, Shoda Y, Mitsuma T, et al. The majority of generalized pustular psoriasis without psoriasis vulgaris is caused by deficiency of interleukin-36 receptor antagonist. J Invest Dermatol 2013;133:2514-21.
8. Setta-Kaffetzi N, Navarini AA, Patel VM, Pullabhatla V, Pink AE, Choon SE, et al. Rare pathogenic variants in IL36RN underlie a spectrum of psoriasis-associated pustular phenotypes. J Invest Dermatol 2013;133:1366-9.
9. Rossi-Semerano L, Piram M, Chiaverini C, De Ricaud D, Smahi A, Koné-Paut I. First clinical description of an infant with interleukin-36-receptor antagonist deficiency (DITRA) successfully treated with interleukin-1-receptor antagonist anakinra. Pediatrics 2013;132:e1043-7.
10. Tauber M, Viguier M, Le Gall C, Smahi A, Bachelez H. Is it relevant to use an interleukin-1-inhibiting strategy for the treatment of patients with deficiency of interleukin-36 receptor antagonist? Br J Dermatol 2014;170:1198-9.
11. Wolf J, Ferris LK. Anti-IL-36R antibodies, potentially useful for the treatment of psoriasis: a patent evaluation of WO2013074569. Expert Opin Ther Pat 2014;24:477-9.

Available online November 12, 2014.
http://dx.doi.org/10.1016/j.jaci.2014.09.043

Is there a risk using hypoallergenic cosmetic pediatric products in the United States?

To the Editor:

Health care providers wisely advise the parents of children with atopic dermatitis (AD) to apply emollients to treat xerotic and inflamed skin. So-called hypoallergenic products are typically recommended because patients with AD have an elevated risk of contact allergy to fragrances, surfactants, and preservatives.[1-3] This is likely explained by more frequent allergen exposure via topical products in combination with an impaired skin barrier facilitating allergen penetration.[4]

Chronic exposure to contact allergens in cosmetics increases the risk of not only allergic contact dermatitis (ACD) but also AD.[5] Repeated cutaneous exposure to skin sensitizers initially leads to ACD characterized by T_H1 inflammation, but then a gradual shift toward T_H2 inflammation, resulting in AD.[4] In addition, AD skin has a specific initial propensity to T_H2 programming following exposure to contact allergens in contrast to the normal T_H1 programming in non-AD skin.[6]

Anecdotally, we have observed a lack of correlation between marketing terms highlighting hypoallergenicity or dermatologist/pediatrician-recommended status and the actual content of contact allergens in topical products. We therefore evaluated the allergen content of 187 unique pediatric cosmetics marketed in the United States as hypoallergenic. Inclusion criteria were products marketed as pediatric and "hypoallergenic," "dermatologist recommended/tested," "fragrance free," or "paraben free."

Products from 6 different retailers in and around Redlands, California, were purchased or photographed in September 2013. The ingredients, name, brand, type, and advertising term for each product were recorded. To identify contact allergens, the ingredients were compared with allergens in the North American Contact Dermatitis Group standard screening tray using a customized search algorithm programmed into Matlab 7.4 (Mathworks, Natick, Mass).

We found that 167 (89%) of the 187 products contained at least 1 contact allergen, 117 (63%) 2 or more, and 21 (11%) 5 or more (Table I). The average number of allergens in each product was 2.4 (95% CI, 2.05-2.51). The most prevalent single allergen was cocamidopropyl betaine, found in 45 (24%) followed by propolis/beeswax in 35 (19%), phenoxyethanol in 33 (18%), tocopherol in 25 (13%), and DMDM hydantoin in 24 (13%) (Table II). Of note, 11.2% of the products contained methylisothiazolinone. By allergen category, the most prevalent sensitizers were preservatives 108 (58%) and fragrances 55 (29%).

TABLE I. Number of allergens in products according to the advertising term used

	Total n	Percent with ≥1 allergen (n)	Percent with ≥2 allergens (n)	Percent with ≥3 allergens (n)	Percent with ≥4 allergens (n)	Percent with ≥5 allergens (n)	95% CI*
All products	187	88.8 (166)	62.6 (117)	38.5 (72)	22.5 (42)	11.2 (21)	NA
By advertising term:							
Dermatologist recommended	66	78.8 (52)	50.0 (33)	21.2 (14)	9.1 (6)	3.0 (2)	73.8-83.8
Fragrance free	52	80.8 (42)	55.8 (29)	30.8 (16)	17.3 (9)	11.5 (6)	75.3-86.2
Hypoallergenic	135	88.2 (119)	65.2 (88)	42.2 (57)	23.7 (32)	11.1 (15)	85.2-90.9
Paraben free	72	88.9 (64)	56.9 (41)	29.2 (21)	18.1 (13)	5.6 (4)	85.2-92.6

NA, Not applicable/available.
*95% CI reflects the CI for % with 1 or more allergen.

METHODS

Mutation screening

The *IL36RN* coding region was screened by using primers and conditions reported elsewhere.[E1] In those instances in which Sanger sequencing uncovered a single disease allele, the possibility that the second mutation might be accounted for by the insertion/deletion of an entire exon was excluded by amplifying the entire *IL36RN* gene region, as previously described.[E2] Nucleotide changes were considered deleterious if (1) experimentally derived evidence was available in the literature or (2) a high-confidence pathogenicity prediction was returned by using at least 4 of the following programs: SIFT,[E3] PolyPhen-2,[E4] Provean,[E5] MutPred,[E6] and MutationTaster.[E7] The sequence of the *IL36RN* transcript ENST00000393200 was used as a reference in all bioinformatics analyses.

Statistical tests

Differences in the frequency distribution of dichotomous clinical findings (presence/absence of PV or systemic inflammation) and mean ages of disease onset were assessed with the Fisher exact test and Student unpaired *t* test, respectively. Both were implemented with the online tools available at http://graphpad.com/quickcalcs/.

The combined frequency of heterozygous *IL36RN* alleles was compared in cases versus control subjects by using the Fisher exact test. Control allele frequencies were determined in the following resources: 284 British subjects sequenced by the 1000 Genomes Project (n = 89) and TwinsUK (n = 195), 89 Japanese and 197 Han Chinese subjects sequenced by the 1000 Genomes Project, and 96 subjects sequenced by the Singapore Sequencing Malay Project.[E8-E10] The meta-analysis of multiple case-control data sets was implemented with Review Manager 5.2.[E11] *P* values of less than .05 were deemed statistically significant.

REFERENCES

E1. Onoufriadis A, Simpson MA, Pink AE, Di Meglio P, Smith CH, Pullabhatla V, et al. Mutations in IL36RN/IL1F5 are associated with the severe episodic inflammatory skin disease known as generalized pustular psoriasis. Am J Hum Genet 2011;89:432-7.

E2. Setta-Kaffetzi N, Navarini AA, Patel VM, Pullabhatla V, Pink AE, Choon SE, et al. Rare pathogenic variants in IL36RN underlie a spectrum of psoriasis-associated pustular phenotypes. J Invest Dermatol 2013;133:1366-9.

E3. Kumar P, Henikoff S, Ng PC. Predicting the effects of coding non-synonymous variants on protein function using the SIFT algorithm. Nat Protoc 2009;4:1073-81.

E4. Adzhubei I, Jordan DM, Sunyaev SR. Predicting functional effect of human missense mutations using PolyPhen-2. Curr Protoc Hum Genet 2013;Chapter 7:Unit 7.20.

E5. Choi Y, Sims GE, Murphy S, Miller JR, Chan AP. Predicting the functional effect of amino acid substitutions and indels. PLoS One 2012;7:e46688.

E6. Li B, Krishnan VG, Mort ME, Xin F, Kamati KK, Cooper DN, et al. Automated inference of molecular mechanisms of disease from amino acid substitutions. Bioinformatics 2009;25:2744-50.

E7. Schwarz JM, Rodelsperger C, Schuelke M, Seelow D. MutationTaster evaluates disease-causing potential of sequence alterations. Nat Methods 2010;7:575-6.

E8. Abecasis GR, Auton A, Brooks LD, DePristo MA, Durbin RM, Handsaker RE, et al. An integrated map of genetic variation from 1,092 human genomes. Nature 2012;491:56-65.

E9. Williams FM, Scollen S, Cao D, Memari Y, Hyde CL, Zhang B, et al. Genes contributing to pain sensitivity in the normal population: an exome sequencing study. PLoS Genet 2012;8:e1003095.

E10. Wong LP, Ong RT, Poh WT, Liu X, Chen P, Li R, et al. Deep whole-genome sequencing of 100 southeast Asian Malays. Am J Hum Genet 2013;92:52-66.

E11. Review Manager (RevMan). Copenhagen: The Nordic Cochrane Centre, the Cochrane Collaboration; 2012.

E12. Marrakchi S, Guigue P, Renshaw BR, Puel A, Pei XY, Fraitag S, et al. Interleukin-36-receptor antagonist deficiency and generalized pustular psoriasis. N Engl J Med 2011;365:620-8.

E13. Farooq M, Nakai H, Fujimoto A, Fujikawa H, Matsuyama A, Kariya N, et al. Mutation analysis of the IL36RN gene in 14 Japanese patients with generalized pustular psoriasis. Hum Mutat 2013;34:176-83.

E14. Li M, Lu Z, Cheng R, Li H, Guo Y, Yao Z. IL36RN gene mutations are not associated with sporadic generalized pustular psoriasis in Chinese patients. Br J Dermatol 2013;168:426-60.

E15. Körber A, Mössner R, Renner R, Sticht H, Wilsmann-Theis D, Schulz P, et al. Mutations in IL36RN in patients with generalized pustular psoriasis. J Invest Dermatol 2013;133:2634-7.

E16. Sugiura K, Takemoto A, Yamaguchi M, Takahashi H, Shoda Y, Mitsuma T, et al. The majority of generalized pustular psoriasis without psoriasis vulgaris is caused by deficiency of interleukin-36 receptor antagonist. J Invest Dermatol 2013;133:2514-21.

E17. Kanazawa N, Nakamura T, Mikita N, Furukawa F. Novel IL36RN mutation in a Japanese case of early onset generalized pustular psoriasis. J Dermatol 2013;40:749-51.

E18. Rossi-Semerano L, Piram M, Chiaverini C, De Ricaud D, Smahi A, Koné-Paut I. First clinical description of an infant with interleukin-36-receptor antagonist deficiency successfully treated with anakinra. Pediatrics 2013;132:e1043-7.

E19. Abbas O, Itani S, Ghosn S, Kibbi AG, Fidawi G, Farooq M, et al. Acrodermatitis continua of Hallopeau is a clinical phenotype of DITRA: evidence that it is a variant of pustular psoriasis. Dermatology 2013;226:28-31.

E20. Sugiura K, Oiso N, Iinuma S, Matsuda H, Minami-Hori M, Ishida-Yamamoto A, et al. il36rn mutations underlie impetigo herpetiformis. J Invest Dermatol 2014;9:1-12.

E21. Renert-Yuval Y, Horev L, Babay S, Tams S, Ramot Y, Zlotogorski A, et al. IL36RN mutation causing generalized pustular psoriasis in a Palestinian patient. Int J Dermatol 2014;53:866-8.

E22. Sugiura K, Endo K, Akasaka T, Akiyama M. Successful treatment with infliximab of sibling cases with generalized pustular psoriasis caused by deficiency of interleukin-36 receptor antagonist. J Eur Acad Dermatol Venereol 2014;9:1-2.

E23. Song HS, Yun SJ, Park S, Lee ES. Gene mutation analysis in a Korean patient with early-onset and recalcitrant generalized pustular psoriasis. Ann Dermatol 2014;26:424-5.

Activating *CARD14* Mutations Are Associated with Generalized Pustular Psoriasis but Rarely Account for Familial Recurrence in Psoriasis Vulgaris

Dorottya M. Berki[1], Lu Liu[2], Siew-Eng Choon[3], A. David Burden[4], Christopher E.M. Griffiths[5], Alexander A. Navarini[6], Eugene S. Tan[7], Alan D. Irvine[8,9], Annamari Ranki[10], Takeshi Ogo[11], Gabriela Petrof[2], Satveer K. Mahil[1], Michael Duckworth[2], Michael H. Allen[2], Pasquale Vito[12], Richard C. Trembath[13], John McGrath[2], Catherine H. Smith[2], Francesca Capon[1,14] and Jonathan N. Barker[2,14]

Caspase recruitment family member 14 (*CARD14*, also known as *CARMA2*), is a scaffold protein that mediates NF-κB signal transduction in skin keratinocytes. Gain-of-function *CARD14* mutations have been documented in familial forms of psoriasis vulgaris (PV) and pityriasis rubra pilaris (PRP). More recent investigations have also implicated *CARD14* in the pathogenesis of pustular psoriasis. Follow-up studies, however, have been limited, so that it is not clear to what extent *CARD14* alleles account for the above conditions. Here, we sought to address this question by carrying out a systematic *CARD14* analysis in an extended patient cohort ($n=416$). We observed no disease alleles in subjects with familial PV ($n=159$), erythrodermic psoriasis ($n=23$), acral pustular psoriasis ($n=100$), or sporadic PRP ($n=29$). Conversely, our analysis of 105 individuals with generalized pustular psoriasis (GPP) identified a low-frequency variant (p.Asp176His) that causes constitutive *CARD14* oligomerization and shows a significant association with GPP in Asian populations ($P=8.4\times10^{-5}$; odds ratio = 6.4). These data indicate that the analysis of *CARD14* mutations could help stratify pustular psoriasis cohorts but would be mostly uninformative in the context of psoriasis and sporadic PRP.

Journal of Investigative Dermatology (2015) **135,** 2964–2970; doi:10.1038/jid.2015.288; published online 13 August 2015

INTRODUCTION

Caspase recruitment family member 14 (*CARD14*, also known as *CARMA2*) is a conserved scaffold protein that mediates TRAF2-dependent activation of NF-κB signaling (Scudiero *et al.*, 2011). The gene is most prominently expressed in the skin, as transcript levels are high in keratinocytes and moderately abundant in dermal endothelial cells (Fuchs-Telem *et al.*, 2012; Harden *et al.*, 2014). Conversely, *CARD14* mRNA is virtually undetectable in T-lymphocytes and monocytes, suggesting that the gene is specifically required for the maintenance of skin immune homeostasis (Fuchs-Telem *et al.*, 2012; Harden *et al.*, 2014). In keeping with this notion, gain-of-function *CARD14* mutations have been linked to a number of inflammatory dermatoses.

Disease alleles resulting in enhanced NF-κB signaling were first described in two multi-generation pedigrees where psoriasis vulgaris (PV) segregated as an autosomal dominant trait (Jordan *et al.*, 2012b). Three further activating mutations were subsequently reported in individuals with familial pityriasis rubra pilaris (PRP), a papulosquamous condition phenotypically related to psoriasis (Fuchs-Telem *et al.*, 2012). Finally, the analysis of a small Japanese resource identified a tentative association between a *CARD14* variant (p.Asp176His) and a generalized pustular psoriasis (GPP), a rare neutrophilic dermatosis that often presents with systemic upset and concurrent PV (Sugiura *et al.*, 2014).

Of note, the follow-up to the findings originally obtained in familial PV has been very limited, with a single survey of

[1]*Department of Medical and Molecular Genetics, King's College London, London, UK;* [2]*St John's Institute of Dermatology, King's College London, London, UK;* [3]*Department of Dermatology, Hospital Sultanah Aminah, Johor Bahru, Malaysia;* [4]*Department of Dermatology, University of Glasgow, Glasgow, UK;* [5]*Department of Dermatology, University of Manchester, Manchester, UK;* [6]*Department of Dermatology, Zurich University Hospital, Zurich, Switzerland;* [7]*National Skin Centre, Singapore, Singapore;* [8]*Paediatric Dermatology, Our Lady's Children's Hospital, Dublin, Ireland;* [9]*Clinical Medicine, Trinity College Dublin, Dublin, Ireland;* [10]*Department of Dermatology, Venereology and Allergic Disease, University of Helsinki and Helsinki University Central Hospital, Helsinki, Finland;* [11]*Department of Cardiology, National Cerebral and Cardiovascular Center, Osaka, Japan;* [12]*Dipartimento di Scienze e Tecnologie, Università degli Studi del Sannio, Benevento, Italy and* [13]*Queen Mary, University of London, Barts and The London School of Medicine and Dentistry, London, UK*

Correspondence: Francesca Capon, Division of Genetics, 9th floor Tower Wing, Guy's Hospital, London SE1 9RT, UK or Jonathan Barker, St John's Institute of Dermatology, 9th floor Tower Wing, Guy's Hospital, London SE1 9RT, UK. E-mail: francesca.capon@kcl.ac.uk or jonathan.barker@kcl.ac.uk

[14]*These authors contributed equally to this work.*

Abbreviations: APP, acral pustular psoriasis; CARD14, *Caspase Recruitment Family Member 14; CC, coiled coil; GPP, generalized pustular psoriasis; PRP, pityriasis rubra pilaris; PV, psoriasis vulgaris*

Received 4 March 2015; revised 16 June 2015; accepted 14 July 2015; accepted article preview online 23 July 2015; published online 13 August 2015

seven North-African pedigrees published in the literature (Ammar *et al.*, 2013). Likewise, studies of *CARD14* in PRP have mostly been restricted to cohorts recruited in the Middle East (Eytan *et al.*, 2014), and the association between p.Asp176His and generalized pustular psoriasis has yet to be validated, as it was only supported by marginal statistical significance. Thus, large gaps remain in our understanding of the phenotypes that are caused by *CARD14* mutations, and it is not clear whether the genetic analysis of this locus might aid disease stratification.

Here, we have sought to address this issue by investigating an extended and an ethnically diverse patient resource. We found that *CARD14* alleles are unlikely to account for a significant proportion of familial PV or sporadic PRP cases.

Table 1. Patient resource summary statistics

Disease	N. of cases	Sex	Ethnicity
Acral pustular psoriasis[1]	100	34M, 66F	North-European
Erythrodermic psoriasis	23	18M, 5F	North-European
Familial psoriasis vulgaris	159	78M, 81F	North-European
Generalised pustular psoriasis	105	34M, 71F	North-European ($n=12$) Chinese ($n=24$) Malay ($n=52$) Indian ($n=17$)
Pityriasis rubra pilaris	29	16M, 13F	North-European ($n=24$) Afro-Caribbean ($n=2$) Unknown ($n=3$)
Total	416	180M, 236F	North-European ($n=318$) Asian ($n=93$) Afro-Caribbean ($n=2$) Unknown ($n=3$)

Abbreviations: F, Female; M, Male.
[1]Including Palmar Plantar Pustulosis ($n=92$) and Acrodermatitis Continua of Hallopeau ($n=8$).

Conversely, we demonstrated that the p.Asp176His variant has a substantial impact on protein function and is strongly associated with generalized pustular psoriasis in the Chinese and Japanese populations.

RESULTS

CARD14 mutations do not have a significant role in the pathogenesis of familial PV, sporadic PRP, or acral pustular psoriasis

As all *CARD14* mutations described to date cluster to exons 3 and 4 (Fuchs-Telem *et al.*, 2012; Jordan *et al.*, 2012b; Eytan *et al.*, 2014; Sugiura *et al.*, 2014), we initially focused our genetic screening on this region. We sequenced the two exons in a total of 416 patients, affected by acral pustular psoriasis (APP; $n=100$), erythrodermic psoriasis ($n=23$), familial PV ($n=159$), GPP ($n=105$), or PRP ($n=29$) (Table 1, Supplementary Table 1 online). Importantly, our calculations showed that all data sets had adequate power (>80%) to detect mutations accounting for >5% of disease cases (Figure 1). In fact, the power of the familial PV, APP, and GPP samples exceeded 95% (Figure 1). This is in keeping with previous analyses of the APP and GPP cohorts, which allowed us to identify a number of low-frequency mutations (Setta-Kaffetzi *et al.*, 2013; Setta-Kaffetzi *et al.*, 2014).

Despite the evidence for adequate power, we could not detect any deleterious alleles among patients affected by APP, familial PV, or erythrodermic psoriasis (Tables 2A and 2B). In fact, the only coding change observed in these data sets was a p.Ser200Asn substitution, which was identified in two cases of APP and four patients affected by familial PV (Table 2A). This variant was, however, classified as benign by multiple pathogenicity prediction algorithms. Moreover, its frequency in APP (1.0%) and familial PV subjects (1.25%) did not exceed that observed in European controls (1.3%, according to the data generated by the Exome Aggregation Consortium).

The screening of the PRP sample revealed a single change with pathogenic potential (p.Gln136Lys; Table 2A). However, this was observed in a patient who underwent parallel investigations of the *GJB4* gene to explore a differential diagnosis of erythrokeratoderma. Given that a damaging p.Cys169Trp change was identified in *GJB4*, it was

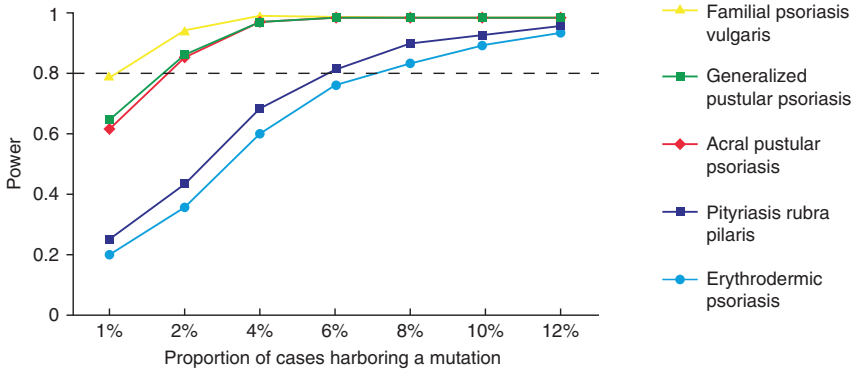

Figure 1. Power calculations. A binomial calculation calculator was used to estimate the power to detect *CARD14* mutations accounting for variable proportions of disease cases. This demonstrated that sequencing exons 3 and 4 in the various patient cohorts would have >80% power to uncover mutations found in >5% of disease cases.

Table 2A. Rare coding variants detected in the study resource

Change (rs ID)	Patient phenotype	Pathogenicity prediction						
		SIFT	Polyphen-2	PROVEAN	Mutation Taster	Align GVGD	CADD score[1]	CONSENSUS[2]
p.Met119Arg (novel)	PRP ($n=1$)	Tolerated	Benign	Neutral	Disease Causing	Pathogenic	Damaging	NEUTRAL
p.Gln136Lys (novel)	PRP ($n=1$)	Damaging	Probably Damaging	Neutral	Disease Causing	Pathogenic	Damaging	DAMAGING
p.Glu168Lys (novel)	GPP ($n=1$)	Tolerated	Benign	Neutral	Polymorphism	Pathogenic	Neutral	NEUTRAL
p.Asp176His (rs144475004)	**GPP ($n=3$)**	**Damaging**	**Probably damaging**	**Neutral**	**Disease Causing**	**Pathogenic**	**Damaging**	**DAMAGING**
p.Ser200Asn (rs114688446)	PV ($n=4$) APP ($n=2$)	Tolerated	Benign	Neutral	Polymorphism	Likely Benign	Neutral	NEUTRAL
p.Ala216Thr (novel)	GPP ($n=1$)	Tolerated	Benign	Neutral	Polymorphism	Likely Pathogenic	Neutral	NEUTRAL

[1]Although the CADD algorithm does not return qualitative pathogenicity predictions, scores >15.0 are generally considered as evidence of pathogenicity. The only variant that is likely to be disease causing (p.Asp176His) is highlighted in bold.
[2]Variants were classified as pathogenic if they were predicted to be deleterious by at least four algorithms.

Table 2B. Rare splicing variant detected in the study resource

Change (rs ID)	Patient phenotype	Pathogenicity prediction					
		Max entropy	SROOGLE	Senepathy	MutationTaster	CADD score[1]	CONSENSUS[2]
c.2569+4T>C (rs146678380)	APP ($n=1$)	Neutral	Neutral	Neutral	Disease Causing	Neutral	NEUTRAL

Abbreviations: APP, acral pustular psoriasis; GPP, generalized pustular psoriasis; PRP, pityriasis rubra pilaris; PV, psoriasis vulgaris.
[1]Although the CADD algorithm does not return qualitative pathogenicity predictions, scores >15.0 are generally considered as evidence of pathogenicity. The only variant that is likely to be disease causing (p.Asp176His) is highlighted in bold.
[2]Variants were classified as pathogenic if they were predicted to be deleterious by at least four algorithms.

not possible to reach a firm conclusion as to which variant was causing the disease phenotype.

Importantly, sequencing of the entire *CARD14* coding region in a representative patient subset ($n=82$; Supplementary Table 2 online) did not identify any additional changes with deleterious potential. Thus, our findings indicate that *CARD14* disease alleles are unlikely to account for a significant proportion of familial PV, sporadic PRP, or APP cases.

The *CARD14* p.Asp176His variant is associated with generalized pustular psoriasis in the Chinese and Japanese populations

The analysis of the generalized pustular psoriasis resource identified three unrelated subjects of Chinese descent, who carried a deleterious p.Asp176His substitution (Figure 2a; Table 2A; Supplementary Table 3 online). Of note, one of the patients had inherited the variant from a maternal aunt, who was also affected by GPP. Although the change occurs at low frequency in the Chinese population, we found that it was more common in GPP cases compared with controls (6.2% vs. 1.0%, $P=0.03$; Table 3). As these observations mirror those previously reported in a small Japanese data set (Sugiura *et al.*, 2014), we undertook a meta-analysis of the two studies. To maximize statistical power, we increased by 4-fold the size of the Japanese control resource by obtaining frequency data for an additional 322 individuals (104 subjects sequenced by the 1000 Genomes Project and 218 screened in-house). This validated the association with the p.Asp176His substitution ($P=0.008$) and showed that the Japanese and Chinese data sets were genetically homogeneous (I^2:0%). The subsequent meta-analysis of the two studies also demonstrated that the p.Asp176His change confers a very substantial increase in disease risk (odds ratio: 6.4; 95% confidence interval: 2.5–16.1; $P=8.4\times10^{-5}$).

As p.Asp176His occurs on the background of a single haplotype in the Japanese population (Sugiura *et al.*, 2014), we typed four tagging single nucleotide polymorphisms in our mutation bearing patients, in order to establish whether they carried the same ancestral chromosome. We found that three subjects were homozygous and one likely heterozygous for the same intragenic haplotype that was described in the Japanese individuals carrying the p.Asp176His variant (Supplementary Table 4 online). Thus, our data strongly support the notion that the spread of the mutation across East Asia is the result of a founder effect.

Sequencing of the entire *CARD14* coding region in a representative patient subset ($n=15$) did not uncover any further disease alleles, indicating that the association with GPP is specific to the p.Asp176His change.

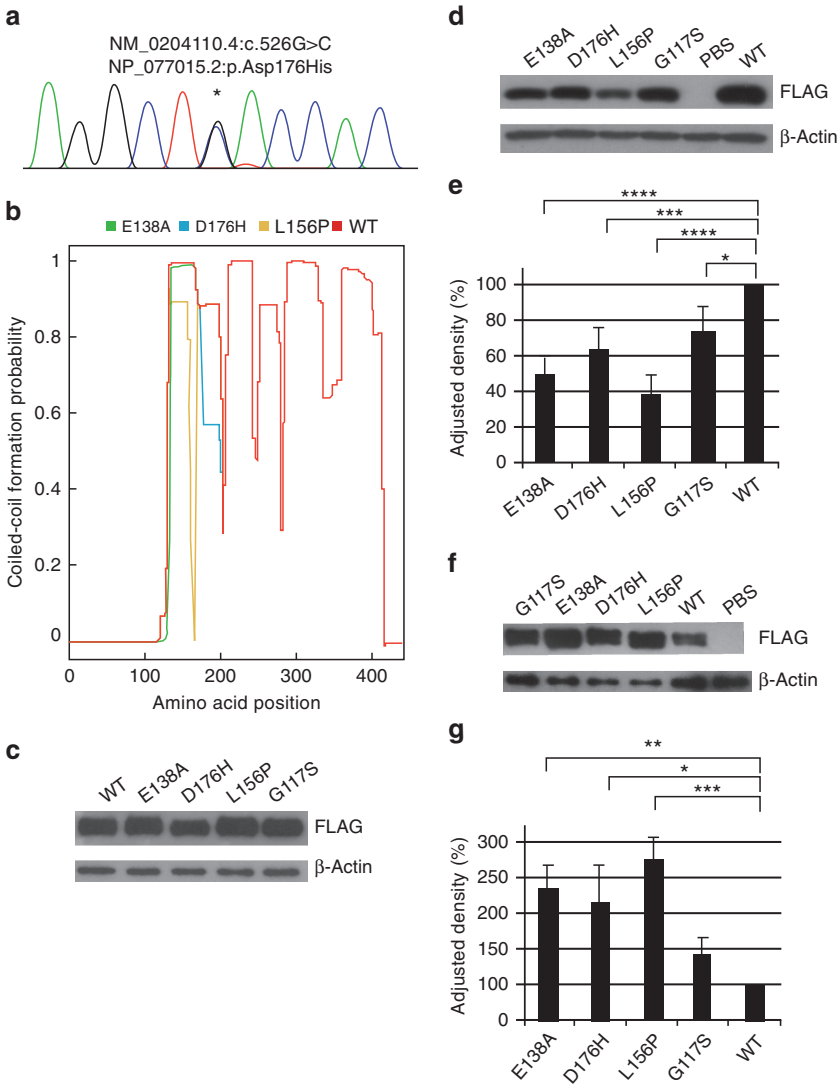

Figure 2. The p.Asp176His substitution causes spontaneous CARD14 oligomerization. (**a**) Chromatogram showing the p.Asp176His (c.526G>C) change, which is predicted to disrupt coiled-coil (CC) formation (**b**). (**c**) Western blotting of total cell lysates shows comparable amounts of wild-type and mutant CARD14. (**d** and **e**) Western blotting and densitometric analysis of soluble proteins shows reduced accumulation of CC mutants (p.Glu138Ala, p.Pro156Leu, p.Asp176His) compared with wild-type CARD14 and the non-CC mutant p.Gly117Ser. (**f** and **g**) Western blotting and densitometric analysis of insoluble proteins shows enhanced aggregation of CC mutants compared with wild-type CARD14 and p.Gly117Ser. All densitometry data are expressed as mean ± SD of at least two independent experiments. Comparable results were obtained when the levels of soluble (or insoluble) protein were normalized to total CARD14, rather than β-actin. *$P<0.05$; ***$P<0.001$; ****$P<0.0001$. WT, wild-type.

Table 3. Genetic analysis of the p.Asp176His variant

	Allele counts (%)		
Ethnicity	**Cases**	**Controls**	***P* value**
Japanese	4/42 (9.5%)	14/844 (1.7%)	0.008
Chinese[1]	3/48 (6.2%)	4/400 (1.0%)	0.030
Meta-analysis			8.4×10^{-5}

[1]As the association analysis was carried out on unrelated cases, the aunt of patient T014369 was excluded from the data set.

The p.Asp176His variant is a deleterious allele associated with constitutive *CARD14* oligomerization

To investigate the functional consequences of the p.Asp176His substitution, we first used bioinformatics to assess its potential effect on the coiled-coil (CC) domain encoded by exons 3 and 4. We found that the change from a negatively charged aspartic acid to a basic histidine significantly reduces the likelihood of CC formation (Figure 2b). This effect is comparable with the predicted impact of p.Leu156Pro and p.Glu138Ala (Figure 2b), two disease alleles previously

associated with PRP and psoriasis (Fuchs-Telem *et al.*, 2012; Jordan *et al.*, 2012b).

Of note, the CC domain of *CARD11* (a well-characterized *CARD14* paralogue) keeps the protein in an inactive conformation, which, in the absence of inflammatory stimuli, precludes auto-oligomerization and downstream signal transduction (Lamason *et al.*, 2010). In fact, gain-of-function mutations within the CC of *CARD11* cause spontaneous protein aggregation and constitutive activation of NF-κB signaling, leading to the onset of diffuse large B-cell lymphoma (Lenz *et al.*, 2008).

To investigate the possibility that the p.Asp176His substitution may also promote protein oligomerization, we transfected HEK293 cells with wild-type or mutant FLAG-CARD14 and monitored recombinant protein levels with an anti-FLAG antibody. Although western blotting of whole-cell extracts showed comparable transfection efficiencies for the two constructs (Figure 2c), the analysis of soluble proteins demonstrated that the p.Asp176His change was associated with a significant decrease in the levels of free *CARD14* (Figure 2d and e). This suggested that the mutant protein was forming insoluble oligomers. To validate this hypothesis, we used the anti-FLAG antibody to analyze the insoluble fraction of the cell extracts. As predicted, we found that *CARD14* aggregates were significantly more abundant in the cells that had been transfected with the p.Asp176His cDNA (Figure 2f and g). Interestingly, a similar effect was noted for the constructs harboring the p.Leu156Pro and p.Glu138Ala disease alleles (Figure 2d, e, f, and g). Thus, our findings indicate that the pathogenic potential of the p.Asp176His change is comparable with that of previously validated mutations.

DISCUSSION

In the last few years, *CARD14* mutations have been associated with a range of inflammatory skin disorders, including familial psoriasis and clinically related conditions such as PRP and generalized pustular psoriasis (Fuchs-Telem *et al.*, 2012; Jordan *et al.*, 2012b; Sugiura *et al.*, 2014). Although these findings have highlighted *CARD14* as a key regulator of skin immune homeostasis, their applicability to clinical practice has been limited. Very little information is available on mutation frequencies in different conditions or ethnic groups, so that it is unclear whether *CARD14* screening would aid the diagnosis or stratification of inflammatory dermatoses. Here, we sought to address this issue by analyzing a sizeable and a well-characterized patient resource, recruited in Europe and East Asia.

We first examined a familial PV cohort including >150 unrelated cases. Despite the significant power of this data set, we could not identify previously unreported disease alleles or detect any of the mutations reported in previous studies (Jordan *et al.*, 2012a; Jordan *et al.*, 2012b). Although it could be argued that our definition of the phenotype allowed the inclusion of many affected sib-pairs who were unlikely to suffer from monogenic psoriasis, our resource also comprised 51 families with four or more affected individuals (Supplementary Table 1 online). Thus, our results indicate that Mendelian forms of psoriasis are likely to be genetically heterogeneous, with *CARD14* mutations accounting for a small minority of cases.

The subsequent analysis of the PRP cohort generated similarly negative results, validating the emerging notion that *CARD14* mutations do not contribute to sporadic forms of the disease (Eytan *et al.*, 2014). Although the idea that *CARD14* has a role in the pathogenesis of PV and PRP is supported by observations of gene overexpression in patient skin and by the results of genome-wide association studies (Tsoi *et al.*, 2012; Eytan *et al.*, 2014), our findings indicate that screening this locus for deleterious mutations is unlikely to help the stratification of patient resources.

The analysis of the GPP data set demonstrated a significant association with a non-conservative amino acid substitution (p.Asp176His) that is only found in Asian populations. The functional characterization of this nucleotide change indicated that it is likely to affect CC formation, leading to the loss of *CARD14* auto-inhibition and spontaneous protein oligomerization. Although we did not formally demonstrate that these abnormalities result in enhanced transcription of NF-κB target genes, this outcome is supported by several lines of evidence. First of all, it has been shown that CARD11 oligomerization levels strongly correlate with increased NF-κB activation (Lenz *et al.*, 2008). Second, the effect of p.Asp176His on CC formation is comparable with that of p.Leu156Pro and p.Glu138Ala, which have been extensively characterized and linked to abnormal NF-κB signaling *in vitro* and *ex vivo* (Fuchs-Telem *et al.*, 2012; Jordan *et al.*, 2012b; Harden *et al.*, 2014). Finally, a systematic analysis of rare *CARD14* variants has shown that overexpression of p.Asp176His mutant constructs results in increased NF-κB reporter activity (Jordan *et al.*, 2012a). Thus, our findings validate p.Asp176His as a deleterious gain-of-function allele.

Of interest, Mossner *et al.* (2015) have very recently observed the p.Asp176His mutation in two APP cases recruited in Estonia. As the p.Asp176His substitution was not detected in any of the European data sets sequenced by the 1000 Genomes Project, it is not surprising that the variant did not appear in our APP cohort. In fact, its presence among Estonian patients is likely to reflect the distinctive population history of the Baltic countries. In this context, the analysis of p.Asp176His in Asian data sets will be required to confirm the association with APP and provide further evidence for a genetic overlap between generalized and localized pustular psoriasis (Setta-Kaffetzi *et al.*, 2013).

Although the evidence presented here strongly supports a pathogenic role for p.Asp176His, no association with GPP was observed in a recent analysis of a Han Chinese resource (Qin *et al.*, 2014). It is interesting, however, that none of the cases that were examined had been screened for mutations in *IL36RN*, the major genetic determinant of GPP (Onoufriadis *et al.*, 2011). Conversely, both our study and the analysis carried out by Sugiura *et al.* (2014) were restricted to *IL36RN*-negative cases. Thus, our results support the notion that the sequential screening of disease genes will enhance the power to detect pathogenic mutations and facilitate the stratification of GPP cohorts.

MATERIALS AND METHODS

Subjects

This study was undertaken in accordance with the principles of the Declaration of Helsinki and with the approval of the ethics committees of all participating institutions. Patients affected by PV, erythrodermic psoriasis, GPP, and APP (including both Acrodermatitis Continua of Hallopeau and Palmar Plantar Pustulosis) were ascertained as described elsewhere (Berki *et al.*, 2014; Hussain *et al.*, 2015). PRP was diagnosed on the basis of established criteria (Judge *et al.*, 2004). All patients with pustular psoriasis had been previously screened for *IL36RN* and *AP1S3* mutations, so as to exclude any subjects carrying disease alleles at known loci (Onoufriadis *et al.*, 2011; Setta-Kaffetzi *et al.*, 2014). Individuals who were affected by PV and had at least one first-degree relative with the same disease were considered cases of familial PV (Supplementary Table 1 online). The demographics of the various patient cohorts are summarized in Table 1.

Allele frequency data for 208 unrelated Chinese controls were initially collated from the 1,000 Genome Project (CHB and CHS data sets) (Abecasis *et al.*, 2012). To match the genetic make-up of cases, eight individuals with *IL36RN* mutations were subsequently excluded from the association analysis. Allele frequency data for 422 independent Japanese controls were obtained from the 1,000 Genome Project (JPT data set, $n = 104$), the work published by Sugiura *et al.* ($n = 100$) (Sugiura *et al.*, 2014), and from the analysis of 218 healthy individuals, recruited at the National Cerebral and Cardiovascular Center in Osaka (Japan) and genotyped in house by Sanger Sequencing. None of the above individuals carried *IL36RN* mutations. Allele frequency data for the European population were obtained by mining the data generated from the Exome Aggregation Consortium (http://exac.broadinstitute.org/).

All study participants granted their written informed consent.

Sanger sequencing and pathogenicity predictions

Primers were designed to amplify all *CARD14* coding exons and exon–intron junctions, as well as the genomic regions spanning haplotype tagging single nucleotide polymorphisms (Supplementary Table 5 online). Sequenced PCR products were loaded on an ABI3730*xl* DNA Analyzer (Applied Biosystems, Waltham, MA), and nucleotide changes were detected using Sequencher 4.10.1 (Gene Codes Corporation, Ann Arbor, MI). The pathogenic potential of non-synonymous sequence variants occurring with a minor allele frequency $<2\%$ was assessed with the following programs: SIFT (Kumar *et al.*, 2009), PolyPhen-2 (Adzhubei *et al.*, 2013), PROVEAN (Choi *et al.*, 2012), MutationTaster (Schwarz *et al.*, 2010), CADD (Kircher *et al.*, 2014), Align GVGD (Mathe *et al.*, 2006), SROOGLE (which was also used to compute Senepathy scores) (Schwartz *et al.*, 2009), and MaxEntScan (Yeo and Burge, 2004). The impact of damaging nucleotide changes on CC domains was further investigated with the NCOILS 1.0 software (Lupas *et al.*, 1991).

Site-directed mutagenesis, cell culture, and transfection

The previously described CARMA2-sh construct (Scudiero *et al.*, 2011) was used as a template for site-directed mutagenesis, as it encodes the *CARD14* isoform with the highest expression in the skin (Jordan *et al.*, 2012b). Reactions were prepared using the QuikChange Lightning Site Directed mutagenesis Kit (Agilent, Santa Clara, CA) and the primers listed in Supplementary Table 6 online. The integrity of all constructs was verified by Sanger sequencing of the *CARD14/CARMA2* coding region, FLAG tag, CMV promoter, and BGH poly-adenylation signal. HEK293 cells were grown in DMEM and supplemented with 1% penicillin/streptomycin and 10% fetal calf serum (all from Life Technologies, Carlsbad, CA). Cells were seeded on 12-well plates at a concentration of 2.5×10^5 per ml and transfected with the indicated constructs, using Lipofectamine 2000 (Life Technologies). All cultures were harvested 48 hours after transfection.

Western blotting and densitometry

Whole-cell protein extracts were prepared by treating cells with a denaturing lysis buffer (5% SDS, 200 Mm Tris-HCl pH 6.8, 1 mM EDTA, 1.5% β-Mercaptoethanol, 8 M Urea, and 1× Complete Protease Inhibitor Cocktail (Roche, Basel, Switzerland)). For the analysis of the soluble and insoluble fractions, cells were initially incubated with a non-denaturing buffer (50 mM Tris-HCl pH 7.4, 50 mM NaCl, 5 mM EDTA, 10% Glycerol, 1% NP40, and 1× Complete Protease Inhibitor Cocktail)and centrifuged for 15 minutes at 13,000 r.p.m., at 4 °C. The supernatant was then stored as a soluble fraction, whereas the pellets containing the insoluble protein aggregates were lysed with the denaturing lysis buffer. Following PAGE and transfer to nitrocellulose membranes, blots were probed with 1:2,500 mouse monoclonal anti-FLAG (Sigma-Aldrich, St Louis, MO) and 1:1,000 rabbit polyclonal anti β-actin (Cell Signaling Technology, Beverly, MA) antibodies. Autoradiography films were scanned, and densitometric analysis was undertaken with the Image J software (Schneider *et al.*, 2012).

Statistical analyses

Power calculations were implemented with the binomial probability calculator available at stattrek.com/online-calculator/binomial.aspx. The frequency of the p.Asp176His substitution was compared in cases versus controls with Fisher's exact test. The meta-analysis of two association studies was undertaken by using the RevMan 5.2 software (Cochrane Collaboration T, 2012) to calculate a weighted pooled odds ratio and Z score. The densitometry data were analyzed with GraphPad Prism 6.0 (GraphPad Software, La Jolla, CA) by one-way analysis of variance followed by the Dunnett's post-test. P values <0.05 were considered statistically significant.

CONFLICT OF INTEREST

The authors state no conflict of interest.

ACKNOWLEDGMENTS

We thank Liisa Vakeva, Hazel H Oon, WS Chong, and Colin T Theng for their contribution to patient ascertainment. We acknowledge support from the Department of Health via the NIHR comprehensive Biomedical Research Centre award to Guy's and St Thomas' NHS Foundation Trust in partnership with King's College London and King's College Hospital NHS Foundation Trust. We also acknowledge the support of the NIHR, through the Dermatology Clinical Research Network, with case ascertainment. This work was supported by a Medical Research Council Stratified Medicine award (grant MR/L011808/1). DMB's PhD studentship is funded by the Psoriasis Association. SKM is supported by a Medical Research Council Clinical Training Fellowship (MR/L001543/1).

SUPPLEMENTARY MATERIAL

Supplementary material is linked to the online version of the paper at http://www.nature.com/jid

REFERENCES

Abecasis GR, Auton A, Brooks LD *et al.* (2012) An integrated map of genetic variation from 1,092 human genomes. *Nature* 491:56–65

Adzhubei I, Jordan DM, Sunyaev SR (2013) Predicting functional effect of human missense mutations using PolyPhen-2. *Curr Protoc Hum Genet* Chapter 7: Unit 7 20

Ammar M, Bouchlaka-Souissi C, Helms CA *et al.* (2013) Genome-wide linkage scan for psoriasis susceptibility loci in multiplex Tunisian families. *Br J Dermatol* 168:583–7

Berki D, Mahil SK, David Burden A *et al.* (2014) Loss of IL36RN function does not confer susceptibility to psoriasis vulgaris. *J Invest Dermatol* 134:271–3

Choi Y, Sims GE, Murphy S *et al.* (2012) Predicting the functional effect of amino acid substitutions and indels. *PLoS ONE* 7:e46688

Cochrane Collaboration (2012) *Review Manager (RevMan)*. The Nordic Cochrane Centre: Copenhagen

Eytan O, Qiaoli L, Nousbeck J *et al.* (2014) Increased epidermal expression and absence of mutations in CARD14 in a series of patients with sporadic pityriasis rubra pilaris. *Br J Dermatol* 170:1196–8

Fuchs-Telem D, Sarig O, van Steensel MA *et al.* (2012) Familial pityriasis rubra pilaris is caused by mutations in CARD14. *Am J Hum Genet* 91:163–70

Harden JL, Lewis SM, Pierson KC *et al.* (2014) CARD14 expression in dermal endothelial cells in psoriasis. *PLoS ONE* 9:e111255

Hussain S, Berki DM, Choon SE *et al.* (2015) IL36RN mutations define a severe auto-inflammatory phenotype of generalized pustular psoriasis. *J Allergy Clin Immunol* 135:1067–70.e9

Jordan CT, Cao L, Roberson ED *et al.* (2012a) Rare and common variants in CARD14, encoding an epidermal regulator of NF-kappaB, in psoriasis. *Am J Hum Genet* 90:796–808

Jordan CT, Cao L, Roberson ED *et al.* (2012b) PSORS2 is due to mutations in CARD14. *Am J Hum Genet* 90:784–95

Judge MR, McLean WHI, Munro CS (2004) Disorder in keratinization. In: *Rook's textbook of Dermatology*. Burns T, Breathnach S, Cox N, Griffiths CE (eds). 7th ed. Vol. 2. Oxford: Blackwell Science, 34.1–111

Kircher M, Witten DM, Jain P *et al.* (2014) A general framework for estimating the relative pathogenicity of human genetic variants. *Nat Genet* 46:310–5

Kumar P, Henikoff S, Ng PC (2009) Predicting the effects of coding non-synonymous variants on protein function using the SIFT algorithm. *Nat Protoc* 4:1073–81

Lamason RL, McCully RR, Lew SM *et al.* (2010) Oncogenic CARD11 mutations induce hyperactive signaling by disrupting autoinhibition by the PKC-responsive inhibitory domain. *Biochemistry* 49:8240–50

Lenz G, Davis RE, Ngo VN *et al.* (2008) Oncogenic CARD11 mutations in human diffuse large B cell lymphoma. *Science* 319:1676–9

Lupas A, Van Dyke M, Stock J (1991) Predicting coiled coils from protein sequences. *Science* 252:1162–4

Mathe E, Olivier M, Kato S *et al.* (2006) Computational approaches for predicting the biological effect of p53 missense mutations: a comparison of three sequence analysis based methods. *Nucleic Acids Res* 34:1317–25

Mossner R, Frambach Y, Wilsmann-Theis D *et al.* (2015) Palmoplantar pustular psoriasis is associated with missense variants in CARD14, but not with loss-of-function mutations in IL36RN in European patients. *J Invest Dermatol*. e-pub ahead of print 19 May 2015

Onoufriadis A, Simpson MA, Pink AE *et al.* (2011) Mutations in IL36RN/IL1F5 are associated with the severe episodic inflammatory skin disease known as generalized pustular psoriasis. *Am J Hum Genet* 89:432–7

Qin P, Zhang Q, Chen M *et al.* (2014) Variant analysis of CARD14 in a Chinese Han population with psoriasis vulgaris and generalized pustular psoriasis. *J Invest Dermatol* 134:2994–6

Schneider CA, Rasband WS, Eliceiri KW (2012) NIH Image to ImageJ: 25 years of image analysis. *Nat Methods* 9:671–5

Schwartz S, Hall E, Ast G (2009) SROOGLE: webserver for integrative, user-friendly visualization of splicing signals. *Nucleic Acids Res* 37:W189–92

Schwarz JM, Rodelsperger C, Schuelke M *et al.* (2010) MutationTaster evaluates disease-causing potential of sequence alterations. *Nat Methods* 7:575–6

Scudiero I, Zotti T, Ferravante A *et al.* (2011) Alternative splicing of CARMA2/CARD14 transcripts generates protein variants with differential effect on NF-kappaB activation and endoplasmic reticulum stress-induced cell death. *J Cell Physiol* 226:3121–31

Setta-Kaffetzi N, Navarini AA, Patel VM *et al.* (2013) Rare pathogenic variants in IL36RN underlie a spectrum of psoriasis-associated pustular phenotypes. *J Invest Dermatol* 133:1366–9

Setta-Kaffetzi N, Simpson MA, Navarini AA *et al.* (2014) AP1S3 mutations are associated with pustular psoriasis and impaired Toll-like receptor 3 trafficking. *Am J Hum Genet* 94:790–7

Sugiura K, Muto M, Akiyama M (2014) CARD14 c.526G>C (p.Asp176His) is a significant risk factor for generalized pustular psoriasis with psoriasis vulgaris in the Japanese cohort. *J. Invest Dermatol 13*4:1755-7.

Tsoi LC, Spain SL, Knight J *et al.* (2012) Identification of 15 new psoriasis susceptibility loci highlights the role of innate immunity. *Nat Genet* 44: 1341–8

Yeo G, Burge CB (2004) Maximum entropy modeling of short sequence motifs with applications to RNA splicing signals. *J Comput Biol* 11:377–94